



HAL
open science

Caractérisation de complexes responsables de la dégradation des ARNm non-sens

Lahari Yeramala

► **To cite this version:**

Lahari Yeramala. Caractérisation de complexes responsables de la dégradation des ARNm non-sens. Génétique. Université Grenoble Alpes, 2017. Français. NNT : 2017GREAV008 . tel-01686304

HAL Id: tel-01686304

<https://theses.hal.science/tel-01686304>

Submitted on 17 Jan 2018

HAL is a multi-disciplinary open access archive for the deposit and dissemination of scientific research documents, whether they are published or not. The documents may come from teaching and research institutions in France or abroad, or from public or private research centers.

L'archive ouverte pluridisciplinaire **HAL**, est destinée au dépôt et à la diffusion de documents scientifiques de niveau recherche, publiés ou non, émanant des établissements d'enseignement et de recherche français ou étrangers, des laboratoires publics ou privés.

THESIS / THÈSE

To obtain the title of / Pour obtenir le grade de

DOCTEUR DE LA COMMUNAUTÉ UNIVERSITÉ GRENOBLE ALPES

Discipline / Spécialité : **Biologie Structurale et Nanobiologie**

Arrêté ministériel : 25 mai 2016

Presented by / Présentée par

Lahari Yeramala

Thesis supervisor / Thèse dirigée par **Prof. Christiane Schaffitzel**

Thesis prepared at / Thèse préparée au sein du **European
Molecular Biology Laboratory (EMBL), Grenoble Outstation**
in / dans l'**École Doctorale de Chimie et Sciences du Vivant**

Characterization of Nonsense- Mediated mRNA Decay Complexes

Caractérisation de complexes responsables de la
dégradation des ARNm non-sens

Public defense on / Thèse soutenue publiquement le **02.06.2017**

Jury members / Devant le jury composé de :

Dr. Bertrand Serpahin Reviewer / Rapporteur
Group Leader, IGBMC, France

Prof. Robbie Joseph Loewith Reviewer / Rapporteur
University Professor, University of Geneva, Switzerland

Dr. Stephen Cusack, FRS Examiner/ Examinateur
Group Leader, EMBL, France

Prof. Uwe Schlattner Examiner/ Examinateur
Professor, University of Grenoble Alpes, France



Dedicated to the people who kept me going

Table of Contents

1 Preface	7
2 Introduction	9
2.1 Life cycle of mRNA.....	10
2.2 Quality control mechanisms	11
2.3 Important factors involved in NMD	23
2.4 Importance of NMD factors.....	32
2.5 Scope of the thesis	34
3 Biochemical and structural characterization of the effect of PABP on mammalian translation termination	35
3.1 Abstract.....	36
3.2 Introduction.....	36
3.3 Results.....	37
3.4 Conclusions.....	54
3.5 General protocols used for the studies	56
3.6 Published Work.....	61
PABP enhances release factor recruitment and stop codon recognition during translation termination	61
4 Biochemical and structural characterization of the effect of UPF1 on mammalian translation termination	63
4.1 Abstract.....	64
4.2 Introduction.....	64
4.3 Results.....	64
4.4 Conclusions.....	68
5 Novel interaction between UPF3B and the SMG1 kinase complex regulates UPF1 phosphorylation	71
5.1 Abstract.....	72
5.2 Introduction.....	72
5.3 Results.....	74
5.4 Discussion	79

5.5	Methods.....	80
5.6	Figures.....	83
5.7	Supplementary Figures	90
6	Conclusions and Discussion	97
7	References.....	104
8	Manuscript	123
9	Appendix.....	125
10	Acknowledgments.....	130

Table of Figures

Figure 2.1 Life cycle of mRNA:	12
Figure 2.2 Non-Stop Decay (NSD):.....	14
Figure 2.3 No-Go Decay (NGD):	15
Figure 2.4 Translation Termination:	18
Figure 2.5 Nonsense-Mediated Decay (NMD):.....	21
Figure 2.6 Decay of mRNA during NMD:	23
Figure 2.7 Schematic representation of the important factors involved in NMD in mammals.:	25
Figure 3.1 Factors required for the reconstituted in vitro translation system:	39
Figure 3.2 Toe-printing assay :	40
Figure 3.3 Capping of the mRNA increases the efficiency of in vitro translation:	42
Figure 3.4 Assembly of Pre termination complexes (PreTCs):	44
Figure 3.5 Biochemical characterization of eRF1-eRF3a-PABP complexes:	48
Figure 3.6 Cyo-EM of pre-terminating ribosome with eRF1-eRF3a-PABP-GTP:	50
Figure 3.7 Cyo-EM of pre-terminating ribosome with eRF1-eRF3a-PABP-GMPPNP:.....	52
Figure 3.8 Interaction between PABP and eRF1:	53
Figure 3.9 Interacting region between PABP and eRF1:.....	54
Figure 4.1 Biochemical characterization of eRF1-eRF3a-UPF1 complexes:.....	66
Figure 4.2 Cyo-EM of pre-terminating ribosome with eRF1-eRF3a-UPF1:.....	67
Figure 5.1 UPF3 forms a complex with SMG1C:	84
Figure 5.2 Interacting region of UPF3B with SMG1C:.....	85
Figure 5.3 UPF3B and UPF3A are substrates for SMG1C kinase:	86
Figure 5.4 UPF2 and /or UPF3B inhibit phosphorylation of UPF1 by SMG1C:	87
Figure 5.5 Mass spectrometry analysis of UPF1, UPF3B and dephosphorylated UPF3B after incubation with SMG1C and ATP:	88
Figure 5.6 Negative stain of SMG1C complex with UPF3B:	89

Nomenclature

3' UTR	3' untranslated region
40S	Eukaryotic small ribosomal subunit
60S	Eukaryotic large ribosomal subunit
80S	Eukaryotic ribosome
ATP	Adenosine 5'-triphosphate
ATPase	ATP hydrolase
CBC	Cap binding complex
Cryo-EM	Electron cryo-microscopy
DNA	Deoxyribonucleic acid
EBD	EJC-binding domain
EBM	Exon junction complex-binding motif
EJC	Exon junction complex
GMPPNP	Guanosine 5'-[β,γ -imido]triphosphate
GTP	Guanosine 5'-triphosphate
GTPase	GTP hydrolase
MIF4G	Middle domain of eukaryotic initiation factor 4G (eIF4G)
NGD	No-go decay
NMD	Nonsense mediated mRNA decay
NSD	No-stop decay
NTC	Normal termination codon
ORF	Open reading frame
PABP	Human cytoplasmic poly (A) binding protein
PAIP	PABP-interacting proteins
PAM2	PABP-interacting motifs 2
PIKK	Phosphatidylinositol 3-kinase-related kinase
PTC	Premature termination codon
PostTC	Post-terminating ribosome
PreTC	Pre-terminating ribosome
RNA	Ribonucleic acid
RNC	Ribosome-nascent chain complex
RRM	RNA-recognition motifs

SMD	STAU1-mediated mRNA decay
SMG	Suppressor with morphogenetic effect on genitalia
UPF	Upstream frameshifting
VCE	Vaccinia capping enzyme
eEF	Eukaryotic elongation factor
eIF	Eukaryotic initiation factor
eRF	Eukaryotic release factor
mRNA	Messenger RNA
mRNP	Messenger ribonucleoprotein
rpm	Rotations per minute
tRNA	Transfer RNA

1 Preface

The aim of my doctoral thesis is to gain a better understanding of the nonsense-mediated mRNA decay (NMD) by studying the cross talk between the translation machinery, termination factors, and NMD factors. The thesis is written in a cumulative style. The second chapter comprises of a general introduction to translation termination and nonsense-mediated mRNA decay. The third and the fourth chapters focus on understanding the role of poly (A) binding protein (PABP) and up-frameshift protein 1 (UPF1) in translation termination respectively. The fifth chapter concentrates on a novel interaction between the NMD factors SMG1 and UPF3B, which is formatted as a manuscript. The final chapter of the thesis includes the conclusions and the future perspectives.

2 Introduction

Résumé en français

L'expression des gènes est un processus très régulé et de nombreux mécanismes de contrôle qualité existent dans les cellules afin d'éliminer les produits de transcription non fonctionnels. Ces processus existent à différentes étapes du cycle cellulaire et sont étroitement régulés. Des ARNs messagers (ARNm) aberrants peuvent résulter d'une édition incorrecte des ARNs, de mutations somatiques, d'erreurs durant la transcription et l'épissage. Il y a différents systèmes de surveillance chez les eucaryotes qui reconnaissent ces ARNm aberrants et qui empêchent la production de protéines non fonctionnelles qui peuvent être toxiques pour les cellules.

Un de ces importants mécanismes de contrôle chez les eucaryotes est la dégradation des ARNm non-sens (nonsense-mediated decay ou NMD) contenant un codon stop prématuré (PTC). La NMD reconnaît les ARNm ayant un PTC durant la traduction et les redirige afin qu'ils soient dégradés. Les facteurs centraux de la machinerie NMD sont les protéines UPF1, UPF2 et UPF3. Les interactions entre les UPFs, les facteurs de terminaison, PABP et le Exon Junction Complexe (EJC) en aval marquent les ARNm afin qu'ils soient dégradés. Le signal majeur du NMD est la phosphorylation de UPF1 par la kinase SMG1. Une fois UPF1 phosphorylé, les facteurs SMGs (SMG5, SMG6 and SMG7) sont recrutés afin de lier les ARNm aberrants avec la machinerie cellulaire de dégradation des protéines.

Dans ce chapitre, une description détaillée est donnée sur les différents mécanismes de contrôle qualité existants et sur les différents facteurs impliqués dans la NMD.

The cell is the basic functional and structural unit of every living organism. The important biologically active molecules in the cell are composed of nucleic acids and proteins. The two different types of nucleic acids are deoxyribonucleic acid (DNA) and the ribonucleic acid (RNA), which carry the genetic information while the proteins are the workhorses of the cell. The central dogma describes the flow of the genetic information in a cell from DNA to proteins. RNA plays a central role in this pathway and the information in the DNA is transferred to the messenger RNA (mRNA) by a process called transcription. Subsequently, mRNA is used as a template by the ribosomes in a process called translation to synthesize proteins (Crick, 1970).

Transcription and translation are tightly regulated at different stages by multiple quality control mechanisms and numerous checkpoints in order to avoid errors that may give rise to diverse diseases.

2.1 Life cycle of mRNA

The pre-mRNAs that are synthesized in the nucleus by RNA polymerase II associate with various proteins to form messenger ribonucleoproteins (mRNPs). During transcription, the pre-mRNA couples with several splicing factors to form the spliceosome at the exon-intron junctions. Spliceosome removes introns in a process known as mRNA splicing. m⁷pppN is added at the 5' end, which is bound by the cap-binding complex (CBC) composed of cap binding proteins CBP80-CBP20. The poly (A) tail at the 3' end is added by polyadenylate polymerase and is then further bound by nuclear poly (A) binding protein. The 5' cap along with the CBC protects the mRNA from 5' to 3' exonucleases (Muhlrad, Decker, & Parker, 1994; Muhlrad & Parker, 1994) whereas the poly (A) tail bound by PABP protects the mRNA from 3' to 5' exonucleases (Mangus, Evans, & Jacobson, 2003). During mRNA splicing, exon junction complex (EJC) is deposited 22-24 nucleotides upstream of the exon-exon junction. The export of these mature RNAs to the cytoplasm occurs through the nuclear pore complexes (NPCs), and is mediated by interactions between the hnRNPs/export factors and the nuclear pore proteins (J. Lykke-Andersen, 2001) (Figure 2.1)

Once the mRNA is exported to the cytoplasm, translation of the mature mRNA occurs by the ribosomes with the help of initiation, elongation, termination factors and transfer RNAs (tRNAs), leading to protein synthesis. After the first round of translation, a complex named eukaryotic initiation factor 4F replaces the CBC. eIF4F comprises the DEAD-box RNA helicase eIF4A, the cap-binding protein eIF4E, and a large scaffold protein eIF4G (Merrick, 2015). Certain mRNA species undergo an additional process of mRNA localization that enables the migration of silenced mRNAs to specific cellular destinations for translation (Ben-Ari et al., 2010).

The mRNA lifetime may vary from a few minutes to days. Eventually, the mRNA is targeted for degradation, which is carried out by the endonucleases and exonucleases and exosomes depending upon the large number of cues within the cell. Interestingly, distinct foci exist within

the cytoplasm of eukaryotic cells called P-bodies (processing bodies), where the enzymes needed for RNA turnover are localized. P-bodies have been shown to have roles in general mRNA decay, nonsense-mediated mRNA decay (NMD), adenylate-uridylate-rich element (AREs)-mediated mRNA decay, and microRNA-induced mRNA silencing (Kulkarni, Ozgur, & Stoecklin, 2010). Any errors in mRNA processing and mRNA assembly gives rise to aberrant RNAs and potentially to truncated, aberrant proteins leading to disease. Hence, it is important to recognize and degrade these incorrectly processed/packaged transcripts immediately. To this end, the cell has evolved many mechanisms to detect and remove these errors. The mRNA is subjected to manifold quality control processes and surveillance systems within the nucleus and the cytoplasm. The regulation of mRNA turnover is crucial for avoiding the production of faulty proteins and controlling the levels of protein expression (C.-Y. a Chen & Shyu, 2011).

2.2 Quality control mechanisms

Cellular gene expression is highly regulated and many quality control processes exist to eliminate non-functional transcripts and their encoded proteins. These processes exist at different stages of the cell cycle and they are tightly regulated.

Aberrant mRNAs can be produced as a result of incorrect RNA editing, somatic mutations, germline mutations, errors during transcription and/or splicing. There are different surveillance systems in eukaryotes, which recognize aberrant mRNAs and thus prevent production of the non-functional proteins that can be toxic to the cell. It is advantageous for the cell to detect and remove these errors in the mRNA as early as possible to avoid any possible dominant negative effects from the aberrant protein products.

Numerous mechanisms exist in the nucleus to target transcripts to the exosome (Schmid & Jensen, 2008). In the cytoplasm cotranslational quality control mechanisms and the ribosome-associated quality control mechanisms exist, which degrade defective mRNAs and the aberrant protein products (Brandman & Hegde, 2016).

Cotranslational quality control mechanisms decide over the fate of the nascent polypeptide chains that are being produced by the ribosomes, removing unfolded or misfolded proteins (J. Lykke-andersen & Bennett, 2014).

In the case of ribosome-associated quality control mechanisms, the state of translation is being detected rather than the folding state of the nascent chain. When translation stalls due to an error, both the nascent polypeptide chain (independent of its folding state) and the mRNA are targeted for degradation. In ribosome-associated quality control mechanisms, the key fate decisions are made by monitoring the translation machinery, especially the ribosome (Shoemaker & Green, 2012).

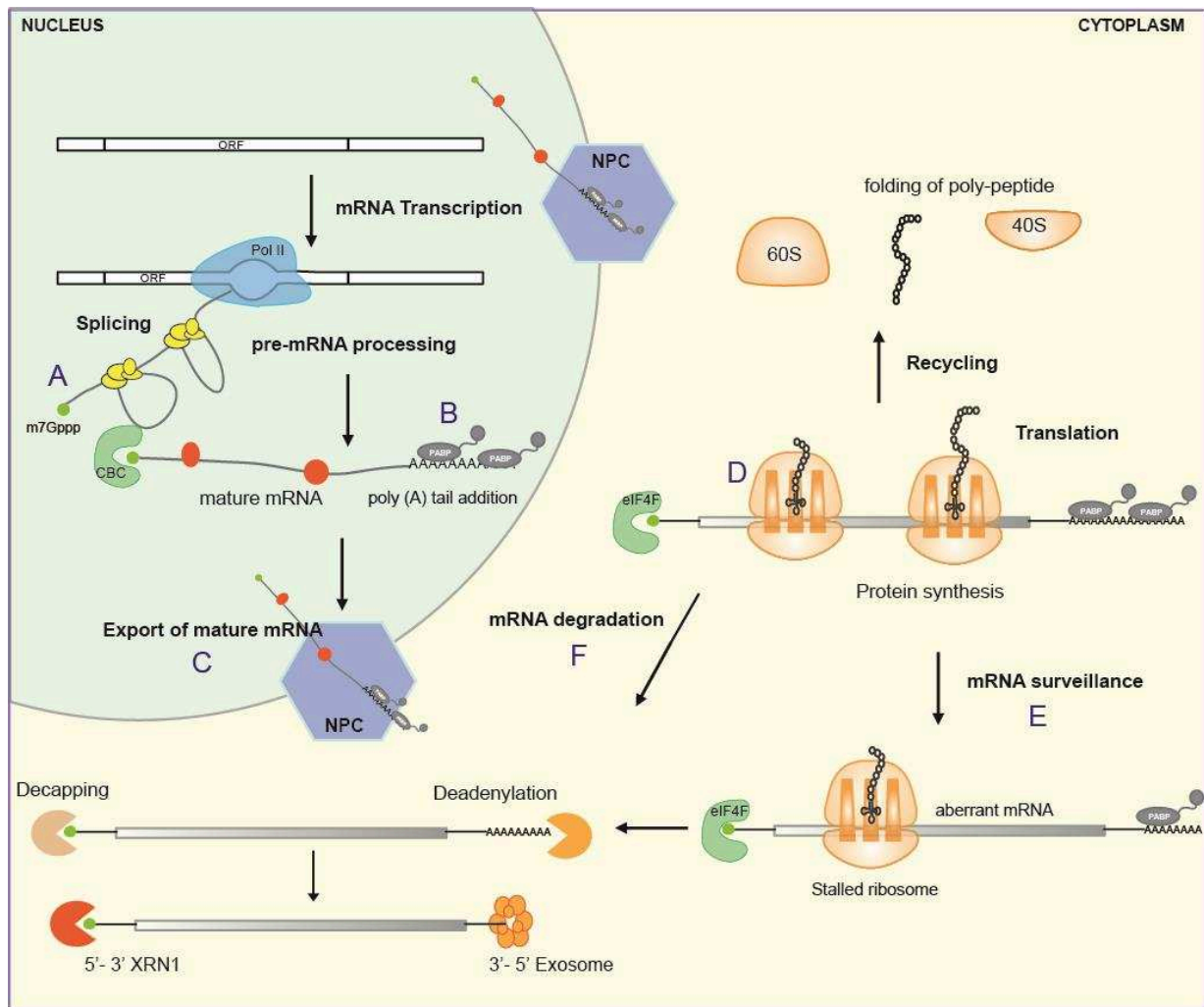


Figure 2.1 Life cycle of mRNA:

Transcription of the DNA by RNA polymerase II generates pre-mRNA in the nucleus. The pre-mRNA is further processed by (a) addition of the 5' cap (b) addition of the poly (A) tail and (c) association with different proteins to form messenger ribonucleoproteins (mRNPs). (d) Removal of introns from the pre-mRNA by the spliceosome to produce mature mRNA. Mature mRNA is then transported to the cytoplasm through the nuclear pore complex (NPC) where it associates with several components of the translational apparatus (ribosomes, initiation, elongation and termination factors). Translation of the mRNA results in the synthesis of the polypeptide chain. After the first round of translation, the cap-binding complex (CBC) is replaced by eIF4F at the 5' cap. Eventually, the mRNA is targeted for degradation to the P-bodies where it is deadenylated, decapped and degraded by specialized nucleases including the exosome. If the ribosome is stalled at any stage during translation due to incorrect RNA editing, somatic mutations, germline mutations, or errors during transcription and splicing, mRNA quality control mechanisms target the aberrant mRNA and its protein product for degradation. Adapted from (Isken & Maquat, 2007; M. J. Moore & Proudfoot, 2009).

The cytoplasmic quality control mechanisms comprise of Staufen1 (STAU1)-mediated mRNA decay (SMD) and other ribosome-associated quality-control mechanisms including Non-Stop mRNA Decay (NSD), No-Go mRNA Decay (NGD) and Nonsense-mediated mRNA Decay (NMD). NMD recognizes and targets mRNAs containing a premature stop codon (UAA, UGA, UAG) for degradation as discussed in detail in section 1.2.3.

2.2.1 Non-Stop mRNA Decay (NSD)

NSD recognizes and degrades mRNAs without a stop codon. NSD involves the protein Ski7 (Super killer 7) a GTPase similar to eukaryotic release factor 3 (eRF3), and a complex composed of the RNA helicase Ski2, the tricopeptide repeat protein Ski3, and the WD40 repeat protein Ski8, named the Ski complex (Brown, Bai, & Johnson, 2000) (Figure 2.2). NSD requires the exosome, which consists of nine core proteins, including Rrp40 and the catalytic protein Rrp44 (Lebreton, Tomecki, Dziembowski, & Seraphin, 2008). Because termination codons are missing in the message, the ribosome continues to translate until the end of the mRNA. Ski7 binds to the ribosome stalled at the 3' end of the mRNA and recruits the exosome to trigger fast 3' to 5' exonucleolytic degradation (Figure 2.2). NSD is translation-dependent (Frischmeyer et al., 2002) but not dependent on deadenylation (Hoof, Frischmeyer, Dietz, & Parker, 2002). The components involved in the yeast NSD mechanism are conserved in mammals except for the key regulator Ski7 that is not found in mammalian cells. In mammalian NSD, the proteins Dom34 and Hbs1 are also required apart from the Ski complex (Saito, Hosoda, & Hoshino, 2013).

2.2.2 No-Go mRNA Decay (NGD)

NGD targets mRNAs that are stalled during translation elongation. Stalling could be caused by stable RNA secondary structures, by depurination of mRNA or by rare codons (Chen et al., 2010; Doma & Parker, 2006; Elzen et al., 2010; Kobayashi et al., 2010). Whereas in bacteria, the trans-translation system rescues stalled ribosomes by employing a specialized RNA called tmRNA (S. D. Moore & Sauer, 2007). The proteins Dom34 (Pelota in mammals) and Hbs1 recognize the stalled ribosomes and recruit a yet unknown endonuclease. This leads to the dissociation of the stalled ribosomes with the help of the ATPase Rli1 (RNase L inhibitor-1, known as ABCE1 in mammals) (Figure 2.3) (Doma & Parker, 2006; Passos et al., 2009; Pisareva, Skabkin, Hellen, Pestova, & Pisarev, 2011; Shoemaker, Eyler, & Green, 2010; Shoemaker & Green, 2011). The mRNA is cleaved near the stalling site and degraded by the exosome or the XRN1 exoribonuclease. After splitting of the ribosomes, the large ribosomal subunit (60S) associated ribosome quality control complex (RQC) is formed which helps in polyubiquitination of the nascent polypeptides by ubiquitin ligase Ltn1 (Listerin in mammals). Polyubiquitination is the signal to subject the polypeptide to rapid degradation (Chu et al., 2009).

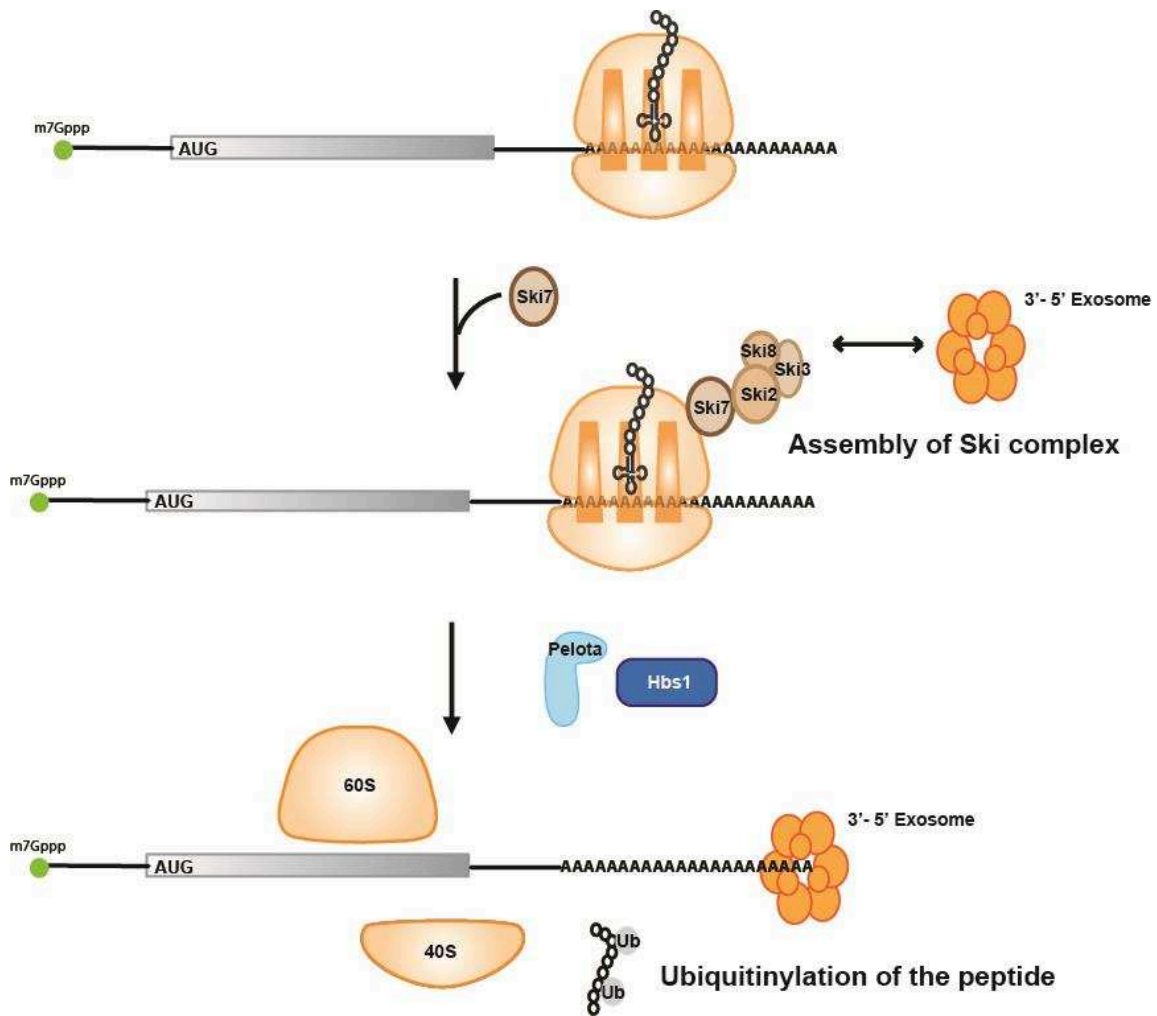


Figure 2.2 Non-Stop Decay (NSD):

Non-Stop decay occurs when the mRNA lacks a stop codon. The ribosome continues to translate and stalls in the 3' poly (A) tail region of the mRNA. Ski7 recognizes the ribosome stalled at the 3' end of the mRNA. It recruits the Ski complex consisting of factors Ski2, Ski3 and Ski8 and the exosome to trigger fast 3' to 5' exonucleolytic degradation of mRNA. The factors Pelota and Hbs1, which are the major players in NGD, have also been associated with recycling of the stalled ribosomes. The nascent polypeptide is ubiquitinated by the ubiquitin ligase Ltn1 and is thus targeted for degradation. Adapted from (J. Lykke-andersen & Bennett, 2014; Shoemaker & Green, 2012).

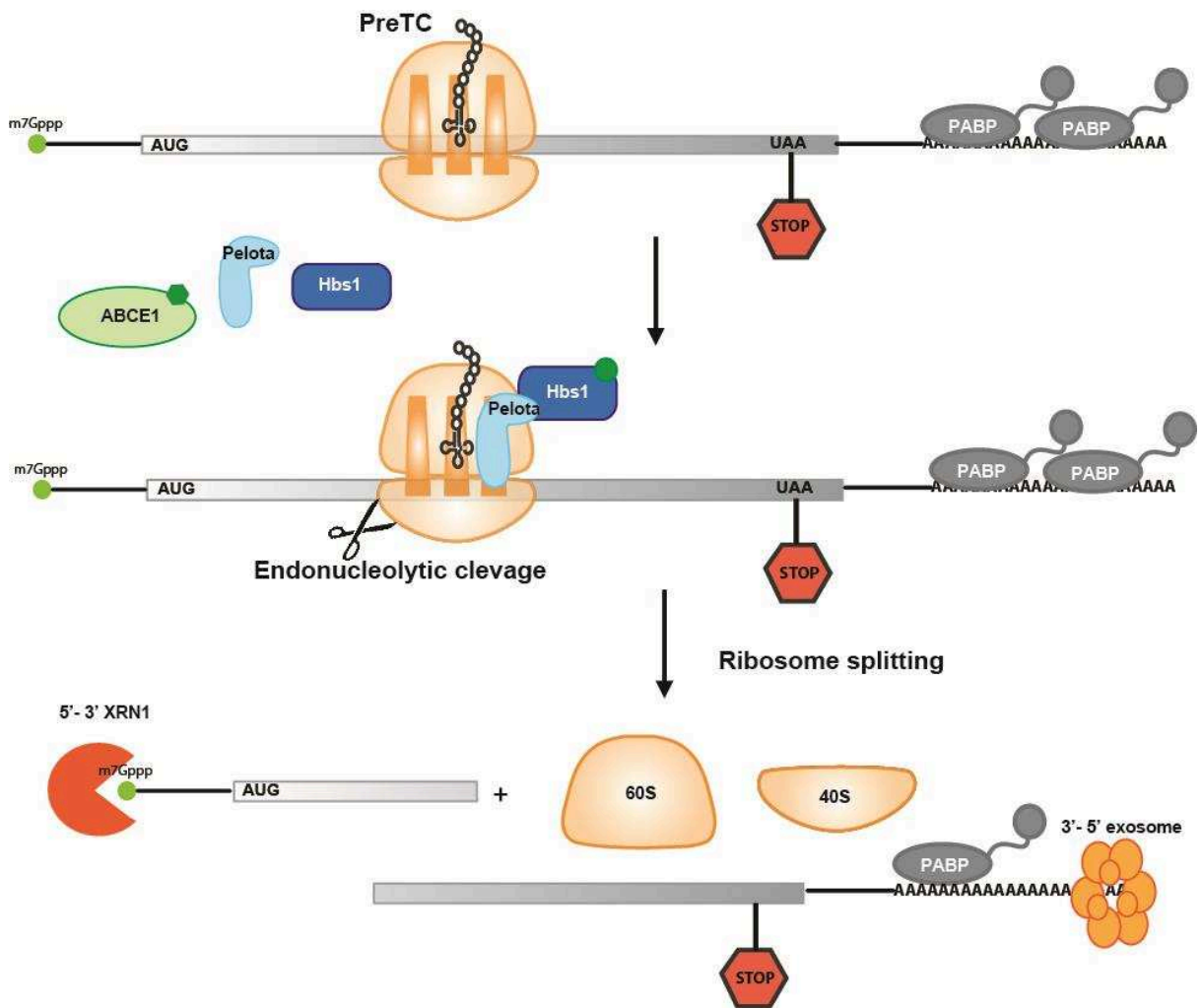


Figure 2.3 No-Go Decay (NGD):

No-go decay occurs when the ribosomes are stalled on the mRNA during the elongation stage of translation. The stalled ribosome recruits the factors Pelota and Hbs1, which are homologs of eRF1 and eRF3a, respectively. This results in an endonucleolytic cleavage of the mRNA. Subsequently, the recycling factor ABCE1 helps in the dissociation of the ribosomes. The cleaved, aberrant mRNA is subjected to rapid degradation by exonuclease XRN1 and the exosome. Adapted from (Shoemaker & Green, 2012)

It has also been shown that Dom34-Hbs1 is not required for the endonucleolytic cleavage of the mRNA, indicating that the ribosome may have this activity (Kobayashi et al., 2010; Passos et al., 2009; Tsuboi et al., 2012). The structure of a stalled ribosome with Dom34-Hbs1 has been solved by electron cryo-microscopy, showing the binding of Dom34 to the ribosomal A site and illustrating how the different interactions of Dom34-Hbs1 with the ribosome lead to destabilization of the interactions of the mRNA and the tRNA with the ribosome (Becker et al., 2011). Recent findings also suggest that Dom34-Hbs1 functions as a non-specific translation termination factor in order to release peptidyl-tRNA and to accelerate recycling of the stalled ribosome (Pisareva et al., 2011; Shoemaker et al., 2010).

2.2.3 Nonsense-mediated mRNA decay (NMD)

Nonsense-mediated mRNA decay (NMD) is a translation-dependent mRNA surveillance mechanism in eukaryotes that degrades mRNAs containing a premature termination codon (PTC) that either results from nonsense or frameshift mutations (Frischmeyer & Dietz, 1999). NMD recognizes the mRNAs containing PTCs during translation and targets them for degradation. PTCs were first reported in 1979 to reduce mRNA abundance (Losson & Lacroute, 1979) and later to reduce mRNA stability in patients with β -thalassemia (Maquat, Kinniburgh, & Ross, 1981). NMD was later observed to be at the basis of many diseases such as triose phosphate isomerase (TPI) deficiency (Daar & Maquat, 1988) or the Marfan syndrome (Caputi, Kendzior, & Beemon, 2002). Other examples for defective transcripts with PTCs leading to diseases include Duchenne muscular dystrophy and cystic fibrosis.

Recent evidence shows that NMD not only regulates aberrant mRNAs containing PTCs but also targets many physiological full-length mRNAs thus regulating the levels of normal gene expression within a cell. Approximately 15% of the transcripts are regulated by NMD (Chan et al., 2007; Imamachi, Tani, & Akimitsu, 2012; Mendell, Sharifi, Meyers, Martinez-murillo, & Dietz, 2004; Yepiskoposyan, Aeschimann, Nilsson, Okoniewski, & Mu, 2011; X. Zhang, Azhar, Huang, & Cui, 2007). NMD function is linked to diverse cellular processes that include neuronal activity or behaviour, cell growth and proliferation, development and differentiation, innate immunity and antiviral or stress responses (He & Jacobson, 2015b; Karousis, Nasif, & Mühlemann, 2016).

The mechanism by which mRNA substrates are recognized by NMD factors is still unclear. There are multiple models that have been proposed. NMD substrates include mRNAs that contain upstream open reading frames, introns in the 3'UTR, or long 3'UTRs. UPF1, UPF2 and UPF3 are the major factors playing a role in NMD and are highly conserved from yeast to humans (He, Brown, & Jacobson, 1997; Melero et al., 2012b).

Understanding NMD depends on elucidating differences between the normal and premature translation termination. Further, it is important to discern the various roles and functional order of the NMD factors and how termination at a PTC is coupled to accelerated mRNA decay.

2.2.4 Translation termination

Translation termination occurs when the ribosome reaches the end of the coding gene and encounters one of the three stop codons (UAA, UAG or UGA). The stop codons, unlike the sense codons, are not recognized by tRNA but instead by dedicated proteins - the release factors. In prokaryotes, different stop codons are recognized by different release factors. RF1 recognizes UAG and UAA and RF2 recognizes UGA and UAA (Ramakrishnan, 2002). Whereas in eukaryotes, eRF1 recognizes all the three stop codons. Upon stop codon recognition, RFs catalyze hydrolysis of the ester bond between the tRNA and the nascent chain polypeptide in the ribosomal peptidyl transferase centre. Class II RFs (RF3 in prokaryotes and eRF3 in eukaryotes) catalyze the reaction and in prokaryotes help to remove the Class I RFs from the ribosomal A site (Petry, Weixlbaumer, & Ramakrishnan, 2008).

Initially, the crystal structures of the RFs with the ribosome in prokaryotes provided us with insights into understanding the molecular basis of the termination (Klaholz BP et al. 2003, Agarwal RK et al. 2004, Petry S et al. 2005). But the recent advances in electron cryo-microscopy (cryo-EM) lead to a significantly improved mechanistic understanding of translation termination catalyzed by the eukaryotic release factors (A. Brown, Shao, Murray, Hegde, & Ramakrishnan, 2015; Matheisl, Berninghausen, Becker, & Beckmann, 2015). These cryo-EM structures answered the long-standing question of how eRF1 specifically recognizes stop codons.

In eukaryotes the termination reaction requires both eRF1 and eRF3, unlike in prokaryotes. eRF1 recognizes the stop codon and eRF3, a ribosome-dependent GTPase stimulates peptide release. eRF3 strongly induces the peptide hydrolysis by eRF1 whereas GMPPNP (a non-hydrolysable GTP analogue) completely abrogates this function (Alkalaeva, Pisarev, Frolova, Kisselev, & Pestova, 2006) indicating that eRF3 GTPase activity couples stop codon recognition with hydrolysis of peptidyl-tRNA (Salas-marco & Bedwell, 2004).

According to the current model of termination, a stable ternary complex of eRF1-eRF3-GTP binds to the A site of the small ribosomal subunit 40S. After recognition of the stop codon by eRF1, eRF3 hydrolyses GTP to GDP leading to a conformational change which positions the GGQ motif of eRF1 in the peptidyl transferase centre of the large ribosomal subunit 60S (Figure 2.4). The eRF1 GGQ motif positions a water molecule to hydrolyse the nascent polypeptide (Preis et al., 2014; Taylor et al., 2012).

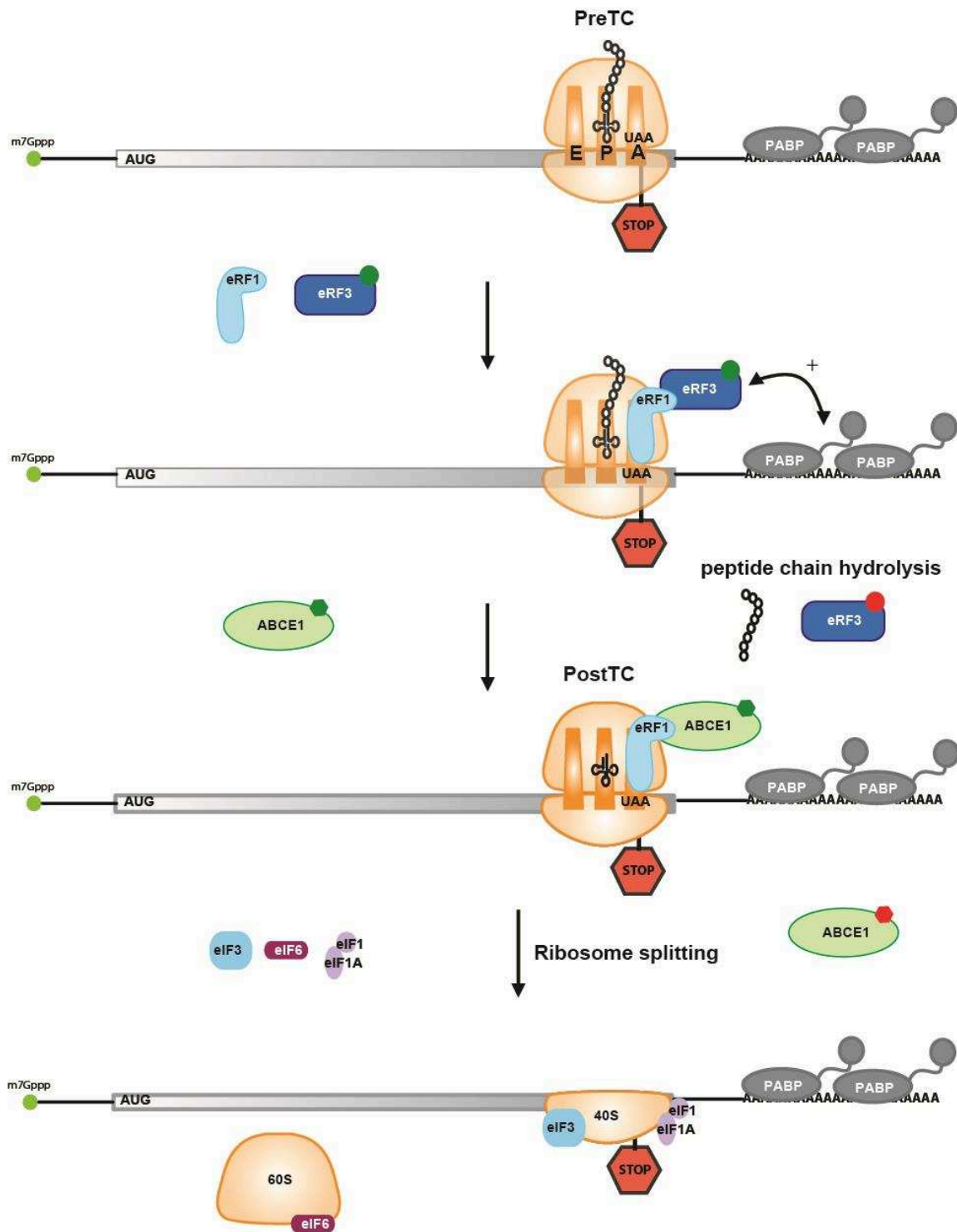


Figure 2.4 Translation Termination:

Termination of the translation occurs when a stop codon (UAA/UAG/UGA) enters the A site of the ribosome. eRF1 and eRF3a are the two release factors: eRF1 recognizes the stop codon and adopts a shape similar to tRNA. eRF3a, a ribosome-dependent GTPase stimulated by GTP hydrolysis, promotes the accommodation of eRF1 in the active site of the large ribosomal subunit and subsequent peptide hydrolysis by eRF1. eRF3a dissociates from the ribosome after peptide release. The dissociation and the recycling of the ribosomes occur with the help of recycling factor ABCE1. The dissociation of mRNA is mediated by eukaryotic initiation factors, which include factors eIF3, eIF3j, eIF6 and eIF1/1A. They also prevent the re-association of ribosomal subunits (green dot represents the GTP/ATP and red dot represents GDP/ADP). Translation termination was suggested to be stimulated further by PABP. Adapted from (Celik, Kervestin, & Jacobson, 2015; He & Jacobson, 2015a)

Once translation termination occurs, eRF3 dissociates from the 80S ribosome. Meanwhile, the ribosomes have to be dissociated so that the components can be recycled for future rounds of translation. The recycling of the ribosomes is mediated by the recycling factors. In eukaryotes, ABCE1 a protein belonging to the ATP-binding cassette (ABC) family of proteins, is the major ribosome-recycling factor. The dissociation of eRF3 after termination is promoted by ABCE1. ABCE1 binds to eRF1-bound postTCs (post-termination complexes) and promotes the splitting of the ribosomes into 60S and 40S subunits with tRNA and mRNA associated (Pisareva et al., 2011). The binding site of ABCE1 overlaps with that of eRF3 and ABCE1-binding is stabilized by the extended conformation of eRF1 (Becker et al., 2012; Preis et al., 2014). Initiation factors eIF3, eIF1, eIF1A and eIF6 help in the recycling process by releasing tRNA and mRNA and preventing the re-association of the ribosomes (He & Jacobson, 2015a; Voigts-Hoffmann, Klinge, & Ban, 2012).

2.2.5 Translation termination at a premature stop codon

When the translation machinery encounters a PTC there are different cues that help the ribosome to differentiate between a normal stop codon and a premature termination codon. Several differences have been observed in the efficiency of translation termination and different models have been proposed based on different studies. However, there is no unified model that can explain the above mentioned observations and the molecular events during translation termination at a PTC (He & Jacobson, 2015a; Karousis et al., 2016; Kurosaki & Maquat, 2016).

When compared to normal translation termination there seems to be a difference in the kinetics and thus efficiency of termination when a PTC is encountered by the ribosome at the A site (Amrani et al., 2004; Ivanov et al., 2008; Singh, Rebbapragada, & Lykke-Andersen, 2008). Inefficient termination is suggested to result in the formation of numerous transient complexes of the terminating ribosome with NMD factors. The major event that marks the mRNA for decay is the hyper phosphorylation of UPF1 by SMG1 kinase (Ohnishi et al., 2003; Okada-Katsuhata et al., 2012; Yamashita, Ohnishi, Kashima, Taya, & Ohno, 2001).

The primary differences that distinguish a PTC from a normal termination codon (NTC) are the presence of exon junction complex (EJC) in the 3'UTR, a long 3'UTR (>2,000 nucleotides) and the absence of termination-stimulating proteins such as PABP which binds to the poly (A) tail (Celik et al., 2015; He & Jacobson, 2015a; Kervestin & Jacobson, 2012).

The EJC is an important stimulatory factor for NMD. The EJC is a multi-subunit complex that is deposited after splicing on the mRNA in the nucleus, 20-24 nucleotides upstream of an exon-exon junction (Hir, Izaurralde, Maquat, & Moore, 2000). The EJC core consists of four conserved core proteins, which are eukaryotic initiation factor 4AIII (eIF4AIII), RNA-binding motif protein 8A (RBM8A / Y14), mago-nashi homolog (MAGOH) and MLN51 (also know as Barentz/ Btz) (Andersen et al., 2006; Bono, Ebert, Lorentzen, & Conti, 2006). PTCs located >50-55 nucleotides

upstream of a 3' exon-exon junction have been shown to efficiently trigger NMD suggesting that the EJC plays a role for the recruitment of NMD factors (Craig, Ashkan, Yu, & Sonenberg, 1998; Nagy & Maquat, 1998). The EJC complex interacts with the NMD factor UPF3 (Kim, Kataoka, & Dreyfuss, 2001a). Accordingly, when EJC factors are deleted, PTC-containing mRNAs are stabilized (Gehring et al., 2005; Shibuya, Tange, Sonenberg, & Moore, 2004).

2.2.6 EJC dependent/enhanced NMD

This model proposes that the presence of EJC downstream of a PTC acts as a platform for the recruitment of NMD factors and activation of UPF1 thus triggering NMD. During the pioneer rounds of translation EJCs are displaced by the ribosomes from the mRNA. However, when a PTC is encountered, EJCs downstream of the PTC remain associated with the mRNA (Dostie & Dreyfuss, 2002; Gehring, Lamprinaki, Hentze, & Kulozik, 2009; Matsuda, Sato, & Maquat, 2008; J. Zhang, Sun, Qian, Duca, & Maquat, 1998). Inefficient translation termination by the ribosome at the PTC is proposed to lead to the recruitment of UPF1 that interacts with the translation termination factor eRF3a and leads to the formation of a SURF complex (SMG1-UPF1-Release-Factors) (Figure 2.5). SMG1 kinase activity is activated by the UPF2-UPF3 that are bound to the downstream EJC (Chamieh, Ballut, Bonneau, & Le Hir, 2008a; Gehring, Neu-Yilik, Schell, Hentze, & Kulozik, 2003; Hwang, Sato, Tang, Matsuda, & Maquat, 2010; Kim, Kataoka, & Dreyfuss, 2001b; Shibuya et al., 2004; Yamashita et al., 2009). The resulting complex is known as the decay-inducing complex (DECID). Phosphorylation of UPF1 by SMG1 kinase and interaction with UPF2 activates UPF1 helicase and promotes unwinding of mRNA and leads to the recruitment of the factors SMG5, SMG6 and SMG7 resulting in degradation of PTC-containing mRNA (Figure 2.6).

The exact role of an EJC in the 3'UTR in NMD is still unclear as EJC-independent NMD has been shown to occur (Gatfield, Unterholzner, Ciccarelli, Bork, & Izaurralde, 2003; Kerényi et al., 2008; Longman, Plasterk, Johnstone, & Cáceres, 2007; Wen & Brogna, 2010). Recent genome wide analysis shows that ~20% of splicing does not result in deposition of an EJC and ~50% of EJCs bind at non-canonical sites (Singh et al., 2012). Moreover, UPF2-independent and UPF3-independent pathways for NMD have been identified (Chan et al., 2007; Gehring et al., 2005; Huang et al., 2011; Ivanov et al., 2008). Recent studies have shown that NMD targets not only mRNA bound to cap-binding complex (CBC) thus restricting it to pioneer rounds of translation, but also eIF4E-bound mRNAs during subsequent rounds of translation where EJC should have already been displaced by the ribosome (Durand & Lykke-andersen, 2013; Rufener & Mühlemann, 2013) thus questioning the concept of a pioneer round of translation for quality control, indicating that the mRNA is constantly monitored during translation for existence of a

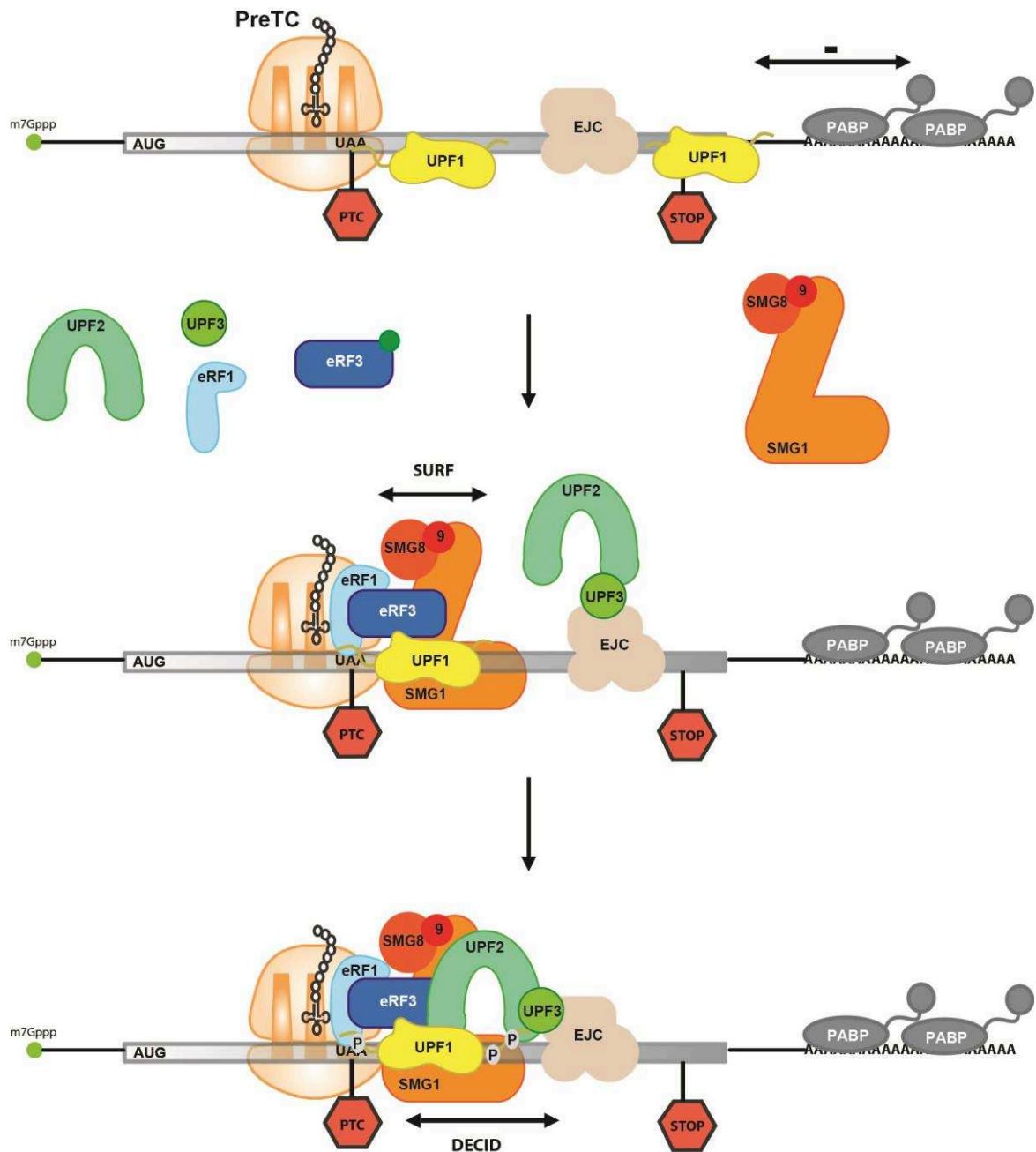
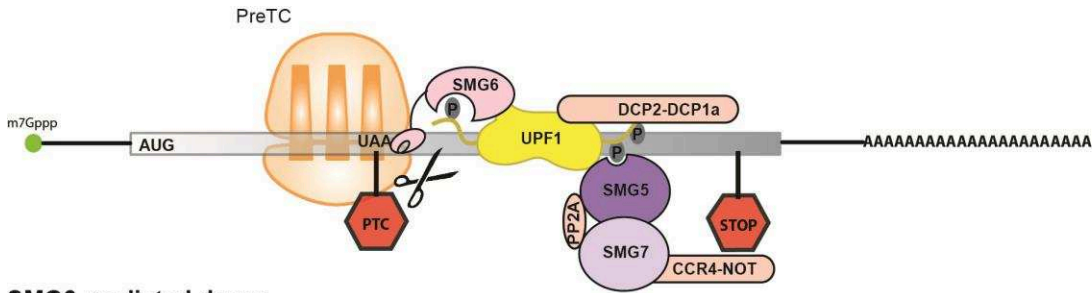
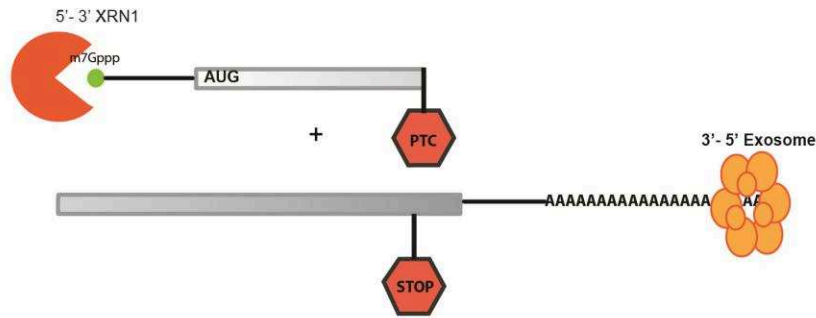


Figure 2.5 Nonsense-Mediated Decay (NMD):

Nonsense-mediated mRNA decay occurs when the mRNA contains a premature termination codon (PTC). NMD activation depends on many factors: Presence of the exon junction complex (EJC) in the 3'UTR of the mRNA and the distance of termination codon (TC) from the poly (A) tail. During normal translation termination the EJC is removed by the translating ribosome. However in case of a PTC the EJC is still present on the mRNA. The pausing of the ribosome at the PTC has been suggested to lead to recruitment of UPF1 rather than binding of PABP. The other NMD factors like UPF2, UPF3 and the SMG1 complex (SMG1C comprising SMG1, SMG8 and SMG9) are recruited thereafter forming the SURF (SMG1-UPF1-Release-Factors) complex. The interaction with UPF2 and UPF3 bound to a downstream EJC leads to the formation of a decay-inducing complex (DECID). SMG1C phosphorylates UPF1 leading to translation termination, remodelling of the mRNP in the 3'UTR and recruitment of SMG6 and SMG5-7, triggering the degradation of the aberrant mRNA. Adapted from (Isken & Maquat, 2007)



SMG6 mediated decay



SMG5-7 mediated decay

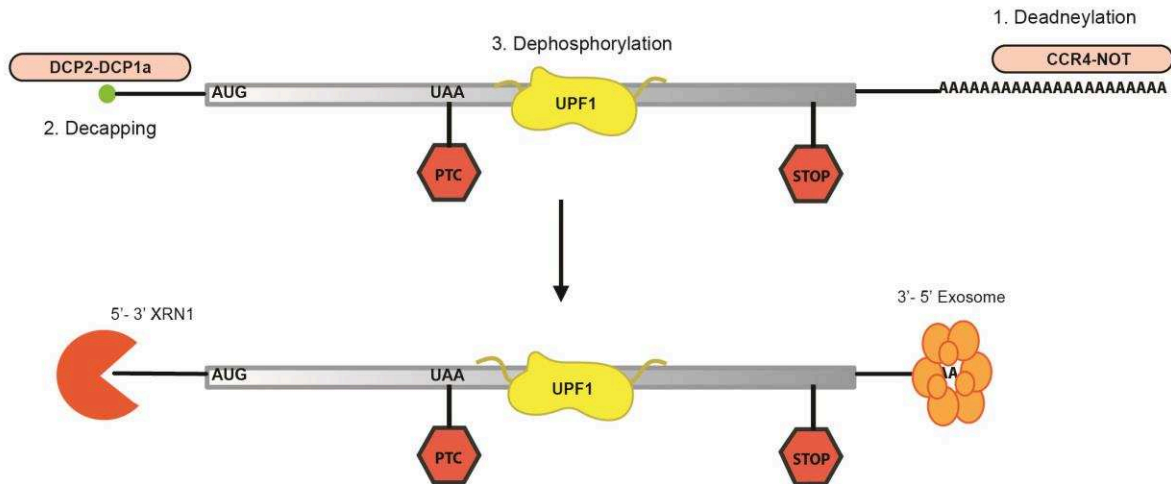


Figure 2.6 Decay of mRNA during NMD:

The aberrant mRNA is recognized by NMD factors UPF1, UPF2 and UPF3 as well as the SMG1C. The important activation step of NMD is the hyper-phosphorylation of UPF1 by SMG1 kinase, which results in remodelling of the 3'mRNP and in the recruitment of the factors SMG6 and SMG5-SMG7. SMG6 recruitment results in endonucleolytic cleavage of the mRNA, followed by rapid 5' to 3' degradation by XRN1 nuclease. The action of exosome results in the 3' to 5' degradation. SMG5-SMG7 recruitment leads to deadenylation of the poly (A) tail by the CCR4-NOT complex and the recruitment of the canonical factors, XRN1 and exosome for further degradation. The SMG5-SMG7 complex also recruits PP2A, which results in the dephosphorylation and recycling of UPF1. UPF1 interaction with the decapping complex DCP2-DCP1a results in the decapping of the mRNA, which subjects the mRNA to various exonucleases. Adapted from (Schweingruber, Rufener, Zünd, Yamashita, & Mühlemann, 2013).

PTC. In yeast, CBC and eIF4E-associated mRNAs are targeted similarly (Gao, Das, Sherman, & Maquat, 2005).

2.2.6.1 3'UTR EJC-independent NMD/ Faux-UTR model

This model was originally proposed for yeast NMD (Amrani et al., 2004). The model suggests that mRNAs with PTCs have longer 3'-UTRs compared to mRNAs with NTCs (Buhler, Steiner, Mohn, Paillusson, & Mühlemann, 2006; Mühlemann, Eberle, Stalder, & Zamudio Orozco, 2008). The longer 3'UTR physically separates the 3' poly (A) tail and its interacting protein PABP from the terminating ribosomes.

In case of PTCs, PABP cannot interact with release factors due to the long distance between the terminating ribosome and the poly (A) tail. Thus it cannot stimulate termination. This change in kinetics results in a slower termination process and may help in the recruitment of UPF1 and the formation of the SURF complex in mammals (Behm-Ansmant et al., 2007; Kertesz et al., 2006; Singh et al., 2008). It was shown that PABP tethering to the downstream 3'UTR close to the PTC or shortening of the distance between the PTC and the poly (A) tail inhibits NMD (Amrani et al., 2004; Eberle, Stalder, Mathys, Orozco, & Mu, 2008; Ivanov et al., 2008; Kervestin & Jacobson, 2012; Liebhaber, Silva, Roma, & Lui, 2008). On the contrary, when the mRNAs 3'UTR is artificially elongated, NMD is triggered (Muhlrad & Parker, 1999).

This model does not explain several observations: how can mRNAs lacking a poly (A) tail be still subject to NMD (Shen et al. 2015) and how can several mRNAs with long 3'UTRs evade NMD (LeBlanc et al. 2004, Quek et al. 2014). In the latter, case there appears to be specific cis-acting elements downstream of the termination codon in the 3'UTR that counteract NMD activity (Withers & Beemon, 2010).

2.3 Important factors involved in NMD

2.3.1 Release factors

The initial knowledge on translational termination was gained from studying the termination in prokaryotes. In prokaryotes, RF1 and RF2 enter the decoding centre to recognize the stop codon in the small ribosomal subunit (Ito, Uno, & Nakamura, 2000). Sequence and mutational studies have shown that the GGQ motif located in domain 3 of RF1 and RF2 mediates the peptide bond hydrolysis in the large ribosomal subunit (L. Y. U. Frolova, Merkulova, & Kisselev, 2000). The highly conserved GGQ loop is surrounded by conserved bases of the peptidyl transferase centre and its placement causes rRNA molecules to rearrange and a water molecule to enter the active site (Shaw & Green, 2007; Youngman, Brunelle, Kochaniak, & Green, 2004). The nucleophilic attack by the water molecule leads to the hydrolysis of the peptidyl-tRNA ester bond. Following

peptide hydrolysis RF3 binds the ribosome and catalyzes the removal and recycling of RF1/RF2 (Klaholz, Myasnikov, & Heel, 2004).

In eukaryotes, eRF1 consists of three domains. The N-terminal domain (N domain) contains the TASNKS, GTS and YxCxxxF motifs that recognize the stop codon (Bertram, Bell, Ritchie, Fullerton, & Stansfield, 2000; A. Brown et al., 2015; Conard et al., 2012; Matheisl et al., 2015; Song et al., 2000).

The M domain contains the conserved GGQ motif that is responsible for peptide hydrolysis. The C-terminal domain (C domain) mediates the interaction with eRF3 and with the ribosome-recycling factor ABCE1 (Korostelev, 2011). In mammals, there are two types of eRF3s: eRF3a and eRF3b, with slight differences in their N-terminal regions (Chauvin et al., 2005). eRF3 is a ribosome dependent GTPase which stimulates the peptide hydrolysis by eRF1. eRF3a consists of a N-terminal domain (1-138aa) that has been shown to interact with PABP but is not essential for the termination reaction *per se*.

The N-terminal domain is followed by the G domain (GTPase domain) and two β -barrel domains: domain 2 and 3. Domain 3 interacts with the domain C of eRF1 mainly through hydrophobic contacts (Cheng et al., 2009b).

The structure of the complex between eRF1 and eRF3a was solved initially using crystallographic techniques and later using cryo-EM (A. Brown et al., 2015; Cheng et al., 2009b; Matheisl et al., 2015).

In the recent high resolution cryo-EM structures, eRF1 was found to be in an extended conformation and the domains (N, M, C) were moved relative to one another when compared to the crystal structures. The mRNA was compacted to incorporate four nucleotides instead of three at the decoding centre of 40S. This mRNA compaction has been suggested to protect one or two additional nucleotides of the mRNA. In toe-printing assays (the equivalent to DNA foot-printing for mRNA), this results in a one- or two-nucleotide shift from pre-termination complexes to post-termination complexes where the stop codon is recognized by eRF1 (Alkalaeva et al., 2006). The NIKS motif located at the end of helix 2 imposes the specificity for uridine at the +1 position. The YxCxxxF motif helps in the stacking of the +2 and +3 bases which results in decoding them as one unit (A and G) and adding specificity for the purines at these positions. (Brown et al., 2015; Matheisl et al., 2015). The cryo-EM structures of eRF1 in complex with eRF3 in the pre-GTP hydrolysis state showed an interaction between the eRF1 domain M and the eRF3a G domain. The GGQ motif is positioned far from the active centre (Brown et al., 2015; Matheisl et al., 2015). Therefore, it has been postulated that GTP hydrolysis by eRF3 positions the GGQ motif into the peptidyl transferase centre.

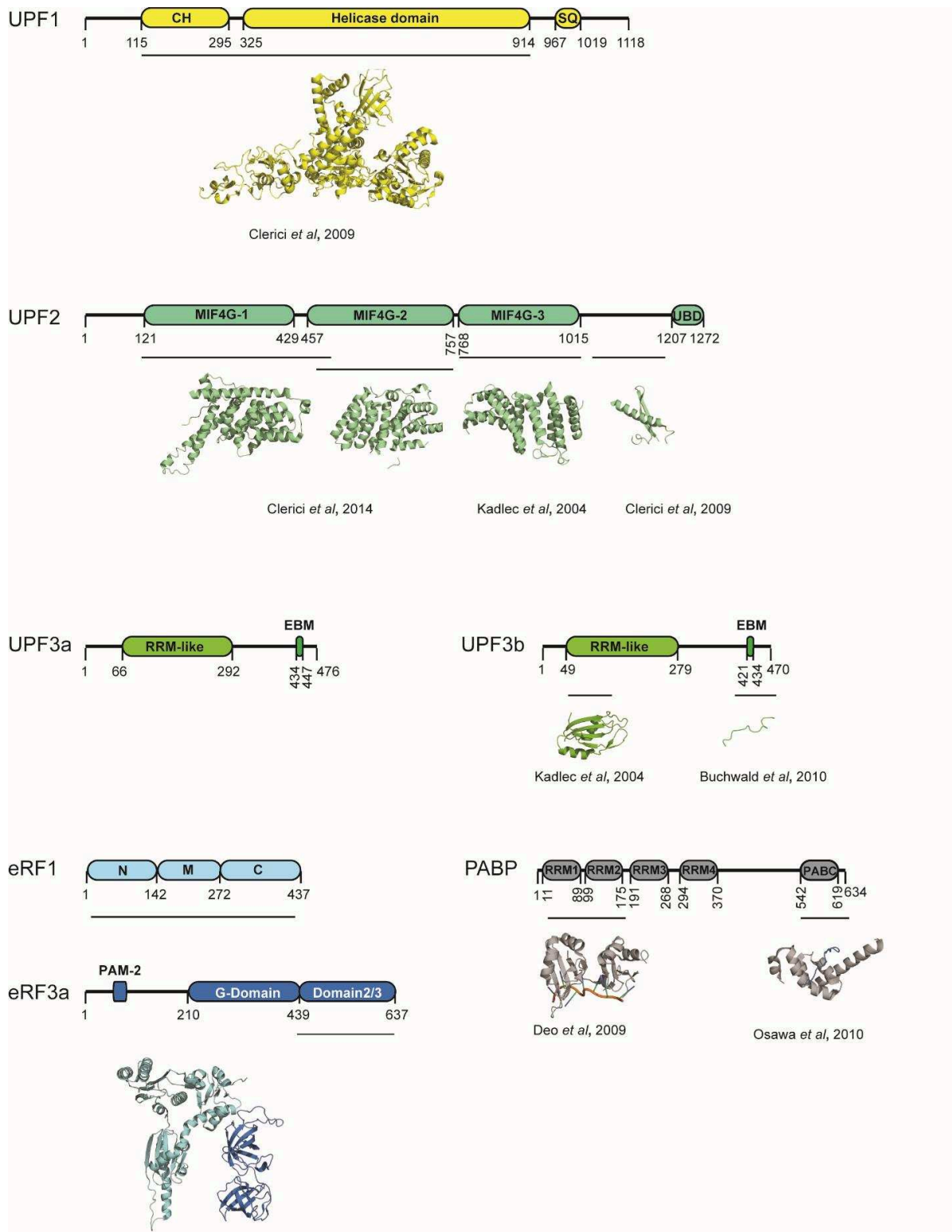
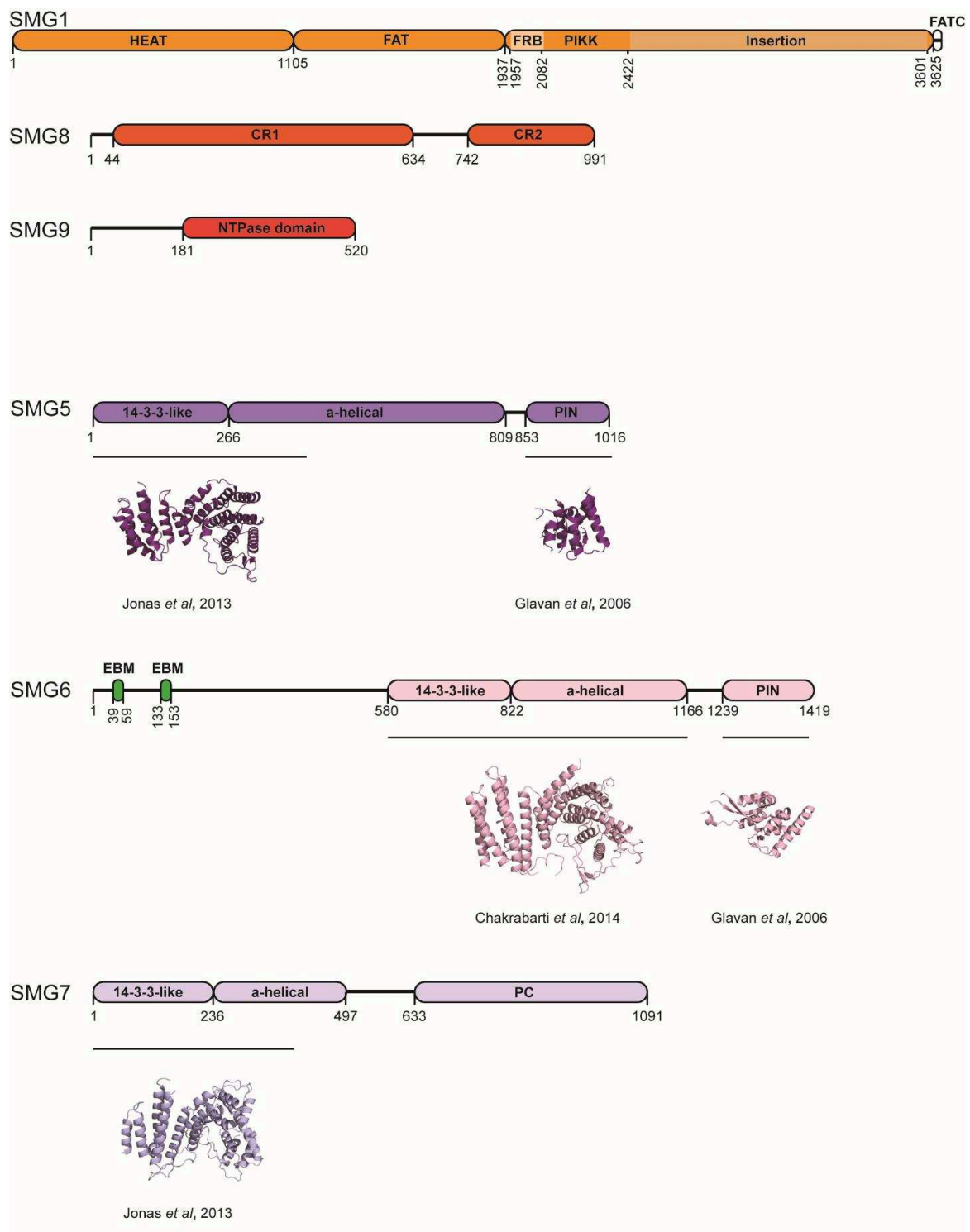


Figure 2.7 Schematic representation of the important factors involved in NMD in mammals:

Crystal structures are shown for proteins/domains where available. All proteins are drawn to the same scale except for SMG1. CH: cysteine-histidine rich domain; SQ: serine-glutamine rich domain; MIF4G: middle of 4G-like domains; UBD: UPF1-binding domain; RRM: RNA recognition motif; EBM: exon junction binding motif; N: N-terminal domain; M: Middle domain; C: C-terminal domain; PAM-2: PABP-interacting motif 2; G-domain: GTPase domain; PABC: PABP C-terminal region;



HEAT: Huntingtin, elongation factor 3 (EF3), protein phosphatase 2A (PP2A), yeast kinase TOR1 domain;
 FAT: focal adhesion kinase domain; PIKK: phosphatidylinositol 3-kinase-related protein kinase domain;
 FATC: C-terminal FAT domain; PIN: PiT N-terminus domain; PC: C-terminal proline- rich region.
 Adapted from (Karousis et al., 2016).

2.3.2 SMG (Suppressor with Morphogenetic effect on Genitalia) proteins

Genetic studies in *C. elegans* showed that there are seven *smg* genes which encode for factors involved in NMD (Cali, Kuchma, Latham, & Anderson, 1999; Hodgkin, Papp, Pulak, Ambrost, & Anderson, 1989; Pulak & Anderson, 1993).

2.3.2.1 Upstream factors (SMG1, SMG8, SMG9)

The gene encoding *smg1* was first identified in *C. elegans* and was found to encode a phosphatidylinositol 3-kinase (PIK)-related protein kinase (PIKK). The homolog of SMG1 does not exist in yeast. In humans SMG1 was identified by Yamashita et al. in 2001. SMG1 kinase phosphorylates the SQ motifs in C-terminus of human UPF1. SMG8 and SMG9 tightly associate with SMG1 resulting in the formation of the SMG1 complex (SMG1C). SMG8 negatively regulates the SMG1 kinase activity (Yamashita et al., 2009).

Human SMG1 is a 410 kDa protein belonging to the phosphatidylinositol 3-kinase (PIK) related protein kinase (PIKK) family, which are serine-threonine kinases and phosphorylate S/TQ motifs. The other proteins that belong to the PIKK family are ATM, ATR, DNA-PKcs, mTOR, and TRAPP. All proteins of the PIKK family share a similar architecture: a conserved N-terminus consisting of HEAT repeats is followed by a FAT (FRAP/TOR, ATM, and TRRAP) domain, the conserved kinase domain (PI3K) and a C-terminal FATC domain (FAT C-terminal). SMG1 presents an exception to this architecture as it contains an insertion domain of >1,000 amino acids between the PI3K and FATC domains. The insertion is poorly characterized. Recently, it was shown to play an important role in the regulation of SMG1 kinase activity in conjunction with SMG8 and SMG9 (Deniaud et al., 2015). Human SMG8 is a 110 kDa protein and SMG9 has a molecular weight of 58 kDa. It has been shown that the C-terminal region of SMG8 interacts with SMG9, independent of SMG1. Moreover, SMG9 contains a putative NTPase domain and can form homodimers (Fernandez et al., 2011).

SMG1 plays an important role in triggering NMD by interacting with UPF1, UPF2 and DHX34 as well as RUVBL1/2 (Izumi et al., 2010). UPF1 phosphorylation by SMG1 kinase is considered to be a key event that targets the mRNA for degradation.

The EM structure of SMG1 revealed that the protein adopts an S-shape with the C-terminal region forming the head and the N-terminal region forming the tail. SMG8 and SMG9 interact with the N-terminal region. It is interesting to note that even though SMG8 interacts with the N-terminal, it has an effect on the catalytic activity of SMG1 that is located in the head region. It has been shown that binding of SMG-8 results in an overall conformational change that affects the activity of SMG1 (Arias-Palomo et al., 2011).

More light has been shed recently on UPF1 phosphorylation by the SMG1C, being the key step of NMD (Deniaud et al., 2015). UPF1 binds near the head domain of SMG1, resulting in the

displacement of C-insertion domain. This insertion domain acts as a scaffold for SMG8 and SMG9 which together with the insertion domain regulate substrate binding and phosphorylation (Deniaud et al., 2015). Moreover, it has also been shown that UPF2 binds to SMG1 in an UPF1-dependent manner and interacts with the FRB domain of SMG1 (Melero et al., 2014).

More recently, the protein DHX34 (DEAH box protein 34) has been shown to activate UPF1 phosphorylation by SMG1 (Hug & Cáceres, 2014) by changing the pattern of interactions between NMD factors that typically lead to NMD activation. DHX34 acts as a scaffold to recruit UPF1 to SMG1 by directly binding SMG1 kinase through its C-terminal domain (López-Perrote et al., 2016).

2.3.2.2 Downstream factors (SMG5, SMG6 and SMG7)

Once the UPF1 is hyperphosphorylated by SMG1, the NMD factors SMG5, SMG6, and SMG7 are recruited by UPF1 to the mRNA thus triggering the decay of the aberrant mRNA (Ohnishi et al., 2003; Okada-Katsuhata et al., 2012). All three factors contain a 14-3-3 like domain that is formed by nine antiparallel α helices (Fukuhara et al., 2005). SMG5 and SMG6 additionally comprise a PIN domain at their C-terminal end which is similar to the RNaseH family ribonucleases. The PIN domain confers endonuclease activity to these proteins. However, SMG5 is an inactive endonuclease as it lacks the canonical motif for nuclease activity (Glavan, Behm-ansmant, Izaurralde, & Conti, 2006).

Different mechanisms appear to coexist in mammals that cooperate or complement each other to ensure the rapid degradation of NMD targets (S. Lykke-Andersen & Jensen, 2015). SMG6 cleaves mRNA endonucleolytically and the cleaved mRNA substrates are further degraded by XRN1 and the exosome (Boehm et al., 2014; Eberle, Lykke-Andersen, Mühlemann, & Heick Jensen, 2009; Gatfield et al., 2003; Huntzinger, Kashima, & Fauser, 2008). SMG5 and SMG7 recruitment results in a decapping-dependent exonucleolytic cleavage of mRNA. Recent studies indicate that SMG6-mediated mRNA degradation is the major pathway for decay (S. Lykke-andersen et al., 2014; S. A. Schmidt et al., 2015) (Figure 2.6).

The 14-3-3-like domains of SMG5 and SMG7 interact with each other to form a heterodimer (Jonas, Weichenrieder, & Izaurralde, 2013). The SMG5-SMG7 heterodimer interacts with the phosphorylated serine residues at the C-terminus of UPF1 (Loh, Jonas, & Izaurralde, 2013; Okada-Katsuhata et al., 2012). SMG5-SMG7 also interacts with protein phosphatase 2A (PP2A) which is responsible for the dephosphorylation of UPF1 and thus recycles UPF1 for future rounds of NMD (Okada-Katsuhata et al., 2012). The proline-rich C-terminal region of SMG7 can additionally interact with POP2 (CNOT8), the catalytic subunit of the CCR4-NOT deadenylase complex (Loh et al., 2013), resulting in deadenylation-dependent decapping and 5' to 3' decay of mRNA followed by XRN1-mediated degradation.

SMG6 interacts with UPF1 either in a phosphorylation-dependent or in a phosphorylation-independent manner, triggering mRNA decay. In the phosphorylation-dependent mechanism, SMG6 interacts with phospho-T28 of UPF1. In the phosphorylation-independent mechanism, the N-terminus of SMG6 interacts with the UPF1 helicase domain and the C-terminal end of UPF1 (Chakrabarti, Bonneau, Sch, & Eppinger, 2014; Nicholson, Josi, Kurosawa, Yamashita, & Mühlemann, 2014). It is interesting to note that SMG6 can also interact with EJC. The N-terminal region of SMG6 consists of two conserved EJC-binding motifs (EBMs) that interact with the same EJC proteins as UPF3B (Kashima et al., 2010).

UPF1 has also been shown to associate with the decapping complex subunits DCP1A, DCP2, and PNRC2 which results in deadenylation-independent decapping (Cho, Kim, & Kim, 2009; Lai et al., 2012). PNRC2 forms the bridge between the UPF1 and the decapping complexes by interacting directly with DCP1A and UPF1. PNRC2 has recently been shown to interact with SMG5 as well (Cho et al., 2013).

2.3.3 Up-Frameshift Proteins (UPFs)

The cross talk between the terminating ribosome and the EJC is mediated by the trans-acting factors UPF1 (also known as SMG2 and RENT1), UPF2 (also known as SMG3) and UPF3 (also known as SMG4). The three UPF proteins (UP-Frameshift proteins) UPF1, UPF2 and UPF3 constitute the core NMD machinery as they are conserved from yeast to humans (He et al., 1997; Lykke-Andersen, Jens, 2000). The UPF proteins were identified initially by using genetic screens in yeast (Leeds, Peltz, Jacobson, & Culbertson, 1991).

2.3.3.1 UPF1

UPF1 is a ~125kDa RNA-binding protein which comprises functions both as a RNA helicase and as an ATPase. UPF1 belongs to the RNA superfamily 1 (SF1) helicases that use ATP hydrolysis to rearrange the RNA-protein complexes or nucleic acids. UPF1 contains a cysteine-histidine-rich (CH) domain at its N- terminus, two recombinase A (RecA)-like domains with an ATP-binding site in the helicase domain which is located in the centre and forms the major part of the protein, followed by the serine- and glutamine-rich (SQ) region at its C-terminus (Bhattacharya et al., 2000; Chakrabarti et al., 2011; Yamashita, 2013). SMG1 kinase phosphorylates the SQ motifs in the C-terminal region and Threonine 28 in the N-terminus of UPF1.

The structural information of UPF1 is derived from crystal structures of its domains. In the absence of UPF2, UPF1 exists in its closed conformation where the N-terminal CH domain packs against the two RecA-like domains to inhibit UPF1's ATPase/helicase activity (Chakrabarti et al., 2011). UPF2 interacts with the CH domain of UPF1, leading to an open conformation, which is due to the large conformational change in the CH domain. This leads to the activation of the

helicase activity of UPF1 (Clerici et al., 2009) resulting in unwinding of RNA. UPF1 requires both its ATPase activity and ATP dependent 5' to 3' helicase for NMD as mutations that affect this activity abolish / reduce NMD (Franks, Singh, & Lykke-andersen, 2010; Weng, Czaplinski, & Peltz, 1996). It has been shown that UPF2 and UPF3B cooperatively stimulate the ATPase and helicase activity of UPF1 (Chamieh et al., 2008a). UPF1 also associates with ribosomes by interacting with ribosomal protein Rps26 and eukaryotic release factors (eRFs) (Kashima et al., 2006; Min, Roy, Amrani, He, & Jacobson, 2013). This led to the proposal that UPF1 recognizes terminating ribosomes at a PTC.

2.3.3.2 UPF2

UPF2 is a 148 kDa RNA-binding protein comprising of three conserved MIF4G (middle domain of translation initiation factor 4G) domains. The structures of MIF4G-1 and MIF4G-2 domains as well as the structure of the MIF4G-2 and MIF4G-3 domains were solved by X ray crystallography (Clerici et al., 2009, 2014). EM studies revealed that full-length UPF2 has an U-shape (Melero et al., 2012a). MIF4G-3 interacts with UPF3B as revealed by the crystal structure of MIF4G-3 bound to the RRM (RNA-recognition motif) domain of UPF3b (Kadlec, Izaurralde, & Cusack, 2004). UPF2 links UPF1 and UPF3B (Chamieh et al., 2008a). However, it has also been shown that the interaction between UPF2 and UPF3B is not essential for all NMD substrates and that an UPF2-independent

NMD branch exists (Gehring et al., 2005, 2003). UPF2 has the potential to interact with several factors required for NMD, including eRF3 at the ribosome, UPF3B at the EJC, as well as UPF1 and SMG1 kinase (Kadlec et al., 2004; López-Perrote et al., 2016; Melero et al., 2012a, 2014). The C-terminus of UPF2 including the MIF4G-3 domain has been shown to interact with eRF3a (Lopez-Perrote et al. 2016). It is unlikely that UPF2 can engage in these interactions simultaneously. Likely, UPF2 is involved in several transient complexes with changing composition during NMD.

2.3.3.3 UPF3

UPF3 is a ~58 kDa protein and is found predominantly in the nucleus (Serin, Gersappe, Black, & Aronoff, 2001). Two paralogues of UPF3 exist in humans, UPF3B and UPF3A. Both contain a N-terminal RRM domain that has been shown not to interact with RNA as it lacks the high abundance of aromatic amino acids (Kadlec et al., 2004). Instead the RRM is required for UPF3's interaction with UPF2. The C-terminus of UPF3 comprises EJC-binding motif (EBM), which interacts with the surface formed by eIF4AIII, MAGO and Y14 of the EJC (Buchwald et al., 2010).

The gene encoding UPF3B resides on the X chromosome whereas that for UPF3A on chromosome 13 in humans. One of the reasons why two paralogs of UPF3 exist, may be that the X chromosome is inactivated during spermatogenesis in many vertebrates. UPF3B is a well-studied NMD factor compared to UPF3A. UPF3A is upregulated in the cell when UPF3B is knocked-down (L S Nguyen et al., 2012). It is interesting to note that upon UPF3B knockdown the protein UPF3A is stabilized but not its mRNA. Mutations in the UPF3B gene are linked to autism, schizophrenia and X-linked intellectual disabilities (Alrahbeni et al., 2015a; Tarpey et al., 2007) indicating an important role of UPF3B in neurodevelopment.

UPF3A has two isoforms: UPF3AL and UPF3AS (containing exon 4 or not) (Lykke-Andersen et al 2000). UPF3a is less efficient in triggering NMD when compared to UPF3B (Kunz, Neu-Yilik, Hentze, Kulozik, & Gehring, 2006) and recently, UPF3A even was shown to have an antagonistic function in NMD by stabilizing several mRNA substrates (Shum et al., 2016).

2.3.4 Poly (A) binding protein (PABP)

PABP is a RNA-binding protein and has an important role in translation control. PABP interacts with the initiation factor eIF4G (part of the eIF4F complex) (Kahvejian, Svitkin, Sukarieh, Boutchou, & Sonenberg, 2005), with the termination factor eRF3a and with the two PABP-interacting proteins (PAIP) (Derry, Yanagiya, Martineau, & Sonenberg, 2006). Moreover, PABP interacts with non-protein-coding RNAs (npcRNAs) to regulate the translation (Khanam, Muddashetty, Kahvejian, Sonenberg, & Brosius, 2006a; H. Wang et al., 2005).

In vitro studies demonstrated an interaction of the PAM2-2 domain in the N-terminal part of eRF3a with the C-terminal domain of PABP (Khanam et al. 2006, Kozlov et al. 2010). It has also been shown that PABP stimulates translation termination at a PTC when tethered close to the stop codon (Ivanov et al., 2008; Silva & Romão, 2009; Singh et al., 2008).

Cytoplasmic PABP stabilizes the mRNA (Bernstein, Peltz, & Ross, 1989). It protects the mRNA from 3' to 5' endonucleases (Derry, M. C, Yanagiya A, 2006; Grange Thierry, Martins de Sa Cezar, 1987). The N-terminus of PABP consists of four conserved RNA-recognition motifs (RRMs) (Burd, Matunis, & Dreyfuss, 1991), whereas the C-terminus consists of an unstructured proline-rich sequence followed by a structured MLLE domain (Kozlov, Gehring, & Kursula, 2010). RRM1 and 2 constitute one functional unit and 3 and 4 the second unit (Deo, Bonanno, Sonenberg, & Burley, 1999). The first two RRM1s have the highest affinity for poly (A). The minimum length that is required for their binding are 12 adenosines (Kühn & Pieler, 1996; Sachs & Davis, 1989) whereas RRM3 and 4 interact with poly (A) and also other RNA sequences (Burd et al., 1991; Deo et al., 1999; Khanam et al., 2006a).

The RRM domain is composed of four β -strands two α -helices assembled in a globular domain shaped as a four-stranded antiparallel β -sheets flanked with two α -helices (Deo et al., 1999). The MLLE domain recognizes and binds to the PABP-interacting motif 2 (PAM2) (Kozlov et al.,

2004) that has been identified in several PABP-interacting proteins such as PAIP1, PAIP2, eRF3a and the deadenylase complexes PAN2-PAN3 and Caf1-Ccr4 (Cosson et al., 2002; Craig et al., 1998; Hoshino, Imai, Kobayashi, Uchida, & Katada, 1999; Kashima et al., 2006; Khaleghpour et al., 2001). Unlike other PAM2-containing proteins, eRF3a comprises two overlapping PAM2 motifs, which independently bind to the MLL domain of PABPC with a low affinity. However, together they bind with increased affinity (Kononenko et al., 2010). The dissociation constant (K_d) between eRF3a and PABP has been determined to be in the micromolar range (Jerbi, Jolles, Bouceba, & Jean-jean, 2016; Kozlov et al., 2004). The structure of the interacting region was solved by NMR and crystallography (Kozlov et al., 2010; Osawa et al., 2012). The structures show that Phe76 is shared between the two PAM motifs and explains why both the motifs are necessary for high affinity-binding to PABP.

2.4 Importance of NMD factors

Knockout experiments of NMD factors show that these factors are essential for mammalian development. UPF3B deletion with shRNA (short hairpin RNA) affects neuronal development and several UPF3B mutations were reported to lead to mental retardation in the affected families (Addington et al., 2011; Alrahbeni et al., 2015b; Jolly, Homan, Jacob, Barry, & Gecz, 2013a; Tarpey et al., 2007). UPF1, UPF2 and SMG1 deletion in mice results in embryonic lethality and shows severe development defects (Mcilwain et al., 2010; Weischenfeldt et al., 2008). SMG5 and SMG6 deletion leads to similar developmental defects as UPF1 deletion (Wittkopp et al., 2009). Similarly, the loss of functional SMG9 results in multiple congenital anomaly syndrome in humans and leads to abnormal embryogenesis in mice (Shaheen et al., 2016).

As mentioned above, UPF3B is widely expressed in neurons and is an important protein in neuronal development. Transcriptome analysis revealed that ~5% of the human transcriptome is impacted in UPF3B patients (L S Nguyen et al., 2012). Mutations in the gene encoding UPF3B leads to neurodevelopmental disorders which include X-linked intellectual disability (XLID), Schizophrenia and autism which lead to mental retardation, apart from other disorders such as Lujan-Fryns and FG syndrome (Szyszka et al., 2012). UPF3B depletion in cultured neuronal cells was found to affect the expression of NMD targets, to change neurite growth and to reduce differentiation of neuronal progenitor cells (Jolly, Homan, Jacob, Barry, & Gecz, 2013b). The UPF3B mutations that lead to mental retardation, autism and schizophrenia generally are nonsense as well as missense mutations both leading to loss of UPF3B expression. The different nonsense mutations that have been identified are Arg225, Gln228, Arg233, Arg361 and Arg430 (Addington et al., 2011; Alrahbeni et al., 2015a; Laumonnier et al., 2010). The missense mutations that have been identified are Tyr160, Arg255, Arg355 and Arg366 (location based in respect to isoform 2 of UPF3B). The mutations generally affect the activity of UPF3B in NMD as evidenced by increased mRNA levels of NMD substrates (Alrahbeni et al., 2015a).

Interestingly it was discovered that deletions of the gene encoding UPF2 in humans leads to similar effects as UPF3B depletion, also causing intellectual disability. The genes that are deregulated when UPF2 is deleted are similar to the ones upon UPF3B depletion. The same study also revealed that UPF3A, SMG6, eIF4A3, RBM8A and RNPS1 are frequently deleted and/or duplicated in these patients (Nguyen et al., 2013).

2.5 Scope of the thesis

Nonsense mediated mRNA decay (NMD) is an important eukaryotic quality control mechanism that recognizes and degrades the mRNA containing a premature termination codon (PTC). The long-standing question in the field has been how a normal termination codon (NTC) is discriminated from a premature termination codon. Current models are based mostly on data from *in vivo* experiments (pull down assays and mutational analyses) and structural information of the complexes involved in NMD is very limited. *In vitro* experiments often used truncated proteins that could be produced as recombinant proteins in *E. coli*. A better understanding of the molecular mechanism of the events at a terminating ribosome leading to recruitment and assembly of the NMD machinery on mRNA with a PTC is required in order to facilitate the development of novel therapeutic strategies for the treatment of PTC-associated diseases.

We have shown that poly (A) binding protein (PABP) stimulates translation termination while Up-frameshift protein (UPF1) inhibits translation termination *in vitro*. The aim of my thesis is to achieve a detailed molecular understanding how the factors PABP and UPF1 modulate translation termination. In order to answer the questions, we used a reconstituted eukaryotic *in vitro* translation system to generate translating ribosomes stalled at a stop codon (PreTC) and we reconstituted termination complexes by addition of purified eukaryotic release factors, PABP or UPF proteins. Full-length factors eRF3a, UPFs and PABP were produced in insect cells. The first section of the thesis focuses on the structural characterization of purified PreTCs with release factors (eRF3a and eRF1) and PABP. We have solved the cryo-EM structure of termination complexes in the presence of UPF1. Moreover, we have studied the role of NMD factors UPF2 and UPF3B in translation termination using peptide release and toe-printing assays. We found that UPF3B interacts with eRF3a and it delays the stop codon recognition and promotes ribosome dissociation. The second section of my thesis focuses on the SMG1C kinase complex. As phosphorylation of UPF1 by SMG1 kinase is required to trigger NMD, regulation of SMG1 activity is a central part of the NMD pathway. We have discovered novel interaction between UPF3B and the SMG1C kinase and additionally that the phosphorylation of UPF1 is affected in the presence of UPF3B. Biochemical and biophysical experiments showed a direct interaction between UPF3B and the SMG1C kinase complex, indicating a new layer of regulation of the NMD pathway.

3 Biochemical and structural characterization of the effect of PABP on mammalian translation termination

Résumé en français

La terminaison de la traduction est un processus hautement régulé qui fait intervenir les facteurs de terminaison eRF1 et eRF3. Il a été montré que l'interaction de eRF3 avec la poly (A) binding protein (PABP) stimule l'arrêt de la traduction, cependant le mécanisme moléculaire régissant ce processus demeure inconnu. Cette étude s'intéresse ainsi à comprendre l'effet de PABP sur la terminaison de la traduction en mettant en œuvre des méthodes biochimiques et de cryo-microscopie électronique (cryo-EM). Plus particulièrement, un système complet de traduction in vitro a été mis en place, de même qu'un protocole de purification des complexes de pré-terminaison (PreTCs). L'interaction entre ces PreTCs et un complexe préformé de PABP, eRF3a and eRF1AGQ a ensuite pu être caractérisée par cryo-microscopie électronique.

3.1 Abstract

Translation termination is a highly regulated process in eukaryotes. Release of the nascent polypeptide chain at the ribosome occurs with the help of eukaryotic release factors eRF1 and eRF3. We have shown that interaction of eRF3 with the poly (A) binding protein (PABP) stimulates translation termination *in vitro*. However, the exact molecular mechanism of this process is unknown. The main aim of my study was to understand how PABP affects translation termination using biochemistry and electron cryo-microscopy (Cryo-EM). To this end, a reconstituted human *in vitro* translation system was established in the lab along with an efficient protocol to purify pre termination complexes (PreTCs). These PreTCs consists of translating / elongating ribosomes stalled at a stop codon. A performed complex between PABP, eRF3a and eRF1AGQ was added to the purified PreTCs to form a termination complex. The complexes were characterized by cryo-EM to solve a structure of the terminating ribosome in the presence of PABP and thus rationalize the stimulatory effect of PABP on translation termination.

3.2 Introduction

Translation termination in eukaryotes occurs with the help of the release factors eRF1 and eRF3. eRF1 recognizes the stop codon in the A site of the ribosome and catalyzes the peptide hydrolysis whereas eRF3, a GTPase helps in the stimulation of the peptide hydrolysis. When a complex between eRF1, eRF3 and GTP is formed, structural rearrangement of the factors and the translocation of the ribosome occurs (Kononenko et al., 2010). Complex formation between eRF1 and eRF3, promotes GTP binding to eRF3 (Hauryliuk, Zavialov, Kisselev, & Ehrenberg, 2006; Pisareva, Pisarev, Hellen, Rodnina, & Pestova, 2006).

eRF3 has been shown to interact with poly (A) binding protein (PABP) and UPF1. Interaction with PABP has been shown to stimulate translation termination and the interaction with UPF1 to inhibit termination or enhance NMD (Hoshino et al., 1999; Ivanov et al., 2008; Kashima et al., 2006; Singh, Rebbapragada, & Lykke-Andersen, 2008). An interaction between eRF3a and PABP was first shown by Hoshino et al. in 1999, *in vitro* and Cosson et al. in 2002, *in vivo*. The conserved N-terminus PABP binding motif 2- 2 (PAM2-2) domain of eRF3a interacts with the C terminal domain of PABP (Khanam et al., 2006; Kozlov et al., 2010). PABP was known to stimulate translation termination *in vivo*. But the molecular mechanism of how PABP stimulates translation termination is unknown.

The aim of the study was to gain an in depth understanding of how PABP affects translation termination and stimulates termination. Pre termination complexes (PreTCs) were reconstituted and purified and the effect of PABP on translation termination was studied using electron cryo-microscopy (Cryo-EM). To this end, a reconstituted human *in vitro* translation system was established in the lab along with an efficient protocol to purify the PreTCs. Purified PABP along

with eRF3a and eRF1AGQ was added to the purified PreTCs and the sample was used for single particle analysis using cryo-EM.

3.3 Results

3.3.1 Reconstitution of the in vitro translation system

We decided to establish a reconstituted in vitro translation system in order to obtain ribosomal complexes at defined stages during translation. Reconstitution of translation in vitro allows studying ribosomal complexes stalled during initiation, elongation, termination or recycling by adding a defined set of translation factors such that translation can proceed only to a certain stage. The subsequent translational step then can be studied in detail in vitro by addition of the required factors and/or additional factors, which are implicated to impact or regulate translation. Moreover, the reconstituted translation system allows preparing defined, homogeneous sample for structural studies.

To reconstitute mammalian in vitro translation many components of the translational apparatus are required. The major components required are: (A) mRNA (B) 40S and 60S ribosomes (C) aminoacylated tRNAs (D) initiation, elongation and termination factors.

3.3.2 mRNA synthesis

The MVHL mRNA used for reconstitution of translation contains four CAA repeats at its 5' end, followed by the 5' untranslated region (5' UTR) from β -globin, the sequence coding for MVHL, the UAA stop codon, and the rest of the β -globin sequence (397 bp) as the 3' UTR. For the production of mRNA, purified pET28-UAA plasmid was linearized using the restriction enzyme XhoI, and transcribed in vitro by T7 RNA polymerase.

The mRNA was purified using LiCl and Ethanol precipitation, followed by resuspension in DEPC-treated, RNase-free H₂O and by using a NAP-25 column (Figure 3.1B). In parallel, CPV-UAA-mRNA containing an IRES (internal ribosomal entry site) from cricket paralysis virus (CPV) was also produced similarly as MVHL mRNA. CPV-UAA-mRNA was used for testing the activity of elongation factors and ribosomes as its IRES allows translation to proceed without the need of any initiation factors and therefore decreases the complexity of the reaction.

3.3.3 Amino-acylation of tRNA

fMet-tRNA (provided by our collaborator Elena Alkaleva) was amino-acylated with Met using purified Methionine tRNA synthetases (purified from HeLa cell lysate as described in Pestova & Hellen., 2003) from E. coli. Bovine total tRNA (Novagen) was amino-acylated with the amino acids Val, His and Leu using purified native aminoacyl synthetases (ARases) from HeLa cell

lysate as described (Pisarev, Unbehaun, Hellen, & Pestova, 2007). The tRNAs were subsequently purified through NAP-25 columns to remove the excess nucleotides used during the reaction.

For preparation of initiator Met-tRNA, 0.025 μ g of fMet tRNA is aminoacylated with 0.15 μ g of MetRNAse in AB3x buffer (50 mM Hepes-KOH pH 7.5, 8 mM MgCl₂, 150 mM NH₄Cl, 4 mM β ME, 2 mM Spermidine) supplemented with 10 μ M of Methionine, 10 mM ATP, 1 mM CTP and 0.375 μ g/ μ l of RNAsin (Promega). The reaction was carried out at 37 °C for 7 min followed by phenol chloroform extraction and precipitation. The resulting pellet was dissolved in 2 mM NaAc at pH 5.3. Bovine total tRNA is amino-acylated similarly using the ARases.

3.3.4 Ribosomes and native factors

The ribosomal subunits were purified from HeLa cell lysate by pelleting the polysomes and dissociating various factors from the ribosomes by using high salt concentration (0.5 M KCl) followed by sucrose gradient centrifugation to separate the 40S and 60S as described (Pestova et al. 2000). 40S ribosomes were always contaminated with 60S ribosomes as shown in Figure 3.1A. The supernatant containing various factors after the high salt wash step during the purification of ribosomes was used for purification of different native initiation factors, elongation factors, and aminoacyl tRNA synthetases (ARSases). Factors eIF2 (3 subunits), eIF3 (13 subunits), eEF1H (4 subunits) and eEF2 were precipitated using different concentrations of ammonium sulfate followed by a series of anion and cation exchange chromatography purifications as described (Pestova & Kolupaeva, 2002; Pestova & Hellen, 2000). The final composition of the buffer comprising the proteins was 20 mM Tris-HCl pH 7.5, 100 mM KCl, 5-10% glycerol and 1mM DTT except for ARSases where the buffer composition was 10 mM Tris-HCl pH 7.5, 1 mM MgCl₂ and 1 mM DTT. All the purified factors are shown in Figure 3.1B and Figure 3.1D.

3.3.5 Recombinant initiation factors

The His-tagged human initiation factors eIF1, eIF1A, eIF4A, eIF5, eIF5B Δ (aa 587-1220), eIF4G Δ (aa 786-1165) were expressed in E. coli (DE3) and purified using Ni²⁺-NTA affinity chromatography (QIAGEN) as described (Frolova et al., 1999; Frolova, Merkulova, & Kisselev, 2000; Pisarev et al., 2007) (Figure 3.1C). All the purifications have been combined with an additional step of anion or cation exchange chromatography (MonoQ/MonoS from GE) to remove RNases. Additionally, care was taken to avoid RNase contamination by using RNase-free buffers, DEPC-treated water, and baked glassware. The final buffer composition of the recombinant proteins was the same as that of the native factors.

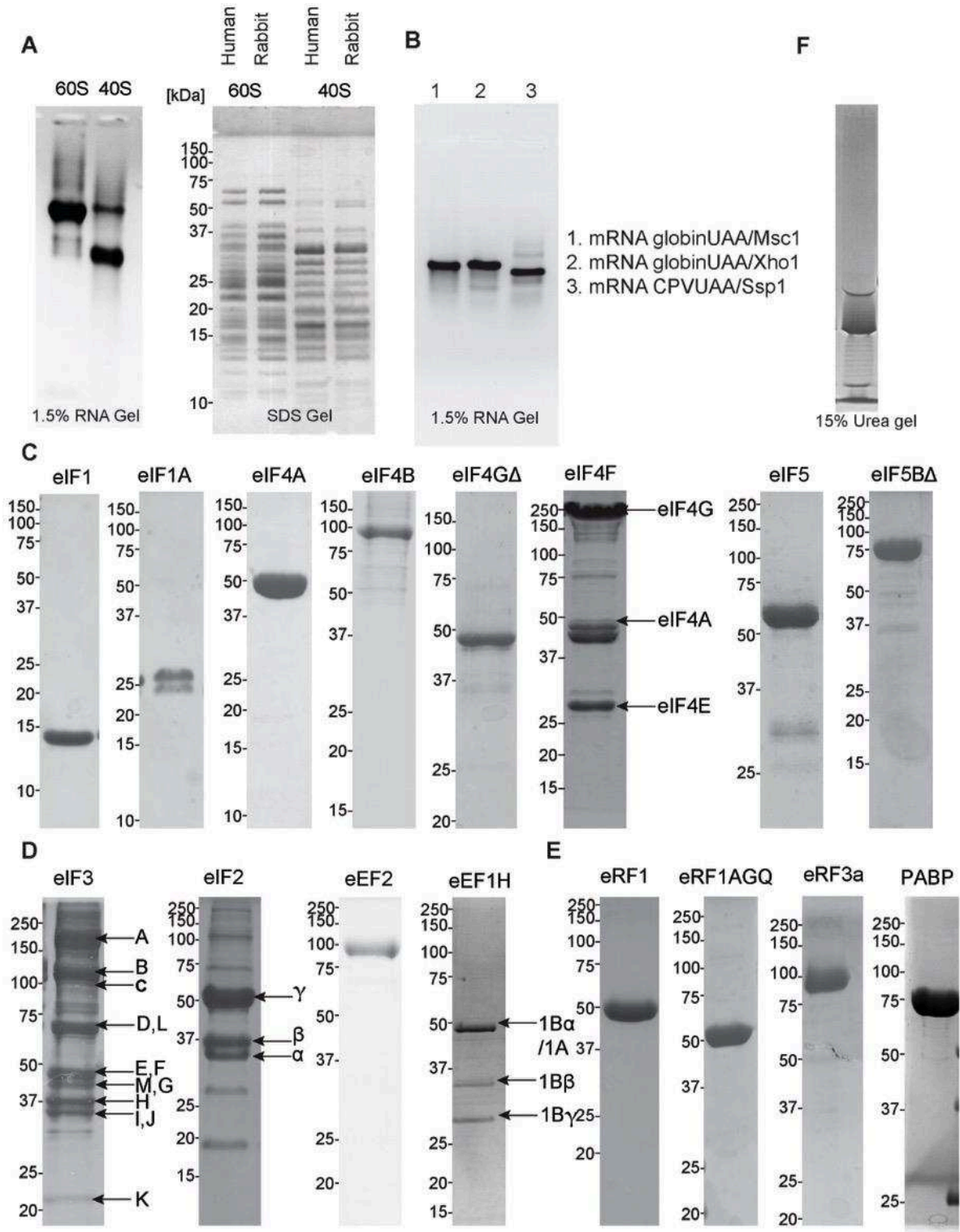


Figure 3.1 Factors required for the reconstituted in vitro translation system:

(A) 60S and 40S ribosomes purified from HeLa cell lysate. Agarose and SDS gels are run to analyze the ribosomal RNA and protein content and integrity. As a control purified ribosomes from rabbit reticulocyte lysate were analyzed (obtained from Elena Alkalaeva) (B) The different mRNAs transcribed using T7 RNA polymerase were used to reconstitute the human translation system (C) Purified recombinant initiation factors required for the translation: eIF1, 1A, 4A, 4G Δ , 5, 5B Δ are purified as recombinant proteins from E.coli. eIF4B and 4F are expressed in insect cells (D) Native factors purified from HeLa cell lysate: eIF3, eIF2, eEF2, eEF1H (E) Factors required for translation termination: eRF1WT, eRF1AGQ and PABP are purified from E. coli; eRF3a is expressed in insect cells. (F) Poly (A) tail RNA of ~30 nucleotides length was synthesized using T7 RNA polymerase and a poly (T) DNA template.

3.3.6 Toe-printing assay

To test whether the reconstituted *in vitro* translation system is active, toe-printing assays are performed. Toe-printing assays are primer extension inhibition assays displaying the position of the ribosome on the mRNA (Figure 3.2). Reverse transcription is carried out with the help of a fluorescently labeled DNA primer binding to the 3' end of the mRNA, which results in various fragments of DNA differing in their lengths. The length of the DNA fragments corresponds to the position of ribosome and thus reveals the different stages of translation (initiation, elongation, termination).

For toeprinting assays, 10 μL of sample is reverse transcribed in translation buffer supplemented with 2.5 μM dNTPs, 40 μM MgCl_2 , 2.5 μM FAM-PTC primer (fluorescently labeled primer complementary to the 3' end of MVHL mRNA) using 0.3 U/ μL of AMV Avian Myeloblastosis Virus (AMV) reverse transcriptase (Promega) at 37 °C for 20 min (Shirokikh et al. 2009). The fragments are purified using phenol-chloroform extraction and precipitated using 70% ethanol and $\frac{1}{3}$ volume of NaAc, and the pellet was sent for fragment analysis.

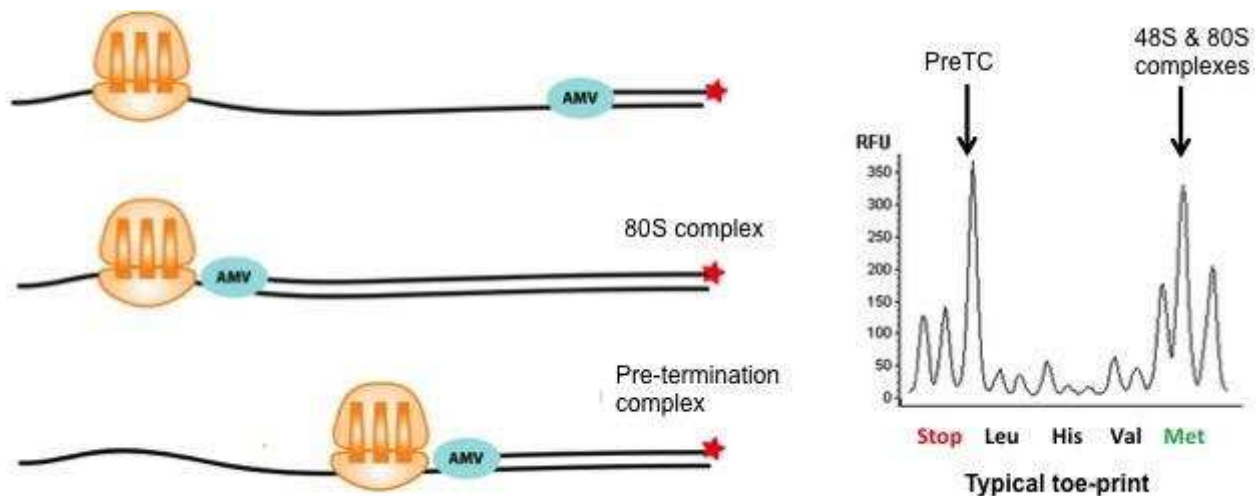


Figure 3.2 Toe-printing assay:

The toe-printing assay displays the position of the ribosome on the mRNA. A fluorescent DNA primer complementary to the 3' end of the mRNA is elongated by a reverse transcriptase generates cDNA fragments complementary to the mRNA. The resulting fragment length of the cDNA indicates the position of the ribosome on the mRNA and thus the stage of translation. A typical toe-print is shown above for an mRNA containing 4 codons. When the ribosome moves from the initiation stage (48S/80S) to the elongation stage a 9-nucleotide shift is observed (PreTC), resulting from the movement of the ribosome along the mRNA.

3.3.7 Optimization of the in vitro translation system

3.3.7.1 Capping of mRNA

The 5' cap structure increases mRNA stability, decreases susceptibility to exonuclease degradation, and promotes the formation of mRNA initiation complexes and thus results in higher efficiency of translation. To increase the efficiency of the in vitro translation system a 5' cap was added to the mRNA MVHL using the vaccinia capping enzyme (VCE). VCE contains two subunits D1 (97 kDa) and D2 (33 kDa) that add a 7-methylguanylate cap structures (Cap 0) to the 5' end of RNA. VCE was expressed in BL21Star (DE3) LysS and purified using Ni²⁺-NTA affinity chromatography and heparin affinity chromatography as described by De la Pena et al. 2007. The protein was dialyzed into the buffer C consisting of 40 mM Tris-HCl pH 7.5 at 25 °C, 200 mM KCl, 10% glycerol and 1 mM DTT and tested for RNases. Purified VCE is shown in Figure 3.3A.

For efficient capping, the vaccinia capping enzyme concentration was optimized using a defined amount of luciferase mRNA reporter and different amounts of VCE in a yeast cell-free translation system. 1 µg of VCE for 2 µg of MVHL mRNA was found to maximize translation yields as indicated by the relative light intensity in the assay (Figure 3.3B). Toe-printing assays showed that capping improved the efficiency of translation at least two-fold (Figure 3.3C). Before the start of the reaction MVHL mRNA is incubated at 65 °C for 10 min to remove any secondary structures. To cap 2 µg of mRNA, 1 µg of VCE is added along with 2 mM GTP and 0.2 mM S-adenosylmethionine in 1X Script cap buffer (50 mM Tris-HCl pH 8.0, 6 mM KCl and 1.25 mM MgCl₂) and incubated at 37 °C for 60 min and purified further using ethanol precipitation and microspin G-50 columns (GE Healthcare).

3.3.7.2 Expression and purification of initiation factors eIF4F and 4B

For the cap binding complex eIF4F (comprising factors eIF4A + eIF4E + eIF4G) yields are very low when purified from HeLa cell lysate. Moreover, the full-length active complex cannot be expressed in *E. coli*, because full-length eIF4B is degraded when purified from *E. coli*. Therefore, the proteins eIF4F (comprising all the 3 subunits: eIF4A + eIF4E + eIF4G) and eIF4B were expressed in SF21 cells using the Multibac system (Figure 3.1A). Cells were lysed in 25 mM HEPES-KOH pH 7.5, 10 mM imidazole, 300 mM KCl, 5 mM βME, 5% v/v glycerol supplemented with protease inhibitor cocktail (Roche) using a sonicator. Lysed cells were centrifuged at 10,000xg, 60 min at 4 °C. The supernatant was subjected to Ni-NTA affinity chromatography (QIAGEN). Factor eIF4F additionally was passed over a 7-methyl-GTP-Sepharose 4B resin column and eluted using 75 µM 7-methyl-GTP. Protein complexes eIF4F and eIF4B were further

purified using anion exchange chromatography (MonoQ from GE Healthcare) and dialysed into the buffer A (20 mM Tris-HCl pH 7.5 at 25 °C, 100 mM KCl, 5% glycerol and 1 mM DTT).

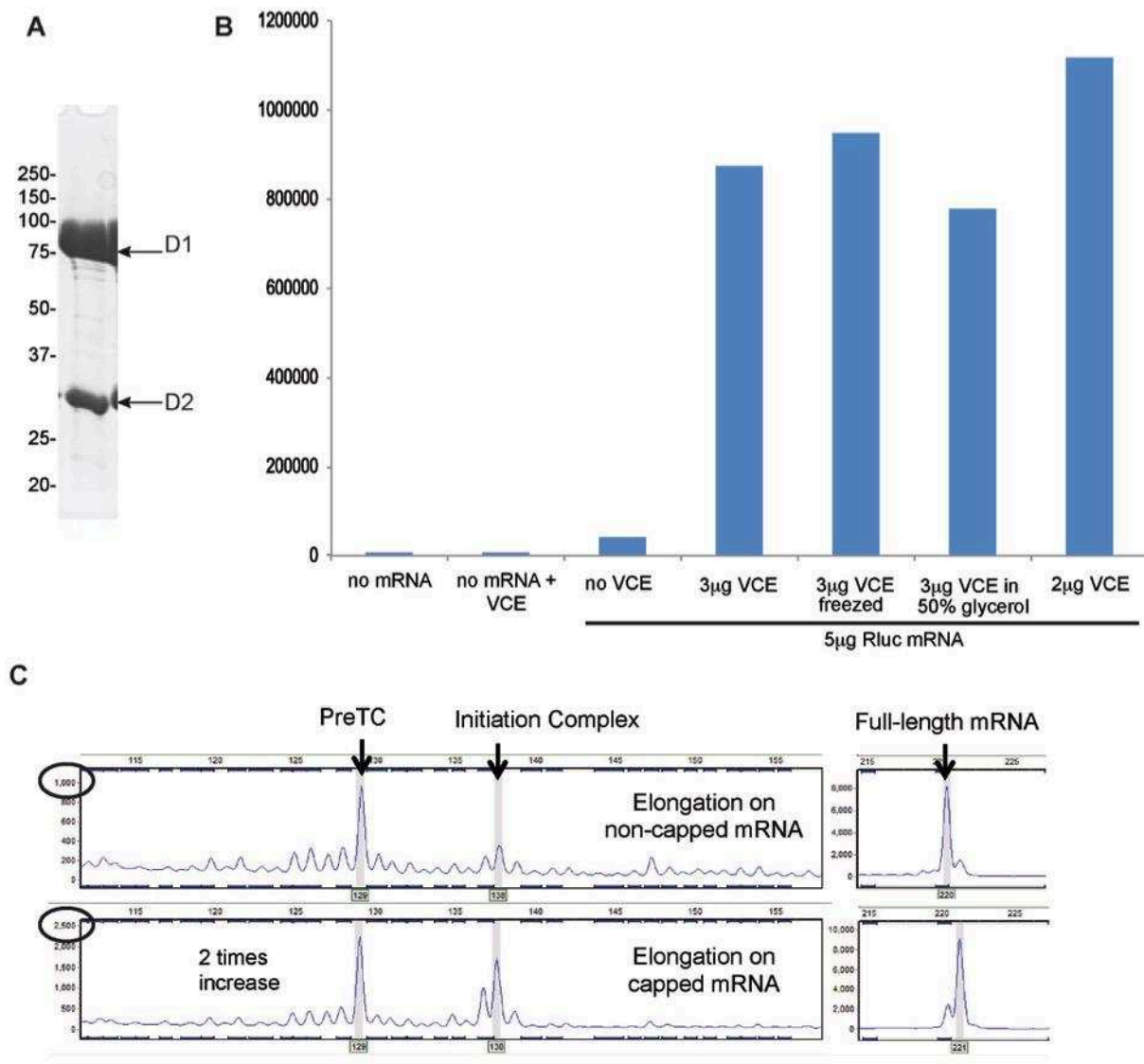


Figure 3.3 Capping of the mRNA increases the efficiency of in vitro translation:

(A) SDS page analysis of purified VCE with subunits D1 and D2 (B) Optimization of the amount of VCE used for the capping reaction using 5µg of luciferase mRNA (C) Toe-printing assay showing that the translation is about two-fold more efficient when capped mRNA is used. The efficiency of capping can be monitored in the full-length cDNA peak (resulting from free mRNA).

3.3.8 Assembly of the Pre-Termination complexes

Pre termination complexes (PreTCs) were assembled as described (Alkalaeva et al., 2006) with the following modifications: The translation reaction was performed in translation buffer (20 mM Tris-HCl, pH 7.5, 50 mM KOAc, 2.5 mM MgCl₂, 2 mM DTT, 0.25 mM Spermidine) supplemented with 200 U RNase inhibitor (RiboLock, Fermentas), 1 mM ATP, 0.2 mM GTP, 35 pmol of MHVL mRNA, 35 pmol methionyl-tRNA^{fmet}, 50 pmol purified 40S human ribosomal subunit, 100 pmol eIF2, 50 pmol eIF3, 80 pmol eIF4F, eIF4A, eIF4B, eIF1, eIF1A each in a total reaction volume of 500 µl and incubated for 15 min at 37 °C to form the 48S initiation complexes (Figure 3.4). 80pmol of eIF5, eIF5BΔ each and 50 pmol 60S human ribosomal subunit is added and and incubated at 37 °C for 10 min to form the 80S initiation complexes. 200 pmol eEF1H, 50 pmol eEF2 and 75 µg total tRNA (aminoacylated with Val, His and Leu was added and incubated at 37 °C for 10 min to form the PreTCs.

3.3.9 Purification of the Pre-Termination complexes

To separate translating ribosomes from non-translating ribosomes and to obtain a homogenous sample for the biochemical and cryo-EM studies, a purification protocol was established and optimized (starting from a procedure published by (Namy, Moran, Stuart, Gilbert, & Brierley, 2006). A RNA oligonucleotide (2'-O-methyl RNA primer) containing six biotin residues and with a complementary sequence to the 3' end of MVHL mRNA was annealed to the mRNA. This mRNA-primer fusion was used for the reconstitution of PreTCs. After the in vitro translation reaction the mRNA was immobilized on to the streptavidin beads via the biotinylated primer.

Immobilized mRNA was washed and eluted from the streptavidin beads using RNaseH directed cleavage. To this end a DNA primer was annealed to the mRNA, subsequently RNaseH cleaves the 3'-O-P bond of the mRNA in the DNA/RNA duplex). This method allowed us to purify mRNA-bound, translating ribosomes from non-translating ribosomes and other translation factors used during reconstitution. The translating ribosomes could be stalled in different stages of translation. Therefore, the PreTC was always confirmed using toe-printing assays. The protocol had to be optimized to optimize the yield of PreTCs, In particular, care had to be taken to keep their integrity and not to disrupt the complexes during the washing steps of the purification.

The following, optimized protocol was used for large-scale PreTC preparations: The streptavidin beads were incubated with BSA and yeast tRNA overnight in translation buffer (20 mM Tris-HCl, pH 7.5, 50 mM KOAc, 2.5 mM MgCl₂, 2 mM DTT, 0.25 mM Spermidine). Before the start of the experiment the beads were washed with 1X beads buffer (BB) (1X BB buffer consists of 20 mM Tris-HCl pH 7.5, 50 mM KOAc, 10 mM Mg(OAc)₂, 2 mM DTT, 0.25 mM Spermidine and 1 mM cycloheximide) to remove tRNA and BSA. This step reduces nonspecific binding of proteins and RNA. The capped mRNA annealed with the biotinylated oligonucleotide (which had been

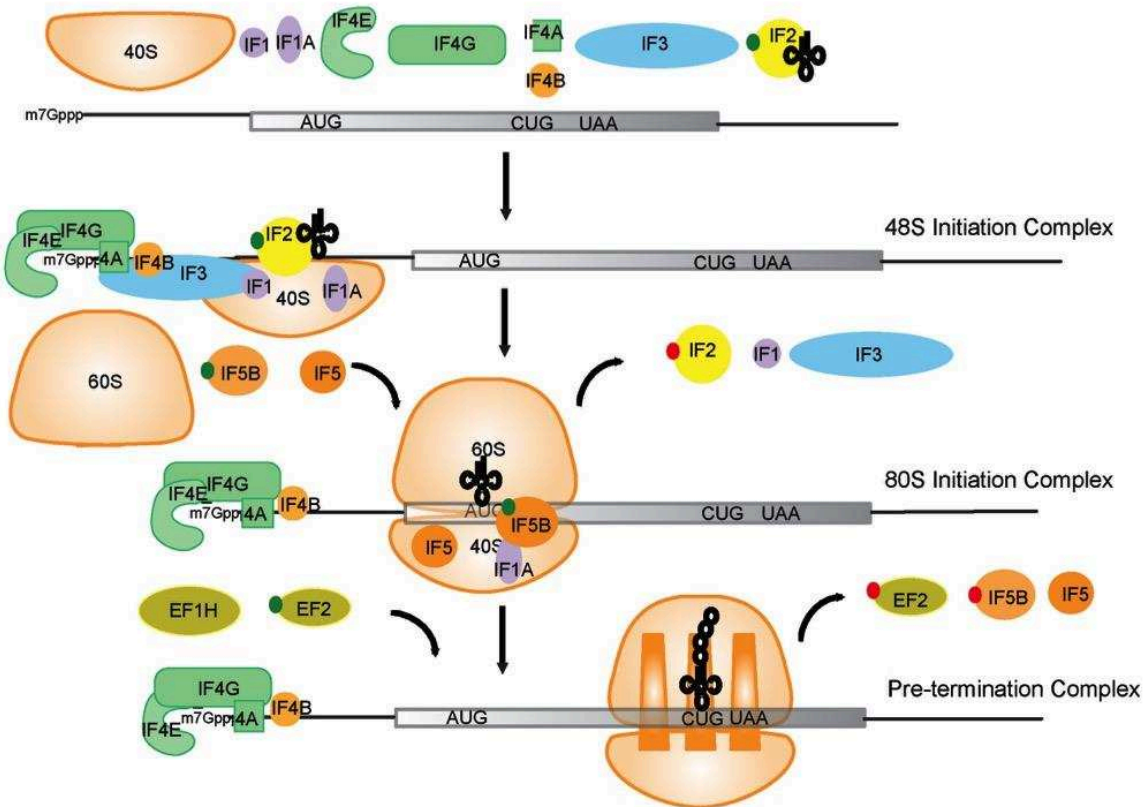


Figure 3.4 Assembly of Pre termination complexes (PreTCs):

A schematic representation of different stages of *in vitro* translation used for the assembly of PreTCs. mRNA, 40S ribosomal subunit, eIF1, 1A, 4F, 4B, 2, 3, methionyl-tRNA^{met}, RNase inhibitor, ATP and GTP are incubated at 37 °C for 15 min for the formation of 48S initiation complexes. eIF5, 5BΔ, 60S ribosomal subunit are added and incubated for 10 min for the formation of 80S initiation complexes. eEF2, eEF1H and amino acylated bovine tRNA are added and incubated for 10 min for the formation of PreTCs.

added in 3fold excess) was heated at 68 °C for 5 min and cooled by incubating at 37 °C for 4 min and then left on ice for 10 min. The biotinylated mRNA was then used for the *in vitro* translation reaction. After the formation of the PreTCs, the mixture was incubated with 100 μL streptavidin beads (Sigma) for 60 min at 4 °C. The magnesium ion concentration was increased to 7.5 mM, and 1 mM cycloheximide was additionally added in order to further stabilize the ribosomal complexes formed on the mRNA. The immobilized complexes were washed with wash buffer (20 mM Tris-HCl, pH 7.5, 30 mM KOAc, 10 mM Mg(OAc)₂, 2 mM DTT, 0.25 mM Spermidine, 1 mM cycloheximide) consisting of lower salt and higher Mg²⁺ concentration. A DNA primer with a sequence complementary to the 3'UTR of the mRNA was added in 7x excess and annealed for 20 min at 4 °C. The site where the DNA primer anneals defines the cleavage site for RNaseH. The excess of the DNA primer is washed away with wash buffer. PreTCs were eluted using RNaseH-directed cleavage for 30 min at room temperature in RNC buffer (20 mM Tris-HCl pH 7.5 at 4 °C, 100 mM KCl, 2.5 mM Mg(OAc)₂, 2 mM DTT, 10 μg/mL cycloheximide). 2.6U of

RNaseH (NEB) was used per 1pmol of mRNA. The enzyme RNaseH was buffer exchanged into the elution buffer before use, to remove the glycerol using a Zebra spin desalting column (Thermo scientific).

3.3.10 Purification of the termination factors eRF1 and eRF3a

The his-tagged eRF1 wild type (WT) and the eRF1 G183A mutant (AGQ) are expressed in *E. coli* (BL21) and purified by combining Ni²⁺-NTA affinity chromatography (QIAGEN) and anion exchange chromatography using a HiTrap QXL column (GE Healthcare) as described (Alkalaeva et al. 2006) (Figure 3.1C). The eRF1AGQ mutant comprises a G183A mutation, which renders it inactive in peptidyl-tRNA hydrolysis. The purified proteins are dialysed into buffer A (20 mM Tris-HCl pH 7.5 at 25 °C, 100 mM KCl, 5% Glycerol and 1mM DTT).

eRF3a FL is expressed in SF21 insect cells and purified using Ni²⁺-NTA affinity chromatography followed by anion exchange chromatography and dialysis into buffer A .

3.3.11 Purification of PABP

His-tagged PABP was expressed from plasmid pET42a-PABP in *E. coli* (C43) by inducing with 0.5mM IPTG for 16hrs at 18 °C. The cells are lysed using a buffer consisting of 20 mM Tris-HCl pH 7.5 at 25 °C, 800 mM KCl, 10% Glycerol and 5mM β ME complemented with protease inhibitors (Roche). The lysate was applied to Ni²⁺-NTA affinity resin (QIAGEN) equilibrated with the lysis buffer. Successive washes were performed using 20 mM Tris -Cl pH 7.5 at 25 °C, 1M KCl, 10% Glycerol, 5mM β ME and 20 mM Tris-HCl pH 7.5 at 25 °C, 800 M KCl, 40 mM Imidazole, 10% Glycerol, 5mM β ME. The protein was eluted using 20 mM Tris-HCl pH 7.5 at 25 °C, 800 mM KCl, 300 mM Imidazole, 10% Glycerol and 1mM DTT. Dialysis was performed overnight and the salt was reduced gradually in the dialysis buffer (20 mM Tris-HCl pH 7.5 at 25 °C, 10% Glycerol, 1mM DTT with 800 mM to 100 mM KCl) in steps consisting of 600 mM, 400 mM, 200 mM of KCl. PABP was further purified using anion exchange chromatography (HiTrap QXL) (Figure 3.1C). PABP was finally dialyzed in buffer A, frozen in small aliquots in liquid nitrogen and stored at -80 °C till further use.

3.3.12 Poly (A) tail synthesis

A 30-nucleotide long poly (A) tail was synthesized using in vitro transcription by T7 RNA polymerase. The DNA primer containing the template sequence and a T7 RNA polymerase binding/ transcription start site was ordered from Invitrogen (5'– ATTATGCTGAGTGATATCCTTTTTTTTTTTTTTTTTTTTTTTTTTTTTTTTTTT – 3'), and the primer with the sequence 5'– CCTATAGTGAGTCGTATTA – 3' was used for elongation. The transcription reaction was carried out at 37 °C for 60 min. The polyA RNA was phenol-

chloroform extracted and ethanol precipitated (Figure 3.1F). The RNA was further purified using an 18% urea gel, extracted, pelleted using isopropanol and resuspended finally in DEPC-treated H₂O.

3.3.13 Biochemical characterization of eRF1, eRF3a and PABP interactions

3.3.13.1 Complex Formation between eRF1AGQ, eRF3a and PABP

eRF1, eRF3a and PABP were purified independently and then used for complex formation. 20 μM eRF1AGQ, eRF3a and PABP were mixed in buffer A (20 mM Tris-HCl pH 7.5, 100 mM KCl, 5% glycerol and 1 mM DTT) and incubated on ice for 60 min. Size Exclusion Chromatography (SEC) was performed (Superdex 200 10/300 or PC32) in buffer A and the fractions were analyzed by 12% SDS PAGE and used for further studies (Figure 3.5A).

A stable complex between the three proteins could be formed even at lower concentrations. The affinity between PABP and eRF3a was reported to be around ~0.7 μM (Kononenko et al. 2010) using iso-thermal titration calorimetry. However, serial dilution of the complex (10 μM to 150 nM) combined with pulldown experiments using immobilized His-tagged PABP showed that the complex was stable even at lower concentrations (e.g. 625 nM; Figure 3.5B). In agreement with my observations, recent work from Jerbi et al. 2016 determined that the K_d between eRF3a and PABP is 1.5 nM using surface plasmon resonance.

3.3.13.2 PABP stimulates translation termination

In collaboration with Elena Alkalaeva, Engelhardt Institute of Molecular Biology, Moscow we could show using toe-printing and peptide release assays that PABP has a stimulating effect on translation termination in vitro. While this stimulating effect had been postulated before based on readthrough experiments using reporter mRNAs (Ivanov et al., 2008) previously, a direct impact on termination had never been demonstrated before, due to the lack of an in vivo termination assay. It was important to use eRF3a FL in these studies because PABP interacts with the N-terminal part of eRF3a. Previous studies on translation termination (Alkalaeva et al., 2006) used eRF3c lacking the N-terminal 138 residues, because the full-length protein cannot be produced in *E. coli*. The toe-prints and the peptide hydrolysis experiments showed that eRF3a FL alone has a higher termination efficiency compared to eRF3c, which is further, stimulated by PABP (Ivanov et al. 2016) (the publication is attached at the end of the chapter).

3.3.13.3 Affinity purification of PreTCs

To avoid non-specific binding of PABP to the mRNA during the affinity purification of the termination complexes, poly (A) RNA with a length of 30 nucleotides corresponding to the

minimal length required was added to the experiments. Pulldown experiments with PreTCs were carried out using mRNA that had been immobilized on streptavidin beads as described in section 1.2.4 above. Preformed eRF1-eRF3a-PABP-poly(A) tail complexes were purified using SEC and added to purified PreTCs. The excess complexes were removed by washing and the complex was eluted from the beads using buffer (20 mM Tris-HCl pH 7.5 at 4 °C, 100 mM KCl, 5 mM Mg(OAc)₂, 2 mM DTT, 10 µg/mL cycloheximide) containing RNaseH. The fractions were analyzed using SDS gel stained with SYPRO ruby stain.

The use of poly (A) RNA prevented the binding of PABP to the mRNA as shown in Figure 3.5C. PABP was found in the eluted fractions of PreTCs suggesting the binding of PABP to the ribosomes. The eRF1-eRF3a-PABP complex was eluted with PreTCs showing that the ribosomal termination complex with PABP can be purified.

3.3.13.4 Sample preparation for electron cryo-microscopy

10X excess of a preformed protein complex between eRF1, eRF3a and PABP (GTP/GMPPNP) along with a 30 nucleotide poly (A) RNA is added to the PreTCs and incubated at 37 °C for 5 min. Subsequently, the sample was applied to a glow discharged Quantifoil grid with a continuous carbon (400 mesh, R1.2/1.3 copper grids).

To increase the concentration of particles on the grids a pre-coated carbon grid was floated on to the sample (30-50 µl) for 30 min. Subsequently, the excess was blotted off and then vitrified in liquid ethane using a Vitrobot Mark III (95% humidity). In another attempt to increase the concentration of the ribosomes for cryo-grid preparation, the preTCs are pelleted through a sucrose cushion by centrifugation at 55000 rpm for 3 h using a TLA55 rotor (Beckman Coulter). Pelleted preTCs were re-suspended in RNC buffer (20 mM Tris-HCl pH 7.5 at 4 °C, 100 mM KCl, 2.5 mM Mg(OAc)₂, 2 mM DTT, 10 µg/mL cycloheximide), and 3 µL of sample was used for freezing grids without flotation.

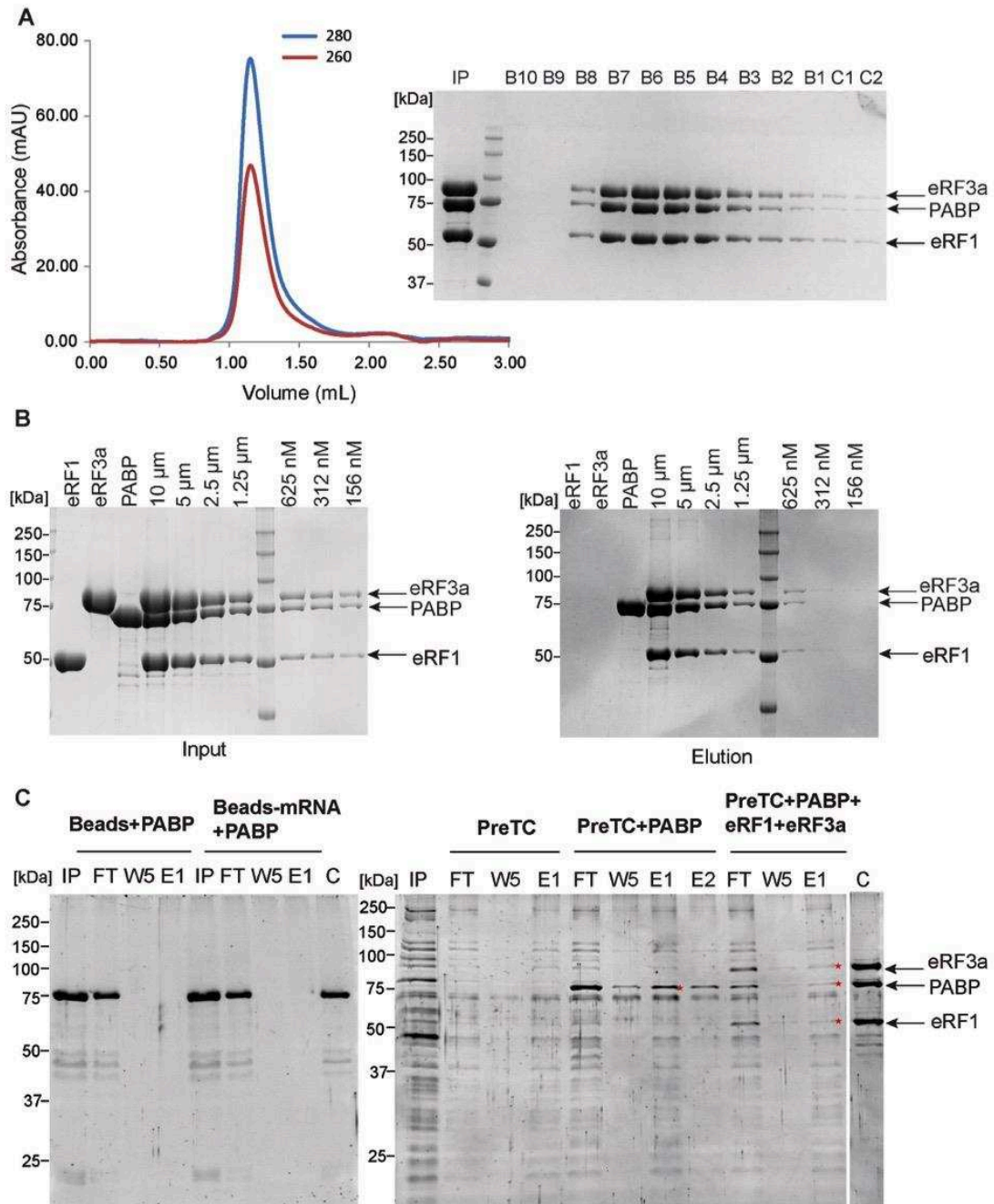


Figure 3.5 Biochemical characterization of eRF1-eRF3a-PABP complexes:

(A) SEC (Superdex 200 10/300) of the preformed eRF1-eRF3a-PABP complex in buffer A. 12% SDS gel showing the peak fractions containing all three proteins. (B) In vitro pulldown of eRF1-eRF3a-PABP complex where His-tagged PABP is immobilized on the Ni²⁺ resin and incubated with tag-free release factors. Protein mixtures before loading onto the beads (input, left) and after elution from the beads (elution, right) were separated on 12% SDS gels followed by Coomassie staining. (C) Affinity purification of PreTCs. PABP pre- incubated with poly (A) RNA does bind to PreTCs in presence and absence of eRF1/eRF3a (right gel), but it does not bind to mRNA (left), suggesting that PABP interacts with the ribosome. The red stars highlight the presence of PABP and eRF1/eRF3a in the eluted fraction. SDS gels are stained using SYPRO Ruby stain.

3.3.13.5 Cryo-EM of the pre-terminating ribosomes with eRF1AGQ, eRF3a, PABP and GTP

PreTCs were purified, pelleted and re-suspended in RNC buffer together with a 10X excess of eRF1-eRF3a-PABP-poly(A)tail complex with 100 μ M GTP. Cryo-EM grids were prepared by adding 3-4 μ L of sample per grid with a thin continuous carbon foil. The data set was collected on TITAN (EMBL, Heidelberg) equipped with a FALCON II electron detector with a pixel size of 1.732 \AA (Figure 3.6A). The micrographs were collected at an under-focus varying between 1.5 and 3.5 μ m. A total of 20 frames accumulating to a dose between 24 and 40 $e^- \text{\AA}^{-2}$ over 1.12s exposure was collected. UNBLUR was used for alignment of the frames. CTFFIND4 was used for CTF estimation, and a total of 2,409 micrographs were used for particle picking. 84,536 particles were picked using RELION autopick. 2D classification was performed with RELION, and the best classes were selected resulting in a data set of 64,535 particles. An initial consensus map was generated using a rabbit 80S ribosome containing P-site tRNA (EMDB 1670; filtered to a resolution of 60 \AA) as reference map. The resulting volume was classified using RELION 3D-classification into 3 classes (Figure 3.6B).

Only Class1 with 20% of the particles yielded an 80S ribosome with a weak density for P site tRNA. Class 2 consisted of 46% of the particles, which resembled a 60S ribosome subunit, and the remaining 32% of particles could not be properly aligned. We speculate that these were particles from thick ice regions.

The class containing the P site tRNA (13,500 particles) was further classified into 3 classes. Class1 consisted of 44% of the dataset (6,000 particles) which showed a density for P site tRNA but the A site was empty and the density accounting for eRF1 and eRF3a and PABP could not be detected. The rest of the particles were empty 80S ribosomes. The particles that contain P site tRNA represent only 10% of the complete dataset. There are several possible explanations. Ribosomal complexes could be dissociated during cryo-EM grid preparation. Moreover, termination could occur despite the fact that we used the eRF1AGQ mutant to prevent peptidyl-tRNA hydrolysis. We suspected that the presence of GTP led to the activation of translation termination. In fact, the eRF1AGQ mutant has been reported to have about 5% of the activity of wildtype eRF1 (Alkalaeva et al., 2006). Therefore, we decided to repeat the experiment with non-hydrolysable nucleotide GMPPNP to better stabilize the complexes.

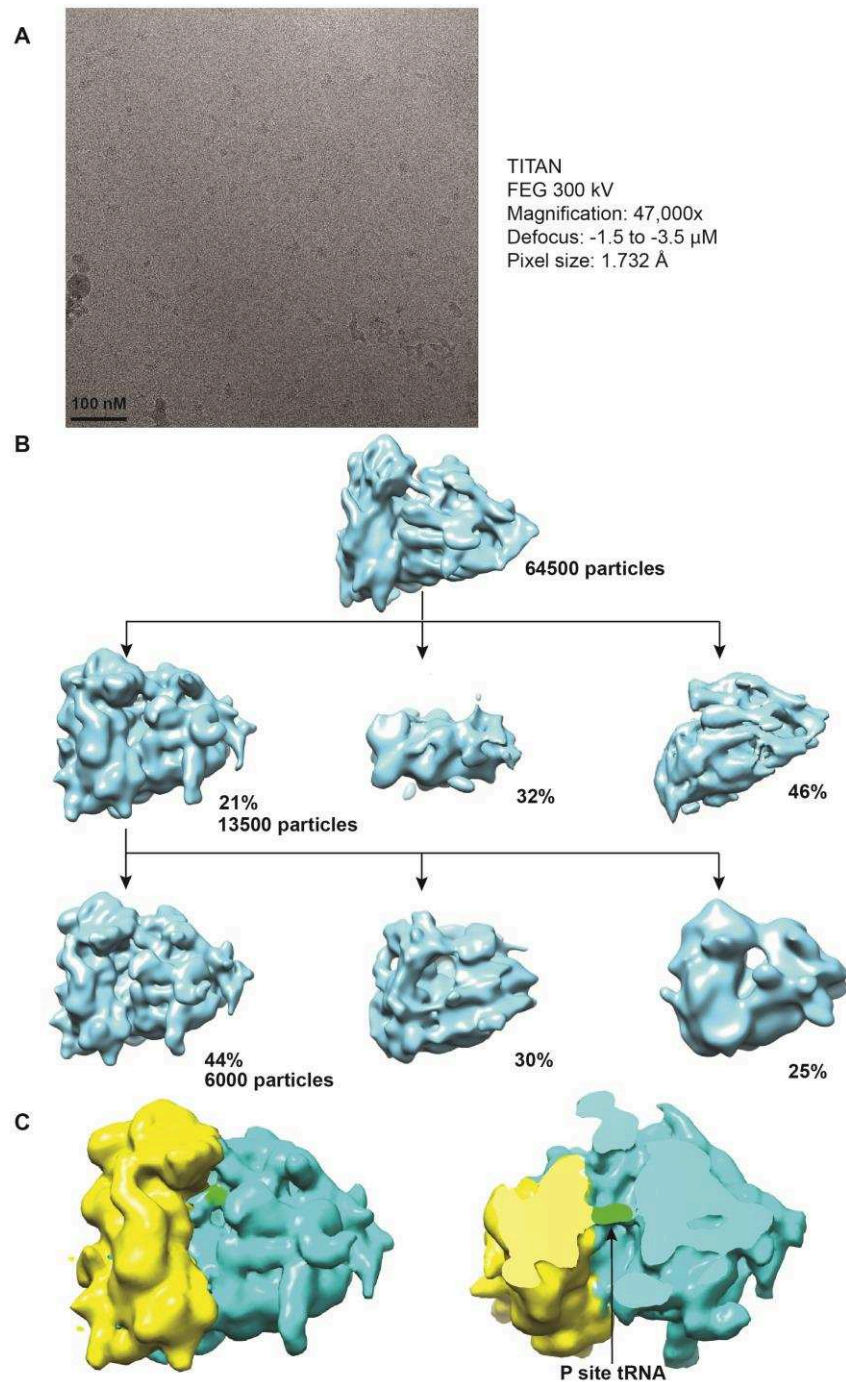


Figure 3.6 Cyo-EM of pre-terminating ribosome with eRF1-eRF3a-PABP-GTP:

(A) A representative image collected from the microscope (B) Sorting of the particles using 3D classification in RELION into 3 classes. A 80S ribosome containing P-site tRNA (EMD 1670) filtered to 60 \AA was used as an initial model for 3D classification (above). The data set comprising 64,500 particles was first sorted into 3 classes (middle). Class1 was used for a second round of 3D classification into 3 classes (below). (C) The final volume from 6,000 particles is shown. 40S is colored in yellow, 60S in cyan and P site tRNA in green. The A site is not occupied.

3.3.13.6 Cryo-EM of the pre-terminating ribosomes with eRF1AGQ, eRF3a, PABP and GMPPNP

PreTCs were purified, pelleted and re-suspended in RNC buffer together with a 10X excess of eRF1-eRF3a-PABP-poly(A)tail complex with 100 μ M GMPPNP. Cryo-EM grids were prepared by adding 3-4 μ L of sample per grid with a thin continuous carbon foil. A test data set of 200 micrographs was collected manually on the Tecnai G2 Polara (IBS microscopy facility) equipped with a K2 direct electron detector with a pixel size of 2.179 \AA (Figure 3.7A). 40 frames accumulating a dose of 17-20 $e^- \text{\AA}^{-2}$ over 12s was used. UNBLUR was used for alignment of micrographs (Brilot et al., 2012; Grant & Grigorieff, 2015). CTF was estimated using CTFFIND4 (Rohou & Grigorieff, 2015) and 185 micrographs were used for particle picking. 58,554 particles were picked using RELION autopick (Scheres, 2012). 2D classification was performed with these particles and the best classes were selected, which yielded a total of 20,329 particles. An initial consensus map was generated using a rabbit 80S ribosome containing P-site tRNA as reference map (EMDB 1670), which was filtered to resolution of 60 \AA . The map was classified using RELION 3D-classification into 3 classes (Figure 3.7B).

Class1 consisted of 38% of the particles: the resulting volume was the empty 80S ribosome. Class2 consisted of 59% of the particles: the resulting volume could be the 60S subunit or damaged 80S particles. The class 3 consisted of 'junk' particles, which accounted for only 2% of the dataset.

The class containing the volume for 80S ribosome (7,800 particles) was further classified into 3 classes. Class1 consisted of 46% of the dataset (3,560 particles) and showed a density for P site tRNA. However, the A site was empty and the density for eRF1 and eRF3a and PABP could not be detected. The rest of the particles were empty 80S ribosomes. We conclude that using of the eRF1AGQ and GMPPNP was not sufficient to successfully stall the complexes for cryo-EM studies. Future efforts need find a new approach to better stabilize the terminating ribosome.

3.3.14 Complex formation between PABP and eRF1

3.3.14.1 Interaction between PABP and eRF1

In SEC experiments, we found that eRF1 and PABP form a complex. This was not observed before. We thus speculated that PABP interacts with the both release factors, and not only eRF3 as previously reported. SEC (Superdex 10/300) was performed in a buffer composed of 20 mM Tris-HCl pH 7.5, 200 mM KCl, 5% glycerol, and 1 mM DTT (Figure 3.8A).

Microscale thermophoresis experiments (MST) were performed to confirm the interaction between eRF1 and PABP. Both PABP and eRF1 were labeled and tested. Both experiments yielded similar Kd values of \sim 880nM (Figure 3.8B).

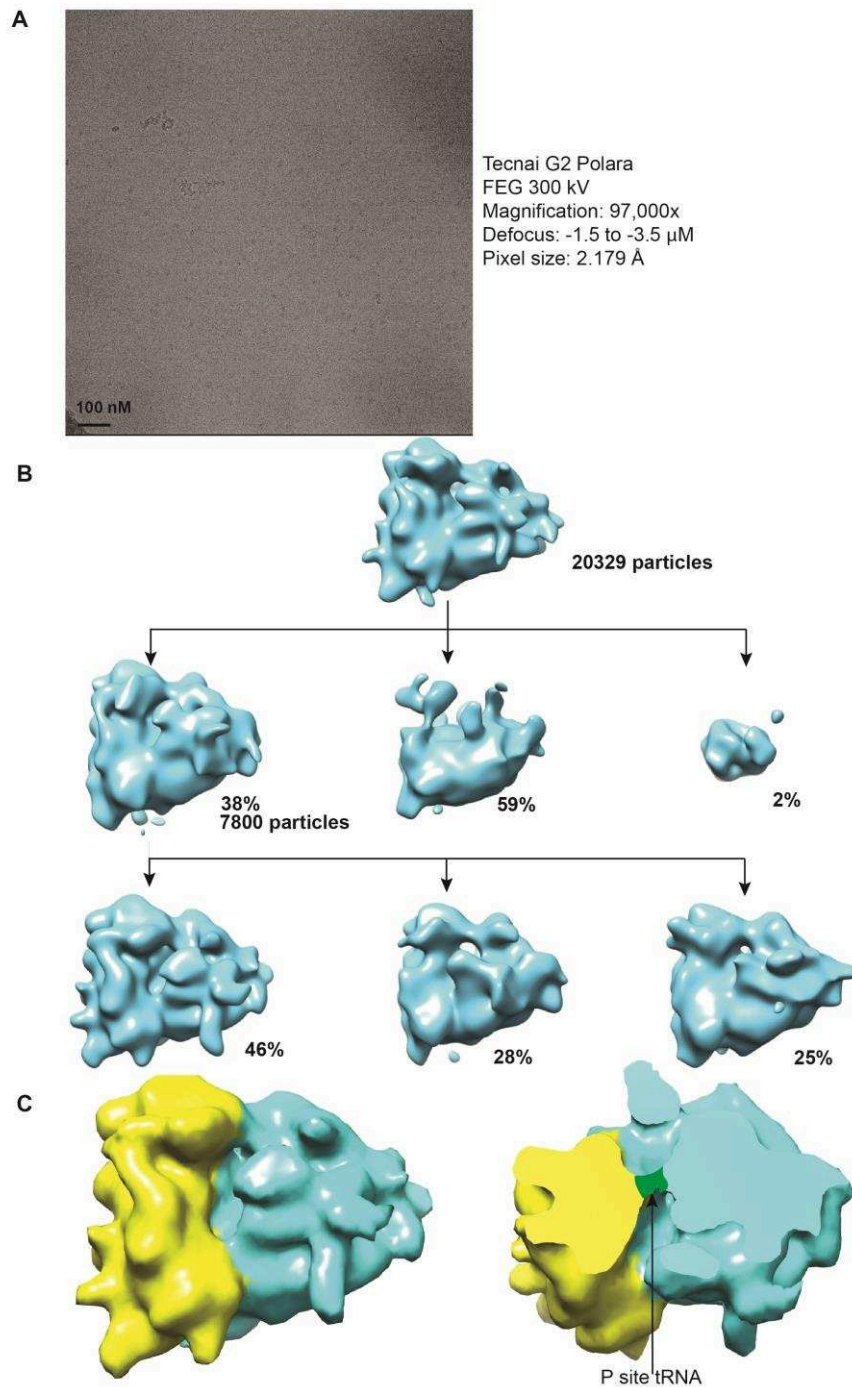


Figure 3.7 Cyo-EM of pre-terminating ribosome with eRF1-eRF3a-PABP-GMPPNP:

(A) A representative image collected from the microscope (B) Sorting of the particles using 3D classification in RELION into 3 classes. An 80S ribosome containing P-site tRNA (EMD 1670) filtered to 60 Å was used as an initial model for 3D classification (above). The data set comprising 64,500 particles was first sorted into 3 classes (middle). Class1 was used for a second round of 3D classification into 3 classes (below). (C) The refined volume is shown: 40S is colored in yellow, 60S in cyan and P site tRNA in green.

3.3.14.2 Interaction region between PABP and eRF1

Two deletion constructs were generated for PABP: PABP 388-634 lacking the RRM domains and PABP 534-634 lacking the proline-rich linker and the RRM domains.

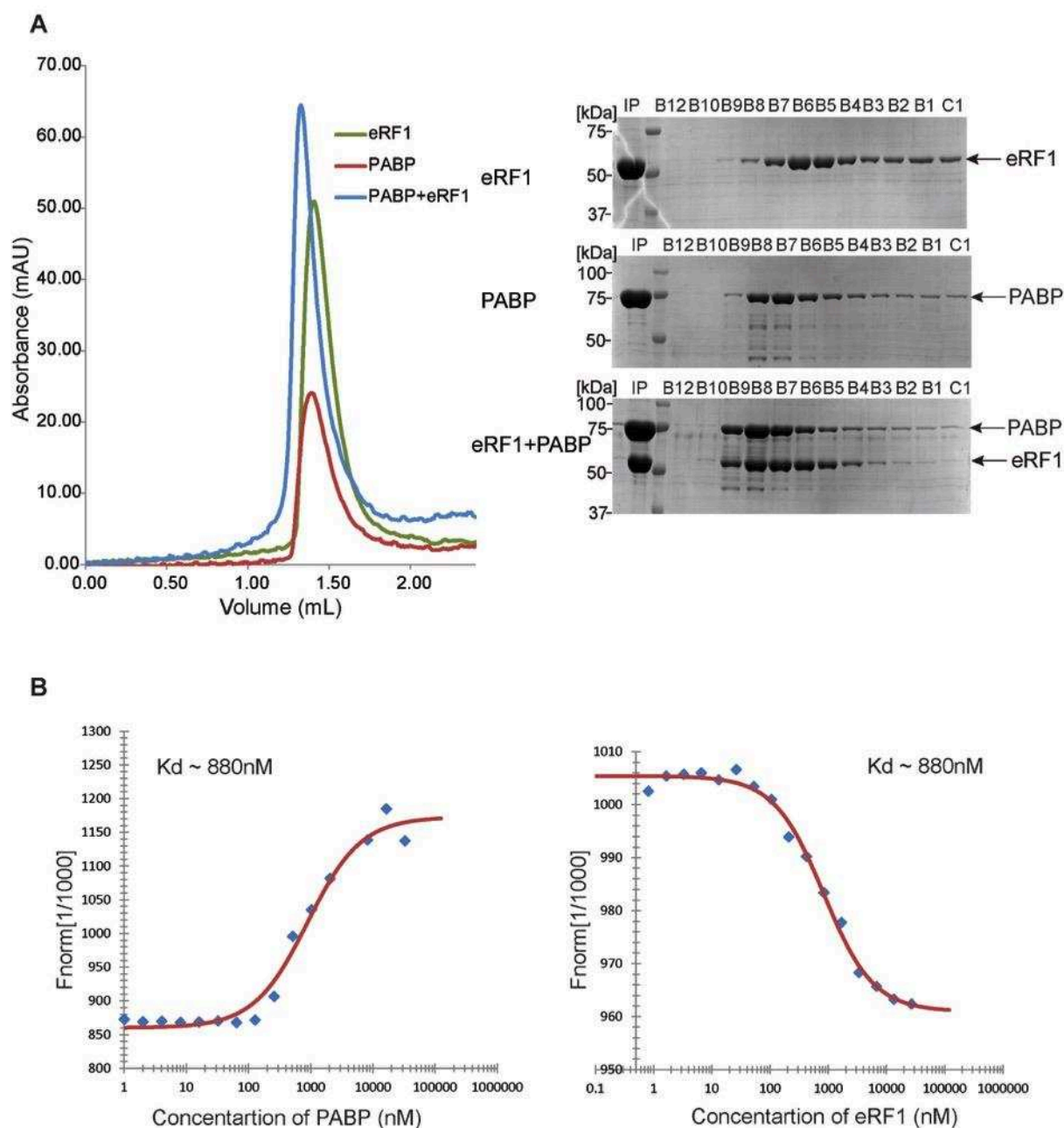


Figure 3.8 Interaction between PABP and eRF1:

(A) SEC (Superdex 200 10/300) analysis of the preformed eRF1-PABP complex in buffer A. 12% SDS gel showing the shift in the fractions indicating an interaction between the proteins. (B) Microscale thermophoresis assays of the PABP and eRF1 interaction. eRF1 (left) or PABP (right) were fluorescently labeled and different concentrations of the other protein were added.

The proteins were generated with a cleavable MBP-tag by a TEV protease using the pMAL vector (NEB). MBP-tagged PABP and its deletion constructs (PABP 388-634 and PABP 534-634) are expressed in *E. coli* (C43) and purified using affinity chromatography (amylose resin) and anion/cation exchange chromatography. The proteins were finally dialyzed in to buffer A (20 mM Tris-HCl pH 7.5 at 25 °C, 100 mM KCl, 5% glycerol and 1 mM DTT).

MBP-PABP, MBP-PABP 388-634 and MBP-PABP 534-634 were immobilized on the amylose resin and pulldowns using eRF1 were performed in buffer A to check the interaction region as shown in Figure 3.9. Only MBP-PABP FL and eRF1 were found to interact. The deletion constructs did not interact, leading to the conclusion that the RRM domains of PABP are important for the interaction between eRF1 and PABP. To corroborate this conclusion, the RRM domains need to be expressed and used for the same pulldown assays

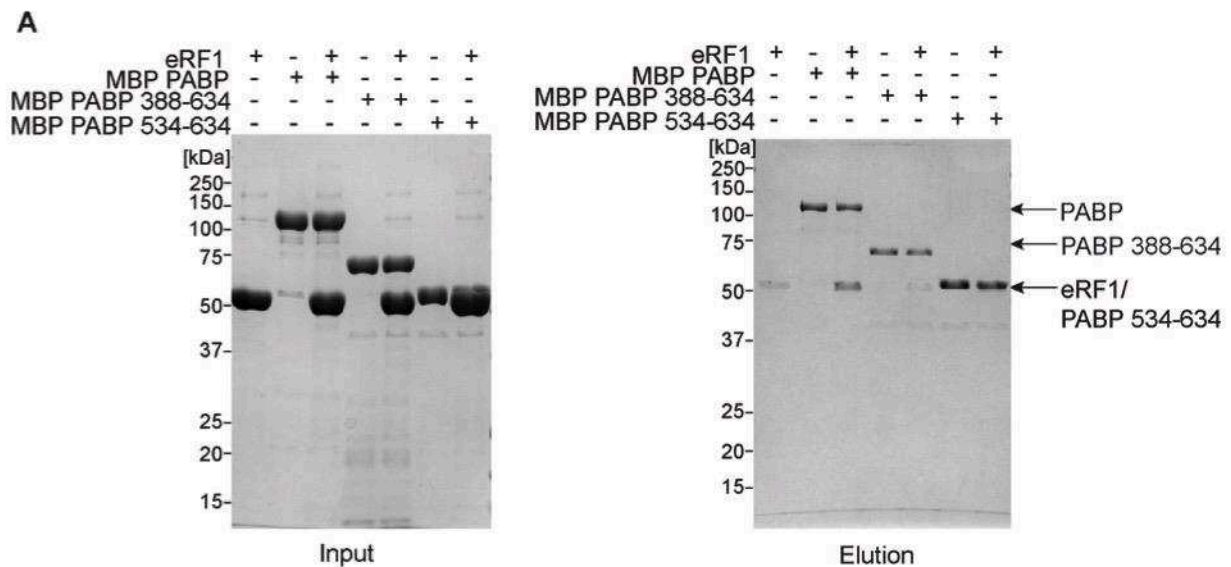


Figure 3.9 Interacting region between PABP and eRF1:

MBP-tagged PABP, PABP 388-634 and PABP 534-634 are immobilized on amylose resin (Input shown on the left panel) and eluted using 10mM maltose (right). Eluted samples are showed in the right panel. 12% SDS gels are run and stained using Coomassie blue.

3.4 Conclusions

We have established a novel method for the purification of mammalian pre-termination complexes using biotinylated mRNA and RNaseH cleavage for elution. This yields a homogeneous pre-TC sample for biochemical and structural studies. The established purification system has been successfully used in the lab to reconstitute initiation and the termination complexes (Chapter 1 and 2).

With our collaborators we performed a biochemical characterization of PABP's effect on translation termination using toeprint analyses and the peptide release assays. This work led to the first demonstration that PABP directly affects translation termination *in vitro*. Simultaneously, we undertook the structural characterization of the ribosome-eRF1-eRF3a-PABP complex described above to understand how PABP interacts with eRF3a and the ribosomes and how its interaction leads to stimulation of translation termination. All biochemical characterizations demonstrate that the termination complex with PABP can be formed and purified *in vitro* successfully. However, the cryo-EM reconstructions lacked release factors and PABP despite the fact that the AGQ mutant of eRF1 was used which is impaired in peptide release. Intriguingly, we observed that the amount of 80S ribosomes containing P-site tRNA after classification is significantly less in our PABP-reconstructions compared to the UPF1 datasets (10% with PABP versus 30% with UPF1, cf. Chapter-2). Based on these numbers and the surprisingly high percentage of empty ribosomes, we conclude that we were not able to efficiently stall termination. Moreover, the termination complex is likely to be very unstable and the factors could dissociate during grid preparation. The eRF1AGQ mutant has 5% residual activity in absence of PABP (Alkalaeva et al., 2006) thus termination could proceed during grid preparation. The non-hydrolysable GMPPNP nucleotide prevents GTP hydrolysis by eRF3a, accommodation of eRF1 in the peptidyl transferase centre of 60S and thus peptide release. Even in the presence of both, eRF1AGQ and GMPPNP, PABP apparently stimulates termination or destabilizes the termination complexes. Release of the nascent peptide very likely also destabilizes the binding of the P-site tRNA and release factors, leading to a large fraction of empty 80S ribosomes and even 60S subunits in cryo-EM reconstructions.

Accordingly, we observe in our reconstructions that there are much less ribosomes with P-site tRNA compared to preparations with eukaryotic release factors and UPF1. At the onset of this project we assumed that we could successfully stall the complexes with the eRF1AGQ mutant. Our recent biochemical studies of PABP's impact however led to a better understanding of how powerful PABP is to stimulate translation termination. In order to effectively stall the translation termination reaction, an inactive PABP mutant would be required or another approach to prevent the dissociation of the termination complex.

3.5 General protocols used for the studies

3.5.1 DNA techniques

3.5.1.1 Oligonucleotides

Desalted DNA oligonucleotides were purchased from ThermoFisher Scientific. The oligonucleotides were resuspended in ultrapure water to a final concentration of 200 nM and stored at -20 °C.

3.5.1.2 Polymerase Chain Reaction (PCR)

PCR was used to amplify the sequence of interest or to introduce mutations. Reactions were carried out using Phusion High-Fidelity PCR Kit (New England Biolabs) following manufacturer's instructions. The reactions were performed in a T3000 Thermocycler (Biometra). The products are checked using agarose gel electrophoresis.

3.5.1.3 Agarose gel electrophoresis

Depending on the size of the DNA to be analyzed, 0.7 - 2% agarose gels were prepared in 1x TBE buffer (178 mM Tris-HCl pH 8.0, 178 mM boric acid, 4 mM EDTA). Agarose was melted in the TBE buffer and cooled to around 50 °C. Ethidium bromide was added to a final concentration of 0.05 µL/mL and poured into the casting tray with a comb. Samples are mixed in a 1:6 [v/v] ratio with loading dye (6x BX-DNA loading dye: 30% [v/v] glycerol, 0.125% [w/v] bromophenol blue, 0.125% [w/v] xylene cyanol FF), loaded into the well and separated at 120 V for 30 min to 1 h depending on the size of DNA molecules and percentage of agarose in the gel.

3.5.1.4 DNA extraction from agarose gels

DNA bands of interest were excised from the gels using scalpel blade under UV light at 365nm. DNA was extracted from the agarose gel using QIAquick Gel Extraction Kit (Qiagen) following manufacturer's instructions.

3.5.1.5 DNA purification:

To clean up the DNA after a digestion reaction and before a ligation reaction, QIAquick PCR purification (Qiagen) kit was used following the manufacturer's instructions.

3.5.1.6 DNA digestion and ligation

Restriction digestion was used to generate compatible ends in PCR products and plasmids before ligation or in order to validate recombinant plasmids by restriction mapping. Restriction

digestions were carried out according to the enzyme manufacturer's recommendations. Ligations were carried out using T4 DNA Ligase (New England Biolabs) in 1x Ligase buffer with 1:3 molar ratio between the vector (usually 150 ng) and the insert in a final volume of 10 μ L for 1 h at room temperature and then transformed into chemically competent cells.

3.5.1.7 SLIC and Self-SLIC

SLIC was performed as described in Li & Elledge, 2007. In order to introduce mutations or generate truncations of the sequence of interest, SLIC reactions without insert were performed. This is referred to as self-SLIC. Briefly, the vector was amplified by PCR using mutagenic primers. 40 U of DpnI enzyme was added to 100 μ L of PCR reaction and incubated at 37°C for 1 h. The DNA was purified using QIAquick PCR purification (Qiagen) kit. Subsequently, 1 μ g of vector was treated with 0.5 U of T4 DNA polymerase in T4 ligase Buffer in 20 μ L at RT for 30 min. The reaction was stopped by adding 1/10 volume of 10mM dCTP and left on ice. Annealing reaction were set up with 150 ng of vector with 1x T4 ligase buffer in a final volume of 10 μ L and incubated at 37 °C for 30 min. 5 μ L of the annealed mixture was transformed into chemically competent E. coli cells.

3.5.1.8 Transformation in E. coli

Plasmids or ligation products are transformed into chemically competent E. coli cells. ~50-100ng of plasmid was added to 100 μ L of cells and incubated for 30 min on ice. Heat-shock was given at 42 °C for 90 s and placed on ice for 2 min. Immediately 500 μ L of sterile LB medium is added and the cells are incubated at 37 °C for 1 h. The cells are pelleted at 3000 rpm for 5 min and resuspended in 100 μ L of LB medium and plated on LB agar plate with the appropriate concentration of antibiotic.

3.5.1.9 Plasmid extraction

Plasmid extraction was performed using Plasmid Preparation Kits (Qiagen), depending on the culture scale, according to manufacturer's protocol. Typically, plasmids from 5-20 mL of culture was extracted using QIAprep Spin Miniprep Kit and eluted in the EB buffer (10 mM Tris-HCl, pH 8.5).

3.5.2 RNA Techniques

3.5.2.1 In vitro transcription using T7 polymerase

100 µg of linearized plasmid was in vitro transcribed with 37.5 µg of T7 RNA polymerase in 200 mM HEPES/KOH, pH 7.6, 30 mM Mg(OAc)₂, 2 mM spermidine, 40 nM DTT, 8.75 mM dNTPs, 0.4 mg/mL RNasin (Promega). Reactions were incubated for 4 h at 37 °C.

3.5.2.2 RNA purification by LiCl and EtOH/NaOAc precipitations

In order to purify mRNA from DNA and proteins, lithium chloride precipitations were performed by the addition of 800 µL of 6 M LiCl in a final volume of 1,600 µL. Reactions were vortexed and kept on ice for at least 30 min. After 30 min of centrifugation at 14,000 g at 4 °C, the pellet was washed with 500 µL of 70% ethanol. The pellet was resuspended in 100 µL RNase-free water. Ethanol precipitations were carried out by the addition of 100 µL 97% ethanol and 4 µL of 3 M sodium acetate. Reactions and wash steps were performed as for the LiCl precipitation. Finally, the pellet was resuspended in 20 µL of RNase-free water.

3.5.2.3 Determination of the mRNA concentration

RNA concentration was determined as follows: 1 µL of sample was diluted 1/10 into RNase-free water and absorbance at 260 nm was determined. RNA concentration was calculated on the basis that OD_{260nm} of 1 corresponds to 40 µg/mL RNA.

3.5.2.4 RNA agarose gel electrophoresis

Analytic RNA agarose gels were run to assess the mRNA quality. RNA molecules were separated on agarose gels containing 1.5 % agarose in freshly prepared RNase free 1x TBE buffer. Guanidinium isothiocyanate and ethidium bromide were added to the agarose gel to a final concentration of 20 mM and 0.05 µL/mL respectively. Before loading, samples were mixed in a 1:2 [v/v] ratio with RNA loading dye (ThermoFisher Scientific, 95% [v/v] formamide, 0.025% [w/v] SDS, 0.025% [w/v] bromophenol blue, 0.025% [w/v] xylene cyanol FF, 0.025% ethidium bromide [w/v], 0.5 mM EDTA) and incubated for 10 min at 70 °C to remove secondary structures. Electrophoresis was carried out at 70 V for 45 min.

3.5.2.5 Test for contamination by RNases

To test protein preparations for contaminating RNases, 100 ng of mRNA was incubated alone or with 2 - 5 pmoles of protein in a final volume of 10 µL at 37 °C for 1h followed by RNA agarose gel electrophoresis as described above. The presence of RNases in the protein sample would

result in degradation of the mRNA, as indicated by a diminution of the full size mRNA band and the appearance of lower molecular weight bands (smear) after gel electrophoresis.

3.5.2.6 mRNA Capping using purified VCE and ScriptCap m⁷G Capping System

To remove potential secondary structures, the uncapped mRNA was denatured at 65 °C for 10 min and transferred immediately on ice. VCE and mRNA were mixed in a 1:2 ratio in 1x Script Capping Buffer (Epicentre Biotechnologies) supplemented with 1 mM GTP and 0.1 mM S-adenosylmethionine (SAM) final concentration. The reactions were incubated for 45 min at 37 °C, frozen in liquid nitrogen and stored at -80 °C, if not used immediately.

3.5.3 Cell Culture

3.5.3.1 E. coli expression

Plasmids were transformed into either chemically competent BL21* (DE3, C43) cells. 20 mL cultures were grown overnight at 37 °C from a single colony in LB medium containing the essential antibiotic. 1 liter of LB medium containing the antibiotic was inoculated with 10 mL of overnight culture and grown until OD₆₀₀=0.6 was reached. The expression was induced by addition of 0.5 mM IPTG at 18 °C and continued overnight. The cells were harvested by centrifugation at 5,500 rpm and 4 °C for 20 min using a JA8.1000 rotor.

3.5.3.2 Insect cell culture expression:

Proteins were expressed in SF21 insect cells using the MultiBac system as described in (Fitzgerald et al. 2006). Briefly, SF21 insect cells were transfected with a recombinant bacmid isolated from DH10-EMBacY cells and grow into Sf-900 media (ThermoFisher Scientific) (Bieniossek et al. 2008). V0 virus was produced in a 6-well plate with 3 mL of culture per well. This virus was used to generate a higher titer V1 virus by infection of 25 mL SF21 cell cultures in a shaker flask. The V1 virus was used for large scale protein production by infection of 400 mL of Hi5 insect cells in Express-Five medium (ThermoFisher Scientific) in 2 L flasks. The cells were harvested 72-96 h following the day of proliferation arrest (DPA) when the expression of the internal expression reporter, yellow fluorescent protein (YFP), was maximal. The cells were harvested by centrifugation at 1,000 x g in a JA8.1000 rotor for 10 min at 4 °C.

3.5.4 Protein Biochemistry

3.5.4.1 Denaturing polyacrylamide gel electrophoresis

Proteins were separated according to their size and resolution range using denaturing sodium dodecyl sulfate polyacrylamide gel electrophoresis (SDS-PAGE). Gels ranging from 10-15% were casted using a Mini-PROTEAN 3 Multi-Casting Chamber (Bio-Rad) using standard protocols (separating gel: 10-15% Acrylamide/Bisacrylamide (30%/0.8% [w/v]), 0.375 M Tris-HCl pH 8.8, 0.1% SDS, 1% APS, 0.5% TEMED; stacking gel: 2.5% Acrylamide/Bisacrylamide (30%/0.8% [w/v]), 0.25 M Tris-HCl pH 6.8, 0.1% SDS, 1% APS, 0.5% TEMED). Before electrophoresis, samples were mixed 1:4 with 4x loading dye (200 mM Tris-HCl pH 6.8, 8% [w/v] SDS, 40% glycerol, 4% [v/v] β -ME, 50 mM EDTA and 0.08% [w/v] bromophenol blue) and denatured at 95 °C for 2 min. Electrophoresis was performed at 150-200 V in running buffer (25 mM Tris-HCl, 192 mM Glycine, 0.1% [w/v] SDS) in a 2-gel vertical electrophoresis system (Bio-Rad). The protein bands were visualized with Coomassie staining (40% [v/v] Ethanol, 10% [v/v] acetic acid and 0.2% [w/v] Coomassie Brilliant Blue G-250). Gels were destained to remove background staining with 5% [v/v] Ethanol and 7.5% [v/v] acetic acid.

3.5.4.2 Western Blotting

The PVDF membrane (Millipore) was activated in 100% methanol for few seconds. Proteins from the SDS-PAGE were transferred to the membrane in transfer buffer (25 mM Tris-Base, 192mM Glycine, 20% EtOH) at 25 V for 1 h using a Trans-Blot SD Semi-Dry Transfer Cell (Bio-Rad). Non-specific interactions were reduced using blocking buffer consisting of 3% BSA in PBS buffer (137 mM NaCl, 2.7 mM KCl, 1 mM Na₂HPO₄, 1.8 mM KH₂PO₄, pH 7.4) supplied with 0.05% [v/v] Tween-20 for at least 1 h at room temperature. The membrane was incubated with the appropriate dilution of antibody or Streptavidin or Strep-Tactin in PSB+0.05% Tween-20 with 0.75% BSA. Streptavidin coupled with Horseradish Peroxidase (HRP) (Sigma) and Strep-Tactin coupled with Alkaline Phosphatase (AP) (IBA Lifesciences) were diluted 1/4000 and incubated for 1 h. His-tagged proteins were detected using 1/10,000 dilution of mouse monoclonal anti-polyHistidine antibody coupled to AP. After washing in PBS+0.05% Tween-20 for 3 times 15 min, blots with AP were developed using BCIP/NBT photoreaction solution (100 mM Tris-HCl, 100 mM NaCl, 5 mM MgCl₂, 1% [v/v] BCIP/NBT(Roche), pH 8.8). Western blots with HRP were developed using 3,3'-Diaminobenzidine tablets (Sigma) in 1 mL of ultrapure water.

3.6 Published Work

PABP enhances release factor recruitment and stop codon recognition during translation termination

PABP enhances release factor recruitment and stop codon recognition during translation termination

Alexandr Ivanov^{1,2}, Tatyana Mikhailova¹, Boris Eliseev³, Lahari Yeramala³,
Elizaveta Sokolova¹, Denis Susorov^{1,2}, Alexey Shuvalov¹, Christiane Schaffitzel^{3,4,*} and
Elena Alkalaeva^{1,*}

¹Engelhardt Institute of Molecular Biology, the Russian Academy of Sciences, 119991 Moscow, Russia, ²Faculty of Bioengineering and Bioinformatics, M.V. Lomonosov Moscow State University, 119992 Moscow, Russia, ³European Molecular Biology Laboratory, Grenoble Outstation, 71 Avenue des Martyrs, 38042 Grenoble, France and ⁴School of Biochemistry, University of Bristol, BS8 1TD, UK

Received November 25, 2015; Revised June 30, 2016; Accepted July 1, 2016

ABSTRACT

Poly(A)-binding protein (PABP) is a major component of the messenger RNA–protein complex. PABP is able to bind the poly(A) tail of mRNA, as well as translation initiation factor 4G and eukaryotic release factor 3a (eRF3a). PABP has been found to stimulate translation initiation and to inhibit nonsense-mediated mRNA decay. Using a reconstituted mammalian *in vitro* translation system, we show that PABP directly stimulates translation termination. PABP increases the efficiency of translation termination by recruitment of eRF3a and eRF1 to the ribosome. PABP's function in translation termination depends on its C-terminal domain and its interaction with the N-terminus of eRF3a. Interestingly, we discover that full-length eRF3a exerts a different mode of function compared to its truncated form eRF3c, which lacks the N-terminal domain. Pre-association of eRF3a, but not of eRF3c, with pre-termination complexes (preTCs) significantly increases the efficiency of peptidyl–tRNA hydrolysis by eRF1. This implicates new, additional interactions of full-length eRF3a with the ribosomal preTC. Based on our findings, we suggest that PABP enhances the productive binding of the eRF1–eRF3 complex to the ribosome, via interactions with the N-terminal domain of eRF3a which itself has an active role in translation termination.

INTRODUCTION

Poly(A)-binding protein (PABP) is one of the major mRNA-interacting proteins in eukaryotes. The protein is widespread and highly conserved among animals. Seven

isoforms of PABP were identified in humans; the most abundant is the cytoplasmic isoform PABPC1 (1). The N-terminal domain of PABP contains four RNA recognition motifs (RRMs) (Figure 1A) each binding 12 adenines, while the whole protein covers 27 adenines (2,3). RRM1 and RRM2 are required for the specific recognition of poly(A) stretches, whereas RRM3 and RRM4 can associate with any RNA. RRM domains 1–4 bind the poly(A) tail from 3' to 5' (4). One of the main functions of the PABP is the protection of the poly(A) tail of cellular mRNAs from nuclease degradation (5). Besides, the protein can associate with other extensive poly(A) stretches like those occurring in certain 5' untranslated regions (5'UTRs) that impact on translation initiation (6).

RRM1 and RRM2 of PABP bind to the N domain of eukaryotic translation initiation factor (eIF) 4G (7). Thus, PABP's interactions with poly(A) and eIF4G together cause the formation of the 5' cap-eIF4E-eIF4G-PABP-poly(A) complex where the 5' and 3' ends of mRNA approach each other to form the closed-loop structure (8). Proximity of the mRNA ends in the closed-loop structure is considered to facilitate the reinitiation of translation, since ribosomes are more easily engaged in the next round of initiation after termination (9). Also, the interaction between eIF4G and PABP is reported to increase the affinity of cap-binding factor eIF4E for the mRNA m⁷G cap (10,11). Thus, PABP can be regarded as a translation initiation-stimulating factor.

The C-terminal domain of PABP (CTC) is joined with the RNA-binding part of the protein by an unstructured proline-rich, ~100 amino acid-long linker. The CTC binds proteins containing PAM2 motifs. Specifically, the PAM2 motif is found in the two main PABP regulators: polyadenylate-binding protein-interacting proteins (Paip) 1 and 2. Paip1 stimulates the activity of PABP in translation initiation (12). Paip1 comprises PAM1 and PAM2 motifs which interact with the N and C-terminal domains of

*To whom correspondence should be addressed. Email: alkalaeva@eimb.ru
Correspondence may also be addressed to Christiane Schaffitzel. Email: schaffitzel@embl.fr

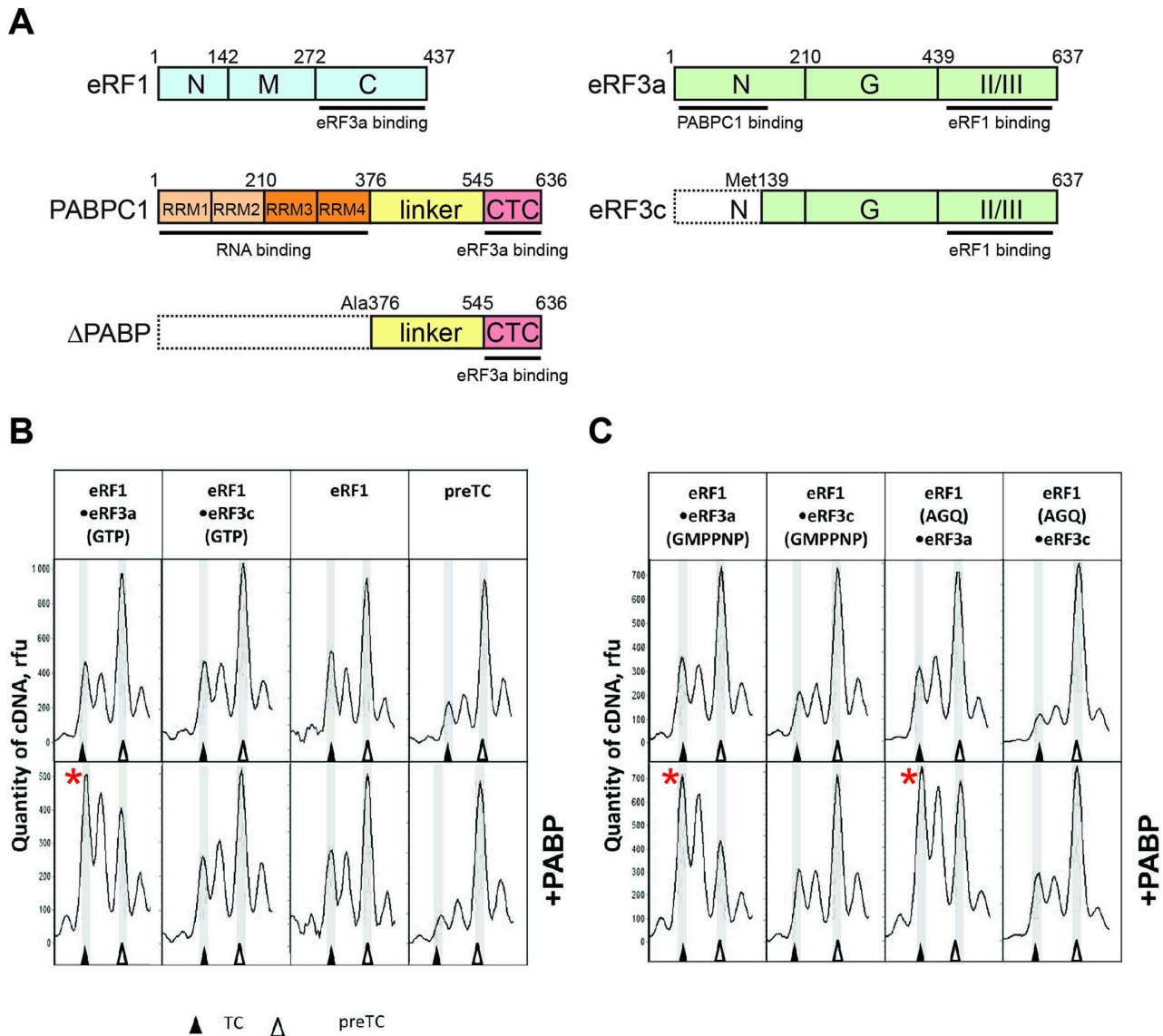


Figure 1. PABP increases the stop codon recognition by release factors. (A) A schematic representation of the release factors and PABP constructs used in this study. Domains involved in protein-protein interactions are indicated. Domains are color-coded and assigned functions and interaction partners are depicted at the corresponding position below the domain. Numbers above represent amino acid positions. (B and C) Toe-print analysis of termination complexes (TCs) formed by addition of the preTCs (B) of eRF1•eRF3a•GTP, eRF1•eRF3c•GTP, eRF1 and PABP; and of (C) eRF1•eRF3a•GMPPNP, eRF1•eRF3c•GMPPNP, eRF1(AGQ)•eRF3a•GTP, eRF1(AGQ)•eRF3c•GTP and PABP. Release factor complexes were associated before addition to the preTCs. Rfu—relative fluorescence unit. Positions of preTCs and TCs are labeled by white and black triangles respectively. Red stars mark the samples where stop codon recognition is enhanced.

PABP respectively. Moreover, Paip1 interacts with eIF3g and eIF4A (13) to form Paip1-eIF3-eIF4G and Paip1-PABP-eIF4G complexes, which increase the stimulatory effect of PABP in translation initiation. In contrast, Paip2 is a repressor of translation initiation (14). Paip2 also contains PAM1 and PAM2 motifs, but complex formation decreases PABP's affinity to the poly(A) tail and to eIF4G, leading to a disruption of the closed-loop structure (15).

Similar to Paip1/2, the eukaryotic release factor 3 (eRF3) contains a PAM2 motif that recognizes the CTC domain of PABP (16). eRF3 is one of two factors required for translation termination (17,18). eRF3 comprises an unstructured N-terminal domain, a G domain which binds nucleotides,

as well as II and III domains which interact with the second essential termination factor eRF1 (Figure 1A) (19). The PAM2 motif of human eRF3 is composed of two mini-domains, PAM2.1 and PAM2.2. These mini-domains are highly conserved among higher eukaryotes, while the remaining sequence of the N-terminal domain is highly variable (20). The PAM2.2 mini-domain of human eRF3 has a higher affinity for PABP when compared with the PAM2.1 mini-domain (21).

The II and III domains of eRF3 interact with the C-terminal domain of eRF1, leading to a conformational change in eRF1 (22). When eRF1 recognizes a stop codon (UAG, UAA, UGA) (23), which is the first step

of translation termination, eRF3 hydrolyzes guanosine-5'-triphosphate (GTP). This results in a conformational rearrangement of eRF1 (18): The M domain of eRF1 enters the A-site of the large ribosomal subunit and reaches into the peptidyl-transferase center (PTC). The second step of translation termination, which is peptidyl-tRNA hydrolysis, is thereby triggered (24). Two human isoforms of eRF3 exist: eRF3a and eRF3b, encoded by different genes (GSPT1 and GSPT2) (25,26). The main isoform is most likely eRF3a which is ubiquitously expressed; in contrast, eRF3b expression is tissue-specific (27). eRF3a and eRF3b differ with respect to their N domains, but both proteins have conserved PAM2.1 and PAM2.2 motifs and thus are able to bind PABP.

PABP has been suggested to have a stimulatory effect on translation termination and was shown to interfere with nonsense-mediated mRNA decay (NMD) (28). Most likely, PABP exerts its function in a position-dependent manner (29,30). Normal stop codons are usually positioned in the last exon of the mRNA, followed by a relatively short 3' untranslated region (3' UTR). In contrast, in the case of a premature stop codon which elicits NMD a long 3'UTR and/or an exon junction complex (EJC) is present. This leads to a larger distance between the terminating ribosome and the PABP bound to the poly(A) tail. In the latter case, NMD factors can interact with the terminating ribosome and initiate the assembly of the mRNA decay-inducing complex. PABP was tethered to the mRNA such that it was positioned closer to the stop codon and upstream of an EJC (29,30). It was shown that this led to suppression of NMD (30,31). Evidence for a stimulatory effect of PABP on translation termination is indirect: It is based on *in vivo* experiments where it was found that stop codon readthrough is increased when PABP is knocked down (29).

The effect of the PABP analog in yeast (Pab1) on translation termination is controversial: On the basis of indirect data Pab1 is thought to decrease termination (32). However, overexpression of Pab1 in yeast strains is suggested to activate termination of translation (33).

The molecular mechanism of PABP's function in termination is enigmatic. Here, we characterize the impact of cytoplasmic human PABP (PABPC1, referred to as PABP here) on translation termination using an *in vitro* reconstituted mammalian translation system. We show that PABP directly stimulates stop codon recognition *in vitro* and that this function is independent of its RNA-binding activity. The termination stimulation effect is most likely caused by the optimal positioning of eRF3a on the ribosome, increasing the efficiency of eRF1 to recognize stop codons and to catalyze peptidyl-tRNA hydrolysis in the PTC.

MATERIALS AND METHODS

Ribosomal subunits and translation factors

The 40S and 60S ribosomal subunits, as well as eukaryotic translation factors eIF2, eIF3, eIF4F, eEF1H and eEF2, were purified from rabbit reticulocyte lysate as described (18). The human translation factors eIF1, eIF1A, eIF4A, eIF4B, eIF5B, eIF5, PABP, Δ PABP lacking RRM1—RRM4 motifs (first 375 amino acids residues),

eRF1, eRF1(AGQ) and eRF3c lacking the N-terminal domain (138 amino acid residues including PAM2) were produced as recombinant proteins in *Escherichia coli* strain BL21 and subsequently purified via Ni-NTA agarose and ion-exchange chromatography (18).

Expression and purification of human eRF3a

Human full-length eRF3a (GSPT1) was cloned into the pFastBac-Htb vector (Life Technologies) and expressed in insect cells Sf21 using the EMBAcy baculovirus from the MultiBac expression system (34). Cells were lysed by sonication in 20 mM Tris-HCl pH 7.5, 100 mM KCl, 6 mM β -mercapthoethanol, 0.1% Tween-20 and 5% glycerol supplemented with protease inhibitors. eRF3a was purified by affinity chromatography using a HisTrap HP column (GE Healthcare) followed by anion-exchange chromatography using a MonoQ column (GE Healthcare). In the final size-exclusion chromatography step (Superdex-200 column, GE Healthcare) using 20 mM Tris-HCl pH 7.5, 100 mM KCl, 6 mM β -mercapthoethanol, 0.1% Tween-20 and 5% glycerol, the protein elutes as a monomer.

In vitro transcription of mRNA

The mRNA was transcribed *in vitro* using T7 RNA polymerase. The MVHL-stop plasmid contains a T7 promoter, four CAA repeats, the β -globin 5'-UTR, open reading frame (encoding for the peptide MVHL), followed by the UAA stop codon with the various next base (U,A,G,C) and a 3'-UTR comprising the rest of the natural β -globin coding sequence (35). For run-off transcription the MVHL-stop plasmid was linearized by restriction digest with XhoI. The MVHC-polyA plasmid contains a T7 promoter, four CAA repeats, an MVHC open reading frame followed by an UAA stop codon, the complete human β -globin 3'-UTR and polyA tail (70 nucleotides). For run-off transcription mRNA plasmids were linearized with EcoRI.

Pre-termination complex assembly and termination analysis

Pre-termination complexes (preTCs) were assembled *in vitro* as described (36) and used in peptide release assays and conformational rearrangement analyses by toe-print assays (37). For peptide release assays aliquots containing 0.2 pmol of the preTCs were incubated at 37°C for 3 min with 0.6 pmol of eRF1/3 and 5 pmol of PABP. For conformational rearrangement analyses aliquots containing 0.2 pmol of the preTCs were incubated at 37°C for 15 min with 0.6 pmol of eRF1/3 and 5 pmol of PABP or 7 pmol of Δ PABP. In case of preTC assembly in the presence of PABP—18 pmol MVHC-polyA and/or 18 pmol MVHL mRNA were used and incubated with 80 pmol PABP at 37°C for 2 min before preTC formation. For toe-print assay of MVHL and MVHC-polyA mRNAs, 5'-FAM labeled toe-primers 1 (5'-GCATGTGCAGAGGACAGG-3') and 2 (5'-GCAATGAAAATAAATTCC-3') were used respectively.

preTC binding assay

Purified preTCs (160 μ l) were incubated with 3.5 pmol eRF1(AGQ), 10 pmol eRF3a or eRF3c, 200 pmol PABP

in buffer with 0.2 mM GTP and with 0.2 mM MgCl₂ at 37°C for 10 min (37). Pre-incubation of PABP with eRF3 was performed to exclude a preliminary binding of eRF3 with eRF1, which can decrease the termination activity of eRFs (Figure 3). The reaction volume was 500 μl. Subsequently, TCs were incubated with 1% formaldehyde at 4°C for 1 h (38). Glycine was added up to 0.1 M to stop the cross-linking reaction. The TCs were purified in a 10–30% (w/w) linear sucrose density gradient (SDG) as described above. The gradients were fractionated into 14 equal fractions followed by precipitation in 10% trichloroacetic acid (TCA). The protein pellets were dried and analyzed by western blot.

RESULTS

PABP stimulates stop codon recognition activity of release factors

PABP and eRF3a were shown to interact directly (16). Therefore, we decided to determine how PABP affects the activity of eRF3a and eRF1 in translation termination. In the presence of PABP, both release factors were added to preTCs which were assembled *in vitro* from individual components on the MVHL mRNA and purified by SDG centrifugation. We then performed toe-print analyses of the ribosomal complexes in order to assess stop codon recognition and termination complex (TC) formation. In Supplementary Figure S1, we show examples of raw data of the toe-print analyses, obtained by capillary electrophoresis of cDNA products generated with fluorescently labeled primers. During stop codon recognition of eRF1, the ribosome protects additional nucleotides on the mRNA, which can be detected in toe-printing assays as a two-nucleotide shift of the ribosomal complex (18,39,40).

Our preTCs contain a UAA stop codon in the ribosomal A-site. Addition of release factors leads to the appearance of a peak, corresponding to the TC. For our experiments, we applied limiting concentrations of release factors (0.6 pmol of eRF1 and eRF3a/c) such that the 2-nt shift of the ribosomal complex was rather inefficient. This allowed us to detect any enhancement of release factor activity in the presence of PABP.

Addition of 5 pmol PABP, release factors and GTP to the preTCs significantly increases the 2-nt shift, i.e. PABP stimulates stop codon recognition (Figure 1B). This stimulatory effect is specific, as it is observed only after the addition of full-length eRF3 (eRF3a) to the reaction: the N-terminally truncated version, eRF3c, which is unable to bind PABP does not show any stimulation of stop codon recognition. Moreover, the stimulatory effect of PABP is not observed in the absence of release factors, or in the presence of eRF1 only (Figure 1B). Addition of PABP to the preTCs in the presence of higher amounts of eRFs (5 pmol of each, corresponding to a 25-fold molar excess of eRFs over preTCs) also stimulates stop codon recognition, but the effect is rather weak (Supplementary Figure S1B).

Our model MVHL mRNA contains an uracil nucleotide (U) in the +4 position after the stop codon. Recently, it was shown that eRF1 binding to a stop codon in the decoding site leads to a conformational change in the 18S rRNA which pulls the +4 nt into the decoding site (39,40). This compaction due to mRNA U-turn motif formation

is the basis of stop codon recognition by eRF1. It pulls downstream mRNA further into the mRNA channel and thus provides an explanation for the toe-printing peak shift, which is observed upon TC formation (Figure 1B) (39,40). We tested the effect of the stop codon context on stimulation of stop codon recognition by PABP: we generated three additional model mRNAs with the various nucleotides (adenine, guanine and cytosine) in the fourth position. We assembled preTCs on these mRNAs and used them for toe-printing assays in the presence and absence of PABP (Supplementary Figure S2). We found that in all possible contexts of the UAA stop codon, PABP equally stimulates stop codon recognition.

Notably, the same stimulatory effect of PABP on stop codon recognition is observed when a non-hydrolysable analog of GTP (GMPPNP) is added to the reaction (Figure 1C). Similarly, PABP stimulates stop codon recognition in the presence of eRF3a and an AGQ mutant of eRF1 (eRF1(AGQ)), which is unable to hydrolyze peptidyl-tRNA (Figure 1C). We conclude that PABP activates TC formation independently of GTP or peptidyl-tRNA hydrolysis. This suggests that the stimulatory effect of PABP on translation termination occurs when the release factors bind to the ribosome and recognize the stop codon.

PABP stimulates stop codon recognition as a cis- and trans-acting factor

We demonstrate in Figure 1 that PABP activates stop codon recognition on the model mRNA lacking a poly(A) tail (MVHL). However, within cells, most molecules of PABP are bound to the poly(A) tail of mRNAs. Therefore, we decided to investigate whether the poly(A) binding of PABP affects its stimulation of translation termination. Therefore, we used MVHC-polyA mRNA which contains the same leader sequence as MVHL mRNA (but a different coding sequence (MVHC)), as well as an UAA stop codon followed by the β-globin 3'UTR and by the poly(A) tail. Different 3'UTRs were used to distinguish cDNA products produced by toe-printing primers 1 and 2 in the mixture of mRNAs (see below).

The MVHC-polyA mRNA was first incubated with PABP and then used for preTC assembly (Figure 2A). Subsequently, the preTCs were purified by SDG centrifugation, subjected to termination reactions and tested in toe-printing assays. We speculate that the different 3'UTR sequence in the MVHC-polyA mRNA leads to a different mobility of the corresponding cDNAs, and TC formation is detected as +1 nt toe-print shift for the MVHC-polyA construct (Figure 2A, B and Supplementary Figure S3). The addition of release factors to preTCs, assembled on MVHC-polyA mRNA and incubated with PABP, results in a more efficient stop codon recognition of the eRF1•eRF3a complex compared to the eRF1•eRF3c complex (Figure 2A). In the absence of PABP, the activities of eRF3a and eRF3c in stop codon recognition are very low and almost equal using the MVHC-polyA construct and limiting amounts of eRFs (Supplementary Figure S3). As a control, we assembled preTCs on MVHL mRNA in the presence of PABP and found almost no differences in stop codon recognition in the presence of eRF3a ver-

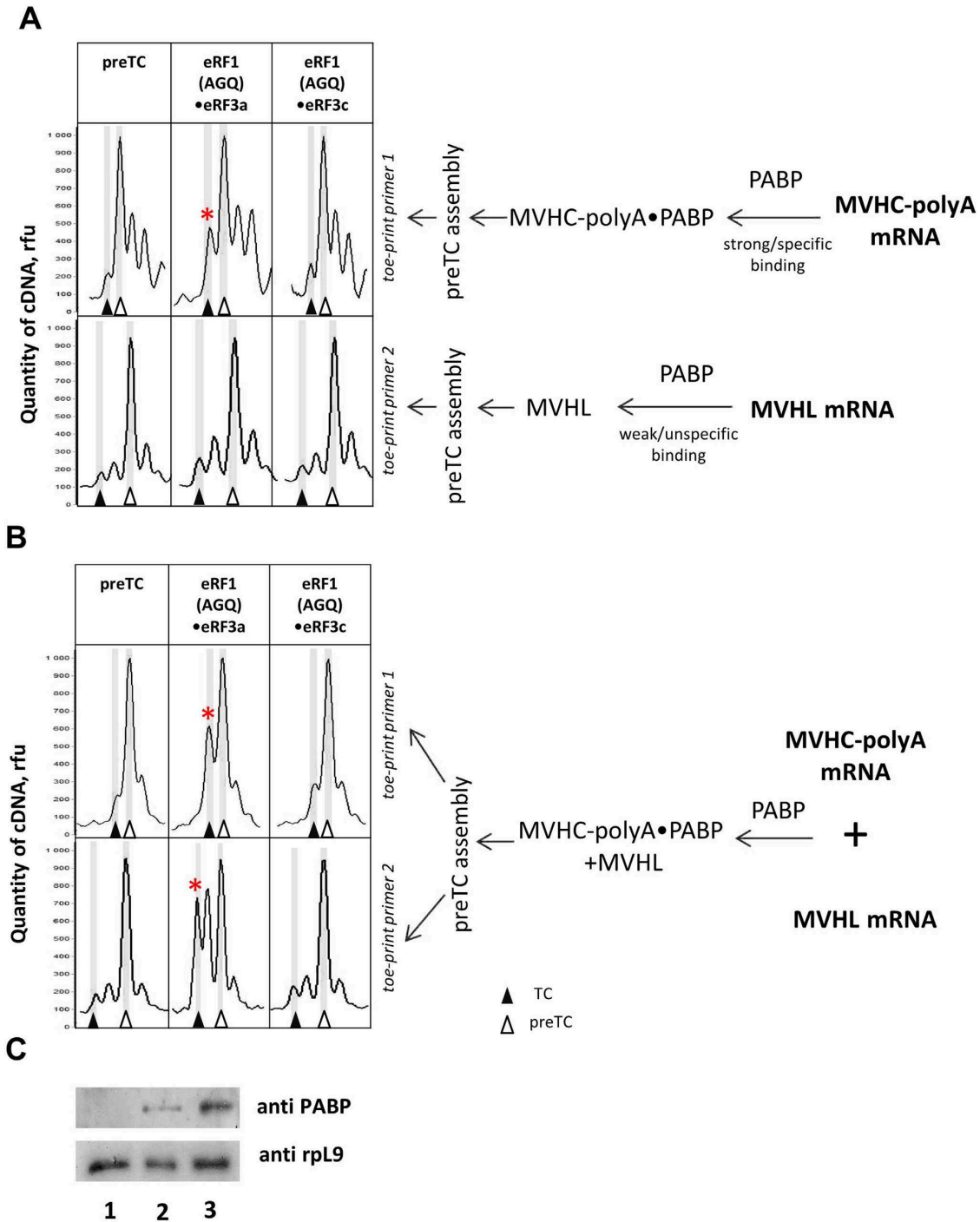


Figure 2. PABP increases the stop codon recognition by release factors in *cis* and *trans*. Toe-print analysis of TCs formed by addition to the preTCs of eRF1(AGQ)•eRF3a•GTP or eRF1(AGQ)•eRF3c•GTP. (A) MVHC-polyA or MVHL mRNAs were incubated with PABP separately and used for reconstitution of preTCs. (B) The mixture of MVHC-polyA and MVHL mRNAs was incubated with PABP and used for reconstitution of preTCs. Release factor complexes were associated before addition to preTCs. Rfu—relative fluorescence unit. Positions of preTC and TC are labeled by white and black triangles respectively. (C) Western blot analysis of fractions after SDG of preTCs assembled on the mixture of MVHL and MVHC-polyA (lane 1), MVHL (lane 2) or MVHC-polyA (lane 3) mRNAs in the absence (lane 1) or presence (lanes 2 and 3) of PABP. Stars mark the samples where stop codon recognition is enhanced.

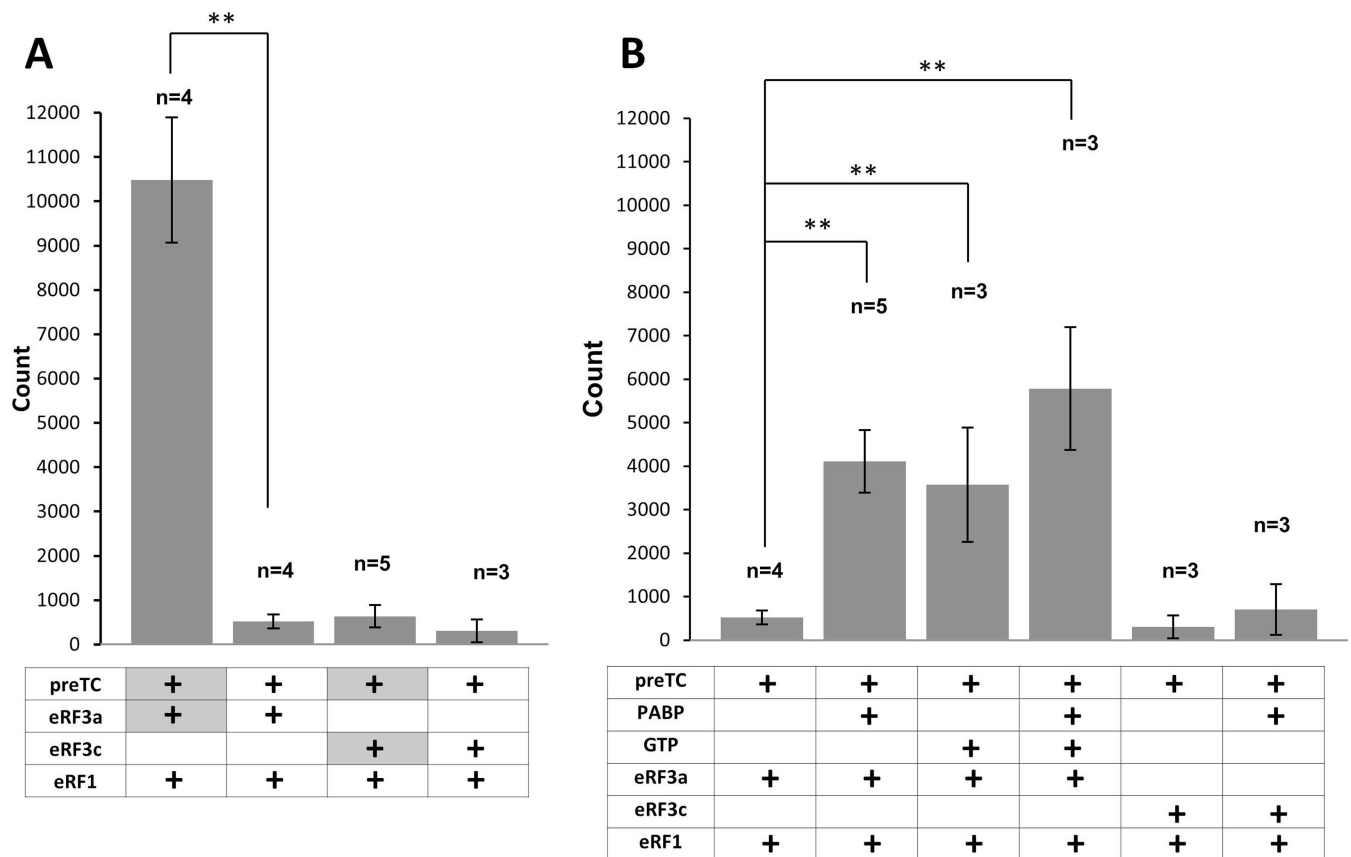


Figure 3. PABP increases the efficiency of peptidyl-tRNA hydrolysis in the presence of release factors. (A) Hydrolysis of peptidyl-tRNA induced by the addition of eRF1 and eRF3 or their preformed complexes. GTP was added first to the reaction. (B) Hydrolysis of peptidyl-tRNA induced by the eRF1•eRF3a or eRF1•eRF3c complexes in the presence/absence of PABP. In experiments 1, 2, 5 and 6, GTP was added to preTCs before the eRFs. In most cases proteins added to the preTCs were pre-associated. The only exceptions are the experiments in panel 3A (lines 1 and 3), where eRF3a/c were pre-incubated with the preTC first (highlighted in gray). n corresponds to the number of measurement repeats. The stars (**) mark a significant difference from the respective control $P < 0,01$.

sus eRF3c (Figure 2A). Moreover, the efficiency of stop codon recognition was similar, irrespective of incubation of MVHL mRNA with PABP (Supplementary Figure S3 and Figure 2A). Western blot analysis of the SDG-purified preTCs shows that PABP binds only very weakly to preTCs assembled on MVHL mRNA and more efficiently binds to the PreTCs assembled on MVHC-poly(A) mRNA (Figure 2C, compare lanes 2 and 3). Thus, the amount of PABP unspecifically bound to MVHL mRNA is apparently not sufficient to detectably activate translation termination (Figure 2A). Taken together, these experiments show that PABP remained bound to the MVHC-poly(A) mRNA during SDG (Figure 2C) and stimulated stop codon recognition in *cis* by interaction with the N-terminal domain of eRF3a.

To test whether PABP can also act in *trans*, MVHC-poly(A) mRNA was mixed with equal amounts of MVHL mRNA and incubated with PABP. After preTC assembly and SDG purification, translation termination reactions were performed followed by toe-printing assays (Figure 2B). The toe-printing results show that stop codon recognition is enhanced for both preTCs. Thus, PABP bound to the poly(A) tail of MVHC-poly(A) mRNA is able to stimulate termination on the own mRNA (i.e. in *cis*) and on preTCs with MVHL mRNA (e.g. in *trans*) (Figure 2B). The ob-

served stimulation is specific because it depends on the presence of the N-terminal domain of eRF3a and accordingly is not observed for eRF3c.

PABP increases peptidyl-tRNA hydrolysis by the release factors

To test whether PABP also affects the peptidyl-tRNA hydrolysis reaction we assembled preTCs on the MVHL mRNA using S^{35} -labeled initiator-tRNA. The efficiency of peptidyl-tRNA hydrolysis was determined by quantification of the radioactive MVHL peptide released from the ribosomal complexes. We observed that the efficiency of peptide release depends on the order of addition of release factors to the preTCs. Incubation of eRF3a with the preTCs and GTP, followed by addition of eRF1, causes effective termination. In contrast, addition of the pre-associated complex of eRF1 and eRF3a to the preTCs decreases termination efficiency by a factor of ~20 (Figure 3A compare lanes 1 and 2). In the same experiment using eRF3c, the efficiency of termination does not depend on the order of factor addition and the peptide release measured after pre-incubation with eRF3c with preTCs, followed by eRF1 addition was virtually identical to the addition of the pre-

associated eRF1•eRF3c complex or eRF1•eRF3a complex to preTCs (Figure 3A compare lanes 2,3,4). Thus, the observed high efficiency of peptide release requires the N-terminal part of eRF3a.

Pre-association of PABP with the eRF1•eRF3a complex stimulates peptidyl-tRNA hydrolysis by approximately 8-fold (Figure 3B, lanes 1 and 2). In contrast, incubation of PABP with the eRF1•eRF3c complex does not significantly affect the efficiency of peptide release (Figure 3B, lanes 5 and 6). We found that the optimal condition for translation termination is the addition of eRF1 after the pre-incubation of eRF3a with the preTCs. Under these conditions, PABP does not change the efficiency of peptide release (Supplementary Figure S4B). However, when we use limiting concentrations of eRFs (three times lower) and the same order for the addition of release factors, the level of peptide release diminishes significantly. Under these sub-optimal conditions, PABP exerts a stimulating effect on termination and increases the efficiency of peptidyl-tRNA hydrolysis ~2-fold (Supplementary Figure S4B). In summary, PABP has a stimulatory effect when the termination efficiency is reduced, for instance due to limiting eRF concentrations or due to the formation of eRF1•eRF3a complexes which seem to be less active in termination.

Notably, pre-association of GTP with eRF1•eRF3a increases the efficiency of peptide release (Figure 3B, lane 3). Formation of eRF1•eRF3a•GTP•PABP complexes also results in a pronounced, 11-fold stimulatory effect on translation termination indicating a moderate additional stimulatory effect compared to eRF1•eRF3a•GTP complexes (7-fold) or eRF1•eRF3a•PABP complexes (8-fold) (Figure 3B, compare lane 4 to lanes 2 and 3).

The C-terminal domain of PABP is essential for improved efficiency of stop codon recognition

We generated an N-terminally truncated PABP protein (Δ PABP) lacking the four RRMs which are necessary to bind mRNA (Figure 1A). The deletion of the RNA-binding motifs of PABP allows assessing whether the RRMs are required for stop codon recognition. Δ PABP comprises the unstructured proline-rich linker and the CTC domain which is able to interact with PAM2 motif of eRF3a (41). To determine an effect of Δ PABP on stop codon recognition, we performed toe-printing assays with reconstituted preTCs on MVHL mRNA. We observed that Δ PABP also promoted stop codon recognition upon addition to eRF1 and eRF3a, although less efficiently than the full-length PABP, requiring high Δ PABP concentrations to achieve a visible effect (compare Figures 1B and 4). The stimulatory effect on stop codon binding can be reproduced in the presence of GMPPNP, which was added instead of GTP (Figure 4). These experiments indicate that the C-terminal part of PABP is required for stimulation of stop codon recognition.

PABP promotes binding of eRF3a to preTCs

In order to study how PABP affects the interaction of release factors with ribosomes and improves stop codon recognition we tested the ability of this protein to bind preTCs in the presence or absence of eRFs (Figure 5).

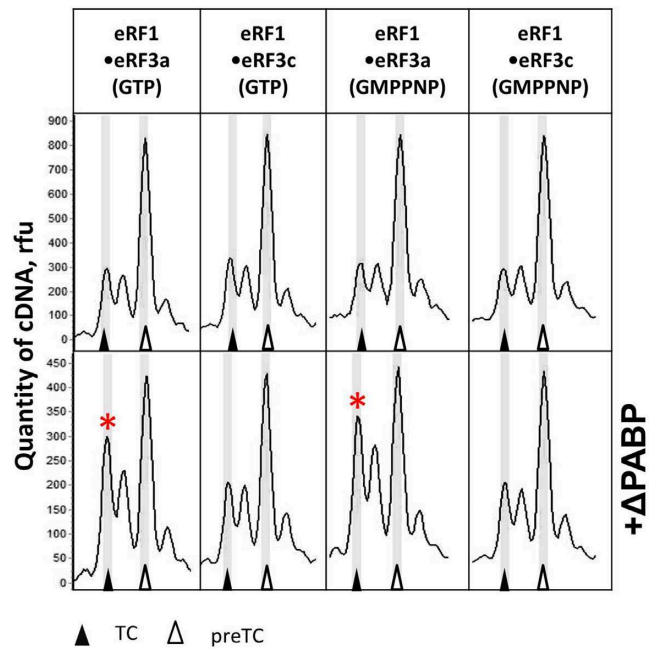


Figure 4. The C-terminal part of PABP (Δ PABP) stimulates stop codon recognition by release factors. Toe-print analysis of TCs formed in the presence of eRF1•eRF3a•GTP, eRF1•eRF3c•GTP, eRF1•eRF3a•GMPPNP, eRF1•eRF3c•GMPPNP in the absence (above) and presence (below) of Δ PABP. Release factor complexes were associated before addition to the preTCs. Rfu—relative fluorescence unit. Positions of preTCs and TCs are labeled by white and black triangles respectively. Red stars mark the samples where stop codon recognition is enhanced.

PreTCs were incubated with PABP, eRF1(AGQ), eRF3a or eRF3c, and GTP. Subsequently, the complexes were centrifuged into an SDG. After fractionation, the proteins were detected by western blotting. The eRF1(AGQ) mutant was used to stabilize TCs, since this mutant is able to bind the stop codon, but is inactive in peptide release. Therefore, it can stabilize the TCs.

PreTCs migrate in fractions 10–14 (Supplementary Figure S5A). To exclude aggregation of proteins in solution, we determined their distribution in the SDG in the absence of ribosomes (Supplementary Figure S5B). All proteins (eRF1, eRF3a, eRF3c and PABP and their complexes) are detected only in the top fractions of the gradient (fractions 1–5). PABP can interact with preTCs. However, the complex is likely low affinity and dissociates during SDG. Accordingly, PABP is found not only in fraction 1–3 (Supplementary Figure S5B), but also in fractions 4–9 in the presence of preTCs (Supplementary Figure S5C).

In the absence of PABP, both eRF3a and eRF3c do not form stable complexes with the preTCs, irrespective of the presence (Figure 5A) or absence of eRF1 (Figure 5B). The presence of PABP in the binding reactions stabilizes the binding of eRF3a to preTCs (Figure 5). In contrast, eRF3c is still not found in the preTC fractions despite the addition of PABP. This was expected because PABP does not interact with either eRF3c or eRF1. It is important to note that the interaction of eRF1(AGQ) with the preTCs is independent from the addition of PABP and from the eRF3 variant (full-length versus truncated).

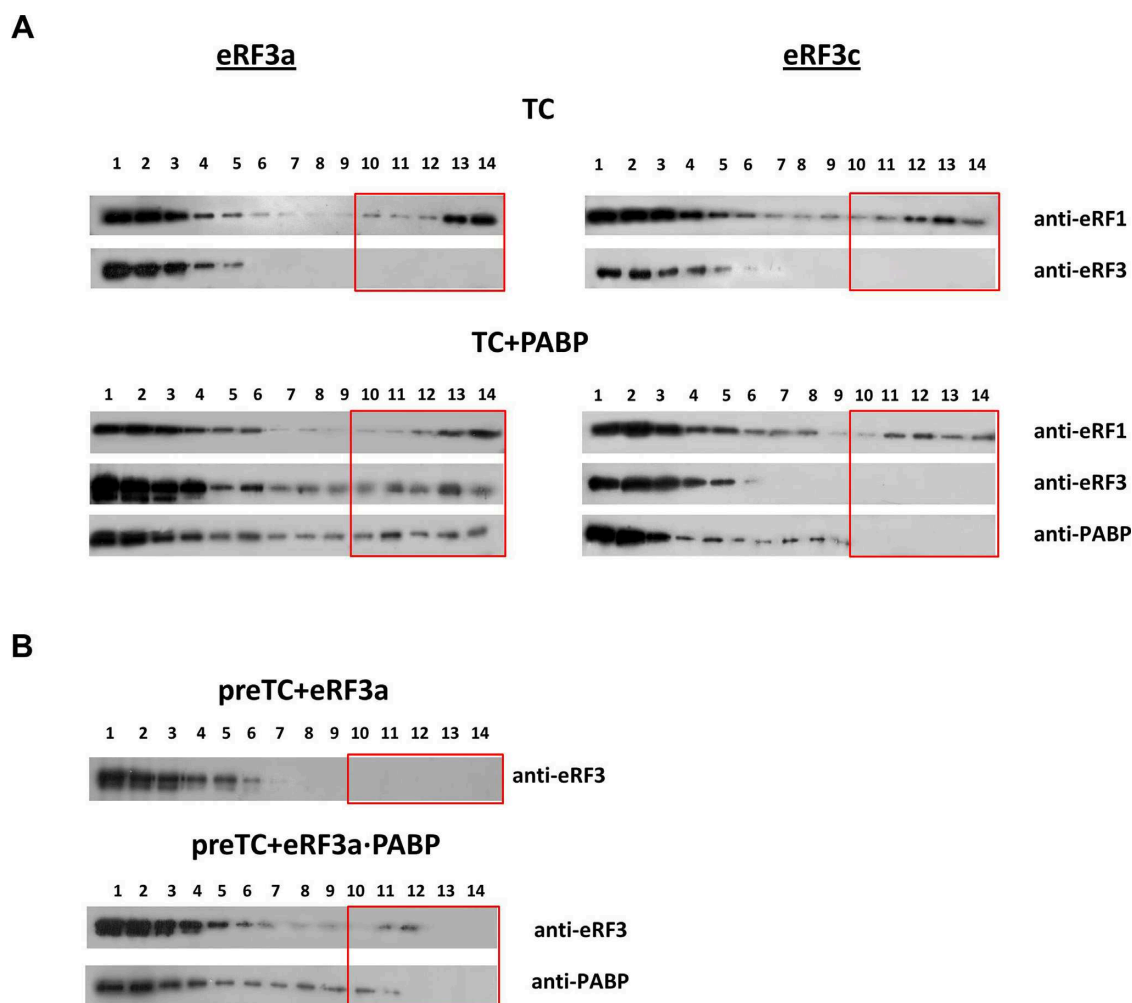


Figure 5. eRF3a and PABP bind preTCs cooperatively. (A) Western blot analysis of TC fractions after SDG of preTCs incubated with GTP, eRF1(AGQ) (upper panel) and eRF3a (left) or eRF3c (right) in presence of PABP (lower panel). Antibodies raised against eRF1, eRF3 and PABP were used for detection. (B) Western blot analysis of preTCs incubated with eRF3a + GTP (above) and eRF3a•PABP + GTP (below) using antibodies against eRF3 and PABP. The fractions of the SDG are indicated above the Western blots; fraction 1 corresponds to the top of the gradient, 14 to the bottom. Boxes indicate the fractions that contain ribosomal complexes.

We conclude that PABP stabilizes the binding of eRF3a to ribosomal complexes. This finding is in agreement with the stimulating effect of PABP on stop codon recognition and peptidyl-tRNA hydrolysis induced by the release factors (Figures 1 and 4).

DISCUSSION

PABP is an important player in eukaryotic translation and its control (42). The role of PABP in stimulation of translation initiation is well-established (10). However, the functions of PABP in translation are not limited to regulation of initiation. Several studies suggest that PABP interferes with NMD and that PABP deletion increases read-through of stop codons, thereby indirectly providing evidence for a role of PABP in stimulation of termination (29–31). Here we show, that PABP directly stimulates translation termination *in vitro*, confirming PABP's role as a regulatory factor in translation termination.

Using a reconstituted *in vitro* translation system we show that PABP stimulates the stop codon recognition activity of eRF1 in the presence of full-length eRF3a (Figure 1). Apparently, this PABP activity is independent of GTP hydrolysis by eRF3a. It can be observed in the presence of a non-hydrolysable GTP analog (GMPPNP) and independent of peptidyl-tRNA hydrolysis, which is inhibited by GMPPNP and by the eRF1(AGQ) mutant (Figure 1B). Moreover, it is independent of the stop codon context (Supplementary Figure S2). In addition, PABP increases the efficiency of peptidyl-tRNA hydrolysis under non-optimal termination conditions, e.g. the formation of eRF1•eRF3a complexes (Figure 3B) or in the presence of limiting amounts of release factors (Supplementary Figure S4B). We show that PABP does not interact with eRF1 directly, but exerts its effect via eRF3a (Figure 1B). Taken together, our experiments show that PABP increases the efficiency of stop codon recognition leading to enhanced formation of TCs. PABP interacts with the N-terminus of eRF3a and the GTPase activity of

eRF3a is not required for stimulation. Therefore, we suggest that the observed increase in efficiency of peptide release is a consequence of more efficient TC formation. Importantly, the observed stimulatory effect does not depend on the RNA-binding motifs of PABP (Figure 4). The C-terminal part of PABP comprising the proline-rich linker and the CTC, is sufficient to elicit increased TC formation in toe-print assays. However, it should be noted that RRM motifs of PABP can participate in the stimulation of termination by binding to the poly(A) tail and thereby positioning PABP closer to the preTCs. Indeed, we demonstrated that the cis-action of PABP in the presence of a mRNA with a poly(A) tail requires significantly less PABP and thus is more efficient compared to the trans-reaction (compare Figures 1 and 2).

We observe that PABP stabilizes the binding of eRF3a to the ribosome (Figure 5). eRF3a is not associated with the TCs after sucrose gradient centrifugation, most likely it dissociates from the complexes in the SDG. In the presence of PABP, eRF3a can be detected in the ribosome-containing fractions indicating that the binding of eRF3a to ribosomes is stabilized by PABP. Previous studies showed that PABP specifically binds ribosomes *in vivo* (43–45). For yeast PABP (Pab1), a specific interaction was shown with the 60S subunit via the C-terminal part of Pab1 comprising the linker region and CTC domain (43). Moreover, it has been suggested that Pab1 interacts with the ribosomal protein rpL39, which is located near the exit of the ribosomal tunnel (44). It should be noted that the linker sequences of the yeast and human PABP are very different, therefore this interaction might not be conserved from yeast to human. Furthermore, rpL39 is located very distant from the eRF3-binding site on the ribosome (46). We assume that the relevant ribosomal binding site for human PABP is not rpL39, but close to the ribosomal A site.

Fundamental differences may exist concerning the role of human PABP and yeast Pab1 in translation termination. However, the exact role of Pab1 in termination is enigmatic: in dual luciferase assays increased stop codon read-through is observed in the presence of Pab1. This is likely due to interaction of Pab1 and eRF3 leading to decreased termination efficiency (32). Based on this, it was suggested that Pab1 is required for maintaining a basic level of read-through in yeast. In contrast, an earlier study showed that overexpression of Pab1 in yeast strains with a mutant eRF3 causes an anti-suppression effect indicating that the interaction of eRF3 and Pab1 stimulates translation termination (33). Importantly, yeast eRF3 interacts via the N and M domains with the linker and C domain of Pab1 (32). This indicates that the underlying protein–protein interactions and molecular mechanisms differ between yeast and human.

Interestingly, we observe that the N domain of eRF3a significantly enhances translation termination, even in the absence of PABP. Pre-association of full-length eRF3a with the preTCs dramatically increases the efficiency of translation termination compared to the N-terminally truncated variant (eRF3c) (Figure 3). The latter was used in most previous termination studies (see below). Pre-association of eRF1•eRF3a complexes in solution abolishes the stimulatory effect of the eRF3a N domain on termination (Figure 3A). However, addition of PABP or GTP to these complexes

partly resumes the activity of full-length eRF3a (Figure 3B). It should be noted that the N-terminal parts of eRF3a and eRF3b vary widely between different species but the PABP-binding motif (PAM2) is conserved (21).

Previous *in vitro* characterizations of release factor activity and all available structures of TCs used truncated eRF3c which is unable to bind PABP, but is active in termination. Until now, the activity of eRF3c was considered to be identical to the one of full-length eRF3a and eRF3b, and thus the N-terminal part of eRF3 was assumed to be dispensable for termination due to its sequence variability (47). This hypothesis is based on a thermodynamic study of eRF1, eRF3a and nucleotide interactions that showed no effect of the N domain of eRF3a on the eRF1–eRF3 association constant in the absence of the ribosome (21). Importantly, the authors noted a change in entropy and enthalpy of the eRF1–eRF3 interaction depending on the presence of the N domain of eRF3. This was interpreted as an enthalpy–entropy compensation, meaning that interactions of eRF1 with either eRF3c or eRF3a use different pathways, but reach the same final state. Notably, that this study was performed in the absence of the ribosome and the association constant of the full-length eRF3a with the ribosome was not determined. Our data indicates that the N domain of eRF3a plays an important role in peptidyl–tRNA hydrolysis and that it is essential for the stimulation of termination by PABP.

We observe that the association of eRF1 with eRF3a in solution prevents efficient binding of the release factors to the preTCs (Figure 3A). One possible explanation could be an unspecific interaction of eRF1 with the N domain of eRF3a. Based on structural data, the PAM2 motif is considered unstructured (41). eRF1–eRF3a interactions may lead to an unfavorable conformation for ribosome binding.

Our data, showing a role of the N domain of eRF3a in translation termination, changes the current concept of termination in higher eukaryotes. Based on our findings, we propose a model for the interaction of release factors with the preTCs and the impact of PABP (Figure 6). We suggest that PABP can specifically bind to the N domain of eRF3a and thereby recruits eRF3a to the preTCs. Possibly, PABP promotes the correct orientation of eRF3a and eRF1 on the ribosome, allowing efficient stop codon recognition. To exert this effect, PABP needs to interact with the ribosome near the factor binding site. Otherwise, PABP could not stimulate termination and would reduce the pool of free eRF3a which would interfere with termination. Efficient peptidyl–tRNA hydrolysis in the presence of PABP may be a consequence of the increased stop codon recognition.

In vivo, a ribosome encountering a normal stop-codon is assumed to be in close vicinity to the poly(A) tail which is bound by PABP (Figure 6). Here, we show that *in vitro* PABP triggers eRF3a binding to ribosomes via its C-terminal domain and thus helps to recruit eRF3a and eRF1. We demonstrate that through the interaction of PABP with the N-terminal domain of eRF3a, the stop codon recognition and peptidyl–tRNA hydrolysis is stimulated under limiting concentrations of eRFs which is likely to be the case *in vivo*. Moreover *in vivo*, PABP is suggested to compete with NMD factor UPF1 for eRF binding thus interfering with NMD. In cases, where the 3'UTR is very long, or when an

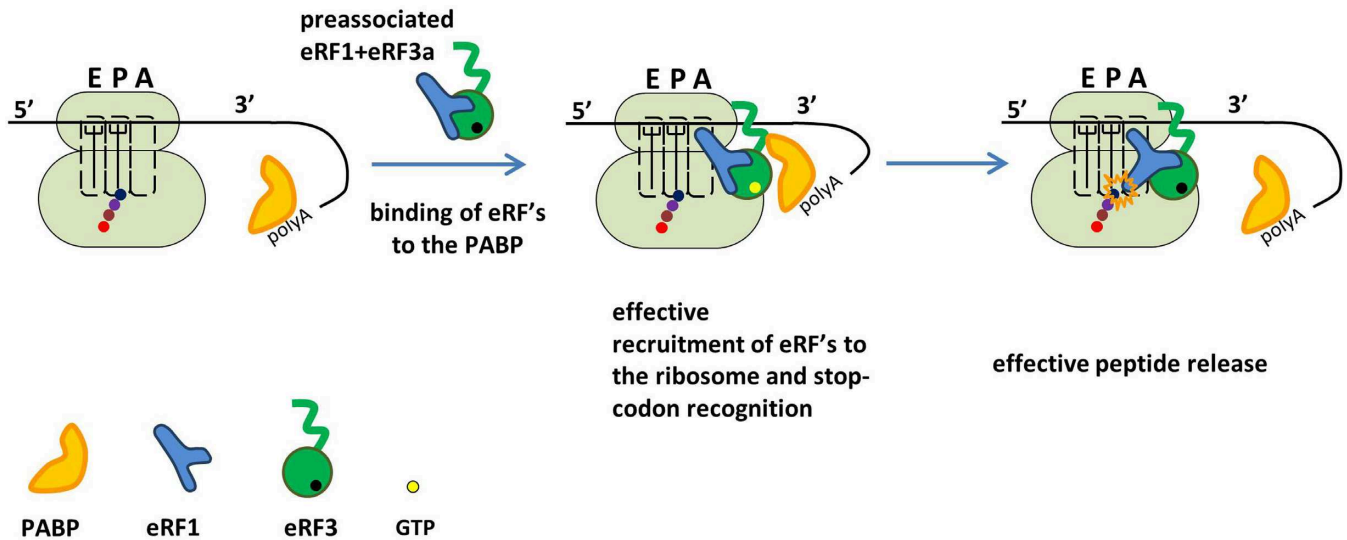


Figure 6. Model for PABP-stimulated translation termination. In the presence of PABP, eRF3a binds efficiently to preTCs and optimally positions eRF1 in the ribosomal complex for stop codon recognition. Accordingly, the termination efficiency is high as indicated by more efficient peptide release. When PABP is pre-bound to the mRNA, it recruits eRF1/3a to the preTCs, thus increasing the local eRF1/3a concentration and stabilizing the eRF binding to the ribosome.

EJC is bound in the 3'UTR, UPF1 may outcompete PABP for preTC binding and trigger mRNA decay (29–31).

In summary, we show here that the N-terminus of eRF3a is important for translation termination in the presence and absence of PABP. The C-terminal part of PABP is sufficient for stimulation of stop codon recognition. PABP enhances eRF3a ribosome binding, stop codon recognition and peptidyl-tRNA hydrolysis. The increased efficiency of TC formation is most likely achieved by optimal positioning of eRF3a on the ribosome.

SUPPLEMENTARY DATA

[Supplementary Data](#) are available at NAR Online.

ACKNOWLEDGEMENTS

We are grateful to Nahum Sonnenberg for plasmid pET3b-PABPC1, to Ludmila Frolova for providing plasmids encoding release factors and to Tatyana Pestova and Christopher Hellen who provided us with plasmids encoding initiation factors. Sequencing of plasmids, coding truncated PABP and cDNA fragment analyses were performed by the center of the collective use 'Genome' of EIMB RAS. We would like to thank Karine Huard, Frederic Garzoni and Etienne Raimondeau for technical assistance and discussions.

FUNDING

The investigation of the activity of PABP in translation termination: RFBR [15-04-08174]; Program of fundamental research for state academies for 2013-2020 years (Subprogram No. 58 Molecular genetics, mechanisms of realization of genetic information, bioengineering); European Research Council Starting grant [ComplexNMD, 281331 to C.S.]. The study of the effect of the eRF3a N domain on the

efficiency of translation termination: Russian Science Foundation [14-14-00487]. Funding for open access charge: European Research Council Starting grant [ComplexNMD, 281331].

Conflict of interest statement. None declared.

REFERENCES

- Eliseeva, I.A., Lyabin, D.N. and Ovchinnikov, L.P. (2013) Poly(A)-binding proteins: structure, domain organization, and activity regulation. *Biochemistry (Mosc.)*, **78**, 1377–1391.
- Kuhn, U. and Pieler, T. (1996) Xenopus poly(A) binding protein: functional domains in RNA binding and protein-protein interaction. *J. Mol. Biol.*, **256**, 20–30.
- Baer, B.W. and Kornberg, R.D. (1983) The protein responsible for the repeating structure of cytoplasmic poly(A)-ribonucleoprotein. *J. Cell Biol.*, **96**, 717–721.
- Deo, R.C., Bonanno, J.B., Sonenberg, N. and Burley, S.K. (1999) Recognition of polyadenylate RNA by the poly(A)-binding protein. *Cell*, **98**, 835–845.
- Bernstein, P., Peltz, S.W. and Ross, J. (1989) The poly(A)-poly(A)-binding protein complex is a major determinant of mRNA stability in vitro. *Mol. Cell Biol.*, **9**, 659–670.
- Wu, J. and Bag, J. (1998) Negative control of the poly(A)-binding protein mRNA translation is mediated by the adenine-rich region of its 5'-untranslated region. *J. Biol. Chem.*, **273**, 34535–34542.
- Imataka, H., Gradi, A. and Sonenberg, N. (1998) A newly identified N-terminal amino acid sequence of human eIF4G binds poly(A)-binding protein and functions in poly(A)-dependent translation. *EMBO J.*, **17**, 7480–7489.
- Wells, S.E., Hillner, P.E., Vale, R.D. and Sachs, A.B. (1998) Circularization of mRNA by eukaryotic translation initiation factors. *Mol. Cell*, **2**, 135–140.
- Rajkowitzsch, L., Vilela, C., Berthelot, K., Ramirez, C.V. and McCarthy, J.E. (2004) Reinitiation and recycling are distinct processes occurring downstream of translation termination in yeast. *J. Mol. Biol.*, **335**, 71–85.
- Kahvejian, A., Svitkin, Y.V., Sukarieh, R., M'Boutchou, M.N. and Sonenberg, N. (2005) Mammalian poly(A)-binding protein is a eukaryotic translation initiation factor, which acts via multiple mechanisms. *Genes Dev.*, **19**, 104–113.

11. Haghighat, A. and Sonenberg, N. (1997) eIF4G dramatically enhances the binding of eIF4E to the mRNA 5'-cap structure. *J. Biol. Chem.*, **272**, 21677–21680.
12. Craig, A.W., Haghighat, A., Yu, A.T. and Sonenberg, N. (1998) Interaction of polyadenylate-binding protein with the eIF4G homologue PAIP enhances translation. *Nature*, **392**, 520–523.
13. Martineau, Y., Derry, M.C., Wang, X., Yanagiya, A., Berlanga, J.J., Shyu, A.B., Imataka, H., Gehring, K. and Sonenberg, N. (2008) Poly(A)-binding protein-interacting protein 1 binds to eukaryotic translation initiation factor 3 to stimulate translation. *Mol. Cell Biol.*, **28**, 6658–6667.
14. Khaleghpour, K., Svitkin, Y.V., Craig, A.W., DeMaria, C.T., Deo, R.C., Burley, S.K. and Sonenberg, N. (2001) Translational repression by a novel partner of human poly(A) binding protein, Paip2. *Mol. Cell*, **7**, 205–216.
15. Karim, M.M., Svitkin, Y.V., Kahvejian, A., De Crescenzo, G., Costa-Mattioli, M. and Sonenberg, N. (2006) A mechanism of translational repression by competition of Paip2 with eIF4G for poly(A) binding protein (PABP) binding. *Proc. Natl. Acad. Sci. U.S.A.*, **103**, 9494–9499.
16. Hoshino, S., Imai, M., Kobayashi, T., Uchida, N. and Katada, T. (1999) The eukaryotic polypeptide chain releasing factor (eRF3/GSPT) carrying the translation termination signal to the 3'-Poly(A) tail of mRNA. Direct association of eRF3/GSPT with polyadenylate-binding protein. *J. Biol. Chem.*, **274**, 16677–16680.
17. Zhouravleva, G., Frolova, L., Le Goff, X., Le Guellec, R., Inge-Vechtomov, S., Kisselev, L. and Philippe, M. (1995) Termination of translation in eukaryotes is governed by two interacting polypeptide chain release factors, eRF1 and eRF3. *EMBO J.*, **14**, 4065–4072.
18. Alkalaeva, E.Z., Pisarev, A.V., Frolova, L.Y., Kisselev, L.L. and Pestova, T.V. (2006) In vitro reconstitution of eukaryotic translation reveals cooperativity between release factors eRF1 and eRF3. *Cell*, **125**, 1125–1136.
19. Kong, C., Ito, K., Walsh, M.A., Wada, M., Liu, Y., Kumar, S., Barford, D., Nakamura, Y. and Song, H. (2004) Crystal structure and functional analysis of the eukaryotic class II release factor eRF3 from *S. pombe*. *Mol. Cell*, **14**, 233–245.
20. Atkinson, G.C., Baldauf, S.L. and Hauryliuk, V. (2008) Evolution of nonstop, no-go and nonsense-mediated mRNA decay and their termination factor-derived components. *BMC Evol. Biol.*, **8**, 290.
21. Kononenko, A.V., Mitkevich, V.A., Atkinson, G.C., Tenson, T., Dubovaya, V.I., Frolova, L.Y., Makarov, A.A. and Hauryliuk, V. (2010) GTP-dependent structural rearrangement of the eRF1:eRF3 complex and eRF3 sequence motifs essential for PABP binding. *Nucleic Acids Res.*, **38**, 548–558.
22. Cheng, Z., Saito, K., Pisarev, A.V., Wada, M., Pisareva, V.P., Pestova, T.V., Gajda, M., Round, A., Kong, C., Lim, M. *et al.* (2009) Structural insights into eRF3 and stop codon recognition by eRF1. *Genes Dev.*, **23**, 1106–1118.
23. Seit-Nebi, A., Frolova, L. and Kisselev, L. (2002) Conversion of omnipotent translation termination factor eRF1 into ciliate-like UGA-only unipotent eRF1. *EMBO Rep.*, **3**, 881–886.
24. Preis, A., Heuer, A., Barrio-Garcia, C., Hauser, A., Eyler, D.E., Berninghausen, O., Green, R., Becker, T. and Beckmann, R. (2014) Cryoelectron microscopic structures of eukaryotic translation termination complexes containing eRF1-eRF3 or eRF1-ABCE1. *Cell Rep.*, **8**, 59–65.
25. Jakobsen, C.G., Seggaard, T.M., Jean-Jean, O., Frolova, L. and Justesen, J. (2001) [Identification of a novel termination release factor eRF3b expressing the eRF3 activity in vitro and in vivo]. *Mol. Biol. (Mosk)*, **35**, 672–681.
26. Hoshino, S., Imai, M., Mizutani, M., Kikuchi, Y., Hanaoka, F., Ui, M. and Katada, T. (1998) Molecular cloning of a novel member of the eukaryotic polypeptide chain-releasing factors (eRF). Its identification as eRF3 interacting with eRF1. *J. Biol. Chem.*, **273**, 22254–22259.
27. Chauvin, C., Salhi, S., Le Goff, C., Viranaicken, W., Diop, D. and Jean-Jean, O. (2005) Involvement of human release factors eRF3a and eRF3b in translation termination and regulation of the termination complex formation. *Mol. Cell Biol.*, **25**, 5801–5811.
28. Behm-Ansmant, I., Gatfield, D., Rehwinkel, J., Hilgers, V. and Izaurralde, E. (2007) A conserved role for cytoplasmic poly(A)-binding protein 1 (PABPC1) in nonsense-mediated mRNA decay. *EMBO J.*, **26**, 1591–1601.
29. Ivanov, P.V., Gehring, N.H., Kunz, J.B., Hentze, M.W. and Kulozik, A.E. (2008) Interactions between UPF1, eRFs, PABP and the exon junction complex suggest an integrated model for mammalian NMD pathways. *EMBO J.*, **27**, 736–747.
30. Eberle, A.B., Stalder, L., Mathys, H., Orozco, R.Z. and Mühlemann, O. (2008) Posttranscriptional gene regulation by spatial rearrangement of the 3' untranslated region. *PLoS Biol.*, **6**, e92.
31. Singh, G., Rebbapragada, I. and Lykke-Andersen, J. (2008) A competition between stimulators and antagonists of Upf complex recruitment governs human nonsense-mediated mRNA decay. *PLoS Biol.*, **6**, e111.
32. Roque, S., Cerciati, M., Gaugue, I., Mora, L., Floch, A.G., de Zamaroczy, M., Heurgue-Hamard, V. and Kervestin, S. (2015) Interaction between the poly(A)-binding protein Pab1 and the eukaryotic release factor eRF3 regulates translation termination but not mRNA decay in *Saccharomyces cerevisiae*. *RNA*, **21**, 124–134.
33. Cosson, B., Couturier, A., Chabelskaya, S., Kiktev, D., Inge-Vechtomov, S., Philippe, M. and Zhouravleva, G. (2002) Poly(A)-binding protein acts in translation termination via eukaryotic release factor 3 interaction and does not influence [PSI(+)] propagation. *Mol. Cell Biol.*, **22**, 3301–3315.
34. Trowitzsch, S., Bieniossek, C., Nie, Y., Garzoni, F. and Berger, I. (2010) New baculovirus expression tools for recombinant protein complex production. *J. Struct. Biol.*, **172**, 45–54.
35. Alkalaeva, E., Eliseev, B., Ambrogelly, A., Vlasov, P., Kondrashov, F.A., Gundllapalli, S., Frolova, L., Soll, D. and Kisselev, L. (2009) Translation termination in pyrrolysine-utilizing archaea. *FEBS Lett.*, **583**, 3455–3460.
36. Kryuchkova, P., Grishin, A., Eliseev, B., Karyagina, A., Frolova, L. and Alkalaeva, E. (2013) Two-step model of stop codon recognition by eukaryotic release factor eRF1. *Nucleic Acids Res.*, **41**, 4573–4586.
37. Susorov, D., Mikhailova, T., Ivanov, A., Sokolova, E. and Alkalaeva, E. (2015) Stabilization of eukaryotic ribosomal termination complexes by deacylated tRNA. *Nucleic Acids Res.*, **43**, 3332–3343.
38. Valasek, L., Szamecz, B., Hinnebusch, A.G. and Nielsen, K.H. (2007) In vivo stabilization of preinitiation complexes by formaldehyde cross-linking. *Methods Enzymol.*, **429**, 163–183.
39. Brown, A., Shao, S., Murray, J., Hegde, R.S. and Ramakrishnan, V. (2015) Structural basis for stop codon recognition in eukaryotes. *Nature*, **524**, 493–496.
40. Matheisl, S., Berninghausen, O., Becker, T. and Beckmann, R. (2015) Structure of a human translation termination complex. *Nucleic Acids Res.*, **43**, 8615–8626.
41. Kozlov, G. and Gehring, K. (2010) Molecular basis of eRF3 recognition by the MLE domain of poly(A)-binding protein. *PLoS One*, **5**, e10169.
42. Mangus, D.A., Evans, M.C. and Jacobson, A. (2003) Poly(A)-binding proteins: multifunctional scaffolds for the post-transcriptional control of gene expression. *Genome Biol.*, **4**, 223.
43. Proweller, A. and Butler, J.S. (1996) Ribosomal association of poly(A)-binding protein in poly(A)-deficient *Saccharomyces cerevisiae*. *J. Biol. Chem.*, **271**, 10859–10865.
44. Sachs, A.B. and Davis, R.W. (1989) The poly(A) binding protein is required for poly(A) shortening and 60S ribosomal subunit-dependent translation initiation. *Cell*, **58**, 857–867.
45. Kuyumcu-Martinez, N.M., Joachims, M. and Lloyd, R.E. (2002) Efficient cleavage of ribosome-associated poly(A)-binding protein by enterovirus 3C protease. *J. Virol.*, **76**, 2062–2074.
46. Ban, N., Nissen, P., Hansen, J., Moore, P.B. and Steitz, T.A. (2000) The complete atomic structure of the large ribosomal subunit at 2.4 Å resolution. *Science*, **289**, 905–920.
47. Kushnir, V.V., Ter-Avanesyan, M.D., Telckov, M.V., Surguchov, A.P., Smirnov, V.N. and Inge-Vechtomov, S.G. (1988) Nucleotide sequence of the SUP2 (SUP35) gene of *Saccharomyces cerevisiae*. *Gene*, **66**, 45–54.

Supplementary Figures

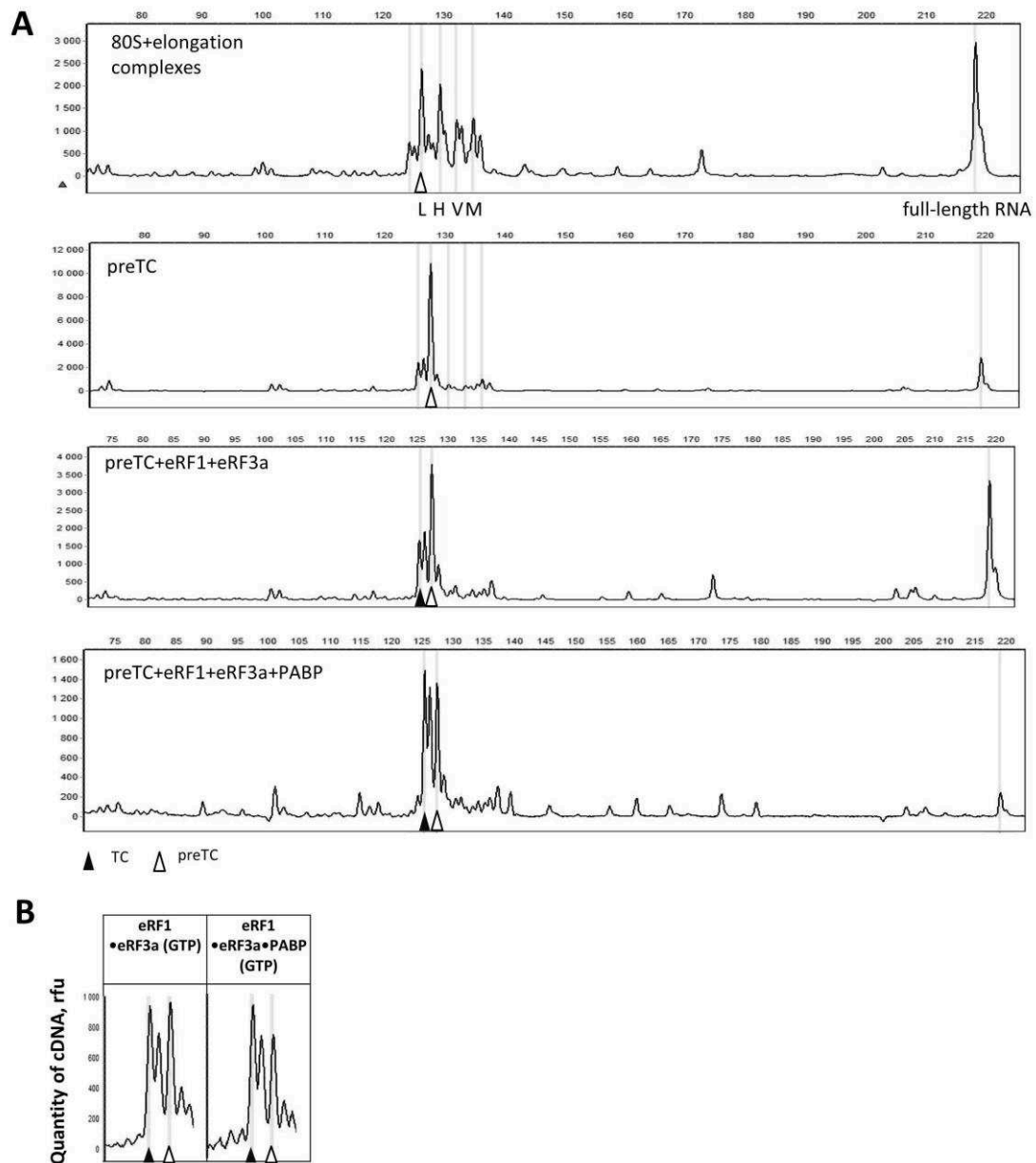


Figure S1. Toe-print analysis of termination complexes on MVHL mRNA.

(A) Examples of raw data from capillary electrophoresis of cDNA products obtained using fluorescently labeled primers for toe-print analysis. Elongation complexes on MVHL mRNA, preTCs after SDG purification, TC formation induced by addition of eRF1 and eRF3a to the preTCs, TC formation induced by addition of eRF1, eRF3a and PABP to the preTCs. (B) Toe-print analysis of termination complexes in the presence of high concentrations of eRFs and PABP. Positions of preTCs and TCs are labeled by white and black triangles respectively. Full-length mRNA corresponds the 219 nt peak.

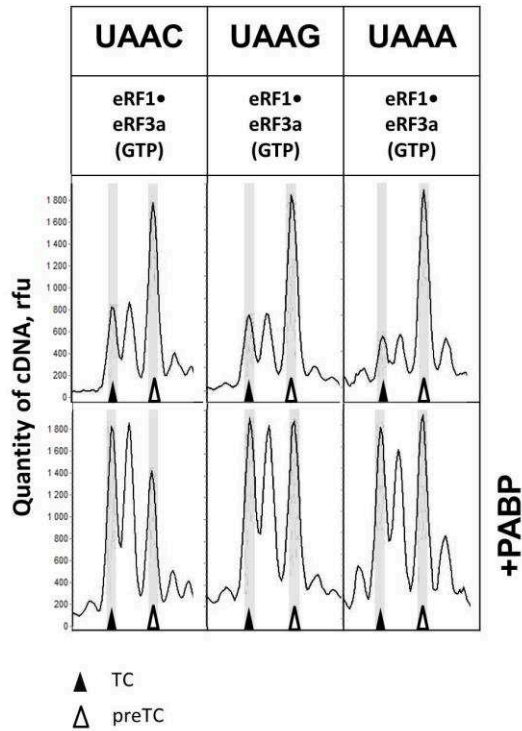


Figure S2. PABP increases the recognition of stop codons on all +4 contexts. Toe-print analysis of termination complexes formed by preTCs containing MVHL-UAAC (left), MVHL-UAAG (middle) and MVHL-UAAA (right) mRNAs in the presence of eRF1•eRF3a•GTP (above and below) and PABP (below). Rfu – relative fluorescence unit. Positions of preTCs and TCs are labeled by white and black triangles respectively. The MVHL mRNA used in this study has a MVHL-UAAU context (Figure 1).

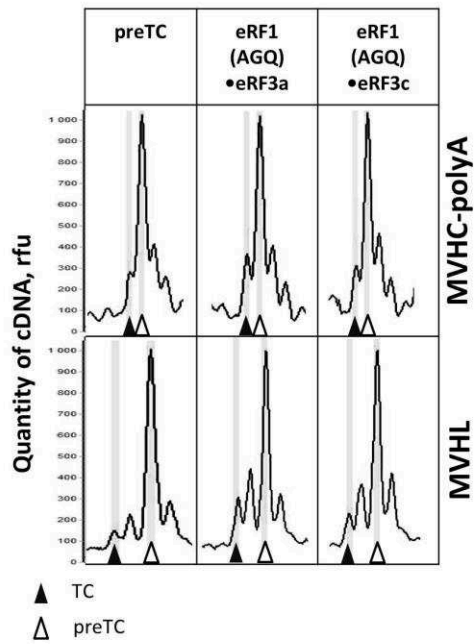


Figure S3. PABP increases stop codon recognition by release factors in *cis* and *trans*. Negativecontrols: Toe-print analysis of termination complexes formed by addition to the preTCs of eRF1(AGQ)•eRF3a•GTP (middle) or eRF1(AGQ)•eRF3c•GTP (right). Complexes were assembled utilizing mixtures of MVHC-polyA and MVHL mRNAs in the absence of PABP. Different toe-printing primers were used to monitor stop codon recognition for complexes bound to MVHC-polyA mRNA (above) or to MVHL mRNA (below). Rfu – relative fluorescence unit. Positions of preTCs and TCs are labeled by white and black triangles respectively.

A

	Maximum Count
eRF1	262,5
eRF3a	116
eRF1+eRF3 a 4pmol each	14125

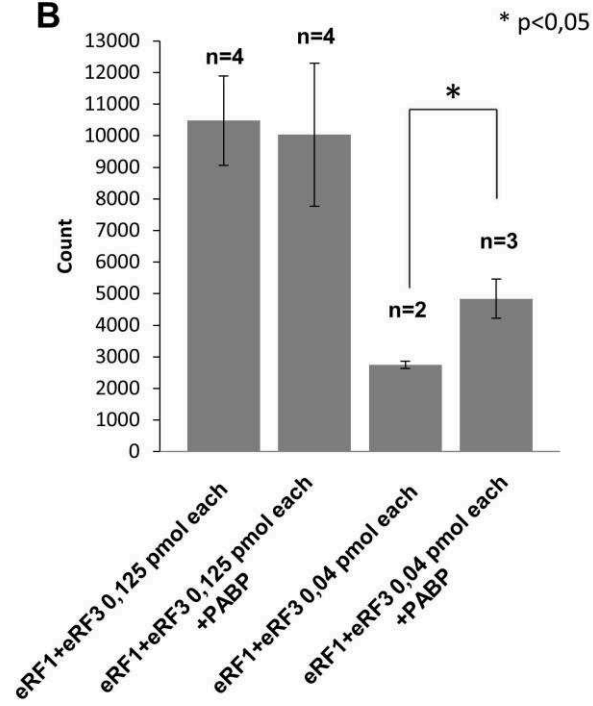
B

Figure S4. PABP increases the efficiency of peptidyl-tRNA hydrolysis in the presence of limiting amounts of release factors. (A) Minimal and maximal level of peptidyl-tRNA hydrolysis in the TCs induced by addition of eRF1 and eRF3. The minimal level of peptide release was determined by incubation of 0.125 pmol of either eRF1 or eRF3a with preTCs for 3 minutes. The maximal level was determined by incubation of 4 pmol of both factors eRF1 and eRF3a with the preTCs for 3 minutes. **(B)** Hydrolysis of peptidyl-tRNA in the TCs induced by different amounts of individual release factors eRF1 and eRF3a in the presence of PABP. The star (*) marks a significant difference from the respective control $p < 0,05$.

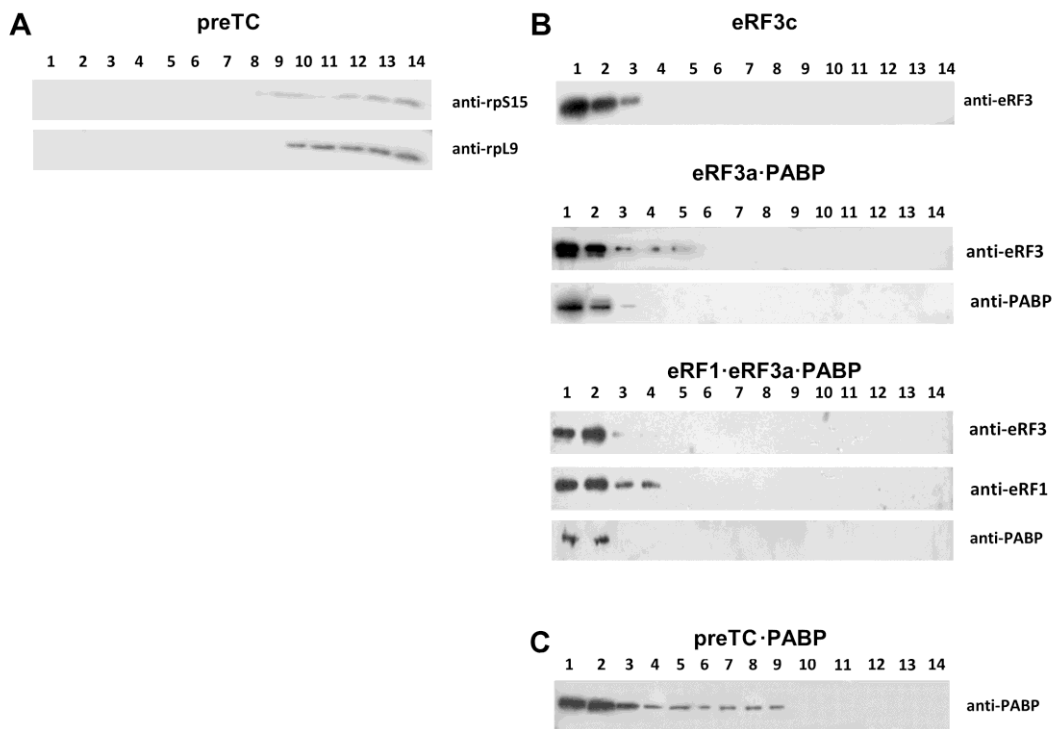


Figure S5. Additional Western blot analyses of eRFs and PABP binding to TCs. (A) Western blot analysis of preTCs separated via SDS centrifugation using antibodies raised against ribosomal proteins S15 and L9. (B) Distribution of eRF3c, eRF3a·PABP and eRF1·eRF3a·PABP in absence of ribosomes in SDS. (C) Western blot analysis of preTCs incubated with PABP using antibodies against PABP. The fractions of the SDS are indicated above the Western blots; 1 corresponds to the top and 14 to the bottom of the gradient.

4 Biochemical and structural characterization of the effect of UPF1 on mammalian translation termination

Résumé en français

Les protéines Up-Framshift (UPFs) jouent un rôle majeur dans la voie de signalisation NMD et constituent le cœur de la machinerie moléculaire impliquée dans ce processus. La relation entre UPF1 et eRF3 est encore énigmatique, alors qu'UPF1 est actuellement perçu comme un frein à la terminaison de la traduction. Ce chapitre se concentre ainsi sur le rôle de UPF1 dans la terminaison de la traduction. Pour ce faire, UPF1 a été fusionnée à eRF3a à l'aide d'un connecteur et a été soumise à des études structurales. Le complexe formé par eRF1AGQ et cette fusion de UPF1 et eRF3a a ensuite été mis en présence des PreTCs et caractérisé par cryo-microscopie électronique.

4.1 Abstract

Up-Frameshift proteins (UPFs) play a major role in NMD and constitute the conserved core of the NMD pathway. UPF1 has been suggested to impede translation termination on a premature termination codon. However, the impact of UPF1 on translation termination and its interaction with eRF3a has not been analyzed in vitro in a defined experimental setup. The main aim of my study was to gain a better understanding of the role of UPF1 in translation termination. To this end, UPF1 was fused with eRF3a using a covalent linker and this fusion protein was used for cryo-EM studies. The complex of UPF1 linker eRF3a and eRF1AGQ was added to purified PreTCs and the structure of the resulting termination complex was solved by cryo-EM.

4.2 Introduction

Up-Frameshift proteins (UPFs) play a major role in NMD and constitute the core machinery of the pathway. UPF1, UPF2 and UPF3 are the important players. Phosphorylation of UPF1 by SMG1 kinase is an important event that results in the degradation of the mRNA. In immunoprecipitation experiments from cell extracts UPF1 has been shown to interact with eRF3 (Kashima et al., 2006). UPF1 was suggested to impede translation termination based on readthrough assays with reporter mRNAs (Ivanov et al., 2008). How UPF1 functions with respect to eRF3 is enigmatic, and the complex formation has not been studied yet, both biochemically and structurally. Using the reconstituted in vitro translation system and electron cryo microscopy we aimed to gain a better understanding of UPF1's role in translation termination on a premature termination codon. PreTCs were reconstituted and purified (see Chapter 3), and termination complexes were reconstituted along with UPF1 for cryo-EM studies.

4.3 Results

4.3.1 Expression and purification of the fusion protein UPF1 linker eRF3a

Fusion proteins were generated as the affinity between the factors eRF3a and UPF1 was expected to be low (with a K_d lower than in the micromolar range as estimated from surface plasmon resonance experiments in the laboratory). In the fusion proteins, the proteins are linked using a flexible, glycine-serine-rich linker (sequence GGGGS) that is 55 amino acids long. The linked proteins comprise an N-terminal His tag and a C-terminal Strep tag for affinity purification. In order to generate fusions proteins, proteins were subcloned into the pFastBac plasmid [pFastBac-11linker (NcoI - SalI - NotI - [GGGGS]_{x11} - NheI - SacI - KpnI - TEV - StrepTag - stop - NsiI - HindIII)]. For UPF1 linker fusion proteins, the UPF1 sequence was amplified by PCR and subcloned into pFastBac-11linker using NcoI and NotI restriction enzymes. eRF3a after PCR amplification was subcloned into the plasmid containing UPF1 using NheI and KpnI restriction

sites. For the eRF3a linker UPF1 protein eRF3a was cloned in between the sites NcoI – SalI and UPF1 between NheI – SacI.

Both constructs were expressed in SF21 cells. Ni²⁺- NTA affinity chromatography was used as the first step of purification followed by anion exchange chromatography (Hi Trap Q XL), Strep-Tactin affinity purification and SEC (Superdex 200) in buffer B (20 mM Tris pH 7.5, 300 mM KCl, 5% glycerol and 1 mM DTT) to remove aggregates. eRF3a linker UPF1 proteins expression was a lower and formed more aggregates. So for subsequent studies UPF1 linker eRF3a was used.

4.3.2 Toe-printing assays

The in vitro translation system described in chapter 1 was used for the reconstitution of the PreTCs. To check whether the UPF1 linker eRF3a was functional i.e. form a complex with eRF1 that still allows for stop codon recognition, toe-print assays were carried out (Figure 4.1A). When UPF1 linker eRF3a was used in termination assays, the stop codon recognition (i.e. +1-2 nt shift in toe-prints) was similar as in the case of unlinked eRF1 + eRF3a proteins. This indicates that the linking of the proteins did not impair the complex formation with eRF1 and the binding to the ribosome.

4.3.3 Preparation of termination complexes

Pre terminating complexes (PreTCs) were prepared from 300 µL in vitro translation reaction. A 10X excess of a preformed complex between eRF1AGQ and UPF1-linker-eRF3a with 50 µM of GMPPNP was added to the PreTCs. The eRF1AGQ: UPF1 linker eRF3a complex was purified by SEC (in 20 mM Tris pH 7.5, 150 mM KCl, 5% glycerol and 1 mM DTT (Figure 4.1B)). The mixture was incubated at room temperature for 10 min (Alkalaeva et al., 2006). Immediately afterwards, cryo-grids were frozen. GMPPNP was used to stabilize the pre termination complex.

4.3.4 Structural characterization of pre-termination complexes with eRF1 and UPF1-eRF3a fusion protein using cryo-EM

Quantifoil grids with pre-coated carbon were used for freezing of the sample using a virobot with 2-3.5 s blotting time and 3-5 blot force.

The data was collected on a Tecnai G2 Polara (IBS microscopy facility) at 300 kV equipped with a 4k X 4k CCD camera at 50,000x magnification which corresponds to a pixel size of 1.93 Å (Figure 4.2A). 1,012 micrographs were CTF corrected using bshow (bsoft). 490 micrographs were used for particle picking using e2boxer total of 9,600 particles. The picked particles were aligned in RELION (Scheres, 2012, 2014) against a rabbit 80S ribosome containing P-site tRNA as reference map, filtered to 60 Å (EMD 1670).

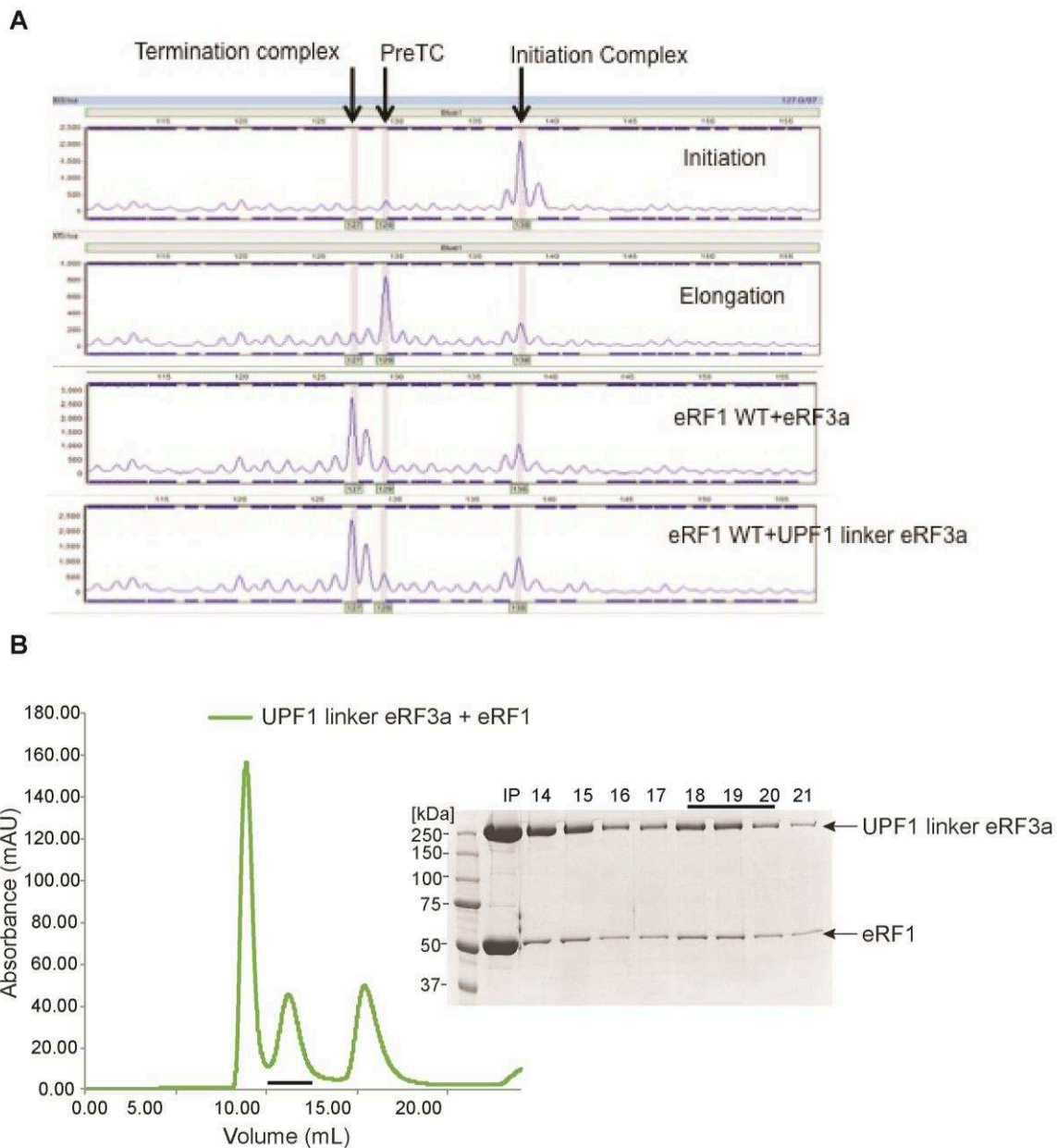


Figure 4.1 Biochemical characterization of eRF1-eRF3a-UPF1 complexes:

(A) Toe-print assays showing the different stages of reconstituted translation. The different peaks indicate ribosomal complexes during initiation, elongation, before and after termination. Addition of eRFs (eRF1 and eRF3a) to PreTCs results in a +1-2 nt peak shift indicating stop codon recognition (Alkalaeva et al., 2006). A similar peak shift is observed when UPF1 linker eRF3a fusion protein is added along with eRF1 WT. (B) SEC of the eRF1 and UPF1 linker eRF3a. The fractions highlighted in black are used for cryo-EM studies.

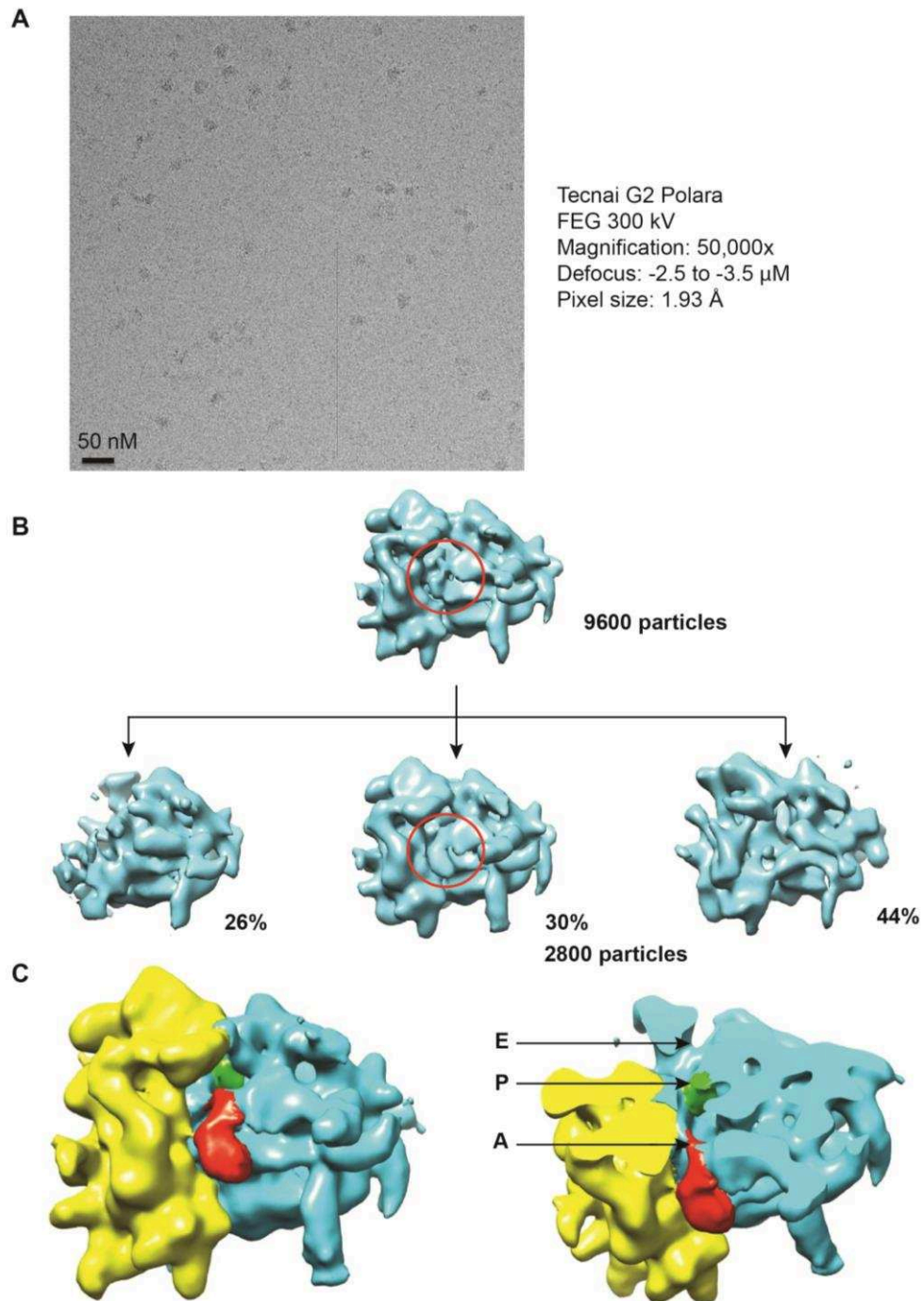


Figure 4.2 Cyo-EM of pre-terminating ribosome with eRF1-eRF3a-UPF1:

(A) A representative micrograph collected from the ribosome-eRF1AGQ-eRF3-UPF1 data set (B) Sorting of the particles using 3D classification in RELION into 3 classes. A map of the 80S ribosome containing P-site tRNA (EMD 1670) was filtered to 60 \AA and used as an initial model for 3D classification. (C) The refined volume is shown. 40S is colored in yellow, 60S in cyan, release factors eRF1 and eRF3a in red and P site tRNA in green.

3D autorefine was used to obtain an initial reconstruction, which then was classified using RELION 3D-classification into 3 classes (Figure 4.2B).

After 3D classification, Class 2 (30% of the particles) contained density at the ribosomal A-site. This map was further refined. Class 3 (44%) comprised empty ribosomes, and the residual 26% particles in Class 1 corresponded to 60S ribosome particles.

The cryo-EM reconstruction of class1 shows a clear density for the release factors eRF1 and eRF3a in the A-site and density for the P-site tRNA. The latter is indicative for a translating ribosome. Thus, the efficiency of our translation system is around 25% as we observe 24% of the particles in cryo-EM with P-site tRNA. The structure is comparable to a previously published cryoEM structure of a mammalian termination complex (Taylor et al., 2012). Unfortunately, density for UPF1 could not be detected in this 3D reconstruction (Figure 4.2C).

With the optimized protocols to increase the ribosome concentration using an Amicon concentrator (Chapter 3), a larger cryo-EM data set was collected in a second attempt. With the optimized protocols for the ribosome concentration for freezing grids, we collected a larger cryo-EM data set allowing for additional classifications.

A total of 1,529 micrographs were collected on the Tecnai G2 Polara at 300 kV with a 4k X 4k CCD camera at 50,000x magnification which corresponds to a pixel size of 1.93 Å. The images were processed as described above. 87,000 particles were used for final reconstruction. A consensus map was generated which was further classified into 3 classes using RELION 3D classification. Class1 (32% of particles) showed a density at the A site for eRF1 and density for eRF3a.

Class 2 (30% of particles) correspond to the 80S ribosome with the P site tRNA. The rest 38% of particles in Class3 were empty 80S ribosomes. A density for UPF1 was not observed in this dataset. However, the percentage of particles containing a density for eRF1 and eRF3a and a P site tRNA is similar to the first smaller dataset, confirming our purification strategy which yields more than 30% terminating ribosomes – this is much better than other purifications where the terminating ribosome presented less than 5% of the entire data set (Taylor et al., 2012). Still, even in this second data set, we could not detect any density corresponding to UPF1. This finding was surprising given the fact that UPF1 is covalently linked to eRF3a (which is clearly present) and that UPF1 was shown to bind to ribosomes. However, recent biochemical experiments in our laboratory support our structural findings; indicating that there is no direct and functional interaction between eRFs and UPF1 (Manuscript attached at the end of the thesis).

4.4 Conclusions

According to Kashima et al., 2006 and Ivanov et al 2008., UPF1 interacts with eRF3a and inhibits translation termination. I have never been able to efficiently pulldown the complex of eRF3a and UPF1 in-vitro and we attributed this to the low-affinity of eRF3a and UPF1 or to the need of a

terminating ribosome in order to form a trimeric complex. Afterwards, in collaboration with Andreas Kulozik and Matthias Hentze we found that UPF1 does not interfere with translation termination *in vitro* in toe-printing assays. The generation of the fusion protein between UPF1 and eRF3a was based on the assumption that eRF3a and UPF1 interact, a finding that was published by the Jacobson lab for yeast (showing a direct interaction for the yeast proteins) and by the Hentze/Kulozik and Lykke-Andersen labs for mammalian cells. The latter used immunoprecipitations from cell extracts (which does not monitor direct interactions) and mutational studies (which can have pleiotropic effects *in vivo*, and also is not a proof for a direct interaction).

In our cryo EM reconstructions, we were only able to observe the density for eRF1 and eRF3a and not UPF1. On the one hand, this shows that our reconstitution of the human termination complexes works. On the other hand, it indicates that the complex between UPF1 and release factors does not form even when enforced by covalently linking the proteins with a long flexible linker. More recent evidence from our and the Hentze/Kulozik labs supports this finding.

Recent work from our laboratory showed that UPF3B interacts with eRF3a and UPF1 opening many new exciting possibilities of how the NMD factors may crosstalk with the translation machinery stalled at a premature stop codon. In fact in collaboration with the Hentze/Kulozik laboratory, we found a direct effect of UPF3B on translation termination *in vitro*. This indicates that UPF3B may have a yet uncharacterized, new role in NMD substrate recognition. UPF3B is a difficult protein to purify with a N-terminal RNA recognition motif (RRM domain) and long, unstructured region. Expressing and purifying the full-length UPF3B protein from insect cells has made these studies possible and allowed us identifying these novel interactions *in vitro*.

Interestingly, we observed a decrease in UPF1 phosphorylation by SMG1 kinase in the presence of UPF3B alone as well as in the presence of UPF2 and UPF3B. This lead to the possible hypothesis that UPF3B may interact directly with SMG1 kinase thus inhibiting the phosphorylation of UPF1. We decided to further analyze the impact of UPF3B on UPF1 phosphorylation by the SMG1C kinase complex (described in Chapter 5).

5 Novel interaction between UPF3B and the SMG1 kinase complex regulates UPF1 phosphorylation

Manuscript under preparation

Résumé en français

La dégradation des ARNm non-sens (NMD) est un système de contrôle qualité important dans le cytoplasme qui reconnaît et dégrade les ARNm contenant un codon stop prématuré. La phosphorylation de UPF1 est l'étape critique de ce processus. Cet événement, qui est régulé par de nombreuses interactions, est permis par le complexe SMG1C comprenant la kinase SMG1 et deux protéines régulatrices SMG8 et SMG9. Une fois phosphorylé, UPF1 recrute de nombreux facteurs de dégradation. Dans cette étude, nous rapportons une nouvelle interaction entre SMG1C et UPF3B. Le motif de RNA recognition (RRM) de UPF3B interagit avec SMG1C. Cette interaction régule la phosphorylation de UPF1 par SMG1C et ajoute donc un nouveau niveau de régulation du processus de NMD.

5.1 Abstract

Nonsense-mediated mRNA decay (NMD) is an important quality control mechanism in the cytoplasm, which degrades mRNA containing premature termination codons. Phosphorylation of UPF1 is considered the major cue for degradation of mRNA. Various interactions regulate the phosphorylation of UPF1 by the SMG1 kinase complex (SMG1C) comprising SMG1 kinase and the two regulatory proteins SMG8 and SMG9. UPF1 phosphorylation leads to the recruitment of downstream decay factors. In this study we report a new interaction between SMG1C and UPF3B. The RNA recognition motif (RRM) of UPF3B interacts with SMG1C. This interaction regulates the phosphorylation of UPF1 by SMG1 kinase and thus presents an additional layer of regulation of the NMD pathway.

5.2 Introduction

Nonsense-mediated mRNA decay (NMD) is one of the important eukaryotic mRNA quality control mechanisms that occur in the cytoplasm. NMD targets aberrant mRNAs containing premature termination codons (PTCs) for degradation and thereby prevents the production of truncated proteins that leads to various diseases (Brandman & Hegde, 2016; He & Jacobson, 2015b; Holbrook, Neu-Yilik, Hentze, & Kulozik, 2004; Karousis et al., 2016; S. Lykke-Andersen & Jensen, 2015). NMD not only recognizes mRNAs with a PTCs but also regulates the expression of ~10% of normal transcripts in the cell (Chan et al., 2007, 2009; Imamachi et al., 2012; Mendell et al., 2004; Yepiskoposyan et al., 2011; X. Zhang et al., 2007). The major cue for the NMD is the hyper-phosphorylation of the factor UPF1 (UP-Frameshift protein 1) CH and SQ domains by the kinase SMG1 (Suppressor with Morphogenetic effect on Genitalia 1) (Bhattacharya et al., 2000; Chakrabarti et al., 2011; Yamashita, 2013). Once UPF1 is phosphorylated, it recruits the downstream NMD factors SMG5, SMG6 and SMG7 that leads to rapid degradation of the faulty mRNA (Ohnishi et al., 2003; Okada-Katsuhata et al., 2012).

In the most widely accepted model for NMD, the pausing of the ribosome at the PTC results in the recruitment of release factors and UPF1, leading to the assembly of the SURF (SMG1-UPF1-eRF1-eRF3a) complex (Kashima et al., 2006). The exon junction complex (EJC) can bind to UPF2 and UPF3 and its presence on an mRNA, downstream of a PTC stimulates NMD. The association between SURF complex and UPF2-UPF3B-EJC activates SMG1 kinase to phosphorylate UPF1. The resulting decay-inducing (DECID) complex leads to a remodeling of the NMD complexes and ultimately to mRNA degradation (Ivanov et al., 2008; Kashima et al., 2006; Yamashita et al., 2009).

The gene encoding SMG1 was first identified in *C. elegans* and was found to encode a kinase belonging to the superfamily of phosphatidylinositol 3-kinase (PIK) related protein kinases (PIKKs) (Pulak & Anderson, 1993). The homolog of SMG1 does not exist in lower eukaryotes

(e.g. yeast). Yamashita et al. first identified SMG1 in the year 2001 in humans, where it was found to phosphorylate the SQ motifs in the C-terminus of UPF1. Later SMG8 and SMG9 have been identified to be tightly associated with SMG1 kinase and to be the essential NMD factors. The complex between SMG1, SMG8 and SMG9 is abbreviated as SMG1C complex (Yamashita et al., 2009).

SMG1 is a 410 kDa serine-threonine kinase recognizing S/TQ motifs. The other members belonging to the PIKK family are ATM, ATR, DNA-PKcs, TOR, TRAPP. All PIKK family members have a similar architecture: A conserved N-terminus comprising HEAT repeats (Huntingtin, elongation factor 3 (EF3), protein phosphatase 2A (PP2A), TOR1) followed by the FAT (FRAP/TOR, ATM, and TRRAP) domain, the conserved kinase domain (PI3K) and a C-terminal FATC domain (FAT C-terminal). SMG1 is an exception regarding this architecture as it contains an insertion domain of >1000 amino acids between the PI3K and FATC domains named as C-insertion domain. The insertion domain is poorly characterized. Moreover, SMG1 has a shorter N-terminal HEAT repeat region when compared to the other PIKK kinases. SMG8 is a 110 kDa protein and SMG9 is 58 kDa protein. The C-terminal region of SMG8 interacts with SMG9, and SMG8-SMG9 can form a complex independent of SMG1. SMG9 contains a putative NTPase domain and can form homodimers (Fernandez et al., 2011).

In Electron-Microscopy (EM), the SMG1C was observed to comprise a head and an arm domain (Arias-Palomo et al., 2011). The head domain comprises the catalytic domain of SMG1 kinase. The protruding arm is formed by N-terminal HEAT repeats of SMG1. SMG8 and SMG9 interact with the N-terminal region of the SMG1 kinase resulting in an overall S shape. Binding of SMG8 and SMG9 has been reported to result in an overall structural change of SMG1 (Arias-Palomo et al., 2011). SMG8 negatively regulates the SMG1 kinase activity (Yamashita et al., 2009). It is interesting to note that even though SMG8 seems to interact with the N-terminal region of SMG1, it thus has an effect on the catalytic domain of SMG1 located in the head region (Arias-Palomo et al., 2011).

In recent years the interactions of SMG1 kinase with various NMD factors are well studied as well as their impact on SMG1 kinase activity (Bono, 2014; He & Jacobson, 2015b; López-Perrote et al., 2016). SMG1 kinase has been shown to interact with UPF1, UPF2, DHX34 (DEXH box helicase 34) and RUVBL1/2 (Izumi et al., 2010). Structural studies by electron microscopy indicate that UPF1 binding to the head domain of SMG1 results in the displacement of C-insertion domain (Deniaud et al., 2015). This conformational rearrangement allows UPF1 to access to the SMG1 kinase active site. The C-insertion domain along with SMG8 and SMG9 was shown to be important to regulate the binding and phosphorylation of UPF1 (Deniaud et al., 2015). UPF1 Thr28, Ser1078, Ser1096 and Ser1116 are the important residues that are phosphorylated by SMG1C *in vivo* in mammals. UPF2 can bind to SMG1 in an UPF1-independent manner, interacting with the FKBP12-rapamycin binding domain which is an

important part of the conserved kinase domain. UPF2 promotes an open SMG1 conformation for UPF1 binding (Melero et al., 2014). More recently, DHX34 helicase was shown to activate UPF1 phosphorylation (Hug & Cáceres, 2014) by acting as a scaffold protein to recruit UPF1 to SMG1. The direct binding of DHX34 to the SMG1 kinase through its C-terminal domain promotes UPF1 phosphorylation (Melero et al., 2016).

Yamshita et al. detected UPF3A in the *in vivo* pulldowns in 2001. But the complex formation between SMG1 kinase and the RRM domain of UPF3B was reported for the first time *in vitro* by Clerici et al. 2014 using surface plasmon resonance. Recent work in our laboratory indicated that UPF1 is less phosphorylated by SMG1C in presence of UPF3B and UPF2 (Neu-Yilik & Raimondeau et al., under review). This interesting observation prompted us to answer the question and resulted in the identification of the interaction between UPF3B and SMG1C. We further characterized this interaction in order to understand whether it could play a role in NMD regulation. The work presented here provides first insights into UPF3's interaction with SMG1C and the regulating effect of this interaction on kinase activity of SMG1C.

5.3 Results

5.3.1 Interaction between SMG1C and UPF3

UPF3 consists of two paralogs UPF3B and UPF3A. UPF3A is upregulated when UPF3B is downregulated (Chan et al., 2009). They have been shown to have antagonistic function in NMD (Shum et al., 2016). In our study we studied both the paralogs.

Full-length UPF3B and UPF3A were successfully produced using an insect cell expression system (Fitzgerald et al., 2007). A stable and active trimeric complex of SMG-1-8-9 (SMG1C) was used for all the studies which was expressed and purified from mammalian cells using the SBP tag and size exclusion chromatography (Deniaud et al., 2015). To investigate whether UPF3B and UPF3A interact with SMG1C, *in vitro* pulldown experiments were performed. Briefly, SMG1C complex was immobilized on streptavidin beads via its N-terminal SBP tag. UPF3B/UPF3A were incubated with SMG1C, the beads were washed and the complex eluted from the streptavidin beads using biotin. The eluate was analyzed using SDS-PAGE followed by silver staining. Analysis of the eluted complexes (Figure 5.1A), shows that UPF3B can be eluted from the beads and a complex is formed between SMG1C and UPF3B. Moreover, the pulldown also indicates that a complex can form between SMG1C and UPF3A *in vitro* (Figure 5.1A, Elution). When we compare the intensities of the silver stained bands of UPF3B or UPF3A and SMG9 in Figure 5.1A, we estimate that the complex is formed in a stoichiometric manner, likely comprising one copy of each protein, as indicated by the fact that the intensities of the bands are virtually identical. We used surface plasmon resonance (SPR) and a streptavidin chip to immobilize SMG1 and thus the SMG1-8-9 complex to determine the dissociation constant (K_d)

of UPF3A and UPF3B from the SMG1C complex. The K_d was determined to be 38nM and 21nM for UPF3B and UPF3A, respectively (Figure 5.1B). Surprisingly the K_d we determined is very similar with that of UPF1 and SMG1C, which was determined to be 38nM, using micro-scale thermophoresis experiments (MST) (Deniaud et al., 2015).

5.3.2 UPF3 affects the interaction between SMG1C and UPF1

To understand how the interaction between SMG1C and UPF3 affects the complex formation between SMG1C and UPF1 or SMG1C-UPF1-UPF2 complex formation, additional pulldowns were carried out. To this end, we purified full-length UPF1 and UPF2 from insect cells (Figure 5.1C). Different combinations of UPF1, UPF2 and UPF3B were incubated with SMG1C immobilized on streptavidin beads or empty beads as control. The complex formation between SMG1C, UPF1 and UPF2 has been reported before (Deniaud et al., 2015; Melero et al., 2014). We find that UPF1 binding to SMG1C is reduced in the presence of UPF2 compared to UPF1 binding alone to SMG1C (Figure 5.1C, (Deniaud et al., 2015)). Interestingly, when UPF1 and UPF3B are added together to SMG1C, the interaction of UPF1 with SMG1C was reduced even more drastically. The pulldown experiments were repeated 5-times, with reproducible results. We therefore conclude that UPF3B weakens the interaction between SMG1C and UPF1. Intriguingly, a novel complex of SMG1C-UPF2-UPF3B was also observed. A macromolecular complex between SMG1C and all the UPFs can be formed as well in vitro. To the best of our knowledge this is the first time that formation of this complex was shown with purified proteins in vitro, the existence of the complex was postulated based on immunoprecipitations from human cell extracts (Yamashita et al., 2009). In conclusion, we find that UPF3B can form complexes with SMG1C alone and in combination with UPF2 as well as in complex with UPF1 and UPF2. UPF3B interaction with UPF1 however seems to interfere with SMG1C binding.

5.3.3 The UPF3B RRM like domain interacts with SMG1C

The exact interaction region between SMG1C and UPF3B was determined using different UPF3B deletion constructs. UPF3B contains a RRM like domain at its N-terminus and an EJC-binding domain (EBD) at its C-terminus. The schematics of the UPF3B deletion constructs used here are depicted in Figure 5.2. All the constructs were expressed in insect cells with the exception of UPF3B fragments containing residues 42-143 and 45-217 that were expressed in *E. coli*. The purified proteins are shown in Supplementary Figure 5.3. We immobilized SMG1C on streptavidin chips via the SBP-tag of SMG1. Subsequently we injected the various UPF3B constructs at a concentration of 100 nM each. We found that the residues at the N-terminus (aa 1-143) comprising the RRM domain are not required for the interaction with UPF3B (Figure 5.2A) as no signal was observed. Similarly the UPF3B deletion constructs lacking residues 256-402 or

residues 380-470 did not show any SMG1C binding. In conclusion, the residues at the C-terminus are also not essential for the interaction of SMG1C with UPF3B (Figure 5.2B).

However, residues 146-217 of UPF3B were found to be essential for interaction between SMG1C and UPF3B (Figure 5.2A). While we could not produce a deletion construct comprising only these residues, we found that a construct comprising the first 217 amino acids of UPF3B binds SMG1C as well as a construct comprising UPF3B residues 179-402 (Figure 5.2A and 5.2C). Interestingly, when we deleted the C-terminal part of UPF3B containing the EBD, UPF3B seemed to have a higher affinity for SMG1C compared to wildtype UPF3B (Figure 5.2C). This indicates that the last 70 C-terminal residues of UPF3B comprising the EBD interfere to some extent with the binding of UPF3B to SMG1C.

It is interesting to note that the fragment 1-217 of UPF3B which was purified from insect cells interacts with SMG1C. In contrast, fragment UPF3B 45-217 purified from *E. coli* does not interact with SMG1C (Figure 5.2D). We speculate that possible post-translational modifications are present in UPF3B purified from insect cells (see next paragraph), but absent when the protein is purified from *E. coli*. These posttranslational modifications in UPF3B may be important for the interaction.

5.3.4 UPF3 is a substrate for SMG1 kinase

UPF1 is the most important and best characterized substrate of SMG1C. UPF1 phosphorylation is the key step for triggering NMD (Okada-Katsuhata et al., 2012; Yamashita, 2013). The phosphorylation of UPF1 was shown to be affected in presence of UPF3B (Neu-Yilik & Raimondeau et al. 2017). Therefore, we decided to further analyze the kinase reaction and to investigate whether UPF3B is a substrate for SMG1C. For the phosphorylation reaction, the purified proteins UPF3B and UPF3A were incubated with SMG1C for 30 min at 37 °C. Subsequently, the reaction was analyzed using SDS-PAGE followed by ProQ as well as Coomassie staining (Thermo Fisher). The resulting ProQ gel showed a clear phosphorylation of UPF1 in the presence of SMG1C confirming the activity of the kinase. For UPF3B we found a slight increase in the intensity (Figure 5.3A). Since the background phosphorylation signal of full size UPF3A and UPF3B was quite high to start with, indicating that UPF3 becomes phosphorylated in insect cells, we dephosphorylated the proteins using lambda phosphatase.

We found that also for dephosphorylated UPF3B and UPF3A the signal slightly increased after incubation with SMG1C (Figure 5.3A). As the intensity of the band stained by ProQ was very low, radioactive ATP was used next to further confirm a phosphorylation of UPF3A and UPF3B by SMG1C. In this case, radioactive phosphate is incorporated into the UPF3B by the SMG1C kinase. Again we found a signal corresponding to UPF3B after incubation with SMG1C and ATP. In summary, UPF3B/UPF3A are substrates for SMG1C in vitro (Figure 5.3B).

Interestingly and in agreement with our conclusion above, dephosphorylated UPF3B and UPF3A showed a lower affinity to SMG1C in SPR experiments compared to phosphorylated UPF3A and UPF3B (Figure 5.3C, Supplementary Figure 2). We conclude that UPF3B and UPF3A are substrates of SMG1C and that the phosphorylation of UPF3B and UPF3A is important for its interaction with SMG1C.

5.3.5 UPF3 inhibits the phosphorylation of UPF1

Phosphorylation of UPF1 by SMG1C is well-characterized biochemically. In vitro at pH 9.0, SMG1C phosphorylates approximately two UPF1 phosphorylation sites within 10 min (Deniaud et al., 2015). We observed that the interaction between UPF1 and SMG1C is affected in the presence of UPF2 and of UPF3B. Therefore, the phosphorylation kinetics of UPF1 by SMG1C in the presence of UPF2, UPF3B or both were tested (Figure 5.4). A deletion construct of UPF2 (UPF2 B31) from *E. coli* was used as UPF2 FL from insect cells was obtained with low yields and additionally was contaminated by a kinase, which could not efficiently be removed from the sample. The presence of UPF2 and UPF3B inhibited the phosphorylation of UPF1 by SMG1C at physiological buffer conditions (Figure 5.4). At pH 7.5 using Mg^{2+} (2.5 mM) rather than Mn^{2+} ions in the reaction, phosphorylation of UPF1 was slower than observed before (Deniaud et al., 2015). The amount of Ser/Thr residues of UPF1 phosphorylated by SMG1C in presence of UPF3B was approximately reduced to 50%. This suggests a more complex regulation of NMD by UPF2 and UPF3B than previously assumed and indicates that UPF3B plays actually a role in regulation of SMG1C kinase activity.

5.3.6 Phosphorylation is important for UPF3B to interact with SMG1C

To identify the sites that have been phosphorylated by SMG1C, UPF3B was analyzed by mass spectrometry (MS) after incubation with SMG1C. UPF3B was treated with SMG1C for 30 min at 37 °C. We also analyzed UPF3B phosphorylation by SMG1C in the presence of UPF1 (Figure 5.5). Even though UPF3B was expressed from insect cells and known to be phosphorylated as seen from ProQ staining (Figure 5.3 and Supplementary Figure 5.3), no phosphorylation sites were detected in MS analysis. However, addition of SMG1C resulted in the phosphorylation of three sites in UPF3B: Thr18, Thr169, and Thr446 residues (Figure 5.5). Thr446 was phosphorylated by SMG1C in both samples, the phosphorylated UPF3B purified from insect cells as well as UPF3B treated with lambda phosphatase ('dephosphorylated UPF3B'). Notably, in the presence of UPF1, UPF3B Thr18 was not phosphorylated by SMG1C but Thr169 and Thr446 are still phosphorylated. This is at odds with our previous finding that in SPR studies UPF3B residues 1-143 are not important for the interaction with SMG1C but the residues from 146 – 256 are required (Figure 5.2). Further studies have to be performed to analyze the importance of UPF3B phosphorylation in general and of the individual impact of the three phosphorylation sites

identified here. When the phosphorylation status of UPF1 was analyzed, Thr922 was the only residue that was found not to be phosphorylated by SMG1C kinase in the presence of UPF3B. There is no evidence in the literature showing that this residue plays a role in NMD.

5.3.7 Negative-stain EM structure of UPF3B bound to SMG1C

In order to further characterize the binding of UPF3B to SMG1C we subjected the complex to negative stain EM. SMG1C was incubated with a 5X excess of UPF3B and then used for grid preparation and data collection. All samples were stained with 2% w/v uranyl acetate. Similarly, SMG1C alone was subjected to negative stain EM as a control. A total of 80 micrographs were collected on a FEI F20 microscope under low dose conditions at a magnification of 50,000x using a 4k × 4k CCD camera. 9,900 particles were picked from the images for SMG1C and after 2D classification 9,400 particles were selected for 3D reconstruction and 3D classification, using the map of SMG1C complex (emd_2663) (Melero et al. 2014) as an initial model. Similarly, 24,600 particles were picked for the SMG1C-UPF3B complex and 24,000 particles were selected for 3D reconstruction after 2D classification. Again the map emd_2663 filtered to 60 Å was used as initial model.

The SMG1C complex architecture has been described before by the Llorca laboratory (Melero et al. 2014). The head domain is formed by the C-terminal part of the SMG1 comprising the FAT domain, the kinase domain and FATC. The tubular arm is formed by the N-terminal HEAT of SMG1 repeats. SMG8 and SMG9 bind to the N-terminal arm region (Arias-Palomo et al. 2011, Yamashita et al. 2009, Melero et al. 2014, Deniaud et al. 2015). Overall, the complex adopts an S-shape.

An overlay of the 3D reconstructions of SMG1C alone and the SMG1C-UPF3B complex is depicted in Figure 5.6. We observe an overall movement of the SMG1 head region in the presence of UPF3B. Extra density is detected near the tubular arm, this density may correspond to parts of UPF3B. Notably, only a crystal structure of the N-terminal RRM domain of UPF3B is available to date (Kadlec et al., 2004) and a small peptide corresponding to the EBD (Melero et al., 2012b). The rest of UPF3B is predicted to be very flexible and its structural organization is unknown. The negative-stain EM reconstruction does not show defined density, which would allow to fit the RRM domain of UPF3B. Thus, at this point it is unclear whether the extra density observed in the UPF3B-SMG1C reconstruction is due to UPF3B or due to a conformational change in SMG1C.

To localize UPF3B in the 3D reconstruction and to determine the UPF3B binding site on SMG1C, we used an IgG antibody specific for UPF3B. The antibody used was specific for the residues 300-350 of UPF3B. The resulting negative stain images show antibody binding to the head region of SMG1C (Figure 5.6B), indicating that UPF3B binds to or next to the head region of SMG1C, which comprises the kinase domain.

5.4 Discussion

NMD is a highly regulated mRNA quality control process in the eukaryotic cell that targets aberrant mRNAs for decay. The major event in NMD is the hyper phosphorylation of UPF1 by SMG1C kinase. Activation of SMG1 kinase is triggered as a result of different transient complexes that are formed when a PTC is encountered by a translating ribosome. The exact compositions of these NMD activating complexes are still unknown.

An interaction between eukaryotic release factor eRF3a and UPF1 on the ribosome stalled at a PTC is assumed to be an important step in activation of NMD. This interaction is assumed to recruit the other key NMD factors to the ribosomal complex, which are UPF2, UPF3B, EJC and SMG1C. Recent studies have shown new interactions of UPF2 with eRF3a, UPF3 with eRF3a and UPF1 with UPF3B (López-Perrote et al., 2016) (Neu-Yilik & Raimondeau et al., submitted). The significance of these new interactions remains to be defined *in vivo*. Clearly, if relevant they add a new level of complexity to the process of NMD. The biochemical experiments presented here characterizing the interactions between the SMG1C and UPF proteins indicates new layers of regulation of UPF1 phosphorylation by SMG1 in the presence of UPF2 and UPF3.

Here, full-length proteins purified from insect cells were used which is assumed to resemble closely the proteins *in vivo*. The studies conducted before have used deletion constructs or proteins that were expressed in *E.coli* (Clerici et al., 2014; Melero et al., 2012a). UPF factors are large in size and contain many post-translational modifications and hence it is important that they are expressed in the right expression system. The interaction between SMG1C and UPF3B that is identified is novel and has been unknown before. It also affects the interaction of UPF1 with that of SMG1C (Figure 5.1) and inhibits the phosphorylation of UPF1 in the presence of UPF3B (Figure 5.4). Moreover, we find that in addition to UPF1, UPF3B is also a substrate of SMG1C as shown in Figure 5.3.

It is assumed that UPF2 is the bridging factor between UPF1 and UPF3 bound to EJC and that the UPF1-2-3 interaction is essential to mark the mRNA for decay. However, UPF2-independent NMD (Chan et al., 2007; Gehring et al., 2005; Huang et al., 2011; Ivanov et al., 2008) has been reported and in these cases UPF3B becomes a major player to activate NMD. We speculate that the direct interaction of UPF3B with UPF1 and SMG1C may play an important role in UPF2-independent NMD.

Phosphorylation is an important post-translational modification that regulates many proteins. When UPF1 is hyper phosphorylated it recruits decay factors to the mRNA. In the present study that has been reported here, UPF3B expressed from insect cells is phosphorylated (Figure 5.3) and its dephosphorylation affects the interaction with SMG1C. Next, we need to identify the insect cell specific phosphorylation sites in UPF3B and see whether UPF3B purified from human

cells has the same phosphorylation pattern. Future work thus needs to confirm the various UPF3B phosphorylation sites identified by MS and their role in regulation of the NMD pathway. Our study underpins the important role of UPF3B in NMD and indicates that the function of UPF3B in NMD activation and regulation requires additional attention.

5.5 Methods

5.5.1 Plasmids

Plasmids encoding UPF1, UPF2, UPF2L, UPF3A and UPF3B were generated by subcloning NcoI/NotI digested fragments from the respective pCI Neo/PcDNA vectors (Promega) into pFastBacHtb (Life Technologies). Deletion constructs for pFastBacHtb_UPF3B were generated by self-SLIC (M.Z. Li & Elledge, 2007) and also by subcloning into pFastBacHtb using restriction enzymes Nco1 and Not1. The plasmid pET21d_UPF2L (121-1227) was generated by subcloning pPROExHtb_UPF2 (121-1227) into pET21d (EMD Biosciences) using restriction enzymes Nco1 and Not1. The gene encoding SMG1 with an N-terminal streptavidin-binding peptide (SBP)-tag was cloned into the pLEXm plasmid. Genes encoding SMG8 with an N-terminal hexahistidine-tag and SMG9 were synthesized (GenScript) and subcloned into the pLEXm and the pcDNA5-frt plasmids, respectively (Deniaud et al., 2015).

5.5.2 Protein production and purification

His-tagged human UPF1, UPF2, UPF3A and UPF3B were expressed using the MultiBac expression system in SF21 cells (Fitzgerald et al., 2007). His-tagged UPF2L was expressed in *E. coli* strain BL21-Gold (DE3) (Life Technologies). The cells were lysed in buffer A (25 mM Hepes-KOH pH 7.5, 10 mM imidazole, 300 mM KCl, 5 mM 2-mercaptoethanol, 5% glycerol (v/v)) supplemented with protease inhibitor cocktail (Roche) and 0.1% NP40 for the insect cell expressed proteins. Lysed cells were centrifuged at 30,000xg for 30 min at 4°C. The supernatant was subjected to Ni-NTA affinity chromatography (QIAGEN). After washing the proteins were eluted with buffer A containing 150 mM KCl and 200 mM imidazole. Proteins were further purified using a HiTrap QXL column (GE Healthcare) equilibrated with 25 mM Hepes-KOH pH 7.5, 150 mM KCl, 1 mM DTT, 5% glycerol (v/v); followed by cation exchange chromatography using a HiTrap SP/HP column (GE Healthcare) for UPF2 and UPF3B similarly. UPF1 was further purified by size exclusion chromatography (SEC) using a Superdex-200 column (GE Healthcare) equilibrated with buffer B (25 mM Hepes-KOH pH 7.5, 300 mM KCl, 5 mM Dithiothreitol (DTT), 5% glycerol (v/v)). All proteins were flash-frozen in liquid nitrogen and stored at -80 °C till further use.

5.5.3 Purification of SMG1C complex

SMG1C was expressed in HEK-293T cells in T300 flasks. A plasmid ratio of 2:1:1 in mass was used for the transfection of SMG1, SMG8 and SMG9 respectively using polyethylimine (PEI). 48 h post-transfection, the cells were recovered by scraping. The cells were pelleted, frozen and stored at -80°C . The cells were lysed using cytobuster (Calbiochem) supplemented with protease and phosphatase inhibitors (Roche). After centrifugation ($100,000\times g$, 30 min, 4°C), the supernatant was mixed with 1 mL of streptavidin beads (Fisher Scientific) equilibrated with SMG1C buffer (20 mM Tris-HCl pH 9.0, 100 mM KCl, 25 mM glycine, 1 mM DTT and 5% sucrose (w/v)) and incubated for 2 h at 4°C . The beads were washed with 50 ml of SMG1C buffer and the complex was eluted by incubation for 30 min with SMG1C buffer containing 2 mM biotin, followed by SEC (Superose-6 10/300, GE-Healthcare) equilibrated using SMG1C buffer. Monomeric SMG1C complexes were concentrated with a 100-kDa-cutoff concentrator, flash-frozen in liquid nitrogen and stored at -80°C till further use (Deniaud et al., 2015).

5.5.4 Dephosphorylation of UPF3B/UPF3A

Purified UPF3B and UPF3A from insect cells were dephosphorylated using lambda phosphatase (λ -PP, NEB) in 1X PMP buffer, 1mM MnCl_2 and buffer B (25 mM Hepes-KOH pH 7.5, 300 mM KCl, 5 mM Dithiothreitol (DTT), 5% glycerol (v/v)). The reaction was allowed to take place at 30°C for 60 min. The UPF3B/UPF3A and λ -PP were separated by SEC (Superdex 200 10/300) equilibrated with buffer B. UPF3 containing fractions were concentrated with a 30-kDa-cutoff concentrator, flash-frozen and stored at -80°C till further use.

5.5.5 SMG1C pull-down experiments

9 μg of SMG1C was mixed with approximately ten-fold molar excess of the UPF1, UPF2FL, UPF3B and UPF3A in buffer C (20 mM Tris-HCl pH 7.5, 100 mM KCl, 1 mM MgCl_2 , 0.01% Tween 20 (v/v), 5% Sucrose (w/v) and 1mM DTT) in a reaction volume of 48 μL . The complexes were incubated for 2 h at room temperature. After centrifugation (10 min, $13,400\times g$ at 4°C), 30 μl of streptavidin beads were added to the mixture and incubated for 2 h at 4°C . The beads were washed three times with 400 μL of buffer C and the complexes were eluted in 30 μl of buffer C supplemented with 4 mM biotin. 12 μL of each sample was supplemented with protein gel loading buffer (PGLB). The samples were boiled for 10 min and subsequently analyzed on 4-12% Bis-Tris gels. The PAGE gels are either Coomassie or silver stained.

5.5.6 Kinase assays

A total of 100 fmoles of SMG1C was mixed with 4 pmoles of UPF1 in buffer D (20 mM Tris-HCl pH 7.5, 100 mM KCl, 5% glycerol (v/v), 1 mM MgCl_2 , 2 mM DTT) in a reaction volume of

30 μ L. The reaction was started by the addition of 12 mM ATP-MgCl₂ (2 mM final concentration). Addition of PGLB and subsequent boiling of the samples for 5 min stopped the reaction. For UPF1 phosphorylation experiments in the presence of UPF2 and UPF3B, 8 pmoles of UPF2 (121–1227) and/or 8 pmoles UPF3B were included in the reaction. 4-12% Bis-Tris gels were used for separation, stained first with Pro-Q Diamond staining (Life Technologies) followed by Coomassie staining. The Pro-Q stained gels were imaged with a Typhoon scanner using 532 nm and 580 nm as excitation and emission wavelength, respectively. The bands were quantified with the Image Quant software. The number of UPF1 phosphorylation sites was determined using ovalbumin as a standard (ovalbumin contains two phosphorylated sites per molecule) (Supplementary Figure 4).

5.5.7 In vitro phosphorylation

100 fmoles of SMG1C was added to 4 pmoles of UPF1/UPF3B in buffer consisting 20 mM Tris-HCl pH 7.5, 100 mM KCl, 5% glycerol (v/v), 1 mM MgCl₂, 2 mM DTT in a final reaction volume of 10 μ L. The reaction was started by adding 2.5 μ L 10 mM ATP and 1.5 μ L γ 32P-ATP and was allowed to proceed for 30 min at 37 °C. Samples were separated by 10% SDS-PAGE and visualized by autoradiography.

5.5.8 Surface plasmon resonance experiments

Surface plasmon resonance (SPR) experiments were performed on a BIAcore3000 machine using streptavidin-coated sensor chips (GE-Healthcare). The first flow cell was not functionalized and used as a control surface. The second flow-cell was functionalized with purified SMG1C to a density of about 2,000 RU. The buffer contained 20 mM Tris-HCl pH 7.5, 250 mM KCl, 0.01% Tween-20 (v/v), 0.5 mM TCEP. UPF3B variants were injected at 60 μ l/min during 5 min followed by a 10 min dissociation phase. To determine the binding sites, all UPF3B variants were injected at 100 nM on both flow-cells. Between each UPF3B injection, the surface was regenerated by 30s injection of assay buffer containing 0.5 M KCl. Data were analyzed by subtracting both the signal from the control flow cell of any UPF3B injection as well as the buffer injection curve. For K_d determination Graph pad prism was used.

5.5.9 Negative-stain electron microscopy

SMG1C complex was diluted to 100 nM using the buffer D (20 mM Tris-HCl pH 7.5, 100 mM KCl, 5% glycerol (v/v), 2 mM DTT). 5 μ L of the sample was adsorbed onto a thin carbon film for 60s. The excess sample was blotted away with a filter paper, followed by 2% (w/v) uranyl acetate staining for 60s. The excess of the stain was blotted away and the grid was allowed to dry in air and stored in vacuum until data collection. SMG1C - UPF3B complexes were assembled by

incubating 100 nM of SMG1C with a 5X molar excess of UPF3B for 30 min on ice. For the SMG1C complex 80 micrographs and for SMG1C-UPF3B 86 micrographs were recorded under low-dose conditions at room temperature on a FEI F20 microscope (EM-platform, IBS Grenoble) at 200kV using a 4k × 4k CCD camera (GATAN) with a defocus of ~2 μM. The magnification used was 50,000x that corresponds to a pixel size of 2.3 Å.

5.5.10 Image-processing

Image processing was performed using the program RELION 1.4 (Scheres, 2012). CTFFIND4 was used for CTF estimation (Rohou & Grigorieff, 2015). The particles were picked manually from the micrographs using e2boxer (from EMAN2 tools) and then given to RELION for 2D and 3D classifications. The negative stain EM reconstruction of the SMG1C complex (EMD-2663, (Melero et al., 2014)) was filtered to 60 Å resolution and then used as the initial model for 3D classification, using RELION 1.4.

5.5.11 Antibody labeling of the SMG1C - UPF3B complexes

SMG1C - UPF3B complexes were mixed with 5X molar excess of anti-UPF3B antibody, recognizing residues 300-350 (Abcam 134566). After 30 min of incubation, 5μL of sample were used to prepare negative stain EM grids (see above). 50 micrographs were recorded at a magnification of 30 000× using a JEOL 1200EX II microscope operated at 100kV equipped with a CCD camera.

5.5.12 Mass-Spectrometry analysis

The phosphorylation reaction was stopped after 30 min using 1X PGLB and send to the Mass-spectrometry platform at EMBL-Heidelberg.

5.6 Figures

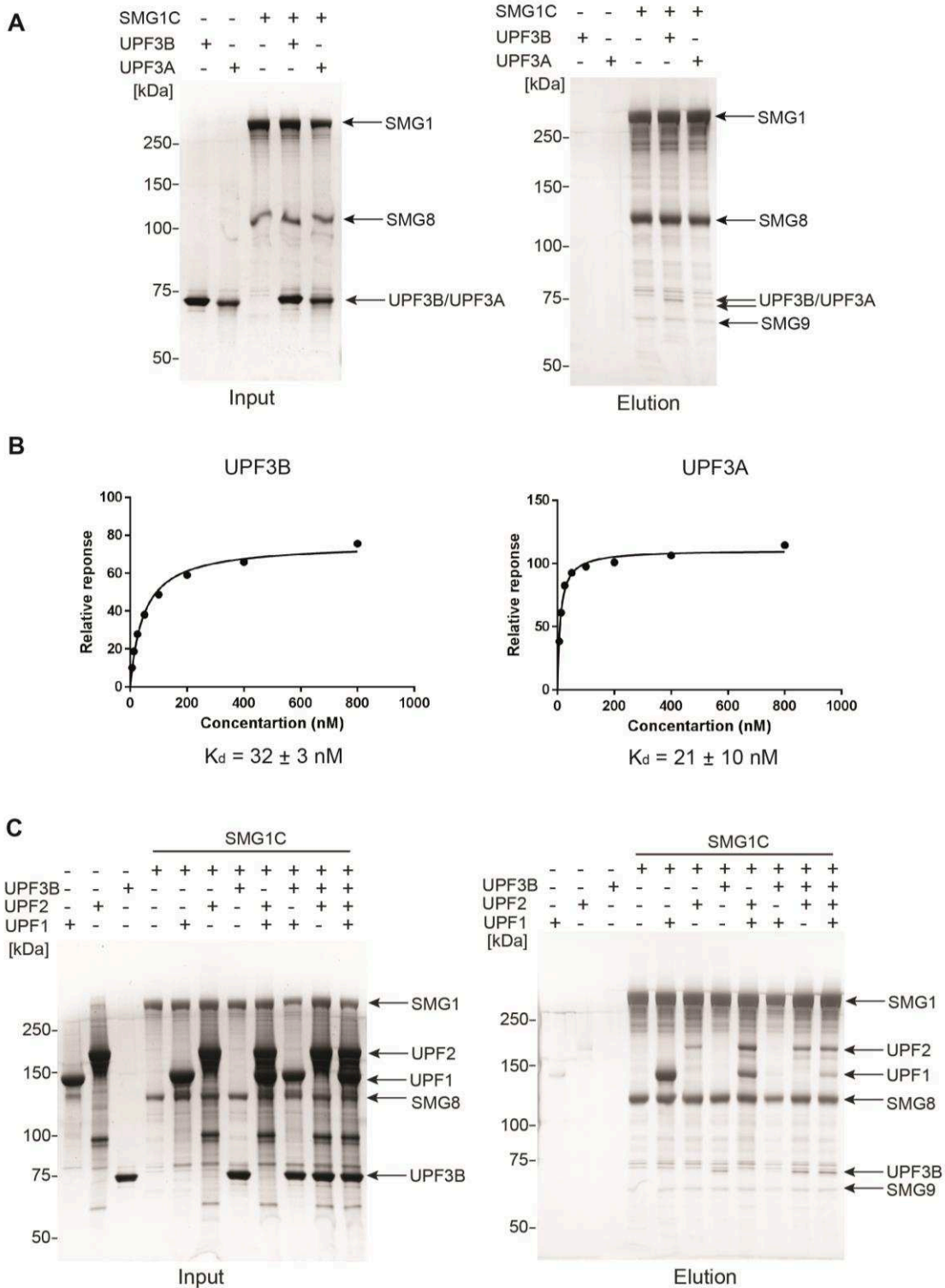


Figure 5.1 UPF3 forms a complex with SMG1C:

(A) In vitro pulldowns of UPF3B and UPF3A with immobilized SBP-tagged SMG1C. Protein mixtures before loading onto the beads (input, left) and after elution from the beads (elution, right) were separated 4-12% Bis-Tris gels and silver stained. The flowthrough and the wash gels are shown in Supplementary Figure 1 (B) Dissociation constants (K_d s) of UPF3B / UPF3A were determined using surface plasmon resonance (SPR). SMG1C was immobilized and different concentrations of UPF3B (left) and UPF3A (right) were injected. Graphpad prism was used for fitting the curve and the determination of the K_d s. A representative curve is shown here. The K_d was calculated from mean of three individual experiments (C) In vitro pulldowns of different combinations full-length UPFs (UPF1, UPF2, UPF3B) with immobilized SMG1C. The proteins were separated by 4-12% Bis-Tris gels and silver stained.

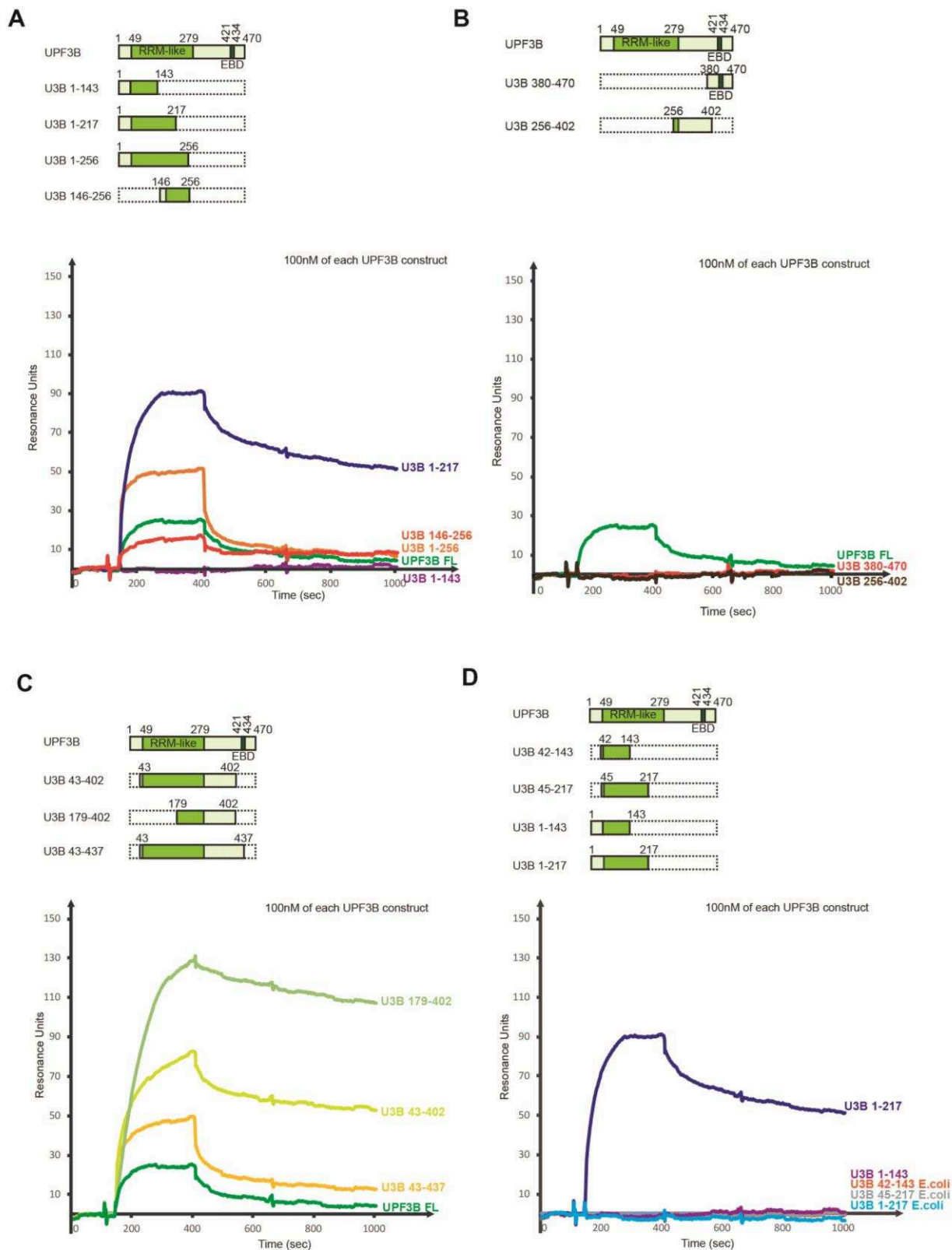


Figure 5.2 Interacting region of UPF3B with SMG1C:

Different deletion constructs of UPF3B were used to determine the interacting region of UPF3B with SMG1C by SPR. 100 nM of each UPF3B deletion construct was injected. All the constructs of UPF3B were expressed in insect cells except UPF3B 42-143 and UPF3B 45-217 which were expressed in *E.coli*. A scheme is presented for each deletion construct of UPF3B. (A) The first 140 amino acids of N-terminal UPF3B are not important for the interaction. (B) The last 200 amino acids of the UPF3B are not important for the interaction with SMG1C. (C) The exon junction binding domain (EBD) affects the interaction with SMG1C. Its deletion leads to a stronger interaction of UPF3B with SMG1C. (D) Phosphorylation of UPF3B in residues 1-217 is important for the interaction with SMG1C.

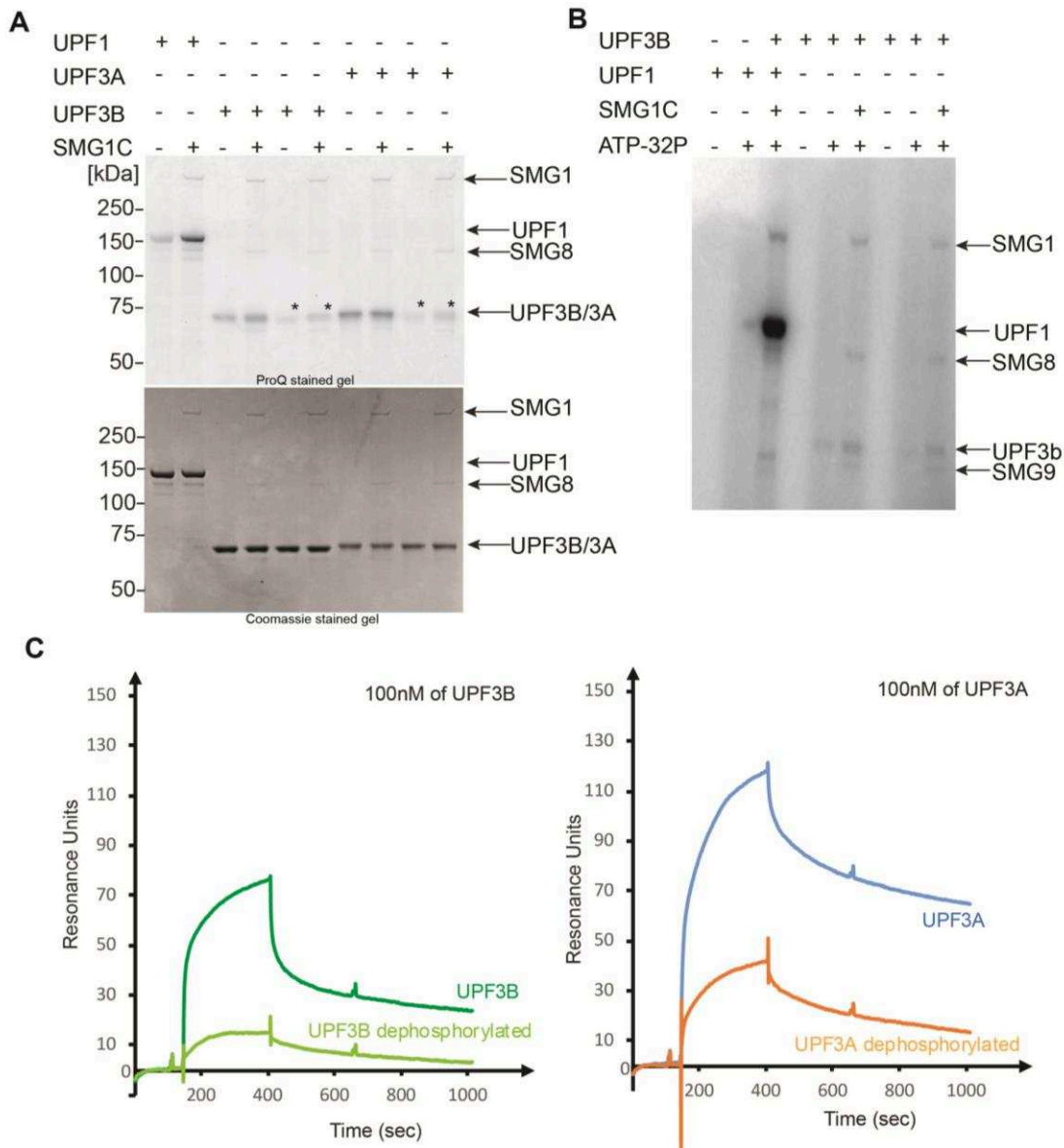


Figure 5.3 UPF3B and UPF3A are substrates for SMG1C kinase:

Phosphorylation of UPF3B and UPF3A is important for their interaction with SMG1C.

(A) UPF1, UPF3B or UPF3A or dephosphorylated UPF3B/UPF3A were incubated with SMG1C and ATP for 30 min and separated by 4-12% Bis-Tris gel electrophoresis. The gel was stained with pro-Q stain and then used for Coomassie staining. (B) UPF1, UPF3B and UPF3A were incubated with SMG1C and γ 32P-ATP for 30 min at 37 °C, the mixtures were separated by gel electrophoresis and the gel was used for autoradiography. (C) 100 nM of UPF3B or dephosphorylated UPF3B were used for SPR experiments and injected onto a surface where SMG1C was immobilized. (D) 100 nM of UPF3A / dephosphorylated UPF3A were used for SPR experiments and injected onto a surface where SMG1C was immobilized.

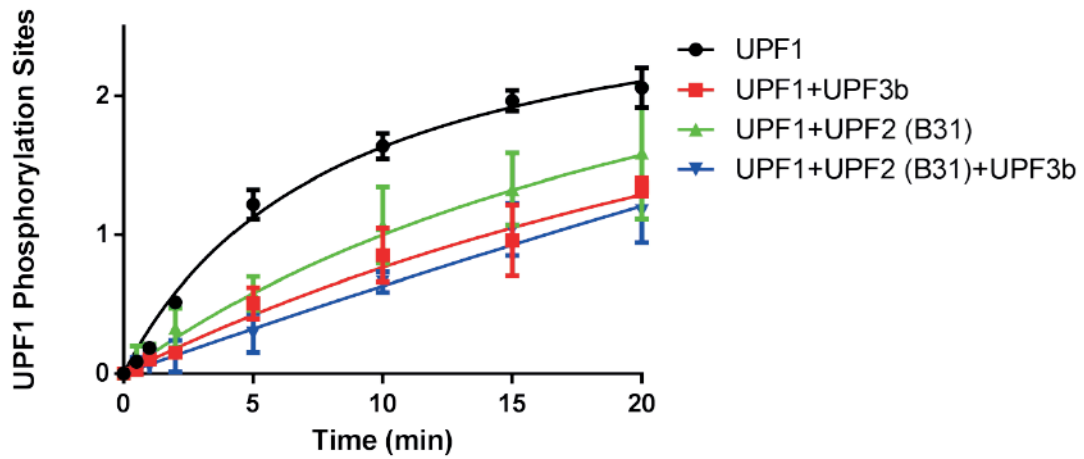
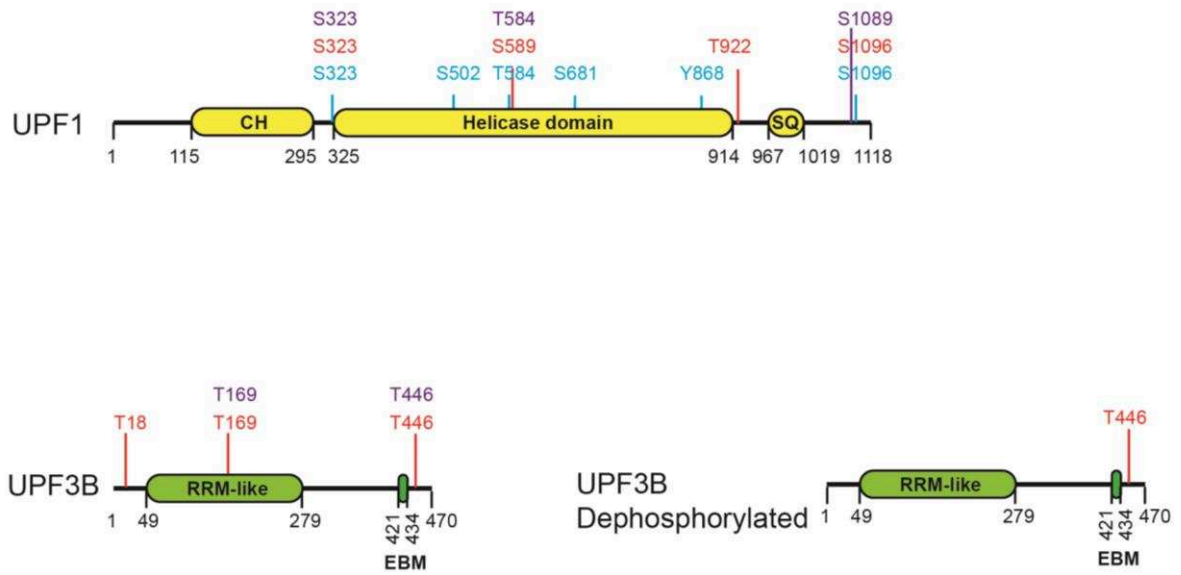


Figure 5.4 UPF2 and /or UPF3B inhibit phosphorylation of UPF1 by SMG1C:

UPF1 was incubated with different combinations of UPF2 (B31) and UPF3B to detect the effect of these NMD factors on phosphorylation of UPF1 by SMG1C. The reaction was stopped by addition of 1X PGLB. Protein mixtures were separated by 4-12% Bis-Tris gels, followed by Pro-Q staining and then Coomassie staining (see also Supplementary Figure 4). Pro-Q stained gels were imaged with a Typhoon scanner.



UPF1/UPF3B

UPF1/UPF3B + SMG1C

UPF1 + UPF3B + SMG1C

Figure 5.5 Mass spectrometry analysis of UPF1, UPF3B and dephosphorylated UPF3B after incubation with SMG1C and ATP:

Blue color indicates the sites that were found in the protein only, prior to incubation with SMG1. Red color indicates the phosphorylation sites of UPF1 or UPF3B only in the presence of SMG1C. The purple color indicates the sites that have been phosphorylated when both UPF1 and UPF3B are present during the reaction and phosphorylated by SMG1C.

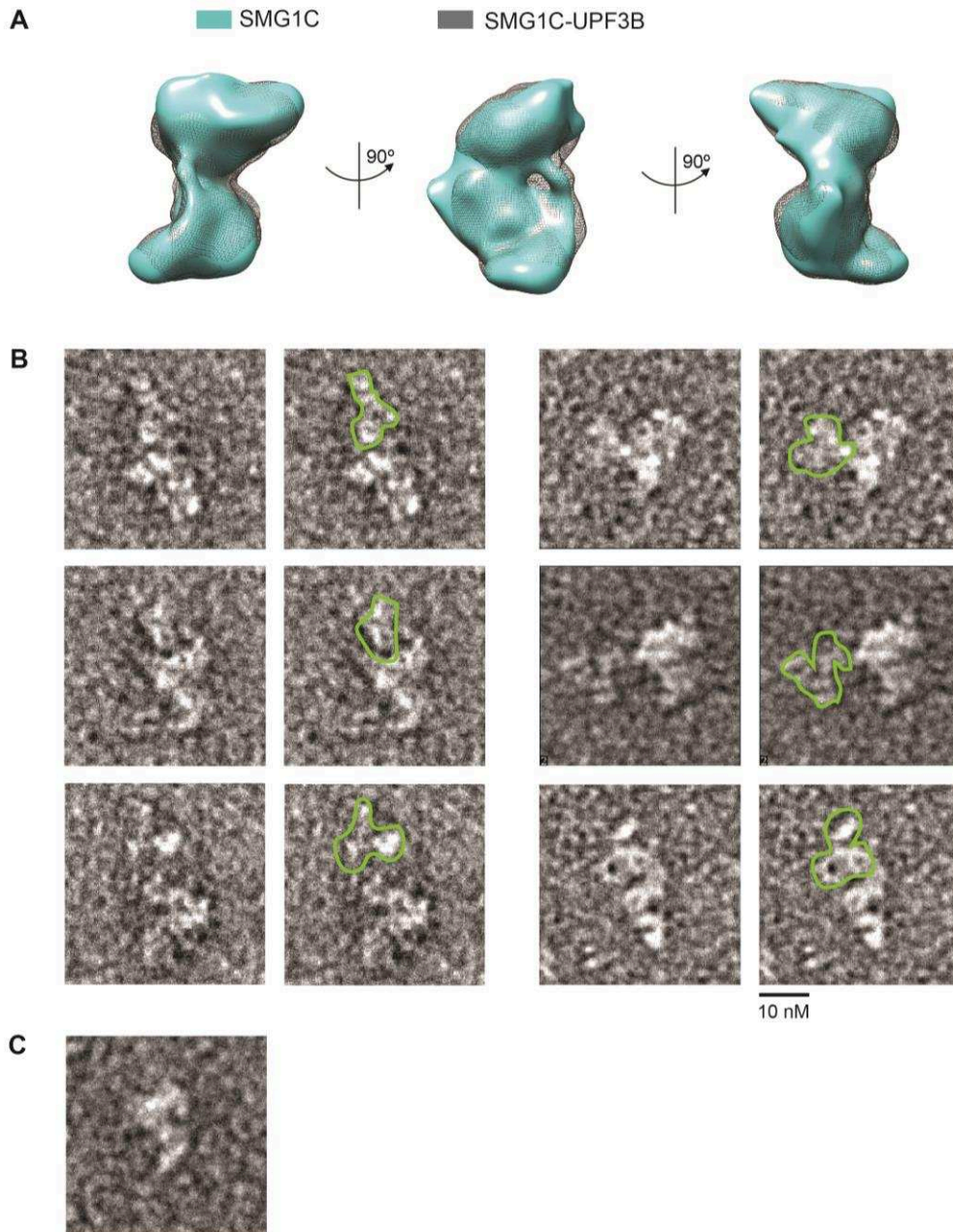
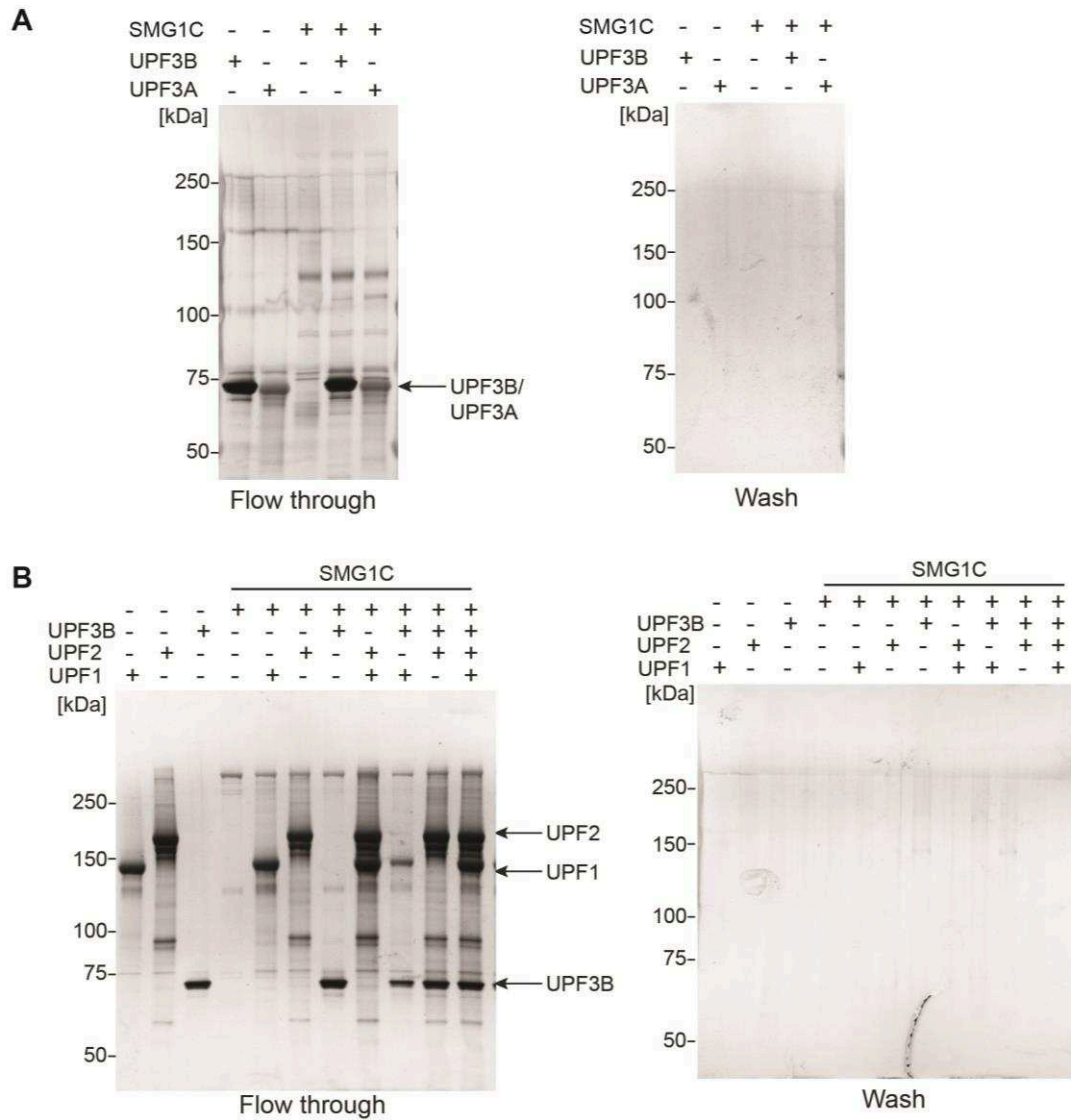


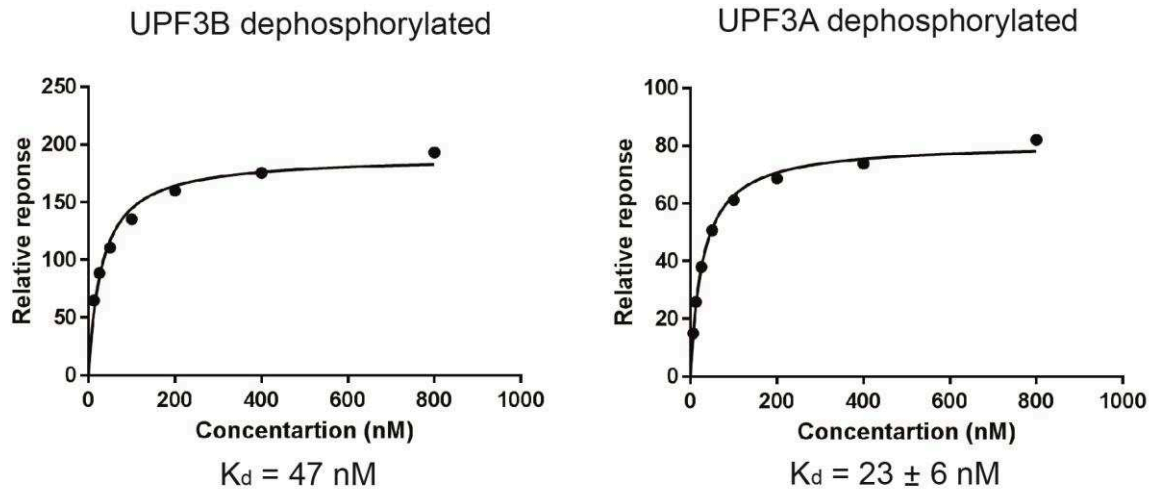
Figure 5.6 Negative stain of SMG1C complex with UPF3B:

(A) Negative stain reconstruction of SMG1C in presence of UPF3B. The light blue color indicates the structure of SMG1C that has been reconstructed using negative stain EM. The grey color indicates the structure of SMG1C-UPF3B. (B) Localization of UPF3B on SMG1C using an antibody specific for UPF3B residues 300-350 (Abcam 134566). The antibody is outlined in green. Binding of the antibody is observed near the head region of the SMG1C-UPF3B complex. (C) A representative image of SMG1C when negative stained

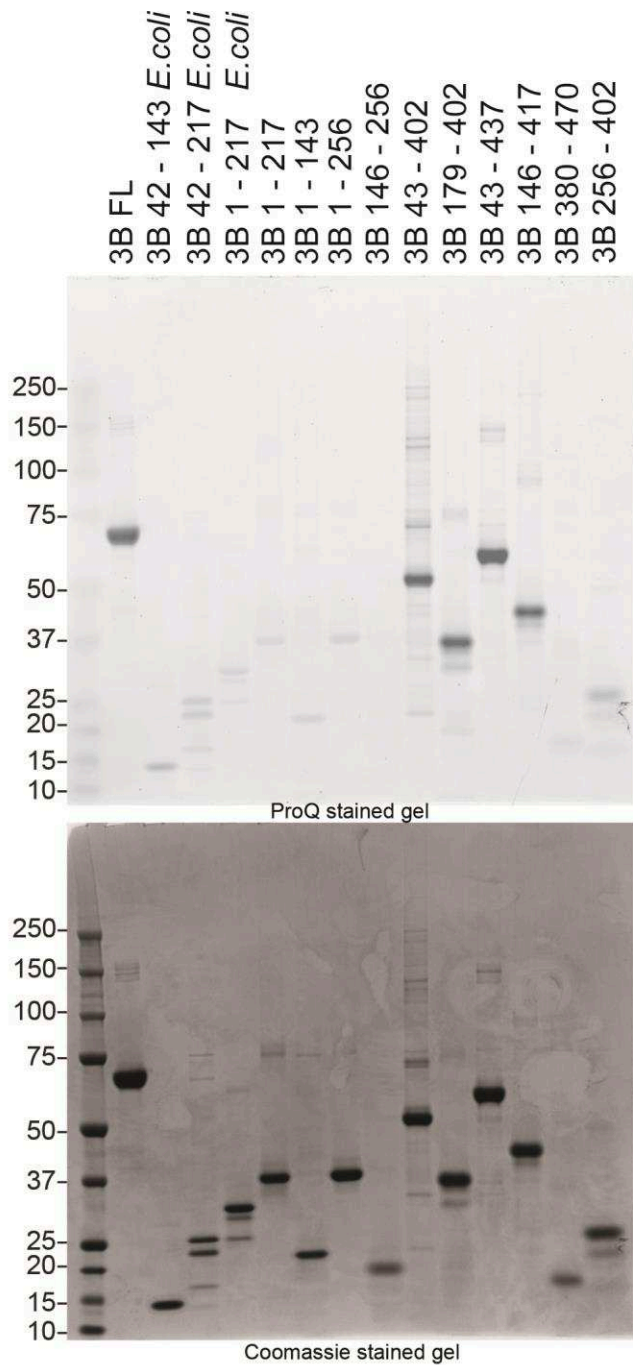
5.7 Supplementary Figures



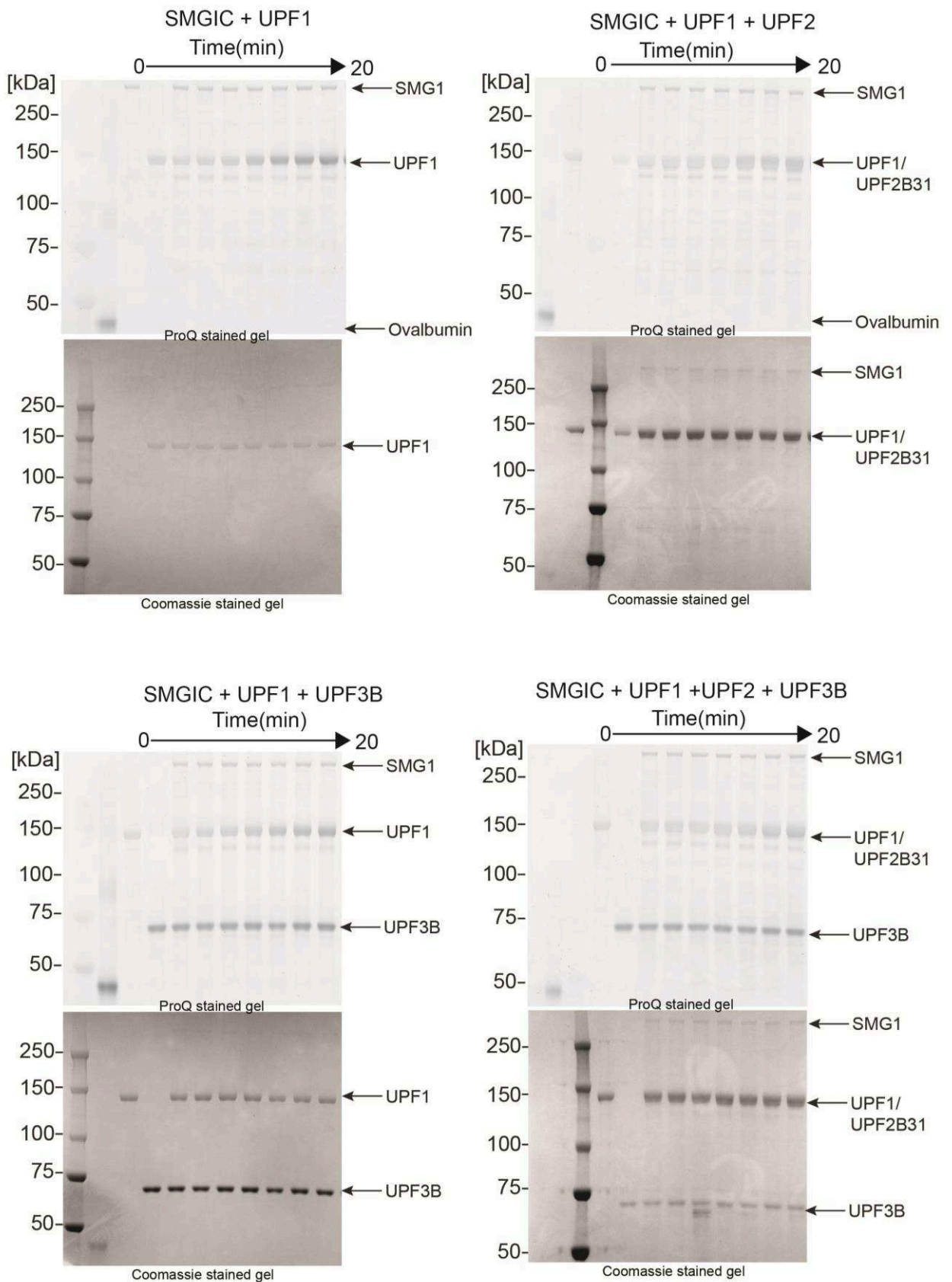
Supplementary Figure 1: (A) In vitro pulldowns of UPF3B and of UPF3A with immobilized SBP-tagged SMG1C. Protein mixtures of flow through and wash were separated by 4-12% Bis-Tris gels and silver stained. (B) In vitro pulldowns of different full-length UPF proteins (UPF1, UPF2, UPF3B) with immobilized SMG1C. Protein mixtures of flow through and wash were separated by 4-12% Bis-Tris gels and silver stained.



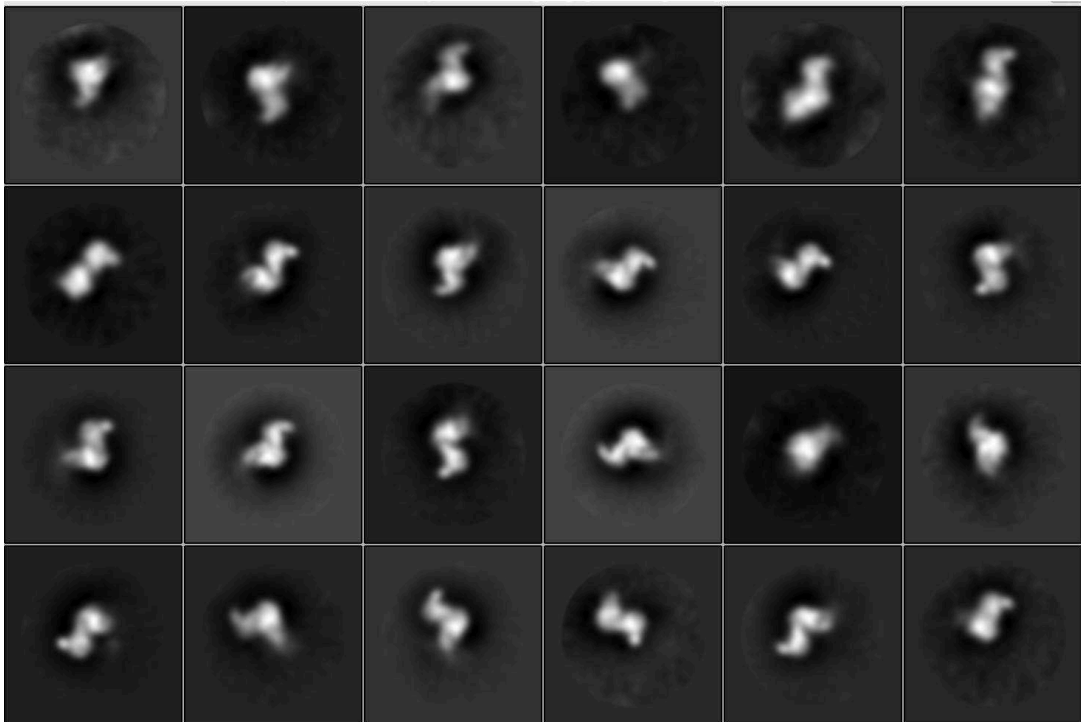
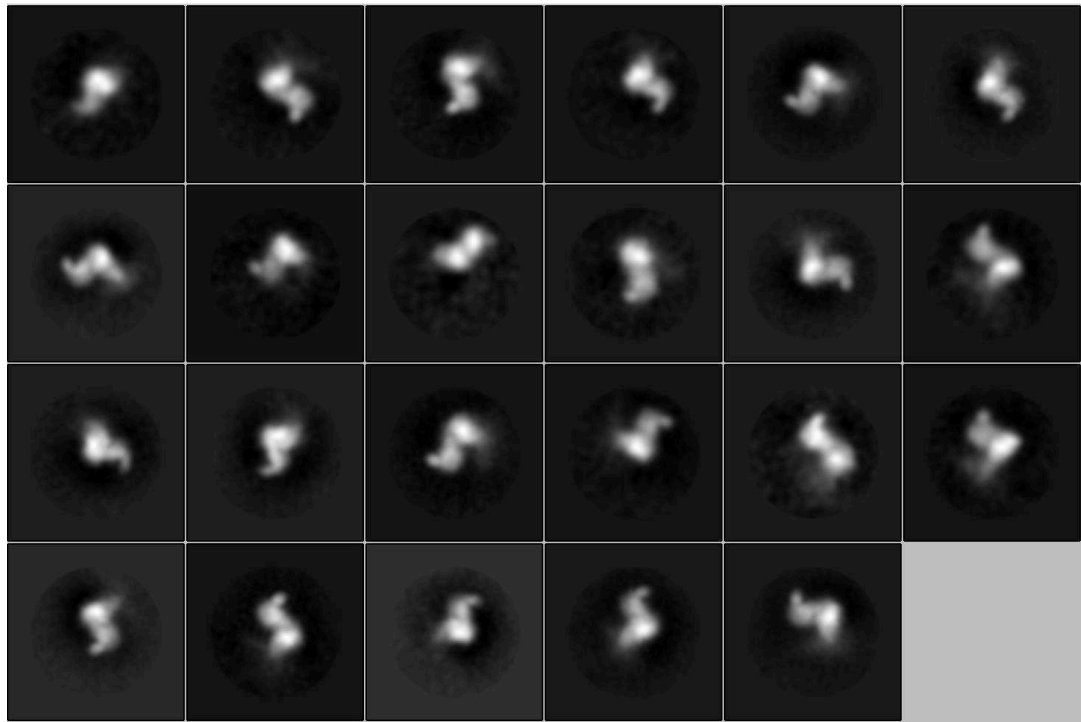
Supplementary Figure 2: K_d (dissociation constant) determination of UPF3B and UPF3A dephosphorylated with lambda phosphatase, using SPR. SMG1C was immobilized and different concentrations of UPF3B or UPF3A were injected. Graphpad prism was used for the fitting the curve and determination of the K_d . A representative curve is shown above. The K_d was calculated from mean of three individual experiments



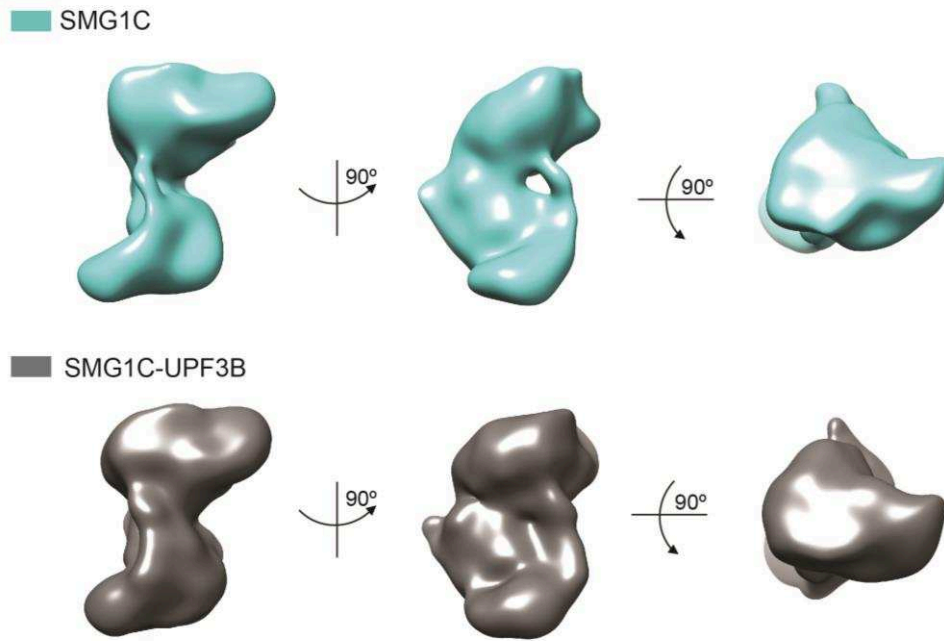
Supplementary Figure 3: The different constructs of UPF3B used in the study. All the constructs are expressed in SF21 cells, except for UPF3B 42-143, UPF3B 42-217 and UPF3B 1-217. 2 μ M of each construct was loaded onto the 4-12% Bis-Tris gel, Pro-Q stained and later Coomassie stained.



Supplementary Figure 4: UPF1 was incubated with different combinations of 2-fold molar excess of UPF2 (B31) and 2-fold molar excess of UPF3B to see their effect on phosphorylation of UPF1 by SMG1C. Different time points (30 s, 1 min, 2 min, 5 min, 10 min, 15 min, 20 min) were used to monitor the reaction. The reaction was stopped by addition of 1X PGLB. Protein mixtures were separated using 4-12% Bis-Tris gels, followed by Pro-Q staining and then Coomassie staining.



Supplementary Figure 5: 2D class averages of SMG1C (A) and SMG1C-UPF3B (B) using RELION 1.4.



Supplementary Figure 6: Negative stain EM reconstruction of SMG1C in presence of UPF3B. The 3D reconstruction of SMG1C using negative stain EM images is shown in light blue. The EM reconstruction of SMG1C-UPF3B is depicted in grey.

6 Conclusions and Discussion

Résumé en français

La dégradation des ARNm non-sens (NMD) est un important mécanisme de contrôle qualité des cellules eucaryotes qui reconnaît et dégrade les ARNm aberrants contenant un codon stop prématuré (PTC). La question centrale dans le domaine de la NMD a toujours été de comprendre comment la NMD différencie un ARNm contenant un codon stop normal d'un contenant un PTC. Alors que les mécanismes de dégradation des protéines situés en aval du NMD sont relativement bien compris, les événements en amont déclenchés à la terminaison d'un ARNm par un PTC et conduisant à l'activation de la machinerie NMD sont énigmatiques. Alors qu'il est clair que les protéines UPFs sont vitales pour la NMD, leurs fonctions précises restent à déterminer. La NMD chez l'humain apparaît plus complexe qu'anticipée avec bien plus de facteurs impliqués et avec une régulation par modification post traductionnel ainsi que par des protéines additionnelles. Le chapitre suivant discute en détails de l'état des connaissances dans le domaine, des résultats de la thèse ainsi que des futures perspectives.

Nonsense mediated mRNA decay is one of the important eukaryotic quality control mechanisms in the cell that recognizes and degrades aberrant mRNAs containing premature termination codons. It also plays an important role in gene expression and regulation by targeting approximately 5-15% of physiological transcripts (He & Jacobson, 2015a; Karousis et al., 2016; Kurosaki & Maquat, 2016; S. Lykke-Andersen & Jensen, 2015). The key question in the field of NMD has always been to understand how the mRNA containing a normal termination codon is discriminated from an aberrant premature translation termination codon by the NMD machinery. While the downstream, degradation pathway of the NMD machinery is comparatively well understood, the upstream events triggered by termination at a PTC and leading to activation of the NMD machinery are enigmatic. While it is clear that the UPF proteins are essential for NMD, the exact functions of these NMD factors are to be yet elucidated precisely.

The most accepted NMD model suggests that when a premature termination codon is encountered by the translating ribosome, the delay in translation termination leads to the recruitment of the NMD factors UPF1 along with the SMG1C kinase complex to the stalled ribosome. This leads to the assembly of the SURF complex which then interacts with the downstream exon junction complex (EJC) through UPF2 and UPF3B, which results in the formation of the decay-inducing complex (DECID complex) and translation termination at the PTC. (Chakrabarti et al., 2011; Chamieh, Ballut, Bonneau, & Le Hir, 2008b). Phosphorylation of UPF1 by SMG1 kinase allows the recruitment of downstream decay factors binding to phospho-UPF1 (Buhler et al., 2006; Eberle et al., 2008; LeBlanc & Beemon, 2004; Matsuda et al., 2008; Singh et al., 2008; J. Zhang et al., 1998).

In the past few years different branches of mammalian NMD have been reported: EJC-independent NMD, UPF2-independent and UPF3B-independent NMD (Chan et al., 2007; Gehring et al., 2005; L S Nguyen et al., 2012). In every instance UPF1 was found to be the major player and accumulation of phosphorylated UPF1 was found on the target mRNAs (Lee et al., 2015). ATP hydrolysis by UPF1 is essential for NMD to occur (Weng et al., 1996) and its dissociation from mRNA requires ATP binding as well as ATP hydrolysis. However, UPF1 has also been shown to bind to transcripts in a translation-independent manner (Kurosaki et al., 2014; Zünd, Gruber, Zavolan, & Mühlemann, 2013), which disagrees with the view that UPF1 is specifically recruited to a ribosome stalled at a PTC. (Kurosaki et al., 2014; Zünd et al., 2013). Taken together, this indicates that UPF1 phosphorylation and ATPase/helicase activity are essential for NMD to occur, but additional triggers which likely include an interaction of the NMD machinery with the PTC stalled ribosome are required to define a NMD substrate. Otherwise it would be hard to rationalize how translation inhibition could interfere with NMD.

Therefore the first step towards understanding NMD activation was to understand how UPF1 modulate the termination as the exact role of UPF1 during translation termination was unknown. UPF1 was shown to inhibit translation termination while the poly (A) binding protein (PABP) was shown to stimulate translation termination in vivo (Ivanov et al., 2008). Addressing this question was complicated by the fact that to date NMD and translation termination could only be analyzed in vivo in cells by using readthrough assays on reporter mRNAs where stop codon suppression was assumed to reflect inefficient translation termination.

Thus the main aim of my thesis was to understand the crosstalk between the translation machinery and the NMD factors. The reconstituted eukaryotic in vitro translation system (adapted from Alkalaeva et al., 2006) was set up in the lab to answer the various questions. The purified pre-termination complexes along with the release factors (eRF1 and eRF3a) and UPF1 / PABP were studied by electron cryo-microscopy to understand the molecular mechanism of translation termination and the regulatory function of PABP / UPF1.

During the period of my thesis, we successfully established and upscaled the human translation system in the laboratory and to highly enrich human pre-termination complexes, as indicated by our cryo-EM reconstructions (chapter 3). Moreover, we produced and purified different full-length proteins: eRF3a, UPF1, UPF2, and UPF3B/UPF3A recombinantly using insect cell expression system (Fitzgerald et al., 2007).

Initially we studied PABP's effect on the termination, i.e. ribosome binding, stop codon recognition and peptide hydrolysis (Ivanov et al., 2016). We could show that PABP binds the ribosome and stimulates stop codon recognition. This stimulatory effect depends on the presence of the C-terminal PABP domain and the N-terminal eRF3a domain. (Khanam et al., 2006; Kozlov, Gehring, & Kursula, 2010). Based on the available biochemical data, we prepared termination complexes with PABP to visualize the molecular mechanism of translation stimulation. However, we underestimated the efficiency of termination in the presence of full-length eRF3a and PABP. The terminating complexes could not be captured successfully for structural studies. Instead, we observed a large portion of empty ribosomes without density in the A site and without P site tRNA. The eRF1AGQ mutation was not sufficient to stall the complexes and prevent peptidyl-tRNA hydrolysis. This could possibly be rationalized by the fact that the eRF1AGQ mutant has 5% residual activity in the absence of PABP, while full-length eRF3a and PABP increase the efficiency of stop codon recognition and peptide hydrolysis compensating the inhibitory effect of the mutation in eRF1. Further mutations in PABP or eRF3a would be required in the future to successfully capture PABP on the terminating ribosome and to stabilize this

complex with the aim to understand the molecular mechanism of how PABP stimulates termination.

In parallel to PABP, we studied the termination complexes along with the NMD factor UPF1. Based on preliminary surface plasmon resonance experiments, we expected the affinity between the eRF3a and UPF1 to be low, i.e. in the micromolar range (Denaud et al, unpublished data). Therefore, we decided to covalently link the proteins UPF1 and eRF3a for subsequent structural studies by cryo-EM. Unfortunately, this strategy was not successful, as UPF1 could not be detected in the cryo-EM reconstructions of terminating ribosomal complexes. Importantly we could detect eRF1 and eRF3a, indicating that UPF1 is part of these complexes. This indicated that UPF1 was flexible and did not interact with the release factors or with the ribosome.

Later studies in the laboratory showed that the NMD factor UPF3B inhibits translation termination *in vitro*. Notably, the NMD factor UPF3B was also found to inhibit the phosphorylation of the UPF1 by the SMG1C kinase complex. This led to the identification of a novel interaction between the SMG1C kinase and UPF3B. A similar termination-inhibiting effect of UPF3B was found in the presence of UPF1, but not in the presence of UPF2. Very recently, it was also shown that human UPF2 and UPF3B both can independently bind to eRF3a, but not in combination (UPF2-UPF3B) (Neu-Yilik & Raimondeau et al., under review). The biological significance of these interactions remains enigmatic and more *in vivo* studies, complemented by *in vivo* analyses (NMD assays and readthrough assays with reporter mRNAs) and step-by-step analysis are required to find out which of these interactions are relevant with respect to translation termination and/or at later phases of NMD.

We also show that the middle domain of UPF3B interacts with the N-terminus of eRF3a. Hence there may be a competition occurring between UPF3B and PABP during translation termination. This hypothesis would be interesting to verify as a direct competition between these factors would provide an attractive model for PTC recognition in NMD versus termination at a normal stop codon. However, this model would not explain how the PTC is recognized in UPF3B-independent NMD. Similarly, further studies need to clarify the function of the interaction between SMG1C kinase and UPF3B.

The field of NMD has moved considerably forward from the time the project has been started in 2012. Many new interactions and the functions have been unraveled. The interaction of termination factor eRF3a with human UPF2, UPF3B is one example (López-Perrote et al., 2016). Role of the N-terminus of eRF3a has been reviewed and also how PABP effects translation termination (Ivanov et al., 2016). New helicases have been found (DHX34, MOV10, DDx19),

and their functions in translation and NMD are being studied in detail (Melero et al., 2016; Montpetit et al., 2011).

Structural information regarding ribosomal termination complexes has been limited to crystal structures of eRF1 and eRF3a at the beginning of this project (Cheng et al., 2009a; Kononenko et al., 2010). First cryo-EM reconstruction of a mammalian termination ribosome from the lab of Joachim Frank was published in 2012 ((Taylor et al., 2012)) and provided initial insights into how the release factors bind the ribosome at the stop codon. Three years later several high-resolution cryo-EM structures are available showing the ribosome in complex with eRF1 and eRF3a and answering the long-standing question of how the different stop codons are recognized by eRF1 (A. Brown et al., 2015; Matheisl et al., 2015). The N-terminus of eRF3a has been always considered as not essential for termination, but our study showed that full-length eRF3a stimulates the peptidyl-tRNA hydrolysis by eRF1 more efficiently than the truncated version lacking the N-terminal 138 amino acids (Ivanov et al., 2016). It is still unclear which role the N-terminal part of eRF3a plays in translation termination and solving a high-resolution structure with eRF3a full-length would be required to understand why and how the presence of the N-terminal part affects efficiency of translation termination.

Our current understanding of NMD is based on genetic data from cells, knockdown or overexpression of NMD factors, immune-precipitation experiments from cell extracts and various *in vivo* and *in vitro* mutational assays as well as yeast genetics. Moreover, several structures exist of NMD factor complexes (Bono et al., 2006; Clerici et al., 2014; Kadlec, Guilligay, Ravelli, & Cusack, 2006; Melero et al., 2012a). Many studies have used yeast as the model organism and assumed that the NMD factors are sufficiently conserved to allow conclusions about NMD in eukaryotes. However, NMD in yeast and humans is different at many levels. For example, yeast does not contain SMG1 kinase and EJC, which has been an important component of the NMD in eukaryotes. Many of the studies have also used the truncated proteins as full-length proteins could not be expressed and even if possible were suspected to be degraded (Clerici et al., 2014; Llorca, 2013; Melero et al., 2012b; Pisarev et al., 2007). But with the novel methods in expression and purification it is now possible to express the full-length proteins and large protein complexes successfully (Fitzgerald et al., 2007; Melero et al., 2016).

Recent developments in the field of genomics have led to the use of more comprehensive studies like transcriptomics and ribosome profiling for the better understanding of the NMD (Colombo, Karousis, Bourquin, Bruggmann, & Mühlemann, 2017; Schweingruber, Soffientini, Ruepp, Bachi, & Mühlemann, 2016; Serdar, Whiteside, & Baker, 2016). Also, the advancements in the field of cryo-EM (direct electron detectors and advanced algorithms leading to improved

computational sorting) have led to high-resolution structures of various ribosomal complexes and to a better understanding of the molecular mechanism of the translation events (e.g. (A. Brown et al., 2015; C. Schmidt et al., 2016).

Improvements in the field of genomics and transcriptomics has lead to the better analysis of the NMD substrates and identification of new markers. The discovery of N⁶-methyladenosine (m⁶A) and its enrichment near stop codons and 3' UTRs (Dominissini et al., 2012; T. Wang, Wei, Sabatini, & Lander, 2014) is interesting. It has also been discovered that m⁶A is selectively recognized by the human YTH domain family 2 (YTHDF2) 'reader' protein to regulate mRNA degradation. A recent work from Zahdeh and Carme et al, 2016 also showed that a higher G content is found near the PTC and in the 3'UTR region. It is known that UPF1 preferentially binds to these G-rich regions (Hurt, Robertson, & Burge, 2013) and also that the helicases pause at G-rich region (Bhattacharya et al., 2000). It is therefore tempting to speculate that the nucleotide composition also plays an important role in the kinetics of NMD.

Helicases are important regulatory subunits and play an important role in mRNA metabolism, processing and quality control (Bourgeois, Mortreux, & Auboeuf, 2016). Transitions between different steps are coupled in time with ATP hydrolysis by helicases (Konarska, Vilardell, & Query, 2006). Numerous helicases are part of the translation system and they play an important role in eukaryotic translation regulation. eIF4A and UPF1 are the best characterized helicases (Bourgeois et al., 2016). However recently, several new helicases have been identified which were linked to translation termination and NMD. The helicase DDX19 has been shown to stimulate translation termination by increasing the peptide release of eRFs (Mikhailova et al., 2017). DHX34 and MOV10 have been shown to interact with UPF1 and to regulate UPF1 phosphorylation by the SMG1C complex. DDX5 has been shown to bind to UPF3B in vivo (Geißler, Altmeyer, Stein, Uhlmann-Schiffler, & Stahl, 2013). The importance of the helicases and there exact function in translation termination and NMD remains to be determined.

In conclusion, despite the many years of NMD research, the key questions remain to be answered. Recent years revealed a much higher complexity of human NMD than anticipated with many more factors and a much higher level of regulation by post-translational modification and additional proteins. Thus, it is unclear how much we can learn from yeast studies. Despite the fact that the UPF proteins are conserved the function of UPF3 remained unclear in general. UPF1 has an ATPase and helicase activity which is essential for NMD in vivo and biochemically well characterized but it is unclear at which point during NMD UPF1 needs to be activated. Understanding the exact role of every conserved and new NMD factor is a challenge which possibly can be overcome by a defined in vitro NMD system where the individual factors can be

added and their impact on NMD/ translation termination directly measured. The fact that an in vitro NMD system does not exist in a way demonstrate that our current understanding of the pathway is incomplete. Here, by reconstitution of a human translation system and by purifying full-length NMD factors we made a first step into this direction. Such a system would be of great value for the study of the NMD pathway and other quality control mechanisms in detail, which would then also help to develop new treatment strategies for the diseases associated with NMD.

7 References

- Addington, A. M., Gauthier, J., Piton, A., Hamdan, F. F., Raymond, A., Gogtay, N., Rouleau, G. A. (2011). A novel frameshift mutation in UPF3B identified in brothers affected with childhood onset schizophrenia and autism spectrum disorders. *Molecular Psychiatry*, 16, 238–239.
- Alkalaeva, E. Z., Pisarev, A. V., Frolova, L. Y., Kisselev, L. L., & Pestova, T. V. (2006). In vitro reconstitution of eukaryotic translation reveals cooperativity between release factors eRF1 and eRF3. *Cell*, 125(6), 1125–36.
- Alrahbeni, T., Sartor, F., Anderson, J., Miedzybrodzka, Z., Mccaig, C., & Müller, B. (2015a). Full UPF3B function is critical for neuronal differentiation of neural stem cells. *Molecular Brain*, 8(33), 1–15.
- Alrahbeni, T., Sartor, F., Anderson, J., Miedzybrodzka, Z., Mccaig, C., & Müller, B. (2015b). Full UPF3B function is critical for neuronal differentiation of neural stem cells. *Molecular Psychiatry*, 8(33), 1–15.
- Amrani, N., Ganesan, R., Kervestin, S., Mangus, D. A., Ghosh, S., & Jacobson, A. (2004). A faux 3'-UTR promotes aberrant termination and triggers nonsense-mediated mRNA decay. *Nature*, 432, 112–118.
- Andersen, C. B. F., Ballut, L., Johansen, J. S., Chamieh, H., Nielsen, K. H., Oliveira, C. L. P., Andersen, G. R. (2006). Structure of the exon junction core ATPase bound to RNA. *Science*, 313(5795), 1968–1972.
- Arias-Palomo, E., Yamashita, A., Fernández, I. S., Núñez-Ramírez, R., Bamba, Y., Izumi, N., Llorca, O. (2011). The nonsense-mediated mRNA decay SMG-1 kinase is regulated by large-scale conformational changes controlled by SMG-8. *Genes and Development*, 25(2), 153–164.
- Becker, T., Armache, J.-P., Jarasch, A., Anger, A. M., Villa, E., Sieber, H., Beckmann, R. (2011). Structure of the no-go mRNA decay complex Dom34–Hbs1 bound to a stalled 80S ribosome. *Nature Publishing Group*, 18(6).
- Becker, T., Franckenberg, S., Wickles, S., Shoemaker, C. J., Anger, A. M., Armache, J., Beckmann, R. (2012). Structural basis of highly conserved ribosome recycling in eukaryotes and archaea. *Nature*, 482(7386), 501–506.
- Behm-Ansmant, I., Kashima, I., Rehwinkel, J., Saulière, J., Wittkopp, N., & Izaurralde, E. (2007). mRNA quality control: An ancient machinery recognizes and degrades mRNAs with nonsense codons. *FEBS Letters*, 581, 2845–2853.
- Ben-Ari, Y., Brody, Y., Kinor, N., Mor, A., Tsukamoto, T., Spector, D. L., Shav-Tal, Y. (2010). The

- life of an mRNA in space and time. *Journal of Cell Science*, 123(10), 1761–1774.
- Bernstein, P., Peltz, S. W., & Ross, J. (1989). The poly (A)-binding protein complex is a major determinant of mRNA stability in vitro. *Molecular and Cellular Biology*, 9(2), 659–670.
- Bertram, G., Bell, H. A., Ritchie, D. W., Fullerton, G., & Stansfield, I. (2000). Terminating eukaryote translation: Domain 1 of release factor eRF1 functions in stop codon recognition. *RNA*, 6, 1236–1247.
- Bhattacharya, A., Czaplinski, K., Trifillis, P., He, F., Jacobson, A., & Peltz, S. W. (2000). Characterization of the biochemical properties of the human Upf1 gene product that is involved in nonsense-mediated mRNA decay. *RNA*, 6, 1226–1235.
- Boehm, V., Haberman, N., Gehring, N. H., Boehm, V., Haberman, N., Ottens, F., Gehring, N. H. (2014). Composition determine endocleavage efficiencies at termination codons 3' UTR length and messenger ribonucleoprotein composition determine endocleavage efficiencies at Termination Codons. *Cell Reports*, 9(2), 555–568.
- Bono, F. (2014). Juggling key players in NMD initiation. *Structure*, 22, 1074–1075.
- Bono, F., Ebert, J., Lorentzen, E., & Conti, E. (2006). The crystal structure of the exon junction complex reveals how it maintains a stable grip on mRNA. *Cell*, 126(4), 713–25.
- Bourgeois, C. F., Mortreux, F., & Auboeuf, D. (2016). The multiple functions of RNA helicases as drivers and regulators of gene expression. *Nature Reviews Molecular Cell Biology*, 17(7), 426–38.
- Brandman, O., & Hegde, R. S. (2016). Ribosome-associated protein quality control. *Nature Publishing Group*, 23(1), 7–15.
- Brilot, A. F., Chen, J. Z., Cheng, A., Pan, J., Harrison, S. C., Potter, C. S., Grigorieff, N. (2012). Beam-induced motion of vitrified specimen on holey carbon film. *Journal of Structural Biology*, 177(3), 630–637.
- Brown, A., Shao, S., Murray, J., Hegde, R. S., & Ramakrishnan, V. (2015). Structural basis for stop codon recognition in eukaryotes. *Nature*, 524(7566), 493–496.
- Brown, J. T., Bai, X., & Johnson, A. W. (2000). The yeast antiviral proteins Ski2p, Ski3p, and Ski8p exist as a complex in vivo. *RNA*, 6, 449–457.
- Buchwald, G., Ebert, J., Basquin, C., Sauliere, J., Jayachandran, U., Bono, F., & Le Hir, H. (2010). Insights into the recruitment of the NMD machinery from the crystal structure of a core EJC-UPF3b complex. *Proceedings of the National Academy of Sciences*, 107(22), 10050–10055.
- Buhler, M., Steiner, S., Mohn, F., Paillusson, A., & Mühlemann, O. (2006). EJC-independent degradation of nonsense immunoglobulin- mRNA depends on 3' UTR length. *Nature Structural & Molecular Biology*, 13(5), 2005–2007.

- Burd, C. G., Matunis, E. L., & Dreyfuss, G. (1991). The multiple RNA-binding domains of the mRNA poly (A)-binding protein have different RNA-binding activities. *Molecular and Cellular Biology*, 11(7), 3419–3424.
- Cali, B. M., Kuchma, S. L., Latham, J., & Anderson, P. (1999). smg-7 is required for mRNA Surveillance in *Caenorhabditis elegans*. *Genetics*, 151, 605–616.
- Caputi, M., Kendzior, R. J., & Beemon, K. L. (2002). A nonsense mutation in the fibrillin-1 gene of a Marfan syndrome patient induces NMD and disrupts an exonic splicing enhancer. *Genes and Development*, 16, 1754–1759.
- Celik, A., Kervestin, S., & Jacobson, A. (2015). NMD: At the crossroads between translation termination and ribosome recycling. *Biochimie*, 114, 2–9.
- Chakrabarti, S., Bonneau, F., Sch, S., & Eppinger, E. (2014). Phospho-dependent and phospho-independent interactions of the helicase UPF1 with the NMD factors SMG5–SMG7 and SMG6. *Nucleic Acids Research*, 42(14), 9447–9460.
- Chakrabarti, S., Jayachandran, U., Bonneau, F., Fiorini, F., Basquin, C., Domcke, S., ...Conti, E. (2011). Molecular mechanisms for the RNA-dependent ATPase activity of Upf1 and its regulation by Upf2. *Molecular Cell*, 41(6), 693–703.
- Chamieh, H., Ballut, L., Bonneau, F., & Le Hir, H. (2008a). NMD factors UPF2 and UPF3 bridge UPF1 to the exon junction complex and stimulate its RNA helicase activity. *Nature Structural & Molecular Biology*, 15(1), 85–93.
- Chamieh, H., Ballut, L., Bonneau, F., & Le Hir, H. (2008b). NMD factors UPF2 and UPF3 bridge UPF1 to the exon junction complex and stimulate its RNA helicase activity. *Nature Structural & Molecular Biology*, 15(1), 85–93.
- Chan, W.-K., Bhalla, A. D., Le Hir, H., Nguyen, L. S., Huang, L., Gécz, J., & Wilkinson, M. F. (2009). A UPF3-mediated regulatory switch that maintains RNA surveillance. *Nature Structural & Molecular Biology*, 16(7), 747–753.
- Chan, W.-K., Huang, L., Gudikote, J. P., Chang, Y.-F., Imam, J. S., MacLean, J. a, & Wilkinson, M. F. (2007). An alternative branch of the nonsense-mediated decay pathway. *The EMBO Journal*, 26, 1820–1830.
- Chang, J. C., & Kan, Y. W. A. I. (1979). Beta thalassemia, a nonsense mutation in man. *Proceedings of the National Academy of Sciences*, 76(6), 2886–2889.
- Chauvin, C., Salhi, S., Goff, C. Le, Viranaicken, W., Diop, D., & Jean-Jean, O. (2005). Involvement of human release factors eRF3a and eRF3b in translation termination and regulation of the termination complex formation. *Molecular and Cellular Biology*, 25(14), 5801–5811.
- Chen, C.-Y. a, & Shyu, A.-B. (2011). Mechanisms of deadenylation-dependent decay. *Wiley*

- Interdisciplinary Reviews. *RNA*, 2(2), 167–83.
- Chen, L., Muhrad, D., Hauryliuk, V., Cheng, Z., Lim, M. K., Shyp, V., Song, H. (2010). Structure of the Dom34 – Hbs1 complex and implications for no-go decay. *Nature Structural & Molecular Biology*, 17(10), 1233–1240.
- Cheng, Z., Saito, K., Pisarev, A. V., Wada, M., Pisareva, V. P., Pestova, T. V., Song, H. (2009a). Structural insights into eRF3 and stop codon recognition by eRF1. *Genes and Development*, 23(9), 1106–1118.
- Cheng, Z., Saito, K., Pisarev, A. V., Wada, M., Pisareva, V. P., Pestova, T. V., Song, H. (2009b). Structural insights into eRF3 and stop codon recognition by eRF1. *Genes & Development*, 23(9), 1106–1118.
- Cho, H., Han, S., Choe, J., Park, S. G., Choi, S. S., & Kim, Y. K. (2013). SMG5 – PNRC2 is functionally dominant compared with SMG5 – SMG7 in mammalian nonsense-mediated mRNA decay. *Nucleic Acids Research*, 41(2), 1319–1328.
- Cho, H., Kim, K. M., & Kim, Y. K. (2009). Human proline-rich nuclear receptor coregulatory protein 2 mediates an interaction between mRNA surveillance machinery and decapping complex. *Molecular Cell*, 33, 75–86.
- Chu, J., Hong, N. A., Masuda, C. A., Jenkins, B. V., Nelms, K. A., Goodnow, C. C., Kay, S. A. (2009). A mouse forward genetics screen identifies LISTERIN as an E3 ubiquitin ligase involved in neurodegeneration. *Proceedings of the National Academy of Sciences*, 106(7), 2097–2103.
- Clerici, M., Deniaud, A., Boehm, V., Gehring, N. H., Schaffitzel, C., & Cusack, S. (2014). Structural and functional analysis of the three MIF4G domains of nonsense-mediated decay factor UPF2. *Nucleic Acids Research*, 42(4), 2673–2686.
- Clerici, M., Gutsche, I., Gehring, N. H., Hentze, M. W., Kulozik, A., Kadlec, J., Cusack, S. (2009). Unusual bipartite mode of interaction between the nonsense-mediated decay factors, UPF1 and UPF2. *The EMBO Journal*, 28(15), 2293–2306.
- Colombo, M., Karousis, E. D., Bourquin, J., Bruggmann, R., & Mühlemann, O. (2017). Transcriptome-wide identification of NMD-targeted human mRNAs reveals extensive redundancy between SMG6- and SMG7-mediated degradation pathways. *RNA*, 23, 189–201.
- Conard, S. E., Buckley, J., Dang, M. A. I., Bedwell, G. J., Carter, R. L., Khass, M., & Bedwell, D. M. (2012). Identification of eRF1 residues that play critical and complementary roles in stop codon recognition. *RNA*, 18, 1210–1221.
- Cosson, B., Berkova, N., Couturier, A., Chabelskaya, S., Philippe, M., & Zhouravleva, G. (2002). Poly(A)-binding protein and eRF3 are associated in vivo in human and *Xenopus* cells. *Biology*

- of the Cell, 94, 205–216.
- Craig, A. W. B., Ashkan, H., Yu, A. T. K., & Sonenberg, N. (1998). Interaction of polyadenylate-binding protein with the eIF4G homologue PAIP enhances translation. *Nature*, 392, 2–5.
- Crick, F. (1970). Central dogma of molecular biology. *Nature*, 227, 561–563.
- Daar, I. R. A., & Maquat, L. E. (1988). Premature translation termination mediates triosephosphate isomerase mRNA degradation. *Molecular and Cellular Biology*, 8(2), 802–813.
- Deniaud, A., Karuppasamy, M., Bock, T., Masiulis, S., Huard, K., Garzoni, F., Schaffitzel, C. (2015). A network of SMG-8, SMG-9 and SMG-1 C-terminal insertion domain regulates UPF1 substrate recruitment and phosphorylation. *Nucleic Acids Research*, 43(15), 7600–7611.
- Deo, R. C., Bonanno, J. B., Sonenberg, N., & Burley, S. K. (1999). Recognition of polyadenylate RNA by the poly(A)-binding protein. *Cell*, 98, 835–845.
- Derry, M. C., Yanagiya A, M. Y. and S. N. (2006). Regulation of poly(A)-binding protein through PABP-interacting proteins. *Cold Spring Harbor Symposia on Quantitative Biology*, 71, 537–543.
- Derry, M. C., Yanagiya, A., Martineau, Y., & Sonenberg, N. (2006). Regulation of poly(A)-binding protein through PABP-interacting proteins. *Cold Spring Harbor Symposia on Quantitative Biology*, 71, 537–543.
- Doma, M. K., & Parker, R. (2006). Endonucleolytic cleavage of eukaryotic mRNAs with stalls in translation elongation. *Nature*, 440, 561–564.
- Dominissini, D., Moshitch-Moshkovitz, S., Schwartz, S., Salmon-Divon, M., Ungar, L., Osenberg, S., Rechavi, G. (2012). Topology of the human and mouse m6A RNA methylomes revealed by m6A-seq. *Nature*, 485(7397), 201–206.
- Dostie, J., & Dreyfuss, G. (2002). Translation is required to remove Y14 from mRNAs in the cytoplasm. *Current Biology*, 12(2), 1060–1067.
- Durand, S., & Lykke-andersen, J. (2013). Nonsense-mediated mRNA decay occurs during eIF4F-dependent translation in human cells. *Nature Structural & Molecular Biology*, 20(6), 37–39.
- Eberle, A. B., Lykke-Andersen, S., Mühlemann, O., & Heick Jensen, T. (2009). SMG6 promotes endonucleolytic cleavage of nonsense mRNA in human cells. *Nature Structural & Molecular Biology*, 16, 49–55.
- Eberle, A. B., Stalder, L., Mathys, H., Orozco, R. Z., & Mu, O. (2008). Posttranscriptional gene regulation by spatial rearrangement of the 3' Untranslated Region. *PLoS Biology*, 6(4), 849–859.
- Elzen, A. M. G. Van Den, Henri, J., Lazar, N., Gas, M. E., Durand, D., Lacroute, F., Graille, M. (2010). Dissection of Dom34 – Hbs1 reveals independent functions in two RNA quality control

- pathways. *Nature Publishing Group*, 17(12), 1446–1452.
- Fernandez, I. S., Yamashita, A., Arias-Palomo, E., Bamba, Y., Bartolome, R. A., Canales, M. A., Llorca, O. (2011). Characterization of SMG-9, an essential component of the nonsense-mediated mRNA decay SMG1C complex. *Nucleic Acids Research*, 39(1), 347–358.
- Fitzgerald, D. J., Schaffitzel, C., Berger, P., Wellinger, R., Bieniossek, C., Richmond, T. J., & Berger, I. (2007). Multiprotein expression strategy for structural biology of eukaryotic complexes. *Structure*, 15(3), 275–279.
- Franks, T. M., Singh, G., & Lykke-andersen, J. (2010). Upf1 ATPase-dependent mRNP disassembly is required for completion of nonsense-mediated mRNA decay. *Cell*, 143(6), 938–950.
- Frischmeyer, P. A., & Dietz, H. C. (1999). Nonsense-mediated mRNA decay in health and disease. *Human Molecular Genetics Review*, 8(10), 1893–1900.
- Frischmeyer, P. A., Hoof, A. Van, O'Donnell, K., Guerrerio, A. L., Parker, R., & Dietz, H. C. (2002). An mRNA surveillance mechanism that eliminates transcripts lacking termination. *Science*, 295(5563), 2258–2262.
- Frolova, L. Y., Tsivkovskii, R. Y., Sivolobova, G. F., Oparina, N. Y., Serpinsky, O. I., Blinov, V. M., ... Kisselev, L. L. (1999). Mutations in the highly conserved GGQ motif of class 1 polypeptide release factors abolish ability of human eRF1 to trigger peptidyl-tRNA hydrolysis. *RNA (New York, N.Y.)*, 5(8), 1014–1020.
- Frolova, L. Y. U., Merkulova, T. I., & Kisselev, L. E. V. L. (2000). Translation termination in eukaryotes: Polypeptide release factor eRF1 is composed of functionally and structurally distinct domains. *RNA*, 6, 381–390.
- Fukuhara, N., Ebert, J., Unterholzner, L., Lindner, D., Izaurralde, E., Conti, E., & Anders, U. P. F. (2005). SMG7 Is a 14-3-3-like adaptor in the nonsense-mediated mRNA decay pathway. *Molecular Cell*, 17, 537–547.
- Gao, Q., Das, B., Sherman, F., & Maquat, L. E. (2005). Cap-binding protein 1-mediated and eukaryotic translation initiation factor 4E-mediated pioneer rounds of translation in yeast. *Proceedings of the National Academy of Sciences*, 102(12), 4258–4263.
- Gatfield, D., Unterholzner, L., Ciccarelli, F. D., Bork, P., & Izaurralde, E. (2003). Nonsense-mediated mRNA decay in *Drosophila*: at the intersection of the yeast and mammalian pathways. *The Journal of Biological Chemistry*, 278(15), 3960–3970.
- Gehring, N. H., Kunz, J. B., Neu-Yilik, G., Breit, S., Viegas, M. H., Hentze, M. W., & Kulozik, A. E. (2005). Exon-junction complex components specify distinct routes of nonsense-mediated mRNA decay with differential cofactor requirements. *Molecular Cell*, 20, 65–75.
- Gehring, N. H., Lamprinaki, S., Hentze, M. W., & Kulozik, A. E. (2009). The hierarchy of exon-

- junction complex assembly by the spliceosome explains key features of mammalian nonsense-mediated mRNA decay. *PLoS Biology*, 7(5), 1–14.
- Gehring, N. H., Neu-Yilik, G., Schell, T., Hentze, M. W., & Kulozik, A. E. (2003). Y14 and hUpf3b Form an NMD-Activating Complex the expression of dominant-negative mutants (hUpf1), by RNAi (hUpf1 and hUpf2), or with antisense strategies. *Molecular Cell*, 11, 939–949.
- Geißler, V., Altmeyer, S., Stein, B., Uhlmann-Schiffler, H., & Stahl, H. (2013). The RNA helicase Ddx5/p68 binds to hUpf3 and enhances NMD of Ddx17/p72 and Smg5 mRNA. *Nucleic Acids Research*, 41(16), 7875–7888.
- Glavan, F., Behm-ansmant, I., Izaurralde, E., & Conti, E. (2006). Structures of the PIN domains of SMG6 and SMG5 reveal a nuclease within the mRNA surveillance complex. *The EMBO Journal*, 25(21), 5117–5125.
- Grange Thierry, Martins de Sa Cezar, O. J. and P. R. (1987). Human mRNA polyadenylate binding protein: evolutionary conservation of a nucleic acid binding motif. *Nucleic Acids Research*, 15(12), 4771–4787.
- Grant, T., & Grigorieff, N. (2015). Measuring the optimal exposure for single particle cryo-EM using a 2.6 Å reconstruction of rotavirus VP6. *eLife*, 4, e06980.
- Hauryliuk, V., Zavialov, A., Kisselev, L., & Ehrenberg, M. (2006). Class-1 release factor eRF1 promotes GTP binding by class-2 release factor eRF3. *Biochimie*, 88(7), 747–757.
- He, F., Brown, A. H., & Jacobson, A. (1997). Upf1p, Nmd2p, and Upf3p are interacting components of the yeast nonsense-mediated mRNA decay pathway. *Molecular and Cellular Biology*, 17(3), 1580–1594.
- He, F., & Jacobson, A. (2015a). Nonsense-mediated mRNA decay: Degradation of defective transcripts is only part of the story. *Annual Review of Genetics*, 49, 339–366.
- He, F., & Jacobson, A. (2015b). Nonsense-mediated mRNA decay: Degradation of defective transcripts Is only part of the story. *Annual Review of Genetics*, 49, 339–366.
- Hir, Â. Le, Izaurralde, E., Maquat, L. E., & Moore, M. J. (2000). The spliceosome deposits multiple proteins 20–24 nucleotides upstream of mRNA exon-exon junctions. *The EMBO Journal*, 19(24), 6860–6869.
- Hodgkin, J., Papp, A., Pulak, R., Ambrost, V., & Anderson, P. (1989). A new kind of information supression in the nematode *Caenorhabditis elegans*. *Genetics*, 123, 301–313.
- Holbrook, J. a, Neu-Yilik, G., Hentze, M. W., & Kulozik, A. E. (2004). Nonsense-mediated decay approaches the clinic. *Nature Genetics*, 36(8), 801–808.
- Hoof, A. Van, Frischmeyer, P. A., Dietz, H. C., & Parker, R. (2002). Exosome-mediated recognition and degradation of mRNAs lacking a termination codon. *Science*, 295(5563), 2262–2264.

- Hoshino, S., Imai, M., Kobayashi, T., Uchida, N., & Katada, T. (1999). The eukaryotic polypeptide chain releasing factor (eRF3/GSPT) carrying the translation termination signal to the 3'-poly(A) tail of mRNA. *Journal of Biological Chemistry*, 274(24), 16677–16680.
- Huang, L., Lou, C., Chan, W., Shum, E. Y., Shao, A., Stone, E., & Karam, R. (2011). RNA homeostasis governed by cell type-specific and branched feedback loops acting on NMD. *Molecular Cell*, 43(6), 950–961.
- Hug, N., & Cáceres, J. F. (2014). The RNA helicase DHX34 activates NMD by promoting a transition from the surveillance to the decay-inducing complex. *Cell Reports*, 8(6), 1845–1856.
- Huntzinger, E., Kashima, I., & Fauser, M. (2008). SMG6 is the catalytic endonuclease that cleaves mRNAs containing nonsense codons in metazoan. *RNA*, 14, 2609–2617.
- Hurt, J. a, Robertson, A. D., & Burge, C. B. (2013). Global analyses of UPF1 binding and function reveals expanded scope of nonsense-mediated mRNA decay. *Genome Research*, 23, 1636–1650.
- Hwang, J., Sato, H., Tang, Y., Matsuda, D., & Maquat, L. E. (2010). UPF1 association with the cap-binding protein, CBP80, promotes nonsense-mediated mRNA decay at two distinct steps. *Molecular Cell*, 39(3), 396–409.
- Imamachi, N., Tani, H., & Akimitsu, N. (2012). Up-frameshift protein 1 (UPF1): Multitalented entertainer in RNA decay. *Drug Discoveries & Therapeutics*, 6(2), 55–61.
- Isken, O., & Maquat, L. E. (2007). Quality control of eukaryotic mRNA: Safeguarding cells from abnormal mRNA function. *Genes and Development*, 21(15), 1833–1856.
- Ito, K., Uno, M., & Nakamura, Y. (2000). A tripeptide “anticodon” deciphers stop codons in messenger RNA. *Nature*, 403, 680–684.
- Ivanov, A., Mikhailova, T., Eliseev, B., Yeramala, L., Sokolova, E., Susorov, D., Alkalaeva, E. (2016). PABP enhances release factor recruitment and stop codon recognition during translation termination. *Nucleic Acids Research*, 44(16), 7766–7776.
- Ivanov, P. V, Gehring, N. H., Kunz, J. B., Hentze, M. W., & Kulozik, A. E. (2008). Interactions between UPF1, eRFs, PABP and the exon junction complex suggest an integrated model for mammalian NMD pathways. *The EMBO Journal*, 27(17), 736–747.
- Izumi, N., Yamashita, A., Iwamatsu, A., Kurata, R., Nakamura, H., Saari, B., ... Ohno, S. (2010). AAA + Proteins RUVBL1 and RUVBL2 coordinate PIKK activity and function in nonsense-mediated mRNA decay. *Science Signaling*, 3(116), 1–14.
- Jerbi, S., Jolles, B., Bouceba, T., & Jean-jean, O. (2016). Studies on human eRF3-PABP interaction reveal the influence of eRF3a N-terminal glycine repeat on eRF3-PABP binding affinity and the lower affinity of eRF3a 12-GGC allele involved in cancer susceptibility. *RNA Biology*, 13(3), 306–315.

- Jolly, L. A., Homan, C. C., Jacob, R., Barry, S., & Gecz, J. (2013a). The UPF3B gene, implicated in intellectual disability, autism, ADHD and childhood onset schizophrenia regulates neural progenitor cell behaviour and neuronal outgrowth. *Human Molecular Genetics*, 22(23), 4673–4687.
- Jolly, L. A., Homan, C. C., Jacob, R., Barry, S., & Gecz, J. (2013b). The UPF3B gene, implicated in intellectual disability, autism, ADHD and childhood onset schizophrenia regulates neural progenitor cell behaviour and neuronal outgrowth. *Human Molecular Genetics*, 22(23), 4673–4687.
- Jonas, S., Weichenrieder, O., & Izaurralde, E. (2013). An unusual arrangement of two 14-3-3-like domains in the SMG5 – SMG7 heterodimer is required for efficient nonsense-mediated mRNA decay. *Genes and Development*, 27, 211–225.
- Kadlec, J., Guilligay, D., Ravelli, R. B., & Cusack, S. (2006). Crystal structure of the UPF2-interacting domain of nonsense-mediated mRNA decay factor UPF1. *RNA*, 12, 1817–1824.
- Kadlec, J., Izaurralde, E., & Cusack, S. (2004). The structural basis for the interaction between nonsense-mediated mRNA decay factors UPF2 and UPF3. *Nature Structural & Molecular Biology*, 11(4), 330–337.
- Kahvejian, A., Svitkin, Y. V., Sukarieh, R., Boutchou, M. M., & Sonenberg, N. (2005). Mammalian poly (A)-binding protein is a eukaryotic translation initiation factor, which acts via multiple mechanisms. *Genes & Development*, 19, 104–113.
- Karousis, E. D., Nasif, S., & Mühlemann, O. (2016). Nonsense-mediated mRNA decay: novel mechanistic insights and biological impact. *WIREs RNA*.
- Kashima, I., Jonas, S., Jayachandran, U., Buchwald, G., Conti, E., Lupas, A. N., & Izaurralde, E. (2010). SMG6 interacts with the exon junction complex via two conserved EJC-binding motifs (EBMs) required for nonsense-mediated mRNA decay. *Genes & Development*, 24(21), 2440–2450.
- Kashima, I., Yamashita, A., Izumi, N., Kataoka, N., Morishita, R., Hoshino, S., Ohno, S. (2006). Binding of a novel SMG-1-Upf1-eRF1-eRF3 complex (SURF) to the exon junction complex triggers Upf1 phosphorylation and nonsense-mediated mRNA decay. *Genes and Development*, 20, 355–367.
- Kerenyi, Z., Merai, Z., Hiripi, L., Benkovics, A., Gyula, P., Lacomme, C., Silhavy, D. (2008). Interkingdom conservation of mechanism of nonsense-mediated mRNA decay. *The EMBO Journal*, 27(11), 1585–1595.
- Kertesz, S., Kerenyi, Z., Merai, Z., Bartos, I., Palfy, T., Barta, E., & Silhavy, D. (2006). Both introns and long 3'-UTRs operate as cis-acting elements to trigger nonsense-mediated decay in plants.

- Nucleic Acids Research, 34(21), 6147–6157.
- Kervestin, S., & Jacobson, A. (2012). NMD: a multifaceted response to premature translational termination. *Nature Reviews. Molecular Cell Biology*, 13(11), 700–712.
- Khaleghpour, K., Kahvejian, A., De Crescenzo, G., Roy, G., Svitkin, Y. V., Imataka, H., Sonenberg, N. (2001). Dual interactions of the translational repressor Paip2 with poly(A) binding protein. *Molecular and Cellular Biology*, 21(15), 5200–5213.
- Khanam, T., Muddashetty, R. S., Kahvejian, A., Sonenberg, N., & Brosius, J. (2006a). Poly(A)-Binding Protein Binds to A-Rich Sequences via RNA-Binding Domains 1+2 and 3+4. *RNA Biology*, 3(4), 170–177.
- Khanam, T., Muddashetty, R. S., Kahvejian, A., Sonenberg, N., & Brosius, J. (2006b). Poly(A)-Binding Protein Binds to A-Rich Sequences via RNA-Binding Domains 1+2 and 3+4. *RNA Biology*, 3(4), 170–177.
- Kim, V. N., Kataoka, N., & Dreyfuss, G. (2001a). Role of the nonsense-mediated decay factor hUpf3 in the junction exon-exon junction complex. *Science*, 293(5536), 1832–1836.
- Kim, V. N., Kataoka, N., & Dreyfuss, G. (2001b). Role of the nonsense-mediated decay factor hUpf3 in the splicing-dependent exon-exon junction complex. *Science*, 293(5536), 1832–1836.
- Klaholz, B. P., Myasnikov, A. G., & Heel, M. Van. (2004). Visualization of release factor 3 on the ribosome during termination of protein synthesis. *Nature*, 427, 3–6.
- Kobayashi, K., Kikuno, I., Kuroha, K., Saito, K., Ito, K., & Ishitani, R. (2010). Structural basis for mRNA surveillance by archaeal Pelota and GTP-bound EF1 α complex. *Proceedings of the National Academy of Sciences*, 107(41), 17575–17579.
- Konarska, M. M., Vilardeell, J., & Query, C. C. (2006). Repositioning of the reaction intermediate within the catalytic center of the spliceosome. *Molecular Cell*, 21(4), 543–553.
- Kononenko, A. V, Mitkevich, V. a, Atkinson, G. C., Tenson, T., Dubovaya, V. I., Frolova, L. Y., ... Hauryliuk, V. (2010). GTP-dependent structural rearrangement of the eRF1:eRF3 complex and eRF3 sequence motifs essential for PABP binding. *Nucleic Acids Research*, 38(2), 548–58.
- Korostelev, A. A. (2011). Structural aspects of translation termination on the ribosome. *RNA*, 17, 1409–1421.
- Kozlov, G., Crescenzo, G. De, Lim, N. S., Siddiqui, N., Kahvejian, A., Elias, D., Gehring, K. (2004). Structural basis of ligand recognition by PABC, a highly specific peptide-binding domain found in poly(A)-binding protein and a HECT ubiquitin ligase. *The EMBO Journal*, 23(2), 272–281.
- Kozlov, G., Gehring, K., & Kursula, P. (2010). Molecular basis of eRF3 recognition by the MLLE domain of poly(A)-binding protein. *PLoS ONE*, 5(4), e10169.
- Kühn, U., & Pieler, T. (1996). *Xenopus* poly(A) binding protein: functional domains in RNA binding

- and protein-protein interaction. *Journal of Molecular Biology*, 256(1), 20–30.
- Kulkarni, M., Ozgur, S., & Stoecklin, G. (2010). On track with P-bodies. *Biochemical Society Transactions*, 38, 242–251.
- Kunz, J. B., Neu-Yilik, G., Hentze, M. W., Kulozik, A. E., & Gehring, N. H. (2006). Functions of hUpf3a and hUpf3b in nonsense-mediated mRNA decay and translation. *RNA*, 12, 1015–1022.
- Kurosaki, T., Li, W., Hoque, M., Popp, M. W.-L., Ermolenko, D. N., Tian, B., & Maquat, L. E. (2014). A post-translational regulatory switch on UPF1 controls targeted mRNA degradation. *Genes & Development*, 28, 1900–1916.
- Kurosaki, T., & Maquat, L. E. (2016). Nonsense-mediated mRNA decay in humans at a glance. *Journal of Cell Science*, 129, 461–467.
- Lai, T., Cho, H., Liu, Z., Bowler, M. W., Piao, S., Parker, R., & Kim, Y. K. (2012). Structural basis of the PNRC2-mediated Llink between mRNA surveillance and decapping. *Structure*, 20(12), 2025–2037.
- Laumonier, F., Shoubridge, C., Antar, C., Nguyen, L. S., Esch, H. Van, Kleefstra, T., Raynaud, M. (2010). Mutations of the UPF3B gene, which encodes a protein widely expressed in neurons, are associated with nonspecific mental retardation with or without autism. *Molecular Psychiatry*, 15, 767–776.
- LeBlanc, J. J., & Beemon, K. L. (2004). Unspliced Rous sarcoma virus genomic RNAs are translated and subjected to nonsense-mediated mRNA decay before packaging. *Journal of Virology*, 78(10), 5139–5146.
- Lebreton, A., Tomecki, R., Dziembowski, A., & Se, B. (2008). Endonucleolytic RNA cleavage by a eukaryotic exosome. *Nature*, 456, 993–997.
- Lee, S. R., Pratt, G. A., Martinez, F. J., Yeo, G. W., & Lykke-Andersen, J. (2015). Target discrimination in nonsense-mediated mRNA decay requires Upf1 ATPase activity. *Molecular Cell*, 59, 413–425.
- Leeds, P., Peltz, S. W., Jacobson, A., & Culbertson, M. R. (1991). The product of the yeast UPF1 gene is required for rapid turnover of mRNAs containing a premature translational termination codon. *Genes & Development*, 5(12a), 2303–2314.
- Liebhaber, S. A., Silva, S. A., Roma, S. A., & Lui, A. N. A. (2008). Proximity of the poly (A)-binding protein to a premature termination codon inhibits mammalian nonsense-mediated mRNA decay. *RNA*, 14, 563–576.
- Llorca, O. (2013). Structural insights into nonsense-mediated mRNA decay (NMD) by electron microscopy. *Current Opinion in Structural Biology*, 23(1), 161–167.
- Loh, B., Jonas, S., & Izaurralde, E. (2013). The SMG5 – SMG7 heterodimer directly recruits the

- CCR4 – NOT deadenylase complex to mRNAs containing nonsense codons via interaction with POP2. *Genes and Development*, 27, 2125–2138.
- Longman, D., Plasterk, R. H. A., Johnstone, I. L., & Cáceres, J. F. (2007). Mechanistic insights and identification of two novel factors in the *C. elegans* NMD pathway. *Genes and Development*, 21, 1075–1085.
- López-Perrote, A., Castaño, R., Melero, R., Zamarro, T., Kurosawa, H., Ohnishi, T., Llorca, O. (2016). Human nonsense-mediated mRNA decay factor UPF2 interacts directly with eRF3 and the SURF complex. *Nucleic Acids Research*, 44(4), 1909–1923.
- Losson, R., & Lacroute, F. (1979). Interference of nonsense mutations with eukaryotic messenger mRNA stability. *Proceedings of the National Academy of Sciences*, 76(10), 5134–5137.
- Lykke-Andersen, J., S. M.-D. and S. A. J. (2000). Human Upf Proteins target an mRNA for Nonsense-Mediated Decay when bound downstream of a Termination Codon. *Cell*, 103(7), 1121–1131.
- Lykke-Andersen, J. (2001). mRNA quality control: Marking the message for life or death. *Current Biology*, 11, 88–91.
- Lykke-Andersen, J., & Bennett, E. J. (2014). Protecting the proteome: Eukaryotic cotranslational quality control pathways. *Journal of Cell Biology*, 204(4), 467–476.
- Lykke-Andersen, S., Chen, Y., Ardal, B. R., Lilje, B., Waage, J., Sandelin, A., & Jensen, T. H. (2014). Human nonsense-mediated RNA decay initiates widely by endonucleolysis and targets snoRNA host genes. *Genes & Development*, 28, 2498–2517.
- Lykke-Andersen, S., & Jensen, T. H. (2015). Nonsense-mediated mRNA decay: an intricate machinery that shapes transcriptomes. *Nature Molecular Cell Biology*, 16(11), 665–677.
- Mangus, D. A., Evans, M. C., & Jacobson, A. (2003). Poly(A)-binding proteins: Multifunctional scaffolds for the post-transcriptional control of gene expression. *Genome Biology*, 4(223).
- Maquat, L. E., Kinniburgh, A. J., & Ross, J. (1981). Unstable β -globin mRNA in mRNA-deficient β Thalassemia. *Cell*, 27, 543–553.
- Matheisl, S., Berninghausen, O., Becker, T., & Beckmann, R. (2015). Structure of a human translation termination complex. *Nucleic Acids Research*, 43(10), 8615–8626.
- Matsuda, D., Sato, H., & Maquat, L. E. (2008). Studying nonsense-mediated mRNA decay in mammalian cells. *Methods in enzymology* (1st ed., Vol. 449). Elsevier Inc.
- McIlwain, D. R., Pan, Q., Reilly, P. T., Elia, A. J., Mccracken, S., Wakeham, A. C., Mak, T. W. (2010). Smg1 is required for embryogenesis and regulates diverse genes via alternative splicing coupled to nonsense-mediated mRNA decay. *Proceedings of the National Academy of Sciences*, 107(27), 12186–12191.

- Melero, R., Buchwald, G., Castaño, R., Raabe, M., Gil, D., Lázaro, M., Llorca, O. (2012a). The cryo-EM structure of the UPF-EJC complex shows UPF1 poised toward the RNA 3' end. *Nature Structural & Molecular Biology*, 19(5), 498–505.
- Melero, R., Buchwald, G., Castaño, R., Raabe, M., Gil, D., Lázaro, M., Llorca, O. (2012b). The cryo-EM structure of the UPF-EJC complex shows UPF1 poised toward the RNA 3' end. *Nature Structural & Molecular Biology*.
- Melero, R., Hug, N., López-Perrote, A., Yamashita, A., Cáceres, J. F., & Llorca, O. (2016). The RNA helicase DHX34 functions as a scaffold for SMG1-mediated UPF1 phosphorylation. *Nature Communications*, 7, 1–12.
- Melero, R., Uchiyama, A., Castano, R., Kataoka, N., Kurosawa, H., Ohno, S., Llorca, O. (2014). Structures of SMG1-UPFs complexes: SMG1 contributes to regulate UPF2-dependent activation of UPF1 in NMD. *Structure*, 22, 1105–1119.
- Mendell, J. T., Sharifi, N. A., Meyers, J. L., Martinez-murillo, F., & Dietz, H. C. (2004). Nonsense surveillance regulates expression of diverse classes of mammalian transcripts and mutes genomic noise. *Nature Genetics*, 36(10), 1073–1078.
- Merrick, W. C. (2015). eIF4F: A Retrospective *. *The Journal of Biological Chemistry*, 290(40), 24091–24099.
- Mikhailova, T., Shuvalova, E., Ivanov, A., Susorov, D., Shuvalov, A., Kolosov, P. M., & Alkalaeva, E. (2017). RNA helicase DDX19 stabilizes ribosomal elongation and termination complexes. *Nucleic Acids Research*, 45(3), 1307–1318.
- Min, E. I. E. I., Roy, B., Amrani, N., He, F., & Jacobson, A. (2013). Yeast Upf1 CH domain interacts with Rps26 of the 40S ribosomal subunit. *RNA*, 19, 1105–1115.
- Montpetit, B., Thomsen, N. D., Helmke, K. J., Seeliger, M. a, Berger, J. M., & Weis, K. (2011). A conserved mechanism of DEAD-box ATPase activation by nucleoporins and InsP6 in mRNA export. *Nature*, 472(7342), 238–242.
- Moore, M. J., & Proudfoot, N. J. (2009). Pre-mRNA processing reaches back to transcription and ahead to translation. *Cell*, 136(4), 688–700.
- Moore, S. D., & Sauer, R. T. (2007). The tmRNA system for translational surveillance and ribosome rescue. *Annual Review of Biochemistry*, 76, 101–124.
- Mühlemann, O., Eberle, A. B., Stalder, L., & Zamudio Orozco, R. (2008). Recognition and elimination of nonsense mRNA. *Biochimica et Biophysica Acta*, 1779(9), 538–549.
- Muhlrad, D., Decker, C. J., & Parker, R. (1994). Deadenylation of the unstable mRNA encoded by the yeast MFA2 gene leads to decapping followed by 5'-3' digestion of the transcript. *Genes and Development*, 8, 855–866.

- Muhlrad, D., & Parker, R. (1994). Premature translational termination triggers mRNA decapping. *Nature*, 370, 578–581.
- Muhlrad, D., & Parker, R. O. Y. (1999). Aberrant mRNAs with extended 3' UTRs are substrates for rapid degradation by mRNA surveillance. *RNA*, 5, 1299–1307.
- Nagy, E., & Maquat, L. E. (1998). A rule for termination-codon position within intron-containing genes : When nonsense affects RNA abundance. *Trends in Biochemical Sciences*, 4(1996), 198–199.
- Namy, O., Moran, S. J., Stuart, D. I., Gilbert, R. J. C., & Brierley, I. (2006). A mechanical explanation of RNA pseudoknot function in programmed ribosomal frameshifting. *Nature*, 441(7090), 244–247.
- Nguyen, L. S., Jolly, L., Shoubridge, C., Chan, W. K., Huang, L., Laumonnier, F., Gecz, J. (2012). Transcriptome profiling of UPF3B/NMD-deficient lymphoblastoid cells from patients with various forms of intellectual disability. *Molecular Psychiatry*, 17(11), 1103–1115.
- Nguyen, L. S., Kim, H.-G., Rosenfeld, J. A., Shen, Y., Gusella, J. F., Yves, L., Gecz, J. (2013). Contribution of copy number variants involving nonsense-mediated mRNA decay pathway genes to neuro-developmental disorders. *Human Molecular Genetics*, 22(9), 1816–1825.
- Nicholson, P., Josi, C., Kurosawa, H., Yamashita, A., & Mühlemann, O. (2014). A novel phosphorylation-independent interaction between SMG6 and UPF1 is essential for human NMD. *Nucleic Acids Research*, 42(14), 9217–9235.
- Ohnishi, T., Yamashita, A., Kashima, I., Schell, T., Anders, K. R., Grimson, A., ... Ohno, S. (2003). Phosphorylation of hUPF1 induces formation of mRNA surveillance complexes containing hSMG-5 and hSMG-7. *Molecular Cell*, 12, 1187–1200.
- Okada-Katsuhata, Y., Yamashita, A., Kutsuzawa, K., Izumi, N., Hirahara, F., & Ohno, S. (2012). N- and C-terminal Upf1 phosphorylations create binding platforms for SMG-6 and SMG-5:SMG-7 during NMD. *Nucleic Acids Research*, 40(3), 1251–1266.
- Osawa, M., Hosoda, N., Nakanishi, T., Uchida, N., Kimura, T., Imai, S., Shimada, I. (2012). Biological role of the two overlapping poly(A)-binding protein interacting motifs 2 (PAM2) of eukaryotic releasing factor eRF3 in mRNA decay. *RNA*, 18(11), 1957–1967.
- Passos, D. O., Doma, M. K., Shoemaker, C. J., Muhlrad, D., Green, R., Weissman, J., Parker, R. (2009). Analysis of Dom34 and its function in No-Go decay. *Molecular Biology of the Cell*, 20, 3025–3032.
- Pestova, T. V., & Kolupaeva, V. G. (2002). The roles of individual eukaryotic translation initiation factors in ribosomal scanning and initiation codon selection. *Genes and Development*, 16(22), 2906–2922.

- Pestova, T. V., & Hellen, C. U. (2000). The structure and function of initiation factors in eukaryotic protein synthesis. *Cellular and Molecular Life Sciences*, 57(4), 651–674.
- Petry, S., Weixlbaumer, A., & Ramakrishnan, V. (2008). The termination of translation. *Current Opinion in Structural Biology*, 18(1), 70–77.
- Pisareva, V. P., Pisarev, A. V., Hellen, C. U. T., Rodnina, M. V., & Pestova, T. V. (2006). Kinetic analysis of interaction of eukaryotic release factor 3 with guanine nucleotides. *Journal of Biological Chemistry*, 281(52), 40224–40235.
- Pisareva, V. P., Skabkin, M. A., Hellen, C. U. T., Pestova, T. V., & Pisarev, A. V. (2011). Dissociation by Pelota, Hbs1 and ABCE1 of mammalian vacant 80S ribosomes and stalled elongation complexes. *The EMBO Journal*, 30, 1804–1817.
- Pisarev, A. V., Unbehauen, A., Hellen, C. U. T., & Pestova, T. V. (2007). Assembly and analysis of eukaryotic translation initiation complexes. *Methods in enzymology (First Edit, Vol. 430)*.
- Preis, A., Heuer, A., Barrio-Garcia, C., Hauser, A., Eyler, D. E., Berninghausen, O., ... Beckmann, R. (2014). Cryoelectron microscopic structures of eukaryotic translation termination complexes containing eRF1-eRF3 or eRF1-ABCE1. *Cell Reports*, 8(1), 59–65.
- Pulak, R., & Anderson, P. (1993). mRNA surveillance by the *Caenorhabditis elegans* stag genes. *Genes & Development*, 7, 1885–1897.
- Ramakrishnan, V. (2002). Ribosome structure and the mechanism of translation. *Cell*, 108(4), 557–572.
- Rohou, A., & Grigorieff, N. (2015). CTFFIND4: Fast and accurate defocus estimation from electron micrographs. *Journal of Structural Biology*, 192(2), 216–221.
- Rufener, S. C., & Mühlemann, O. (2013). eIF4E-bound mRNPs are substrates for nonsense-mediated mRNA decay in mammalian cells. *Nature Structural & Molecular Biology*, 20(6), 710–717.
- Sachs, a B., & Davis, R. W. (1989). The poly(A) binding protein is required for poly(A) shortening and 60S ribosomal subunit-dependent translation initiation. *Cell*, 58(5), 857–867.
- Saito, S., Hosoda, N., & Hoshino, S. (2013). The Hbs1-Dom34 protein complex functions in non-stop mRNA decay in mammalian cells. *The Journal of Biological Chemistry*, 288(24), 17832–17843.
- Salas-marco, J., & Bedwell, D. M. (2004). GTP hydrolysis by eRF3 facilitates stop codon decoding during eukaryotic translation termination. *Molecular and Cellular Biology*, 24(17), 7769–7778.
- Scheres, S. H. W. (2012). RELION: Implementation of a Bayesian approach to cryo-EM structure determination. *Journal of Structural Biology*, 180(3), 519–530.
- Scheres, S. H. W. (2014). Single-particle processing in RELION-1 . 3, 1–38.
- Schmid, M., & Jensen, T. H. (2008). The exosome : a multipurpose RNA-decay machine. *Trends in Biochemical Sciences*, 33(10), 501–510.

- Schmidt, C., Kowalinski, E., Shanmuganathan, V., Defenouillère, Q., Braunger, K., Heuer, A., Beckmann, R. (2016). The cryo-EM structure of a ribosome-Ski2-Ski3-Ski8 helicase complex. *Science*, 354(6318), 1431–1433.
- Schmidt, S. A., Foley, P. L., Jeong, D., Rymarquis, L. A., Doyle, F., Tenenbaum, S. A., Green, P. J. (2015). Identification of SMG6 cleavage sites and a preferred RNA cleavage motif by global analysis of endogenous NMD targets in human cells. *Nucleic Acids Research*, 43(1), 309–323.
- Schweingruber, C., Rufener, S. C., Zünd, D., Yamashita, A., & Mühlemann, O. (2013). Nonsense-mediated mRNA decay - Mechanisms of substrate mRNA recognition and degradation in mammalian cells. *Biochimica et Biophysica Acta*, 1829(6–7), 612–623.
- Schweingruber, C., Soffientini, P., Ruepp, M., Bachi, A., & Mühlemann, O. (2016). Identification of interactions in the NMD complex using proximity-dependent biotinylation (BioID). *PLoS ONE*, 11(3), 1–27.
- Serdar, L. D., Whiteside, D. L., & Baker, K. E. (2016). ATP hydrolysis by UPF1 is required for efficient translation termination at premature stop codons. *Nature Communications*, 7, 1–8.
- Serin, G., Gersappe, A., Black, J. D., & Aronoff, R. (2001). Identification and characterization of human orthologues to *Saccharomyces cerevisiae* Upf2 protein and Upf3 protein (*Caenorhabditis elegans* SMG-4). *Molecular and Cellular Biology*, 21(1), 209–223.
- Shaheen, R., Anazi, S., Ben-Omran, T., Seidahmed, M. Z., Caddle, L. B., Palmer, K., Alkuraya, F. S. (2016). Mutations in SMG9, encoding an essential component of nonsense-mediated decay machinery, cause a multiple congenital anomaly syndrome in humans and mice. *The American Journal of Human Genetics*, 98, 1–10.
- Shaw, J. J., & Green, R. (2007). Two distinct components of release factor function uncovered by nucleophile partitioning analysis. *Molecular Cell*, 28, 458–467.
- Shibuya, T., Tange, T. Ø., Sonenberg, N., & Moore, M. J. (2004). eIF4AIII binds spliced mRNA in the exon junction complex and is essential for nonsense-mediated decay. *Nature Structural & Molecular Biology*, 11(4), 346–351.
- Shoemaker, C. J., Eyler, D. E., & Green, R. (2010). Dom34:Hbs1 promotes subunit dissociation and peptidyl-tRNA drop-off to initiate no-go decay. *Science*, 330(6002), 369–372.
- Shoemaker, C. J., & Green, R. (2011). Kinetic analysis reveals the ordered coupling of translation termination and ribosome recycling in yeast. *Proceedings of the National Academy of Sciences*, 108(51), 1392–1398.
- Shoemaker, C. J., & Green, R. (2012). Translation drives mRNA quality control. *Nature Structural & Molecular Biology*, 19(6), 594–601.
- Shum, E. Y., Jones, S. H., Shao, A., Dumdie, J., Krause, M. D., Chan, W. K., Wilkinson, M. F.

- (2016). The antagonistic gene paralogs Upf3a and Upf3b govern nonsense-mediated RNA decay. *Cell*, 165(2), 382–395.
- Silva, A. L., & Romão, L. (2009). The mammalian nonsense-mediated mRNA decay pathway: to decay or not to decay! Which players make the decision? *FEBS Letters*, 583(3), 499–505.
- Singh, G., Kucukural, A., Cenik, C., Leszyk, J. D., Shaffer, S. A., Weng, Z., & Moore, M. J. (2012). The cellular EJC interactome reveals higher-order mRNP structure and an EJC-SR protein nexus. *Cell*, 151(4), 750–764.
- Singh, G., Rebbapragada, I., & Lykke-Andersen, J. (2008). A competition between stimulators and antagonists of Upf complex recruitment governs human nonsense-mediated mRNA decay. *PLoS Biology*, 6(4), e111.
- Song, H., Mugnier, P., Das, a K., Webb, H. M., Evans, D. R., Tuite, M. F., Barford, D. (2000). The crystal structure of human eukaryotic release factor eRF1--mechanism of stop codon recognition and peptidyl-tRNA hydrolysis. *Cell*, 100(3), 311–321.
- Szyszkka, P., Sharp, S. I., Dedman, A., Gurling, H. M. D., & McQuillin, A. (2012). A nonconservative amino acid change in the UPF3B gene in a patient with schizophrenia. *Psychiatric Genetics*, 22(3), 150–151.
- Tarpey, P. S., Raymond, F. L., Nguyen, L. S., Rodriguez, J., Hackett, A., Vandeleur, L., Ge, J. (2007). Mutations in UPF3B , a member of the nonsense- mediated mRNA decay complex , cause syndromic and nonsyndromic mental retardation. *Nature Genetics*, 39(9), 1127–1133.
- Taylor, D., Unbehaun, A., Li, W., Das, S., Lei, J., Liao, H. Y., ... Frank, J. (2012). Cryo-EM structure of the mammalian eukaryotic release factor eRF1-eRF3-associated termination complex. *Proceedings of the National Academy of Sciences of the United States of America*, 109(45), 18413–18418.
- Tsuboi, T., Kuroha, K., Kudo, K., Makino, S., Inoue, E., Kashima, I., & Inada, T. (2012). Dom34: Hbs1 plays a general role in quality-control Ssystems by dissociation of a stalled ribosome at the 3' end of aberrant mRNA. *Molecular Cell*, 46(4), 518–529.
- Voigts-Hoffmann, F., Klinge, S., & Ban, N. (2012). Structural insights into eukaryotic ribosomes and the initiation of translation. *Current Opinion in Structural Biology*, 22, 1–10.
- Wang, H., Iacoangeli, A., Lin, D., Williams, K., Denman, R. B., Hellen, C. U. T., & Tiedge, H. (2005). Dendritic BC1 RNA in translational control mechanisms. *The Journal of Cell Biology*, 171(5), 811–821.
- Wang, T., Wei, J. J., Sabatini, D. M., & Lander, E. S. (2014). Genetic screens in human cells using the CRISPR-Cas9 system. *Science*, 343(6166), 80–85.
- Weischenfeldt, J., Damgaard, I., Bryder, D., Theilgaard-mönch, K., Thoren, L. A., Nielsen, F. C.,

- Porse, B. T. (2008). NMD is essential for hematopoietic stem and progenitor cells and for eliminating by-products of programmed DNA rearrangements. *Genes & Development*, 22, 1381–1396.
- Wen, J., & Brogna, S. (2010). Splicing-dependent NMD does not require the EJC in *Schizosaccharomyces pombe*. *The EMBO Journal*, 29(9), 1537–1551.
- Weng, Y., Czaplinski, K., & Peltz, S. W. (1996). Genetic and biochemical characterization of mutations in the ATPase and helicase regions of the Upf1 protein. *Molecular and Cellular Biology*, 16(10), 5477–5490.
- Withers, J. B., & Beemon, K. L. (2010). Structural features in the Rous sarcoma virus RNA stability element are necessary for sensing the correct termination codon. *Withers and Beemon Retrovirology*, 7(65), 1–15.
- Wittkopp, N., Huntzinger, E., Weiler, C., Schmidt, S., Sonawane, M., & Izaurralde, E. (2009). Nonsense-mediated mRNA decay effectors are essential for Zebrafish embryonic development and survival. *Molecular and Cellular Biology*, 29(13), 3517–3528.
- Yamashita, A. (2013). Role of SMG-1-mediated Upf1 phosphorylation in mammalian nonsense-mediated mRNA decay. *Genes to Cells*, 18, 161–175.
- Yamashita, A., Izumi, N., Kashima, I., Ohnishi, T., Saari, B., Katsuhata, Y., Ohno, S. (2009). SMG-8 and SMG-9, two novel subunits of the SMG-1 complex, regulate remodeling of the mRNA surveillance complex during nonsense-mediated mRNA decay. *Genes and Development*, 18, 161–175.
- Yamashita, A., Ohnishi, T., Kashima, I., Taya, Y., & Ohno, S. (2001). Human SMG-1, a novel phosphatidylinositol 3-kinase-related protein kinase, associates with components of the mRNA surveillance complex and is involved in the regulation of nonsense-mediated mRNA decay. *Genes & Development*, 15, 2215–2228.
- Yepiskoposyan, H., Aeschmann, F., Nilsson, D., Okoniewski, M., & Mu, O. (2011). Autoregulation of the nonsense-mediated mRNA decay pathway in human cells. *RNA*, 17, 2108–2118.
- Youngman, E. M., Brunelle, J. L., Kochaniak, A. B., & Green, R. (2004). The active site of the ribosome is composed of two layers of conserved nucleotides with distinct roles in peptide bond formation and peptide release. *Cell*, 117, 589–599.
- Zhang, J., Sun, X., Qian, Y., Duca, J. P. L. A., & Maquat, L. E. (1998). At least one intron is required for the nonsense-mediated decay of triosephosphate isomerase mRNA: A possible link between nuclear splicing and cytoplasmic translation. *Molecular and Cellular Biology*, 18(9), 5272–5283.
- Zhang, X., Azhar, G., Huang, C., & Cui, C. (2007). Alternative splicing and nonsense-mediated

mRNA decay regulate gene expression of serum response factor. *Gene*, 400, 131–139.

Zünd, D., Gruber, A. R., Zavolan, M., & Mühlemann, O. (2013). Translation-dependent displacement of UPF1 from coding sequences causes its enrichment in 3' UTRs. *Nature Structural & Molecular Biology*, 20(8), 936–43.

8 Manuscript

Under revision

Dual function of UPF3B in early and late translation termination

Authors

Gabriele Neu-Yilik^{1,2,6}, Etienne Raimondeau^{3,6}, Boris Eliseev³, Lahari Yeramala³, Beate Amthor^{1,2}, Aurélien Deniaud³, Karine Huard³, Kathrin Kerschgens^{1,2}, Matthias W. Hentze^{2,4,7}, Christiane Schaffitzel^{3,5,7}, Andreas E. Kulozik^{1,2,7}

Correspondence:

Hentze@embl.de

christiane.berger-schaffitzel@bristol.ac.uk

Andreas.Kulozik@med.uni-heidelberg.de

Affiliations:

- (1) Department of Pediatric Oncology, Hematology and Immunology, University of Heidelberg, Im Neuenheimer Feld 430, 69120 Heidelberg, Germany
- (2) Molecular Medicine Partnership Unit, University of Heidelberg and European Molecular Biology Laboratory, Im Neuenheimer Feld 350, 69120 Heidelberg, Germany
- (3) European Molecular Biology Laboratory, Grenoble Outstation, 71 Avenue des Martyrs, 38042 Grenoble, France
- (4) European Molecular Biology Laboratory, Meyerhofstr. 1, 69117 Heidelberg, Germany
- (5) School of Biochemistry, University of Bristol, Bristol, BS8 1TD, United Kingdom
- (6) Co-first author
- (7) Corresponding author

Running title: Dual function of UPF3B

Keywords: NMD, translation termination, UPF3B

Summary

Nonsense-mediated mRNA decay (NMD) is a cellular surveillance pathway that recognizes and degrades mRNAs with premature termination codons (PTCs). The mechanisms underlying translation termination are key to the understanding of RNA surveillance mechanisms such as NMD and crucial for the development of therapeutic strategies for NMD-related diseases. Here, we have used a fully reconstituted *in vitro* translation system to probe the NMD proteins for interaction with the termination apparatus. We discovered that UPF3B (1) delays translation termination and (2) dissociates post-termination ribosomal complexes that are devoid of the nascent peptide. These previously unknown functions of UPF3B in early and late phases of translation termination suggest that UPF3B is involved in the crosstalk between the NMD machinery and the PTC-bound ribosome, a central mechanistic step of RNA surveillance.

Introduction

Nonsense-mediated mRNA decay (NMD) is a eukaryotic surveillance mechanism that controls the expression of aberrant mRNAs, degrading transcripts with premature termination codons (PTCs). PTCs can be introduced into mRNAs by mutations, transcriptional errors, and aberrant splicing, but are also contained in 5 -15 % of normal transcripts. By modulating the expression of physiological target mRNAs, NMD serves as a posttranscriptional regulator of gene expression and thus controls important cellular and organismal processes in development, cellular stress responses, immunity, and neuronal differentiation (Kurosaki & Maquat, 2016, Linder, Fischer et al., 2015, Lykke-Andersen & Jensen, 2015, Ottens & Gehring, 2016). NMD is also of medical importance as it limits the production of truncated proteins that may otherwise exert dominant negative functions but can also result in loss of function when mRNAs encoding (partially) functional truncated proteins are degraded (Bhuvanagiri, Schlitter et al., 2010, Nguyen, Wilkinson et al., 2014). Mutations or copy number variations in NMD factors are linked to genetic diseases, specifically to neurodevelopmental disorders and intellectual disabilities (Linder et al., 2015, Nguyen et al., 2014).

Conceptually, NMD can be divided into a translation termination phase and an mRNA degradation phase. During the past two decades a wealth of information has accumulated documenting the interplay between the core NMD factors and decay enzymes that enable the recognition and degradation of NMD substrates (Fatscher, Boehm et al., 2015, Schweingruber, Rufener et al., 2013). However, the mechanism by which translation termination at a PTC is distinguished from termination at a normal termination codon (NTC) is still poorly understood. Two prevailing models, the “downstream marker model” and the “faux 3’UTR model”, have been proposed to explain the difference between normal and aberrant termination (reviewed in (Bhuvanagiri et al., 2010, He & Jacobson, 2015)). The “downstream marker model” posits the

formation of an aberrant termination complex at a PTC consisting of the terminating ribosome, the central NMD effector UPF1, the SMG1-8-9 kinase complex, and the release factors eRF1 and eRF3. This so-called SURF complex (Kashima, Yamashita et al., 2006) is thought to delay translation termination and to sense the presence of an mRNP complex on the extended 3'UTR which in mammalian cells is represented by an exon junction complex (EJC) downstream of the PTC. The terminating ribosome and the EJC are thought to be bridged by UPF2 that, according to this model, interacts with UPF1 at the termination site and EJC-bound UPF3B, leading to the formation of a decay inducing complex that remodels the 3' mRNP and recruits mRNA decay enzymes.

The faux 3'UTR model posits that NMD can be induced by an aberrant 3'UTR mRNP characterized by the absence of at least one termination-enhancing factor that is associated with a normal 3'UTR (Amrani, Ganesan et al., 2004). Consequently, termination at a PTC is delayed and inefficient. Such an aberrant 3'UTR mRNP can be caused by inappropriate spacing between the termination codon and the poly(A) tail, preventing the termination-promoting interaction between eRF3a and poly(A) binding protein, and instead allowing the recruitment of UPF1.

Both models converge on the central NMD effector UPF1 that interacts with the release factors (eRFs) at the terminating ribosome. For yeast NMD, all three UPF proteins are essential, whereas in higher eukaryotes, UPF2-independent, UPF3B-independent, and EJC-independent NMD branches have been described (Bühler, Steiner et al., 2006, Chan, Huang et al., 2007, Gehring, Kunz et al., 2005). How UPF2 and UPF3 are recruited to the termination site in EJC-independent NMD is unknown. UPF2 and UPF3B are thought to stimulate the phosphorylation of UPF1 and to activate UPF1's ATPase and helicase functions that are necessary to remodel the 3'UTR mRNP and to recruit mRNA degradation enzymes (Chamieh, Ballut et al., 2008, Fiorini, Bagchi et al., 2015, Ivanov, Gehring et al., 2008, Kashima et al., 2006).

Although the necessity of an interaction between the UPF proteins and the translation termination apparatus is generally accepted, the sequence and timing of NMD factor recruitment to the termination site has not been addressed experimentally. The hypothesis that UPF1 is specifically recruited to aberrant termination events as an anchor point for the assembly of an NMD-mRNP has been challenged by the finding that UPF1 is bound along the entire length of transcripts and that this binding occurs in a translation-independent fashion (Hogg & Goff, 2010, Hurt, Robertson et al., 2013, Zünd, Gruber et al., 2013).

Translation termination, whether regular or aberrant, needs to recycle ribosomes to avoid deleterious consequences for the translation apparatus (Graille & Seraphin, 2012, Lykke-Andersen & Bennett, 2014). In ribosome recycling the ATPase ABCE1/Rli1 is needed for the ultimate dissociation of post-termination ribosomes from the mRNA (Dever & Green, 2012,

Franckenberg, Becker et al., 2012, Graille & Seraphin, 2012, Jackson, Hellen et al., 2012). In yeast and human cells, depletion of the UPF proteins induces readthrough at PTCs in vivo as well as delayed termination in vitro (Amrani et al., 2004, Peixeiro, Inacio et al., 2012). A recent attempt to reconcile all available data into a new NMD model posits that UPF1, UPF2, and UPF3 have roles in early and late phases of premature termination (He & Jacobson, 2015). Accordingly, UPF1's initially weak association with elongating ribosomes is proposed to be stabilized by UPF2 and UPF3 when a ribosome terminates prematurely, stimulating the initially delayed termination at a PTC by either recruiting the release factors or by enhancing peptide release. Subsequently, UPF2 and UPF3 promote ATP hydrolysis by UPF1 to fuel the dissociation of post-terminating ribosomal complexes. UPF1, still bound to the 40S ribosomal subunit, then recruits mRNA decay enzymes to initiate mRNA degradation.

To shed light on these critical aspects of translation termination in an NMD context, we adopted an approach that combines a fully reconstituted in vitro translation termination system with in vitro and in vivo interaction studies to decipher the UPF-eRF interactome in translation termination. We find that UPF3B interacts with eRF3a and forms a trimeric complex with both eRF3a and eRF1. Moreover, UPF3B binds to RNA, the ribosome, and to UPF1. Unexpectedly, UPF1 plays no discernible functional role in this context, suggesting that it acts downstream to promote NMD. Importantly, UPF3B delays translation termination when release factors are limiting and dissolves post-termination complexes after peptidyl-tRNA hydrolysis.

Results

Validation of the experimental system

During termination at a PTC, the UPF1-eRF interaction is thought to impede translation termination (Ivanov et al., 2008, Kashima et al., 2006). Here, we analyze whether UPF1 alone or together with UPF2 and/or UPF3B affects the efficiency of mammalian translation termination in vitro.

We produced full-length eRF1, eRF3a, UPF1, and UPF3B. Because both the N- and C-termini of purified full length UPF2 are unstable when expressed in *Escherichia coli* or insect cells, we produced a stable UPF2 variant (UPF2L) comprising amino acids (aa) 121–1227 (Fig EV1A). UPF2L contains the UPF1- and UPF3B-binding domains and has the same activities as full length UPF2 (Chakrabarti, Jayachandran et al., 2011, Chamieh et al., 2008). Ribosomal pre-termination complexes (translating ribosomes stalled at a stop codon; preTCs) were assembled on a model mRNA using ribosomal subunits, aminoacylated tRNAs, and purified initiation and elongation factors. The model mRNA (MVHC-STOP) contained the β -globin 5'-UTR and a short open reading frame encoding a MVHC tetrapeptide followed by a UAA stop codon and a 3'UTR of

~400 nt (Fig 1A) (Alkalaeva, Pisarev et al., 2006, Fan-Minogue, Du et al., 2008). The formation of defined ribosomal complexes was analyzed by sucrose density gradient (SDG) centrifugation and primer extension inhibition (toeprinting). PreTCs containing the peptidyl-tRNA^{Cys} in the ribosomal P-site and the stop codon in the A-site are characterized by specific toeprints at position +16 nt 3' to the U of the UGC (Cys) codon (Fig 1B, lane 1, Fig EV1B).

During translation termination, eRF1 in complex with eRF3a binds to the stop codon (Brown, Shao et al., 2015) inducing conformational rearrangements. The formation of such post-termination complexes (postTCs) is manifested by a +1-2 nt forward shift relative to the preTC toeprint (Fig 1B, lane 2; Fig EV1B) (Shirokikh, Alkalaeva et al., 2010). These shifted toeprint bands arise from mRNA compaction in the mRNA channel of the 40S subunit upon binding of the eRFs to the stop codon in the ribosomal A site (Brown et al., 2015, Ivanov, Mikhailova et al., 2016, Matheisl, Berninghausen et al., 2015). GTP hydrolysis by eRF3a leads to accommodation of the GGQ motif of eRF1 in the peptidyl transferase centre of the large ribosomal subunit, resulting in rapid peptide release. eRF1 (together with eRF3a or after dissociation of eRF3a) remains associated with postTCs, thus maintaining the +1-2 nt shift of their toeprint (Alkalaeva et al., 2006).

To confirm the biological activity of purified UPF1, UPF2L, and UPF3B, we performed ATP hydrolysis experiments. In previous studies (Chakrabarti et al., 2011, Chamieh et al., 2008) maximal ATP hydrolysis by UPF1 was achieved at low pH (6-6.5) using N- and C-terminally truncated UPF1 fragments UPF1L and UPF1 Δ CH (Fig EV1C). Using these UPF1 isoforms as controls, we first tested ATP hydrolysis by UPF1 in end-point experiments at pH 6.5 (Fig EV1D). UPF1 \square CH (aa 295-914) lacks the CH domain and exhibits high ATPase activity that cannot be further stimulated (Fig EV1D, lanes 6, 7), whereas UPF1L (aa 115-914) contains the CH domain and exhibits similar ATPase activity when stimulated by UPF2 and UPF3B (Fig EV1D, lanes 4,5) (Chamieh et al., 2008). In full-length UPF1 (UPF1) the C-terminus contributes to maintaining UPF1 in an inactive state (Fiorini, Boudvillain et al., 2013). Accordingly, UPF1 exhibited only modest ATPase activity at 30°C and pH 6.5 which was doubled in the presence of UPF2L/3B (Fig EV1D, lanes 2 and 3). These results, using our recombinant UPF1 isoforms at pH 6.5 fully conformed to previous findings (Chakrabarti et al., 2011, Chamieh et al., 2008, Fiorini et al., 2013). At physiological pH 7.5 the activity of all proteins was lower, but followed a similar pattern (Fig EV1D, lanes 8-13). Under in vitro translation conditions at pH 7.5 and 37°C (Fig EV1E) neither UPF2L (lane 5) nor UPF3B (lane 6) had a significant effect on the ATPase function of UPF1. When used in combination, the ATPase function of UPF1 was slightly enhanced (lane 7). Taken together, these data show that our UPF proteins are biologically active.

UPF3B delays inefficient translation termination in a fully reconstituted translation termination system

Termination at a PTC contrasts with termination at a normal termination codon by being slowed and less efficient. This kinetic difference is thought to be either caused by the absence of the termination-stimulating protein PABPC1 and/or by inefficient recruitment of the eRFs in the presence of UPF1 (Amrani et al., 2004, He & Jacobson, 2015, Ivanov et al., 2016, Peixeiro et al., 2012). To mimic this situation in vitro and to avoid missing relevant modulatory effects of the UPF proteins, we used limiting concentrations of eRFs for our termination experiments as judged by the retention of a faint, but discernible preTC toeprint in addition to the appearance of postTC signals after termination (Fig EV2A, Fig 1B, 1E, EV2D, lanes 2).

To test if UPF proteins affect the efficiency of translation termination, preTCs were incubated with UPF1, UPF2L, UPF3B or combinations of these proteins (Fig 1B, lanes 3-9). UPF proteins were added in excess to saturate their interaction with the release factors, the mRNA, and preTCs. In fact, their local concentration, e.g. associated with the 3'UTR of natural NMD substrates, is impossible to estimate and might be in excess of terminating ribosomes (Hauer, Sieber et al., 2016, Zünd & Mühlemann, 2013). As controls, preTCs were either left untreated (lane 1) or the UPF proteins were replaced by BSA (lane 2). Subsequently, limiting amounts of eRFs were added to the reactions (except in lane 1), and translation termination was allowed to proceed for 5 min, followed by toeprinting analysis.

Neither UPF1 nor UPF2L individually (Fig 1B, lanes 3, 4) or together (lane 6) affected the intensity of pre- or postTC bands, compared to the control sample (lane 2). These findings indicate that when the eRFs are limiting, neither UPF1 nor UPF2L have a direct effect on translation termination in vitro.

By contrast, UPF3B (lane 5) substantially reduced the preTC to postTC transformation rate to about 40 % of the rate observed in the control reaction (lane 2) as estimated by calculating the ratio between the preTC and postTC signal intensities using a phosphoimager. Notably, the addition of UPF1 to UPF3B resulted in a similar delay of termination (lane 7) and did not have an additive, synergistic or reversing effect. Addition of UPF2L abolished the effect of UPF3B on translation termination (lane 7, 8) confirming that the termination delay is specifically caused by UPF3B and indicating that binding to UPF2L may prevent UPF3B from interfering with the termination reaction. We observed that the toeprint signals corresponding to the full length RNA and to the termination complexes as well as to the traces of initiating and elongating ribosomes present in preTC preparations were always stronger in the presence of UPF3B than in reactions without UPF3B. Therefore, we performed toeprinting of preTCs that had been incubated with

UPF3B but without eRFs. We found that here, too, all toeprint signals were stronger than in the absence of UPF3B (Fig 1B, lanes 1 and 10), which is likely to be caused by a more efficient recovery of ribosomal complexes and RNA. UPF3B has a basic pI of 9.48 and contains an RNA recognition motif (RRM). To exclude that the inhibitory effect of UPF3B on the preTC-postTC transition is due to unspecific binding to ribosomes and/or RNA, we tested other proteins with similar biochemical properties. Neither eIF4B (RNA- and ribosome-binding), nor IRP1 (RNA-binding), or SXL (RNA-binding, pI 9,53) had an influence on in vitro translation termination (Fig EV2B). Likewise, we tested truncated versions of UPF3B for their capacity to delay translation termination. UPF3B-N (aa 42-217, pI 7,98), comprising the RNA recognition motif (RRM) domain (Kadlec, Izaurralde et al., 2004), and UPF3B-M (aa 147-419, pI 9,73) comprising the middle domain had no influence on translation termination. In contrast, a UPF3B variant lacking the exon junction complex binding domain (EBD; aa 421-434) but retaining both the RRM and the middle domain (UPF3B Δ EBD, (Gehring, Neu-Yilik et al., 2003)) delayed the preTC-postTC transition (Fig EV2C).

UPF3B reduces the efficiency of peptidyl-tRNA hydrolysis at low concentrations of release factors

Toeprinting assays of termination reactions monitor stop codon recognition. To investigate if UPF3B also affects peptidyl-tRNA hydrolysis, preTCs assembled on the MVHC-STOP mRNA using ³⁵S-labeled initiator-tRNA were incubated with or without UPF3B, and with limiting amounts of eRFs. In comparison to the maximal rate of peptidyl-tRNA hydrolysis achieved within the observed time window, peptide release efficiency was reduced in the presence of UPF3B by ~40-50 % (Fig 1C). Both, the +1-2 nt toeprint shift can only occur when the eRFs bind to the stop codon in the ribosomal A site. Therefore, we conclude that UPF3B impairs stop codon recognition and peptidyl-tRNA hydrolysis by the eRFs and thereby reduces termination efficiency.

Translation termination in vitro is independent of ATP-binding or the ATPase activity of UPF1

ATP binding and hydrolysis by UPF1 are essential for NMD. We repeated the toeprinting experiment described above in the presence of either ATP (Fig EV2D, lanes 1-8) or its non-hydrolyzable analogue AMPPNP (lanes 9-15). Under these conditions, neither UPF1 nor UPF2L individually (lanes 3, 4, 10, 11) or together (lanes 6, 13) affected the intensity of pre- or postTC signals compared to the control samples (lanes 2, 9). By contrast, UPF3B both alone and following addition of UPF1 reduced termination efficiency. These findings were independent of

the presence of ATP or AMPPNP, indicating that neither the ATP-binding nor the ATPase function of UPF1 influences the transition of preTCs to postTCs.

Translation termination is independent of UPF1 phosphorylation and the presence of the SMG1-8-9 complex

According to current models, UPF1, the eRFs, and the SMG1-8-9 complex form the termination-stalling SURF complex (Kashima et al., 2006). UPF1 phosphorylation by SMG1 is thought to trigger UPF1's release from the eRFs (Kashima et al., 2006, Okada-Katsuhata, Yamashita et al., 2012). Here, we explored whether *in vitro* phosphorylation of UPF1 affects translation termination. Maximal *in vitro* phosphorylation of UPF1 by SMG1 or SMG1-8-9 is achieved at pH 9.0, corresponding to the pH-optimum of the kinase (Chakrabarti, Bonneau et al., 2014, Deniaud, Karuppasamy et al., 2015, Morita, Yamashita et al., 2007). We examined phosphorylation of UPF1 by SMG1-8-9 at physiological pH in the absence or presence of UPF2L, UPF3B and the eRFs (Fig 1D). UPF2L only slightly stimulates UPF1 phosphorylation (Fig 1D, compare lane 1 with lanes 4, 10) by SMG1-8-9. In contrast, UPF3B alone (lanes 5, 11) moderately and together with UPF2L (lanes 6, 12) strongly inhibits UPF1 phosphorylation by SMG1-8-9 irrespective of the presence of equimolar concentrations of the eRFs. We confirmed that our UPF2L or UPF3B preparations do not contain a phosphatase by co-incubating the phosphorylated UPF1 (P-UPF1) with the preparations of UPF2L and UPF3B for 15 min at 37°C (lanes 13-16), which did not affect the abundance of the phosphorylated UPF1.

We next investigated whether UPF1 phosphorylation or the presence of SMG1-8-9 *per se* affects *in vitro* translation termination. UPF1 alone or together with either UPF2L, UPF3B, or both was incubated with SMG1-8-9 and ATP for 30 min and subsequently mixed with preTCs for another 10 min at 37°C (Fig 1E, lanes 9-12) followed by termination with eRF1 and eRF3a and toeprint analysis. Reactions without SMG1-8-9 served as controls (lanes 3-8). We found that irrespective of the presence of either UPF2L or UPF2L and UPF3B, neither UPF1 phosphorylation nor the presence of SMG1-8-9 have a detectable influence on termination efficiency as judged by the rate of transformation of preTCs to postTCs (compare lanes 3 and 9, lanes 6 and 10, lanes 8 and 12). The inhibitory effect of UPF3B on this transformation was independent of the presence of SMG1-8-9 and UPF1 (compare lanes 7 and 11).

UPF1 and UPF3B are part of release factor-containing complexes *in vivo*

We next analyzed the interaction of the UPF proteins with the termination complex *in vivo*. Based on co-immunoprecipitation (co-IP) experiments, human UPF1 has been suggested to interact with both eRF1 and eRF3a, and thereby physically link the NMD apparatus with translation termination (Ivanov et al., 2008, Kashima et al., 2006, Singh, Rebbapragada et al., 2008). In

yeast, all three Upf proteins were reported to bind to eRF3 (Sup35) (Wang, Czaplinski et al., 2001). We thus transiently co-transfected HeLa cells with FLAG-tagged eRF1 or eRF3a and full length versions of V5-tagged UPF1, UPF2, or UPF3B, and immunoprecipitated on FLAG-antibody beads in the presence of RNase A. Co-IPs of FLAG-eRF1 with V5-eRF3a and of FLAG-eRF3a with V5-eRF1 served as positive controls and yielded strong eRF1-eRF3a interactions (Fig 2A, B, lanes 2). Co-IPs of FLAG-eRFs with the EJC-disassembly factor PYM (Gehring, Lamprinaki et al., 2009) served as specificity controls (Fig 2A, B, lanes 10).

Using FLAG-eRF1 as bait, UPF1 (Fig 2A, lane 3), but not UPF2 (lanes 4, 6, 8, 9) or UPF3B (lane 5, 7-9) was co-immunoprecipitated with eRF1. Importantly, co-transfection of UPF3B and UPF1 prevented the formation of a complex containing eRF1 and UPF1 (lane 7) indicating that UPF3B either directly or indirectly competes with eRF1 for UPF1 binding.

Using FLAG-eRF3a as bait, only little UPF2 (Fig 2B, lane 4) but considerably more UPF1 and UPF3B (lanes 3 and 5) were co-immunoprecipitated. Interestingly, we found UPF3B in FLAG-eRF3a immunoprecipitates together with UPF1 (lanes 7 and 9), indicating that UPF1 and UPF3B can bind to eRF3a complexes both, individually and together, but that these proteins do not compete for eRF3a-binding. Although co-transfection of UPF2 strongly enhanced the ability of UPF1 to co-immunoprecipitate with eRF3a (compare lane 3 to lane 6), UPF2 was excluded from these complexes as well as from complexes containing eRF3a and UPF3B (lanes 6, 8 and 9). We conclude that UPF2 stimulates the direct or indirect interaction between UPF1 and eRF3a, but does not partake in complexes containing eRF3a together with UPF1, UPF3B, or both.

UPF3B directly interacts with eRF3a in a magnesium-sensitive manner forming a ternary complex with eRF1

Co-IP experiments do not reveal whether the interactions identified are direct or indirect. Therefore, we performed *in vitro* pulldown assays to analyse whether purified UPF proteins and release factors interact directly.

We incubated reaction mixtures containing His-tagged UPF1, UPF2L or UPF3B and one or both untagged eRF(s) (Fig 3A) with Ni-NTA beads, washed extensively and eluted the bound proteins with imidazole. We found that neither eRF1 nor eRF3a individually, nor the eRF1-eRF3a complex, detectably bound to UPF1 (Fig 3B, lanes 5-7), or to UPF2L (Fig 3C, lanes 5-7). UPF2 has recently been reported to directly interact with eRF3a (Lopez-Perrote, Castano et al., 2016). However, under the conditions tested, UPF2L did not bind to eRF3a, although it comprises the part that was reported to interact with eRF3a. In contrast, eRF3a and, to a lesser extent, eRF1 co-eluted with UPF3B individually (Fig 3D, lanes 5, 6) as well as simultaneously (lane 7) indicating that UPF3B directly interacts with both release factors.

Reciprocal control experiments using His-eRF3a as a bait for both UPF1 and UPF3B (Fig EV3) corroborated the eRF3a-UPF3B interaction (Fig EV3B) and confirmed that UPF1 does not co-elute with eRF3a irrespective of the presence of eRF1 (Fig EV3A).

Translation is modulated by the Mg^{2+} concentration both in vivo and in vitro. In our in vitro translation termination assays (Fig 1) we used 1mM free Mg^{2+} which corresponds to the physiological intracellular level of unbound Mg^{2+} (MacDermott, 1990, Veloso, Guynn et al., 1973). We explored the impact of Mg^{2+} on the UPF3B-eRF interaction. At physiological $[Mg^{2+}]$ a substantial amount of UPF3B bound to eRF3a, whereas at >5 mM Mg^{2+} the interaction between UPF3B and eRF3a was considerably weaker (Fig 3E, lanes 4-6). Notably, UPF1 did not directly interact with the eRFs at all Mg^{2+} concentrations tested (Fig EV3C).

To corroborate UPF3B-eRF complex formation by an independent, established biophysical method, we incubated UPF3B with combinations of eRF1 and eRF3a and resolved the protein mixtures by size exclusion chromatography (SEC) under physiological buffer conditions. Co-incubation of equimolar amounts of eRF3a and UPF3B resulted in a complex eluting at a higher apparent molecular weight than the individual proteins (Fig 3F), corroborating a direct interaction between eRF3a and UPF3B. Because UPF3B alone eluted at a higher apparent molecular weight than expected (Fig 3F), indicating possible oligomerisation or a deviation from the globular shape, we subjected UPF3B to SEC coupled to on-line detection by Multi-Angle Laser Light-Scattering (SEC-MALLS) and refractometry index measurements. The determined weight-averaged molecular mass confirmed that UPF3B is monomeric in solution. This suggests a non-globular shape of UPF3B (Fig EV3D).

In contrast, after co-incubation of eRF1 and UPF3B the proteins eluted in two peaks (Fig EV3E). The first peak eluted at the same volume as UPF3B when analysed individually and thus corresponds to UPF3B. The second peak eluted at a higher apparent molecular weight than eRF1 alone (1.55 mL vs. 1.50 mL). Accordingly, in the SDS-PAGE analysis a slight shift of the eRF1 containing fractions can be observed in the gel analysing co-migration of UPF3B and eRF1 in SEC as compared to the gel analysing the eRF1-SEC fractions (Fig EV3E) suggesting a very weak interaction between eRF1 and UPF3B.

When UPF3B was mixed with both eRF1 and eRF3a, a single peak containing all three proteins eluted at a higher apparent molecular weight than each individual protein (Fig 3G) demonstrating that UPF3B, eRF1, and eRF3a can form a stable trimeric complex. The complex is likely stabilized by eRF3a, which can bind both UPF3B and eRF1. These findings suggest that the effect of UPF3B on translation termination can be fully or partially mediated by a direct interaction of UPF3B with either eRF3a or the eRF1-eRF3a complex.

UPF3B and UPF1 interact directly

In EJC-dependent NMD, UPF2 is thought to bridge the termination complex and the EJC by simultaneously binding to UPF1 at the termination site and UPF3B at the EJC (Chamieh et al., 2008, Kashima et al., 2006). However, UPF3B but not UPF1 binds to eRF3a *in vitro* and UPF2, in contrast to UPF1 and UPF3B, is excluded from eRF3a-bound complexes *in vivo* (Fig 2, 3). Although earlier *in vitro* binding studies using a truncated UPF1 variant revealed no direct interaction (Chamieh et al., 2008), we tested full length UPF1 binding to UPF3B. We incubated His-UPF3B with UPF1 either in the presence or in the absence of eRF3a and found that UPF1 directly interacts with UPF3B (Fig 4A, lane 6). Binding of eRF3a to UPF3B was not affected by UPF1, suggesting that the two proteins can bind to UPF3B independently (lanes 5 and 7). In SEC analysis, a single peak containing both UPF1 and UPF3B eluted earlier than UPF1 and UPF3B alone, confirming the formation of a UPF1-UPF3B complex. SDS-PAGE analysis revealed that the elution profile of UPF1 and UPF3B within this peak was not fully symmetric, indicating that the UPF1-UPF3B complex partly dissociates during SEC (Fig 4B).

The eRF3a-UPF3B interaction requires the N-terminus of eRF3a *in vitro* and *in vivo*

The N-terminus of eRF3a is not required for the function of eRF3a in translation termination (Ter-Avanesyan, Kushnirov et al., 1993). We explored whether an eRF3a variant lacking the first 138 aa (eRF3a Δ N) (Fig 5A) can bind UPF3B and found that in contrast to eRF3a (Fig 5B, lane 4), eRF3a Δ N was not co-eluted with His-UPF3B (lane 5). In the reciprocal experiment using His-eRF3a or His-eRF3a Δ N as bait, UPF3B co-eluted with eRF3a (Fig 5C, lane 4) but not with eRF3a Δ N (lane 5).

We further characterized the eRF3a-UPF3B interaction using truncated versions of His-UPF3B comprising the RNA recognition motif (RRM) domain (aa 42-217, UPF3B-N) (Kadlec et al., 2004), the middle domain (aa 147-419, UPF3B-M), part of the middle domain (aa 147-256, UPF3B-SM), or the EJC-binding motif (EBM) (aa 380-470, UPF3B-C) (Fig 5D). UPF3B-N and UPF3B-C did not bind eRF3a, indicating that neither the RRM domain which binds UPF2 nor the EBM are sufficient to interact with eRF3a (Fig 5E, lanes 8, 11). In contrast, UPF3B-M and UPF3B-SM, comprising the hitherto uncharacterized middle domain of UPF3B, bound to eRF3a, albeit less efficiently than the full length protein (lanes 7, 9, 10). The protein-protein contact between eRF3a and UPF3B is thus established by binding between the eRF3a N-terminus and the middle domain of UPF3B. Notably, most UPF3B mutations linked to neurodevelopmental disorders are located in this region (Alrahbeni, Sartor et al., 2015).

To examine if the interaction between UPF3B and N-terminally truncated eRF3a was also impaired *in vivo*, we transiently co-transfected HeLa cells with plasmids encoding a FLAG-

tagged version of eRF3a lacking the first 199 aa (FLAG-eRF3a Δ 199) and with V5-eRF1 or V5-UPF1, -UPF2, or -UPF3B, either individually or simultaneously (Fig 5F). We found that UPF1 still co-precipitated with eRF3a Δ 199 when it was co-transfected individually or with UPF2 (Fig 5F, lanes 3, 6). In contrast, only trace amounts of UPF3B were found in FLAG-eRF3a Δ 199 complexes (lanes 5, 7-9), illustrating that the eRF3a N-terminus is necessary for the interaction with UPF3B *in vivo*.

Next, we examined if the inability of eRF3a Δ N to interact with UPF3B affects the termination-delaying function of UPF3B (Fig 5G). However, the pre- and postTC toeprints generated in the presence of UPF3B and eRF3a (lanes 3, 5) or eRF3a Δ N (lanes 4, 6), respectively, were very similar.

We reasoned that the effect of UPF3B in delaying translation termination may involve direct binding to the ribosome, and that its potential role in eRF3a recruitment can be bypassed by eRF1 in the *in vitro* translation system. With an isoelectric point of 9.48, UPF3B is positively charged at physiological pH, and may interact with negatively charged rRNAs or ribosomal proteins. We used a 24 nt RNA oligomer in SEC to analyse the RNA-binding capacity of full length UPF3B (Fig EV4A). UPF3B incubated with RNA eluted earlier than UPF3B alone from the SEC column (1.22 mL vs 1.30 mL), and had a higher OD_{260nm} signal, indicating the presence of nucleic acids in this peak. The second peak (~ 1.77 mL) contained unbound RNA oligomer. The majority of the RNA oligonucleotide shifted to the position of the UPF3B peak, demonstrating that full length UPF3B binds RNA, a finding that is consistent with recent iCLIP and RNA interactome data (Hauer et al., 2016).

To explore the ability of UPF3B, UPF1, and UPF2L to interact with ribosomes we performed co-sedimentation assays. Centrifugation without ribosomes served as controls (Fig EV4B). UPF1 and UPF3B individually and simultaneously co-sedimented with 80S ribosomes (Fig EV4C, lanes 2, 6, 8), indicating that both proteins can bind independently to ribosomes. In contrast, the weak ribosome binding of UPF2L alone (lane 4) was considerably enhanced in the presence of UPF3B (lane 10). This finding indicates that UPF2L can be recruited to the ribosome by UPF3B, and that the interaction with UPF2L on the ribosome may interfere with the function of UPF3B in termination.

UPF3B triggers the disassembly of post-termination complexes

The ability of UPF3B to form complexes with UPF1 and the release factors suggests the existence of a previously unknown dynamic UPF-eRF protein network. We reasoned that the influence of the UPF proteins on translation termination might differ from what we had observed with limiting

amounts of the eRFs at equimolar and saturating amounts of eRFs and UPF proteins, allowing free interplay of all factors.

We thus complemented the experiments described in Fig 1B, 1E, and EV2 by experiments with saturating amounts of eRFs (Fig 6A, EV5). Addition of the eRFs induced the transformation of all preTCs to postTCs as indicated by a shift of the toeprint by +1-2 nt relative to the preTC toeprint (Fig 6A, EV5, lanes 2). Irrespective of the presence of ATP or AMPPNP, this pattern was essentially the same when preTCs were pre-incubated with either UPF1, UPF2L, both of these proteins (Fig 6A, EV5A, B, lanes 3, 4, and 6), with UPF2L and UPF3B (lanes 8), or with all three UPF proteins (lanes 9). We also investigated whether the phosphorylation of UPF1 by SMG1-8-9 either alone (Fig EV5C, lane 7), in presence of UPF2L and/or UPF3B (8-10), or before (lanes 11-14) addition of UPF2L and/or UPF3B influenced UPF1 function. We found that irrespective of the phosphorylation status, toeprints generated by termination with phosphorylated UPF1 (lanes 7-14) were indistinguishable from those generated with non-phosphorylated UPF1 (lanes 3-6). Thus, independent of its functions in ATP-binding or ATP-hydrolysis or of its phosphorylation status, UPF1 has no impact on translation termination even when eRFs are present at saturating concentrations.

In termination reactions including UPF3B either alone or together with UPF1 a small amount of preTCs was retained, suggesting that here, too, UPF3B delayed termination. However, most preTCs were transformed to postTCs in the presence of either UPF3B alone or in the presence of both, UPF1 and UPF3B, when eRFs were not limiting (Fig 6A, EV5A, B, lanes 5, 7, EV5C lanes 5, 9, 13). Importantly, the postTC toeprints resulting from termination reactions in the presence of UPF3B (or of UPF1 and UPF3B; Fig 6A, EV5A, EV5B, lanes 5 and 7) were considerably weaker and the readthrough full length signal clearly stronger than toeprints resulting from termination reactions without UPF3B (Fig 6A, EV5A, B, lanes 2-4, 6, 8, 9; EV5C, lanes 3, 4, 7, 8, 11, 12). This finding indicates that UPF3B induced the release of postTCs from the mRNA. We thus conclude that UPF3B destabilizes postTCs when release factors are abundant. This activity is independent of UPF1 and is prevented by UPF2L (Fig 6A, EV5A, B, lanes 8, 9; EV5C, lanes 6, 10, 14). The UPF2-dependent inhibition of UPF3B's impact on termination confirms that both termination delay and ribosome dissociation are caused by UPF3B, and not by a potential low-level contaminant escaping detection on Coomassie-stained gels and which might be co-purifying with recombinant UPF3B (Fig 1,3-5, EV1,3,5). We next included UPF3B-N, UPF3B-M, and UPF3B Δ EBD into termination reactions with saturating amounts of eRFs. Only UPF3B \square EBD exerted a similar postTC dissociating activity as UPF3B, indicating that the EBD is dispensable for this function (Fig EV5D). Taken together with the results described in Fig EV2C and D this indicates that neither RNA/ribosome-binding features nor a basic pI per se influence the preTC-

postTC transition or the dissolution of postTC complexes and that neither the RRM nor the middle domain of UPF3B alone are sufficient to exert these functions.

The formation of postTCs in toeprinting assays reflects stop codon recognition by eRF1. To explore if UPF3B performs its postTC-dissociating activity before or after peptide release, we interfered with the termination reaction by adding GMPPNP, eRF1AGQ, or the peptide-releasing reagent puromycin to the preTCs, or by omitting eRF3a (Fig 6B). eRF1AGQ (Fig EV1A, lane 2) with a G183A mutation in the GGQ motif is inactive in peptide release, but recognizes stop codons, stimulates the GTPase activity of eRF3a, and together with eRF3a can induce the ribosomal rearrangements reflected by the +1-2 nt shift in the toeprint (Fig 6B, lanes 4, 5) (Alkalaeva et al., 2006, Frolova, Simonsen et al., 1998). Likewise, eRF3a supports stop codon recognition in the presence of GMPPNP (lane 3), but impairs peptidyl-tRNA hydrolysis by eRF1. eRF1 alone can induce termination and ribosomal rearrangements as well as peptide release, but the reaction is considerably less efficient than in the presence of eRF3a and GTP (lane 6) (Alkalaeva et al., 2006). UPF3B efficiently dissociated postTCs generated in the presence of eRF1, eRF3a and GTP (Fig 6B, lane 10), but not ribosomal complexes that were deficient in peptide release either due to blocking the activity of eRF3a by GMPPNP (lane 11), the peptide-hydrolysis defective eRF1AGQ (lane 12), or the absence of eRF3a (lane 14). When peptide release was enforced by the addition of puromycin, UPF3B effectively dissociated the resulting postTCs (lanes 13, 15), which was also reflected by a concomitant increase of the toeprint corresponding to the ribosome-free full length mRNA. Notably, UPF3B was unable to dissociate preTCs in the absence of eRFs (Fig 6B, lane 9) or residual preTCs in reactions that were incubated with eRF1 or puromycin alone (lanes 15, 16). These data indicate that UPF3B dissociates postTCs after both GTP and peptidyl-tRNA hydrolysis, but not preTCs or postTCs before peptide hydrolysis. UPF3B also dissociates postTCs that have been generated in the absence of eRF3a (Fig 6B, lane 15). Therefore, the eRF3a-UPF3B interaction is not required for the function of UPF3B in ribosome dissociation.

The ability of UPF3B to promote the dissociation of postTC is reminiscent of the energy-free ribosome recycling activity mediated by eIF3, eIF1, and eIF1A (Pisarev, Hellen et al., 2007a), which is apparent only at low Mg^{2+} concentrations. Furthermore, ribosomal inter-subunit association is dynamic and more flexible at physiological rather than at higher Mg^{2+} concentrations (Shenvi, Dong et al., 2005). Therefore, we investigated the ability of UPF3B to dissociate postTCs at Mg^{2+} concentrations higher than 1 mM (Fig 6C) and found that no dissociation occurred at 2.5 or 5 mM Mg^{2+} , respectively (compare lanes 7 to lanes 8, 9). These findings suggest that UPF3B dissociates postTCs with flexible subunit association, possibly by accessing the ribosome subunit interface which is stabilized at higher Mg^{2+} concentrations.

Discussion

How translation termination at a premature termination codon differs from termination at a normal termination codon has long been a matter of debate. All prevailing models from yeast to man ascribe a critical role to UPF1 not only in the mRNA degradation phase, but already in the translation termination phase of NMD. These hypotheses are founded on the interaction of UPF1 with eRF1 and eRF3a, which were identified in co-IP experiments (Ivanov et al., 2008, Singh et al., 2008, Wang et al., 2001) (Fig 2). UPF1 is thought to recruit the eRFs to ribosomes that are stalled at a PTC in an early phase of termination and to promote ribosome disassembly in a late phase of termination via its ATPase function that is activated by UPF2 and UPF3 binding (reviewed in (Brognna, McLeod et al., 2016, Celik, Kervestin et al., 2015, He & Jacobson, 2015)). However, it has not been possible to experimentally address the hypothetical functions of NMD factors in translation termination in cells and organisms, because no adequate *in vivo* termination assay is available to date. Deletion of the UPF genes in yeast leads to increased stop codon suppression (Keeling, Lanier et al., 2004, Wang et al., 2001), whereas RNAi-mediated depletion of UPF1 in human cells reduces stop codon readthrough (Ivanov et al., 2008). Yet, it is unclear, if these manipulations disturb or reflect direct interactions of UPF proteins with the translation termination machinery.

Here, we tested the functional interactions of key NMD factors *in vitro* using a fully reconstituted translation termination system that has been demonstrated to faithfully mirror all phases of eukaryotic translation (Alkalaeva et al., 2006, Pisarev, Unbehauen et al., 2007b, Pisareva, Pisarev et al., 2008). Although this system cannot per se differentiate between termination at a NTC and a PTC, respectively, we simulated the situation at a PTC by combining terminating ribosomes and NMD factors as well as by omitting termination-stimulating factors. In agreement with current models we hypothesized that in such a system the central NMD factor UPF1 interacts with the eRFs and possibly the ribosome (Min, Roy et al., 2013), thereby delaying translation termination. In these models, UPF2 and UPF3B serve as activators of UPF1 functions. They support UPF1 phosphorylation by SMG1-8-9 which is thought to dissolve the UPF1-eRF interaction, to release UPF1-induced ribosomal stalling and to activate its RNP remodeling function in a post-termination phase (Ivanov et al., 2008, Kashima et al., 2006). Accordingly, we hypothesized that the addition of UPF2, UPF3B, ATP and/or SMG1-8-9 would release the UPF1-induced break and allow for efficient termination.

Surprisingly, we find that neither UPF1 per se nor its biochemical functions such as ATP-binding, ATP-hydrolysis or its phosphorylation play a discernible role in early or late phases of translation termination. Furthermore, UPF1 does not appear to bind eRF1 and eRF3a directly, and the previously described interactions between UPF1 and the eRFs, found in co-IP experiments, are

thus likely to be indirect. Cumulatively, our data demonstrate that UPF1 remains inactive or functionally dispensable during translation termination, and that the essential role of UPF1 in human NMD as well as the function of UPF2, may be exerted in the post-termination phase of NMD. This conclusion is supported by findings that show UPF1 phosphorylation and its ATPase and helicase activities in metazoans to be important for its functions in 3'UTR mRNP remodeling and the recruitment of mRNA decay factors (Fiorini et al., 2015, Franks, Singh et al., 2010, Kurosaki, Li et al., 2014, Okada-Katsuhata et al., 2012). However, in yeast Upf1 has recently been implicated in translation termination and ribosome release at PTCs (Serdar, Whiteside et al., 2016), an activity that required Upf1's ATPase function as well as Upf2 and Upf3. These divergent findings may reflect the higher complexity of metazoan NMD involving several NMD branches as well as a considerably larger number of factors, regulatory steps and feedback mechanisms as compared to yeast NMD.

Unexpectedly, we discover that UPF3B exerts the bifunctional influence on translation termination that has hitherto been attributed to UPF1. When release factors are limiting and translation termination is inefficient, UPF3B further delays termination and inhibits peptide release. After release of the nascent peptide UPF3B promotes the dissociation of post-termination ribosomal complexes. Both activities are prevented by UPF2L, which is likely caused by interference with its function at the termination site. This dual function of UPF3B is in excellent accord with the observation that termination at PTCs is considerably slower than termination at NTCs (Amrani et al., 2004, Peixeiro et al., 2012), and that deletion of any of the UPF genes in yeast causes defects in ribosome release both *in vitro* and *in vivo* (Ghosh, Ganesan et al., 2010). It has been suggested that the kinetics of termination determines the discrimination between NTCs and PTCs *in vivo* (Hilleren & Parker, 1999, Zünd & Mühlemann, 2013). Slow termination defines aberrant termination events and triggers the recruitment of decay enzymes, whereas fast termination is promoted by the interaction of PABPC1 with eRF3a. Mechanistically, we suggest that in the absence of PABPC1 either EJC-bound or free UPF3B binds to the terminating ribosome, interacts with the release factors and then delays termination by sterically impeding stop codon recognition and peptide release by eRF1. This hypothesis also provides a mechanistic rationale for the NMD-enhancing effect of EJCs, which may increase the local concentration of UPF3B at the premature termination site.

Because UPF3B interferes with translation termination we assign a central role to UPF3B in a modified model for NMD. According to this model, UPF3B binds in the vicinity of the A site of the ribosome and assists in the recruitment of eRF1-eRF3a during the initial slow phase of termination at a PTC (Fig 7, phase 1). UPF1 molecules bound to the 3'UTR nearby may interact with terminating ribosomes as well but remain inactive in the proceedings of termination. As our eRF3a co-IP experiments indicate (Fig 2B), UPF2 could assist with this interaction, but is not

itself part of a complex that contains both, UPF1 and the terminating ribosome. After peptide release (Fig 7, phase 2) UPF3B, possibly promoted by a conformational or positional change at the ribosome, contributes to the rescue of ribosomes stalled at a PTC and dissolves the postTC (Fig 6A, 6B, Fig 7, phase 3). This phase is independent of eRF binding and may be promoted by interactions of UPF3B with the ribosome subunit interface. Because UPF2 is not detected in complexes that contain both UPF3B and eRF3a (Fig 2B), we propose that UPF2 is recruited to postTCs after the release of eRF3a and dissociation of the ribosome by UPF3B. Subsequently UPF1, supported by UPF2 and UPF3B and possibly other proteins, can engage in 3'UTR remodeling and the recruitment of decay enzymes triggering the decay phase of NMD (Fig 7, phase 4).

Importantly, UPF3B can neither destabilize preTCs nor postTCs, when either GTP hydrolysis by eRF3a or peptidyl-tRNA hydrolysis are inhibited (Fig 6B). Ribosome recycling after proper or faulty translation termination is crucial for the protein synthesis machinery to avoid sequestration of essential components of the translation apparatus. In normal termination, no-go decay (NGD) and non-stop decay (NSD) postTCs or stalled ribosomes are dissociated by ABCE1 (reviewed in (Graille & Seraphin, 2012, Lykke-Andersen & Bennett, 2014)). A specific mechanism for ribosome rescue in NMD has not yet been identified. UPF1 has been proposed to dissolve ribosomes stalled at a PTC, possibly because eRF3a is not able to leave the complex and therefore prevents the interaction of ABCE1 with eRF1 (Celik et al., 2015, Serdar et al., 2016). Here, we uncover that UPF3B dissociates postTCs and may, therefore, function as a dedicated NMD ribosome dissociation factor in metazoans. This conclusion is indirectly supported by the finding that directing UPF3B close to the 3' end of the ORF stimulates translation of a reporter RNA in vivo (Kunz, Neu-Yilik et al., 2006). Since UPF3B is not an ATPase, its activity is reminiscent of the energy-free activity of initiation factors that can recycle post-termination complexes only at a narrow range of low Mg^{2+} (Pisarev et al., 2007a, Pisarev, Skabkin et al., 2010). Dissociation of postTCs by eIF3 alone is relatively inefficient and is enhanced by eIF1, eIF1A, and eIF3j. Similarly, UPF3B does not dissolve all postTCs even when present in large excess over the preTCs (Fig 6). Hence, future work will determine whether UPF3B-mediated ribosome dissociation is simply slower than ribosome release in normal termination as has been suggested (He & Jacobson, 2015), or if it can be stimulated by other proteins reminiscent of the cooperation of initiation factors and ABCE1 (Pisarev et al., 2010).

Remaining questions concern the role of UPF3B both in NMD and in NMD-related diseases. Loss-of-function mutations of the UPF3B gene result in X-linked intellectual disability disorders. However, their underlying molecular mechanisms are unknown (Jolly, Homan et al., 2013, Tarpey, Raymond et al., 2007). Most of these mutations impair NMD and have been mapped to the functionally uncharacterized middle domain of UPF3B (Alrahbeni et al., 2015). We show here

that this domain mediates the interaction with eRF3a (Fig 5E). This finding will enable investigation of whether disruption of the UPF3B-eRF3a interaction leads to the deregulation of genes that are required for normal neurodevelopment.

Upf3 is essential for NMD in yeast. For human NMD both UPF2-independent and UPF3B-independent branches have been reported (Chan et al., 2007, Gehring et al., 2005). Our discovery that UPF1 can directly interact with UPF3B contributes to the understanding of the UPF2-independent NMD branch, since UPF2 was assumed to bridge between UPF1 and UPF3B. However, if a major role of UPF3B in NMD is confined to translation termination, it remains to be investigated how ribosomes stalled at a PTC are recognized in the UPF3B-independent branch. Notably, UPF3 exists in two paralogs in higher eukaryotes, UPF3A and UPF3B. UPF3A has hitherto been considered to be a “backup molecule” that can substitute for UPF3B in NMD (Chan, Bhalla et al., 2009). By contrast, UPF3A has recently been shown to also act as an antagonist of UPF3B and to function as a suppressor of NMD (Shum, Jones et al., 2016). Therefore, it will be interesting to probe if UPF3A can either substitute or antagonize the role of UPF3B in translation termination.

Materials and Methods

Recombinant proteins were expressed in the Multi-Bac system, in *E. coli*, or in HEK 293 cells and purified as described (Deniaud et al., 2015). Assembly of preTCs on the MVHC-STOP mRNA, in vitro translation and toeprinting was performed essentially as described (Alkalaeva et al., 2006). In vitro ATPase and phosphorylation assays were performed as described (Chamieh et al., 2008) with modifications explained in the Supplementary Materials and Methods. For Co-IP experiments in Fig 2 and 4, HeLa cells were transiently transfected with protein-expression constructs described elsewhere (Ivanov et al., 2008) using the JetPrime transfection system (Polyplus). Immunoprecipitation and immunoblotting were performed as described (Gehring et al., 2003). All procedures are described in detail in the Supplementary Material and Methods. All experiments were performed between two and four times with comparable results using different batches of cells, of recombinant proteins, and/or preTCs.

Author contributions

GN-Y, CS, AEK, and MWH designed the study and wrote the manuscript with input from ER, BE, and LY; GN-Y, BA, and KK performed toeprinting experiments, ATPase assays, in vitro phosphorylation, and Co-IPs; ER, BE, LY, AD, and KH produced proteins; ER performed in vitro pulldown, co-sedimentation, and SEC (SEC-MALLS) experiments; BE generated preTCs and performed peptide release experiments.

Acknowledgements

We are much obliged to Tatyana Pestova for generously introducing KK to the reconstituted in vitro translation system and for providing the MVHC-STOP plasmid. We thank Hervé Le Hir for the UPF1L and UPF1 \square CH expression plasmids and providing protocols for their production as well as for the ATPase assay, Ludmila Frolova for providing the plasmid pET15b-eRF3a, and Stephen Cusack for plasmids pPROExHtb_UPF2 (121-1227), pPROExHtb_UPF3B-N, and the RNA oligonucleotide for RNA interaction assays. We thank Elena Alkalaeva for providing Met-tRNA and the plasmids for initiation factors used for in vitro translation, Alain Miller (Cilbiotech S.A., Mons, Belgium) for providing HeLa cytoplasmic extracts, Jan Medenbach for the gift of SXL, and Dmytro Dziuba for the gift of IRP1. AD acknowledges support by an EC-EMBL CoFUNDS EIPOD fellowship, CS is supported by a European Research Council Starting Grant (ComplexNMD, 281331). The experimental work of MWH and AEK is supported by the DFG through the SFB 1036 grant and together with GN-Y through the SPP1935 grant.

Conflict of interest

The authors declare that they have no conflict of interest

References

- Alkalaeva EZ, Pisarev AV, Frolova LY, Kisselev LL, Pestova TV (2006) In vitro reconstitution of eukaryotic translation reveals cooperativity between release factors eRF1 and eRF3. *Cell* 125: 1125-36
- Alrahbeni T, Sartor F, Anderson J, Miedzybrodzka Z, McCaig C, Muller B (2015) Full UPF3B function is critical for neuronal differentiation of neural stem cells. *Mol Brain* 8: 33
- Amrani N, Ganesan R, Kervestin S, Mangus DA, Ghosh S, Jacobson A (2004) A faux 3'-UTR promotes aberrant termination and triggers nonsense-mediated mRNA decay. *Nature* 432: 112-8
- Bhuvanagiri M, Schlitter AM, Hentze MW, Kulozik AE (2010) NMD: RNA biology meets human genetic medicine. *Biochem J* 430: 365-77
- Brogna S, McLeod T, Petric M (2016) The Meaning of NMD: Translate or Perish. *Trends Genet* 32: 395-407
- Brown A, Shao S, Murray J, Hegde RS, Ramakrishnan V (2015) Structural basis for stop codon recognition in eukaryotes. *Nature* 524: 493-6
- Bühler M, Steiner S, Mohn F, Paillusson A, Mühlemann O (2006) EJC-independent degradation of nonsense immunoglobulin- μ mRNA depends on 3' UTR length. *Nat Struct Mol Biol* 13: 462-4
- Celik A, Kervestin S, Jacobson A (2015) NMD: At the crossroads between translation termination and ribosome recycling. *Biochimie* 114: 2-9
- Chakrabarti S, Bonneau F, Schussler S, Eppinger E, Conti E (2014) Phospho-dependent and phospho-independent interactions of the helicase UPF1 with the NMD factors SMG5-SMG7 and SMG6. *Nucleic Acids Res* 42: 9447-60
- Chakrabarti S, Jayachandran U, Bonneau F, Fiorini F, Basquin C, Domcke S, Le Hir H, Conti E (2011) Molecular mechanisms for the RNA-dependent ATPase activity of Upf1 and its regulation by Upf2. *Mol Cell* 41: 693-703
- Chamieh H, Ballut L, Bonneau F, Le Hir H (2008) NMD factors UPF2 and UPF3 bridge UPF1 to the exon junction complex and stimulate its RNA helicase activity. *Nat Struct Mol Biol* 15: 85-93
- Chan WK, Bhalla AD, Le Hir H, Nguyen LS, Huang L, Gecz J, Wilkinson MF (2009) A UPF3-mediated regulatory switch that maintains RNA surveillance. *Nat Struct Mol Biol* 16: 747-53
- Chan WK, Huang L, Gudikote JP, Chang YF, Imam JS, MacLean JA, 2nd, Wilkinson MF (2007) An alternative branch of the nonsense-mediated decay pathway. *EMBO J* 26: 1820-30
- Deniaud A, Karuppusamy M, Bock T, Masiulis S, Huard K, Garzoni F, Kerschgens K, Hentze MW, Kulozik AE, Beck M, Neu-Yilik G, Schaffitzel C (2015) A network of SMG-8, SMG-9 and SMG-1 C-terminal insertion domain regulates UPF1 substrate recruitment and phosphorylation. *Nucleic Acids Res* 43: 7600-11
- Dever TE, Green R (2012) The elongation, termination, and recycling phases of translation in eukaryotes. *Cold Spring Harb Perspect Biol* 4: a013706
- Fan-Minogue H, Du M, Pisarev AV, Kallmeyer AK, Salas-Marco J, Keeling KM, Thompson SR, Pestova TV, Bedwell DM (2008) Distinct eRF3 requirements suggest alternate eRF1 conformations mediate peptide release during eukaryotic translation termination. *Mol Cell* 30: 599-609
- Fatscher T, Boehm V, Gehring NH (2015) Mechanism, factors, and physiological role of nonsense-mediated mRNA decay. *Cell Mol Life Sci* 72: 4523-44
- Fiorini F, Bagchi D, Le Hir H, Croquette V (2015) Human Upf1 is a highly processive RNA helicase and translocase with RNP remodelling activities. *Nat Commun* 6: 7581
- Fiorini F, Boudvillain M, Le Hir H (2013) Tight intramolecular regulation of the human Upf1 helicase by its N- and C-terminal domains. *Nucleic Acids Res* 41: 2404-15
- Franckenberg S, Becker T, Beckmann R (2012) Structural view on recycling of archaeal and eukaryotic ribosomes after canonical termination and ribosome rescue. *Curr Opin Struct Biol* 22: 786-96

Franks TM, Singh G, Lykke-Andersen J (2010) Upf1 ATPase-dependent mRNP disassembly is required for completion of nonsense-mediated mRNA decay. *Cell* 143: 938-50

Frolova LY, Simonsen JL, Merkulova TI, Litvinov DY, Martensen PM, Rechinsky VO, Camonis JH, Kisselev LL, Justesen J (1998) Functional expression of eukaryotic polypeptide chain release factors 1 and 3 by means of baculovirus/insect cells and complex formation between the factors. *Eur J Biochem* 256: 36-44

Gehring NH, Kunz JB, Neu-Yilik G, Breit S, Viegas MH, Hentze MW, Kulozik AE (2005) Exon-junction complex components specify distinct routes of nonsense-mediated mRNA decay with differential cofactor requirements. *Mol Cell* 20: 65-75

Gehring NH, Lamprinaki S, Kulozik AE, Hentze MW (2009) Disassembly of exon junction complexes by PYM. *Cell* 137: 536-48

Gehring NH, Neu-Yilik G, Schell T, Hentze MW, Kulozik AE (2003) Y14 and hUpf3b form an NMD-activating complex. *Mol Cell* 11: 939-49

Ghosh S, Ganesan R, Amrani N, Jacobson A (2010) Translational competence of ribosomes released from a premature termination codon is modulated by NMD factors. *RNA* 16: 1832-47

Graille M, Seraphin B (2012) Surveillance pathways rescuing eukaryotic ribosomes lost in translation. *Nat Rev Mol Cell Biol* 13: 727-35

Hauer C, Sieber J, Schwarzl T, Hollerer I, Curk T, Alleaume AM, Hentze MW, Kulozik AE (2016) Exon Junction Complexes Show a Distributional Bias toward Alternatively Spliced mRNAs and against mRNAs Coding for Ribosomal Proteins. *Cell Rep* 16: 1588-603

He F, Jacobson A (2015) Nonsense-Mediated mRNA Decay: Degradation of Defective Transcripts Is Only Part of the Story. *Annu Rev Genet* 49: 339-66

Hilleren P, Parker R (1999) mRNA surveillance in eukaryotes: kinetic proofreading of proper translation termination as assessed by mRNP domain organization? *RNA* 5: 711-9

Hogg JR, Goff SP (2010) Upf1 senses 3'UTR length to potentiate mRNA decay. *Cell* 143: 379-89

Hurt JA, Robertson AD, Burge CB (2013) Global analyses of UPF1 binding and function reveal expanded scope of nonsense-mediated mRNA decay. *Genome Res* 23: 1636-50

Ivanov A, Mikhailova T, Eliseev B, Yeramala L, Sokolova E, Susorov D, Shuvalov A, Schaffitzel C, Alkalaeva E (2016) PABP enhances release factor recruitment and stop codon recognition during translation termination. *Nucleic Acids Res* 44: 7766-76

Ivanov PV, Gehring NH, Kunz JB, Hentze MW, Kulozik AE (2008) Interactions between UPF1, eRFs, PABP and the exon junction complex suggest an integrated model for mammalian NMD pathways. *EMBO J* 27: 736-47

Jackson RJ, Hellen CU, Pestova TV (2012) Termination and post-termination events in eukaryotic translation. *Adv Protein Chem Struct Biol* 86: 45-93

Jolly LA, Homan CC, Jacob R, Barry S, Gecz J (2013) The UPF3B gene, implicated in intellectual disability, autism, ADHD and childhood onset schizophrenia regulates neural progenitor cell behaviour and neuronal outgrowth. *Hum Mol Genet* 22: 4673-87

Kadlec J, Izaurralde E, Cusack S (2004) The structural basis for the interaction between nonsense-mediated mRNA decay factors UPF2 and UPF3. *Nat Struct Mol Biol* 11: 330-7

Kashima I, Yamashita A, Izumi N, Kataoka N, Morishita R, Hoshino S, Ohno M, Dreyfuss G, Ohno S (2006) Binding of a novel SMG-1-Upf1-eRF1-eRF3 complex (SURF) to the exon junction complex triggers Upf1 phosphorylation and nonsense-mediated mRNA decay. *Genes Dev* 20: 355-67

Keeling KM, Lanier J, Du M, Salas-Marco J, Gao L, Kaenjak-Angeletti A, Bedwell DM (2004) Leaky termination at premature stop codons antagonizes nonsense-mediated mRNA decay in *S. cerevisiae*. *RNA* 10: 691-703

Kunz JB, Neu-Yilik G, Hentze MW, Kulozik AE, Gehring NH (2006) Functions of hUpf3a and hUpf3b in nonsense-mediated mRNA decay and translation. *RNA* 12: 1015-22

Kurosaki T, Li W, Hoque M, Popp MW, Ermolenko DN, Tian B, Maquat LE (2014) A post-translational regulatory switch on UPF1 controls targeted mRNA degradation. *Genes Dev* 28: 1900-16

Kurosaki T, Maquat LE (2016) Nonsense-mediated mRNA decay in humans at a glance. *J Cell Sci* 129: 461-7

Linder B, Fischer U, Gehring NH (2015) mRNA metabolism and neuronal disease. *FEBS Lett* 589: 1598-606

Lopez-Perrote A, Castano R, Melero R, Zamarro T, Kurosawa H, Ohnishi T, Uchiyama A, Aoyagi K, Buchwald G, Kataoka N, Yamashita A, Llorca O (2016) Human nonsense-mediated mRNA decay factor UPF2 interacts directly with eRF3 and the SURF complex. *Nucleic Acids Res* 44: 1909-23

Lykke-Andersen J, Bennett EJ (2014) Protecting the proteome: Eukaryotic cotranslational quality control pathways. *J Cell Biol* 204: 467-76

Lykke-Andersen S, Jensen TH (2015) Nonsense-mediated mRNA decay: an intricate machinery that shapes transcriptomes. *Nat Rev Mol Cell Biol* 16: 665-77

MacDermott M (1990) The intracellular concentration of free magnesium in extensor digitorum longus muscles of the rat. *Exp Physiol* 75: 763-9

Matheisl S, Berninghausen O, Becker T, Beckmann R (2015) Structure of a human translation termination complex. *Nucleic Acids Res* 43: 8615-26

Min EE, Roy B, Amrani N, He F, Jacobson A (2013) Yeast Upf1 CH domain interacts with Rps26 of the 40S ribosomal subunit. *RNA* 19: 1105-15

Morita T, Yamashita A, Kashima I, Ogata K, Ishiura S, Ohno S (2007) Distant N- and C-terminal domains are required for intrinsic kinase activity of SMG-1, a critical component of nonsense-mediated mRNA decay. *J Biol Chem* 282: 7799-808

Nguyen LS, Wilkinson MF, Gecz J (2014) Nonsense-mediated mRNA decay: inter-individual variability and human disease. *Neurosci Biobehav Rev* 46 Pt 2: 175-86

Okada-Katsuhata Y, Yamashita A, Kutsuzawa K, Izumi N, Hirahara F, Ohno S (2012) N- and C-terminal Upf1 phosphorylations create binding platforms for SMG-6 and SMG-5:SMG-7 during NMD. *Nucleic Acids Res* 40: 1251-66

Ottens F, Gehring NH (2016) Physiological and pathophysiological role of nonsense-mediated mRNA decay. *Pflugers Arch* 468: 1013-28

Peixeiro I, Inacio A, Barbosa C, Silva AL, Liebhaber SA, Romao L (2012) Interaction of PABPC1 with the translation initiation complex is critical to the NMD resistance of AUG-proximal nonsense mutations. *Nucleic Acids Res* 40: 1160-73

Pisarev AV, Hellen CU, Pestova TV (2007a) Recycling of eukaryotic posttermination ribosomal complexes. *Cell* 131: 286-99

Pisarev AV, Skabkin MA, Pisareva VP, Skabkina OV, Rakotondrafara AM, Hentze MW, Hellen CU, Pestova TV (2010) The role of ABCE1 in eukaryotic posttermination ribosomal recycling. *Mol Cell* 37: 196-210

Pisarev AV, Unbehauen A, Hellen CU, Pestova TV (2007b) Assembly and analysis of eukaryotic translation initiation complexes. *Methods Enzymol* 430: 147-77

Pisareva VP, Pisarev AV, Komar AA, Hellen CU, Pestova TV (2008) Translation initiation on mammalian mRNAs with structured 5'UTRs requires DExH-box protein DHX29. *Cell* 135: 1237-50

Schweingruber C, Rufener SC, Zünd D, Yamashita A, Mühlemann O (2013) Nonsense-mediated mRNA decay - mechanisms of substrate mRNA recognition and degradation in mammalian cells. *Biochim Biophys Acta* 1829: 612-23

Serdar LD, Whiteside DL, Baker KE (2016) ATP hydrolysis by UPF1 is required for efficient translation termination at premature stop codons. *Nat Commun* 7: 14021

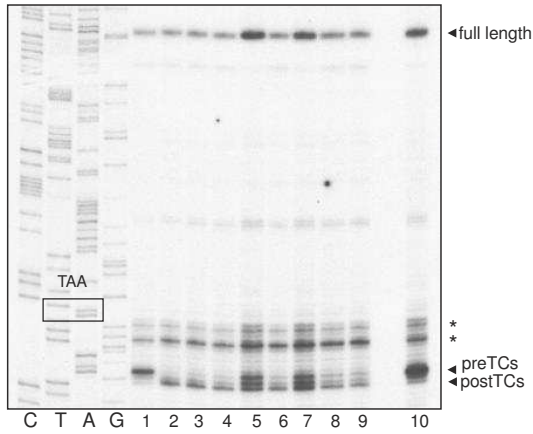
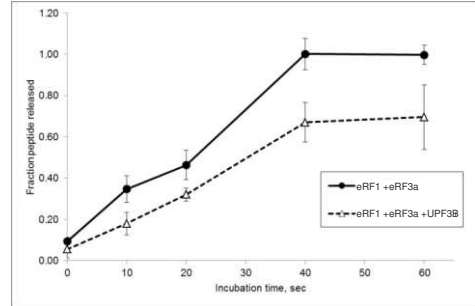
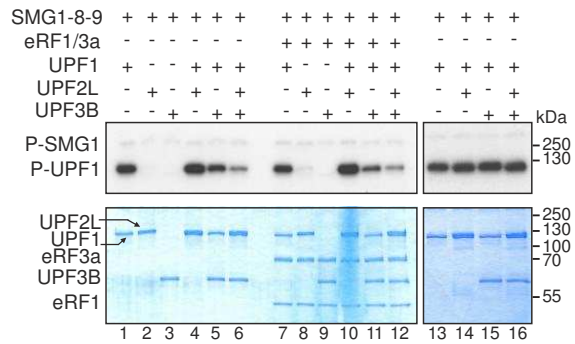
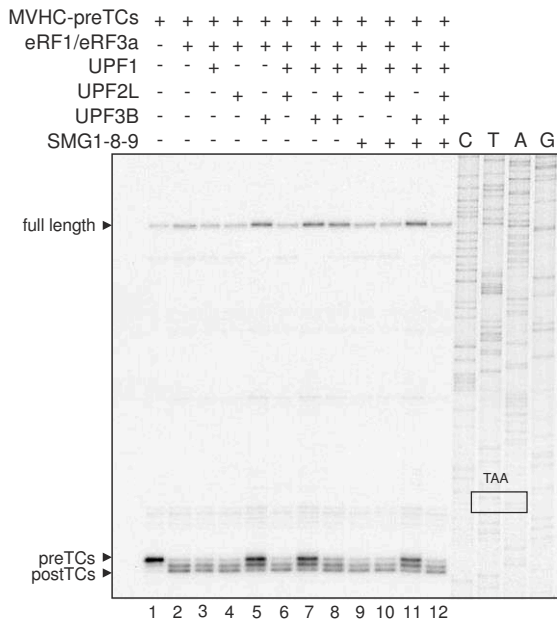
- Shenvi CL, Dong KC, Friedman EM, Hanson JA, Cate JH (2005) Accessibility of 18S rRNA in human 40S subunits and 80S ribosomes at physiological magnesium ion concentrations--implications for the study of ribosome dynamics. *RNA* 11: 1898-908
- Shirokikh NE, Alkalaeva EZ, Vassilenko KS, Afonina ZA, Alekhina OM, Kisselev LL, Spirin AS (2010) Quantitative analysis of ribosome-mRNA complexes at different translation stages. *Nucleic Acids Res* 38: e15
- Shum EY, Jones SH, Shao A, Dumdie J, Krause MD, Chan WK, Lou CH, Espinoza JL, Song HW, Phan MH, Ramaiah M, Huang L, McCarrey JR, Peterson KJ, De Rooij DG, Cook-Andersen H, Wilkinson MF (2016) The Antagonistic Gene Paralogs Upf3a and Upf3b Govern Nonsense-Mediated RNA Decay. *Cell* 165: 382-95
- Singh G, Rebbapragada I, Lykke-Andersen J (2008) A competition between stimulators and antagonists of Upf complex recruitment governs human nonsense-mediated mRNA decay. *PLoS Biol* 6: e111
- Skabkin MA, Skabkina OV, Hellen CU, Pestova TV (2013) Reinitiation and other unconventional posttermination events during eukaryotic translation. *Mol Cell* 51: 249-64
- Tarpey PS, Raymond FL, Nguyen LS, Rodriguez J, Hackett A, Vandeleur L, Smith R, Shoubridge C, Edkins S, Stevens C, O'Meara S, Tofts C, Barthorpe S, Buck G, Cole J, Halliday K, Hills K, Jones D, Mironenko T, Perry J et al. (2007) Mutations in UPF3B, a member of the nonsense-mediated mRNA decay complex, cause syndromic and nonsyndromic mental retardation. *Nat Genet* 39: 1127-33
- Ter-Avanesyan MD, Kushnirov VV, Dagkesamanskaya AR, Didichenko SA, Chernoff YO, Inge-Vechtomov SG, Smirnov VN (1993) Deletion analysis of the SUP35 gene of the yeast *Saccharomyces cerevisiae* reveals two non-overlapping functional regions in the encoded protein. *Mol Microbiol* 7: 683-92
- Veloso D, Guynn RW, Oskarsson M, Veech RL (1973) The concentrations of free and bound magnesium in rat tissues. Relative constancy of free Mg²⁺ concentrations. *J Biol Chem* 248: 4811-9
- Wang W, Czaplinski K, Rao Y, Peltz SW (2001) The role of Upf proteins in modulating the translation read-through of nonsense-containing transcripts. *EMBO J* 20: 880-90
- Zünd D, Gruber AR, Zavolan M, Mühlemann O (2013) Translation-dependent displacement of UPF1 from coding sequences causes its enrichment in 3' UTRs. *Nat Struct Mol Biol* 20: 936-43
- Zünd D, Mühlemann O (2013) Recent transcriptome-wide mapping of UPF1 binding sites reveals evidence for its recruitment to mRNA before translation. *Translation* 1: e26977

A**MVHC-STOP mRNA**5'G (CAA)_n-(\square -globin 5'UTR)-AUG-GUG-CAC-UGC-UAA-3'UTR (~400nt)

Met Val His Cys

B

MVHC-preTCs	+	+	+	+	+	+	+	+	+	+	+	+	+	+
eRF1/eRF3a	-	+	+	+	+	+	+	+	+	+	+	+	-	-
UPF1	-	-	+	-	-	+	+	-	+	-	+	-	-	-
UPF2L	-	-	-	+	-	+	-	+	+	-	+	+	-	-
UPF3B	-	-	-	-	+	-	+	+	+	+	+	+	-	-

**C****D****E****Figure 1 UPF3B delays translation termination in vitro.****A** Structure of the MVHC-STOP mRNA.

B Toeprinting analysis of ribosomal complexes obtained by incubating preTCs assembled on MVHC-STOP mRNA (MVHC-preTCs) with UPF1, UPF2L, UPF3B, or BSA at 1 mM free Mg²⁺ followed by termination with limiting amounts of eRF1 and eRF3a. The positions of preTCs, postTCs, and full length cDNA are indicated. Asterisks mark initiation and elongation complexes. Representative of 5 independent experiments

C Kinetics of [³⁵S]-peptidyl-tRNA hydrolysis in the presence of eRF1 and eRF3a (black circles) or eRF1, eRF3a, and UPF3B (white triangles). A value equal to 1 corresponds to the maximum value for peptide release triggered by eRF1 and eRF3a. Data points show the mean of 3 experiments +/- SEM.

D UPF1 in vitro phosphorylation by SMG1-8-9 in the presence of UPF2L and/or UPF3B and in the presence (lanes 7-12) or absence (lanes 1-6) of the eRFs. In lanes 13-16 UPF2L and/or UPF3B were added after UPF1 phosphorylation. Samples were analysed by SDS-PAGE, Coomassie-stained to control for equal loading (lower panel) and autoradiographed (upper panel). SMG1 autophosphorylation (P-SMG1) confirms equal SMG1-activity in all samples. UPF1 is represented by the lower and UPF2L by the upper of the two closely migrating bands between 125 and 130 kDa in the Coomassie stained gel. Representative of 2 independent experiments.

E Toeprinting analysis of ribosomal complexes obtained by incubating MVHC-preTCs with UPF1, UPF2L, UPF3B, SMG1-8-9, or BSA as indicated followed by translation termination by eRF1 and eRF3a. See also Fig EV2. Representative of 3 independent experiments

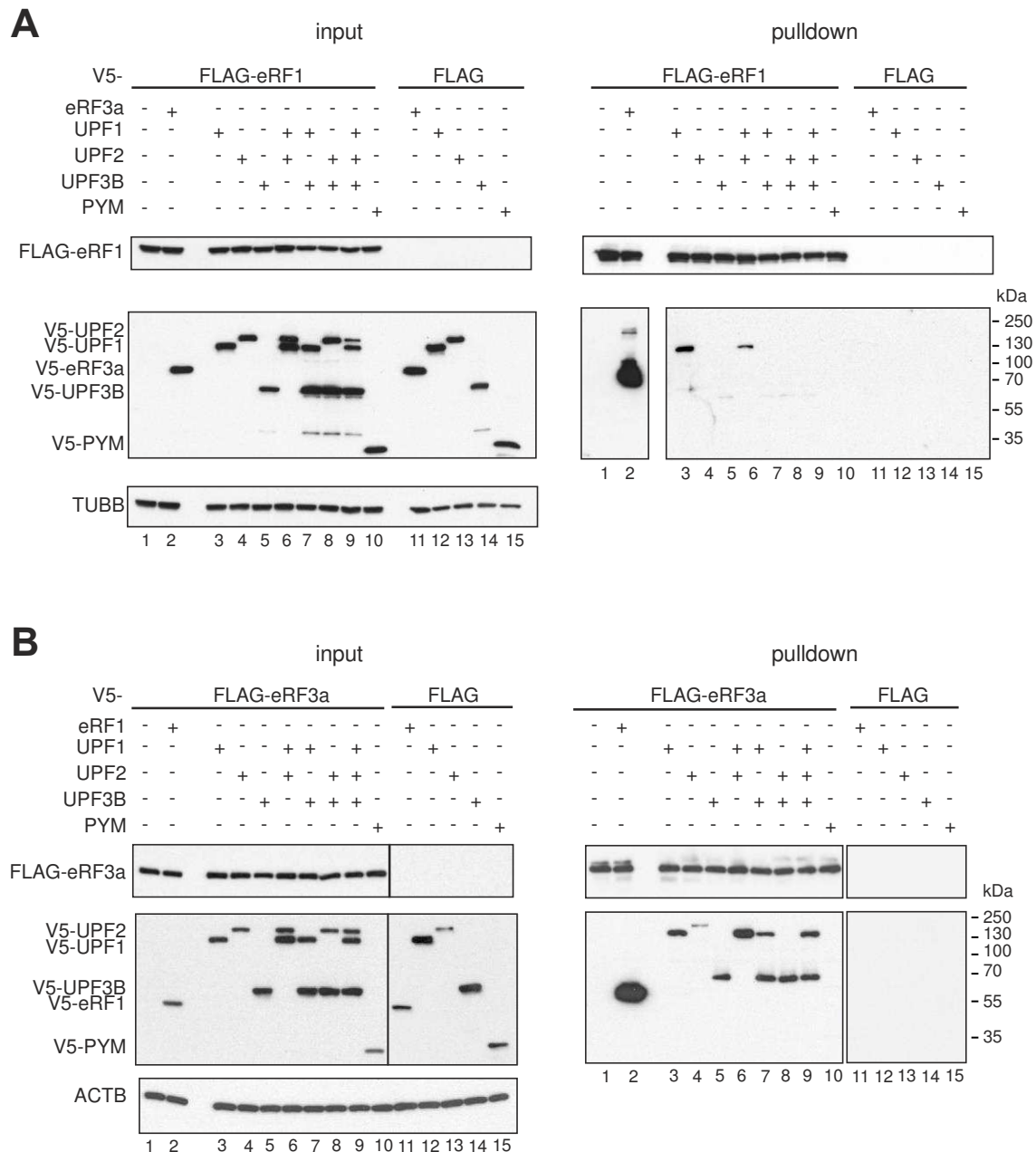


Figure 2 In vivo interaction between release factors and UPF proteins

A Co-immunoprecipitation from RNase A-treated lysates of HeLa cells transfected with FLAG-eRF1 (lanes 1-10) or unfused FLAG (lanes 11-15) and V5-eRF3a, V5-UPF1, V5-UPF2, V5-UPF3B, or V5-PYM. Co-precipitated proteins were detected using an anti-V5 antibody. Lysate used for the immunoprecipitations was loaded in the input lanes (left). Re-probing with anti-TUBB antibody served as loading control.

B Co-IP experiment as in (A) with FLAG-eRF3a. Re-probing with anti-ACTB served as loading control. Because TUBB migrates at virtually the same position as FLAG-eRF3a and ACTB migrates very closely to FLAG-eRF1, TUBB was used as loading control for Fig 2A and ACTB for Fig 2B. A,B each represent 2 independent experiments

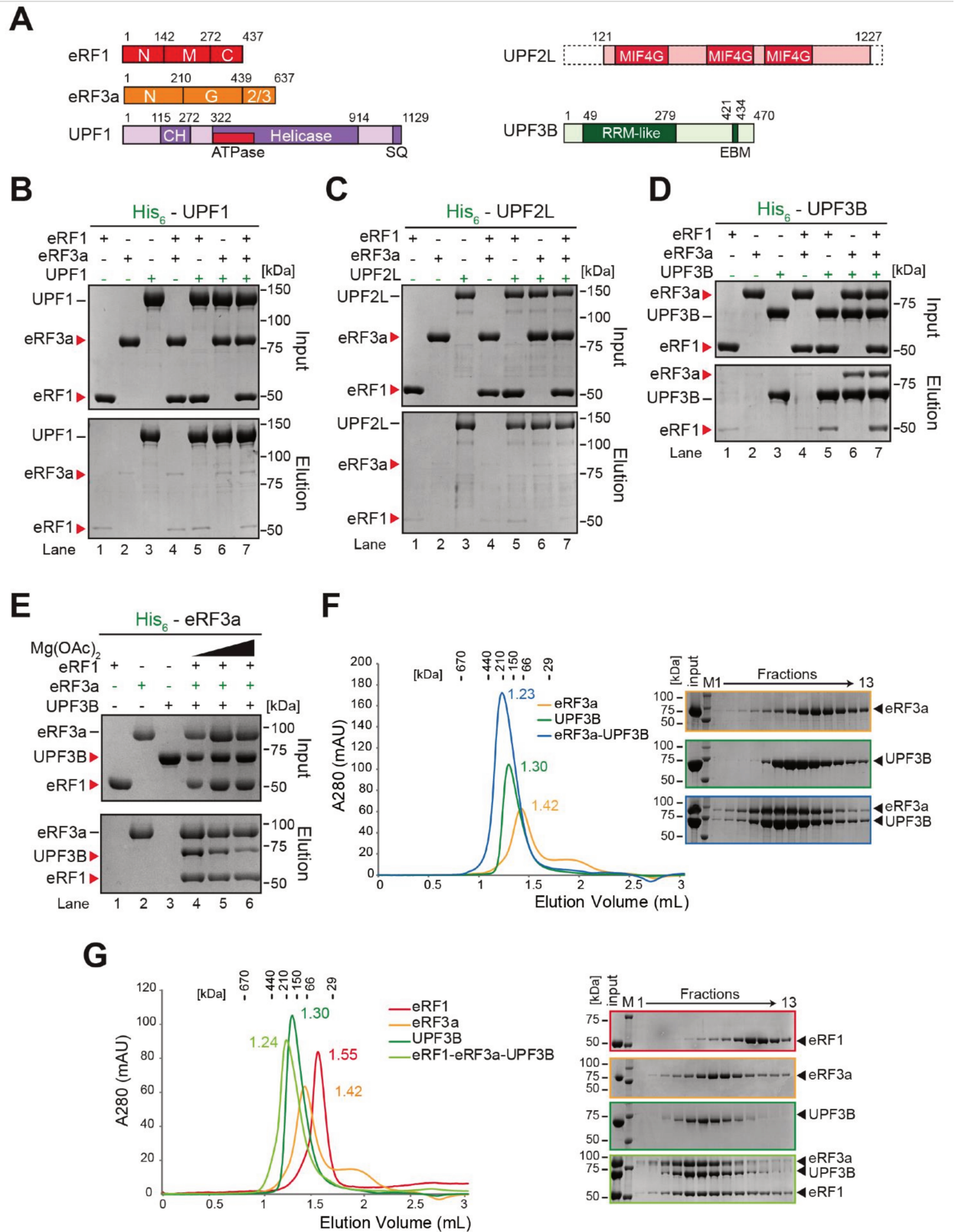


Figure 3 UPF3B forms a complex with eRF3a and eRF1.

A Schematic representation of eRFs, UPF1, UPF2L and UPF3B proteins. Domains of known function and structural motifs are indicated. N, M, C, G, CH stand for N-terminal, middle, C-

terminal, GTP-binding- and cysteine-histidine-rich domain, respectively. 2/3: domains 2 and 3. MIF4G: middle fragment of eIF4G, RRM: RNA-recognition motif, EBM: EJC-binding motif.

B In vitro pulldown of eRF1 and/or eRF3a with His-UPF1. Protein mixtures before loading onto the beads (input) or after elution (eluate) were separated by SDS-PAGE.

C Pulldown as in (B), with His-UPF2L as bait.

D Pulldown as in (B), with His-UPF3B as bait.

E Pulldown of eRF1, UPF3B, or both with His-eRF3a at 0, 2.5, or 5 mM Mg^{2+} respectively.

F Left: SEC elution profile of eRF3a (yellow), UPF3B (green), or both (blue). The elution volume (in mL) is indicated for each experiment. Column calibration was performed with globular proteins (shown above). Right: SDS-PAGE analysis of eluate fractions. M: protein molecular weight standards (kDa).

G SEC elution profile and SDS-PAGE analysis as in (F) of eRF1 (red), eRF3a (orange), UPF3B (dark green) or all three (light green). See also Fig EV3.

B-C each represent 3 independent experiments. E-G each represent 2 independent experiments.

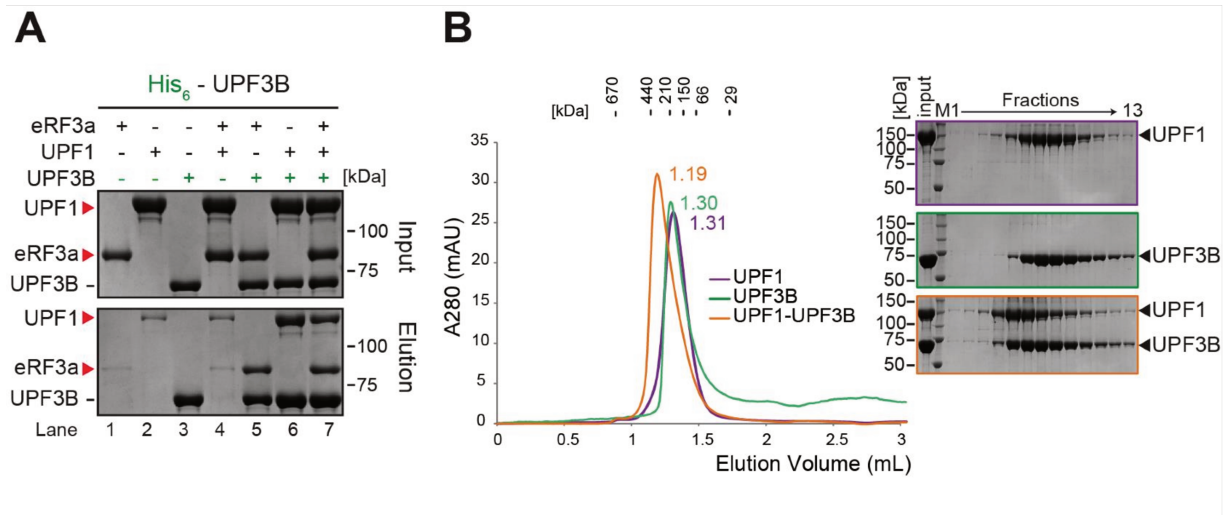


Figure 4 UPF3B can directly interact with UPF1.

A In vitro pulldown of eRF3a, UPF1, or both with His-UPF3B. Protein mixtures before loading onto the beads (input) or after elution (eluate) were separated by SDS-PAGE. Representative of 4 independent experiments.

B Left: SEC elution profile of UPF1 (purple), UPF3B (green) or both (orange). Right: SDS-PAGE analysis of eluate fractions. Representative of 2 independent experiments.

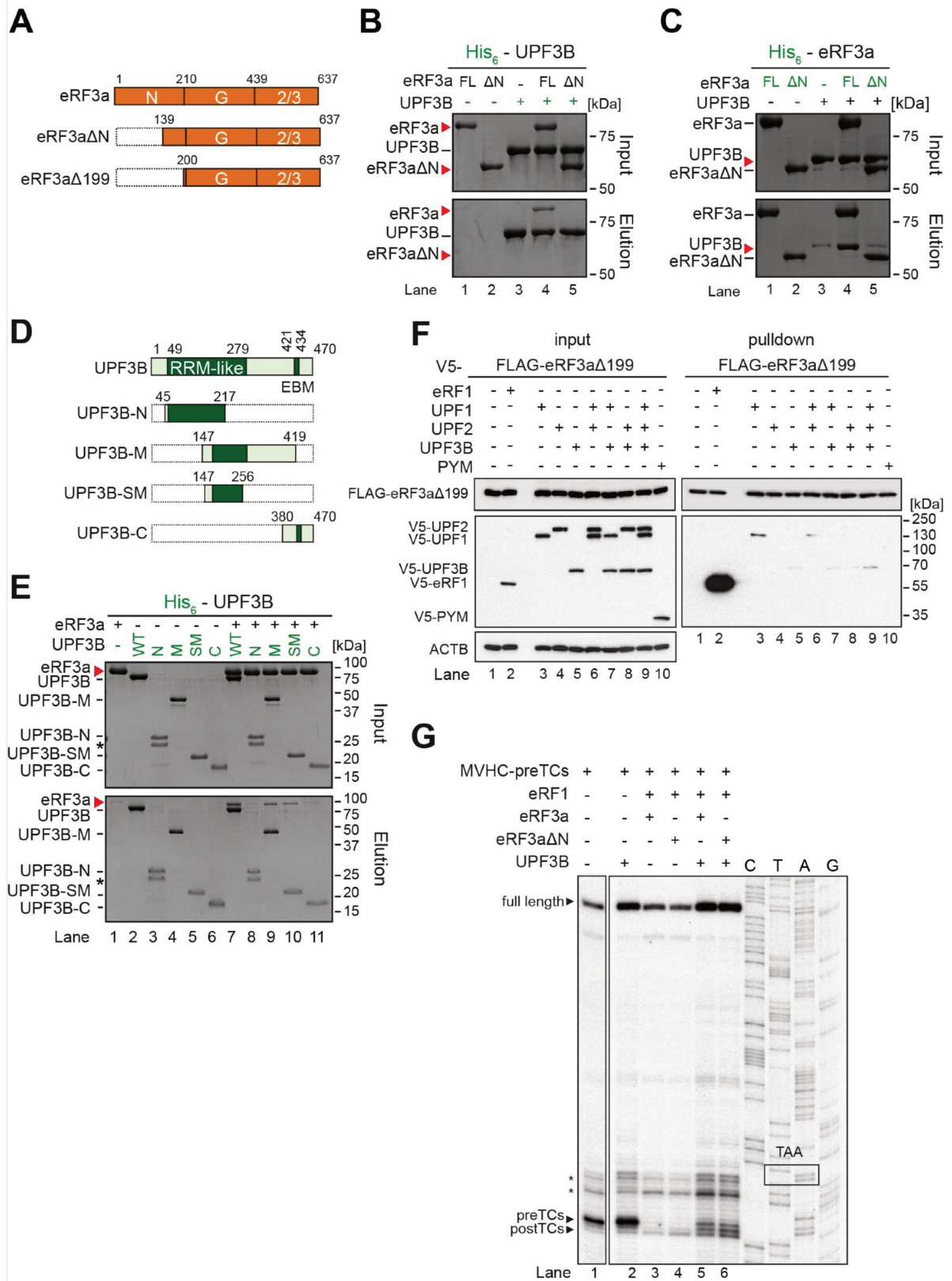


Figure 5 UPF3B interacts with the N-terminus of eRF3a.

A Schematic representation of eRF3a constructs used for this Figure. eRF3aΔN, eRF3aΔN199: eRF3a variants lacking amino acids 1-100 and 1-199, respectively.

- B In vitro pulldown as in Fig 3 of eRF3a (FL) or eRF3a Δ N (Δ N) with His-UPF3B.
- C Pulldown of UPF3B with His-eRF3a or His-eRF3a Δ N.
- D Schematic representation of UPF3B constructs.
- E Pulldown as in Fig 3 of eRF3a with His-UPF3B variants.
- F Co-IP experiment as in Fig 2 with FLAG-eRF3a Δ 199 and V5-UPF1, -UPF2L, -UPF3B, or -PYM.
- G Toe-printing analysis of ribosomal complexes obtained by incubating MVHC-preTCs with BSA or with UPF3B as indicated. Termination was completed with limiting amounts of eRF1 and either eRF3a (lanes 3,5) or eRF3a Δ N (lanes 4,6), respectively.
- B, E each represents 3 independent experiments. C, F, G each represents 2 independent experiments.

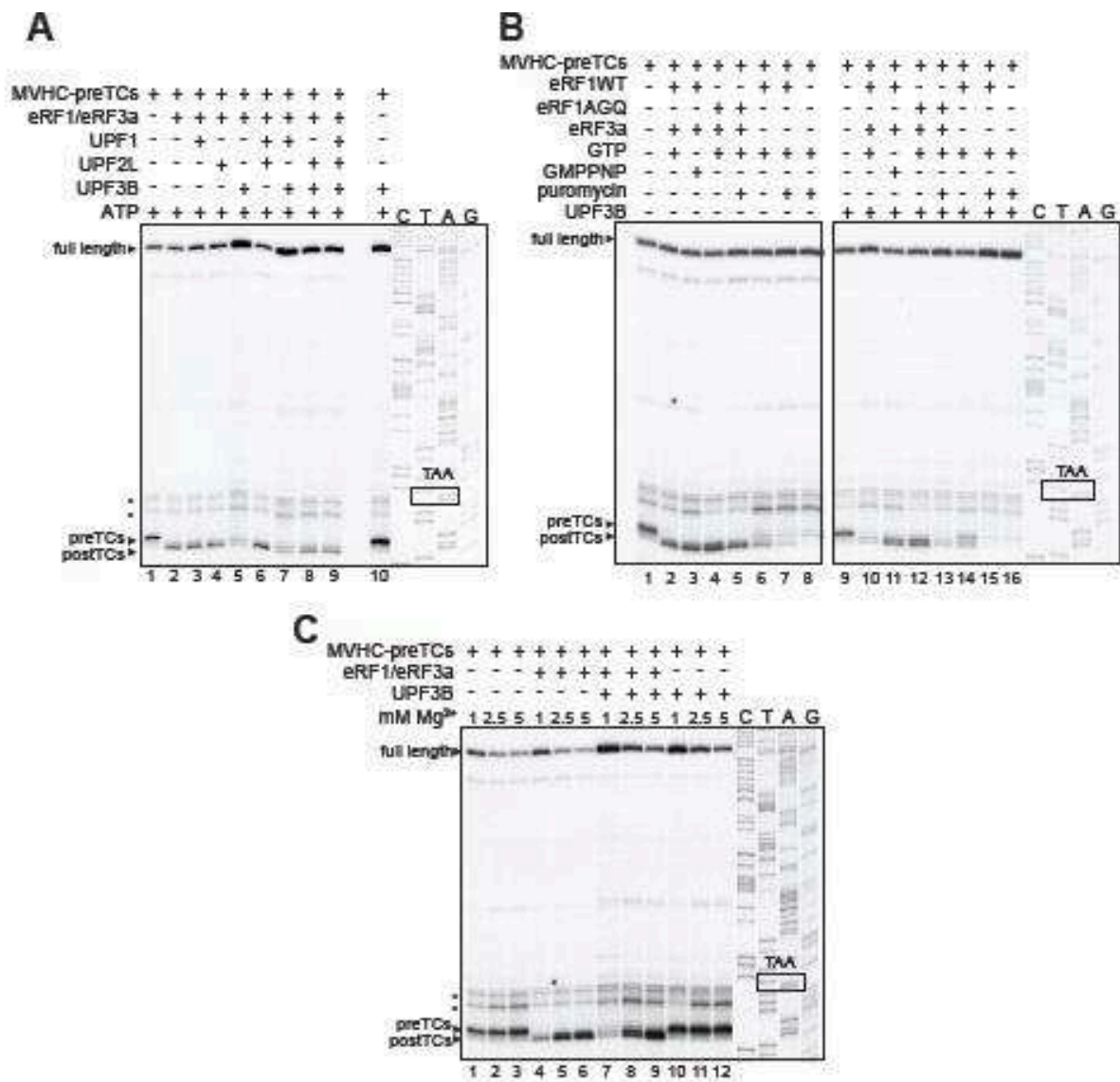


Figure 6. UPF3B dissociates postTCs

A Toeprinting analysis of ribosomal complexes obtained by incubating MVHC-preTCs with UPF1, UPF2L, UPF3B, or BSA at 1 mM free Mg²⁺ and 1 mM ATP followed by termination with saturating amounts of eRF1 and eRF3a.

B Toeprinting analysis of ribosomal complexes obtained by incubating preTCs as in (A) with UPF3B or BSA and combinations of eRF1, eRF1AGQ, eRF3a, and puromycin in the presence of GTP or GMPPNP. Gel on the left was exposed 2x longer than gel on the right. Note that puromycin-treated preTCs are relatively unstable at low Mg²⁺ (Skabkin, Skabkina et al., 2013).

C Mg²⁺-sensitivity of postTC dissociation by UPF3B. Toe-printing analysis of ribosomal complexes obtained by incubating MVHC-preTCs with BSA (lanes 1-6) or UPF3B (lanes 7-12) and at the indicated concentrations of free Mg²⁺. Termination was completed by adding eRF1 and eRF3a to the samples in lanes 4-9.

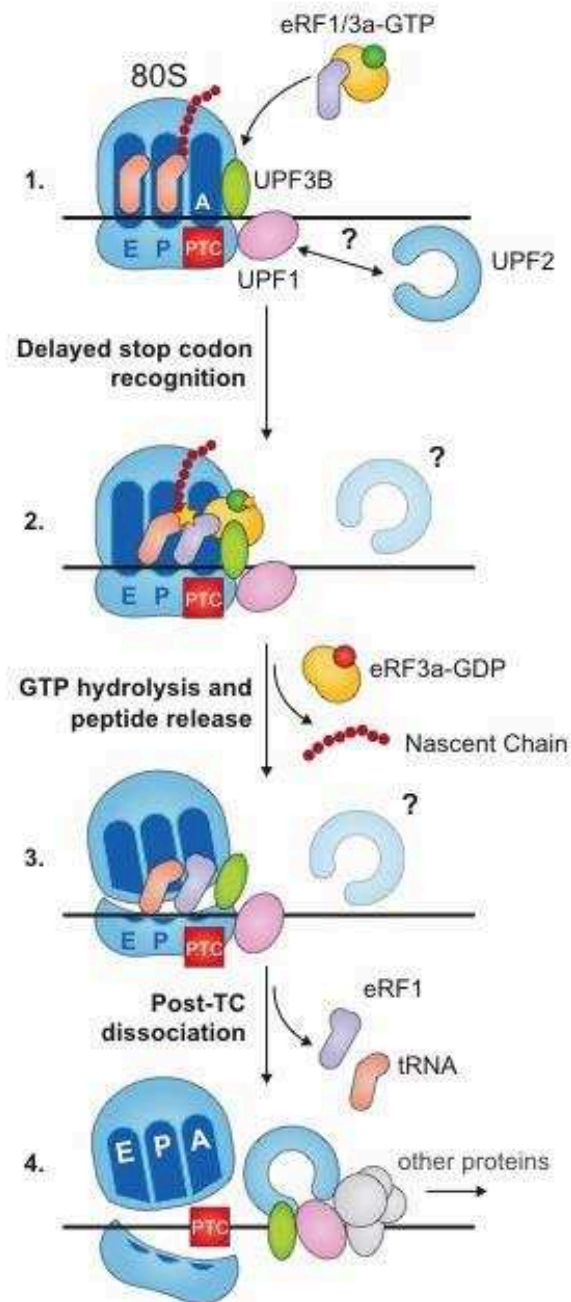


Figure 7. Model for early and late UPF3B function in translation termination

During termination at a PTC ribosome-bound UPF3B interacts the eRF1/eRF3a-GTP complex impeding efficient stop codon recognition. UPF1 bound to the 3'UTR and stimulated by UPF2 can contact the termination complex, but does not interfere with termination. After GTP hydrolysis and peptide release UPF3B destabilizes the post-termination ribosomal complex leading to its dissociation. Subsequently, UPF3B, UPF1, UPF2 and other factors activate UPF1's ATPase and helicase functions to remodel the 3' UTR mRNP and attract decay enzymes.

Expanded View Figure legends

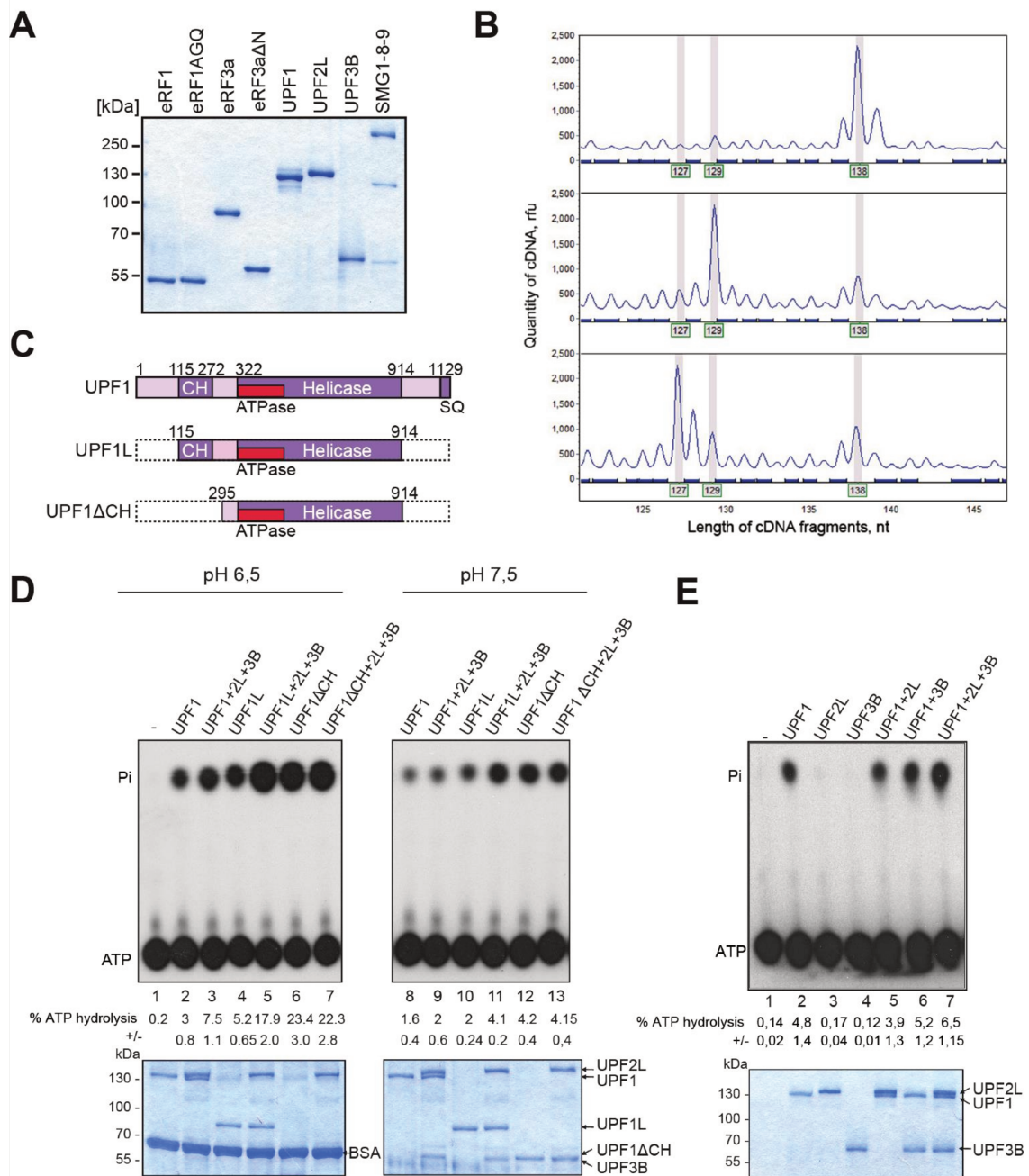


Figure EV1 Validation of the experimental system

A SDS-PAGE analysis of purified recombinant proteins used in the toe-printing experiments as indicated.

B Toe-print analysis of translation complexes prepared by the reconstituted in vitro translation system. Above: 80S initiation complex; middle: pre-termination complex (preTC); below: termination complex formed in presence of eRF1, eRF3a and GTP. Peaks at 138 nt indicate the position of the 80S initiation complex on mRNA, peaks at 129 nt indicate the position of preTC

and peaks at 127 nt correspond to the termination complex (postTC). Rfu – relative fluorescence units.

C Schematic representation of UPF1 variants used in (D).

D Thin layer chromatography (TLC) analysis of the ATPase activity of UPF1 variants in the absence or presence of UPF2L and/or UPF3B at 30°C in MES buffer (pH6.5, lanes 1-7) or translation buffer (pH7.5, lanes 8-13), respectively. 1.5 µl of the samples were spotted on the TLC plates and the residual 18.5 µl were analysed on SDS-PAGE gels for loading control (lower panels). The positions of $\gamma^{32}\text{P}$ -ATP and $\gamma^{32}\text{P}$ -Pi are indicated.

E. ATP hydrolysis experiment as in (D) at 37 °C in translation buffer. % ATP hydrolysis in C and D was calculated using a phosphoimager and displays the means \pm SEM of 4 independent experiments.

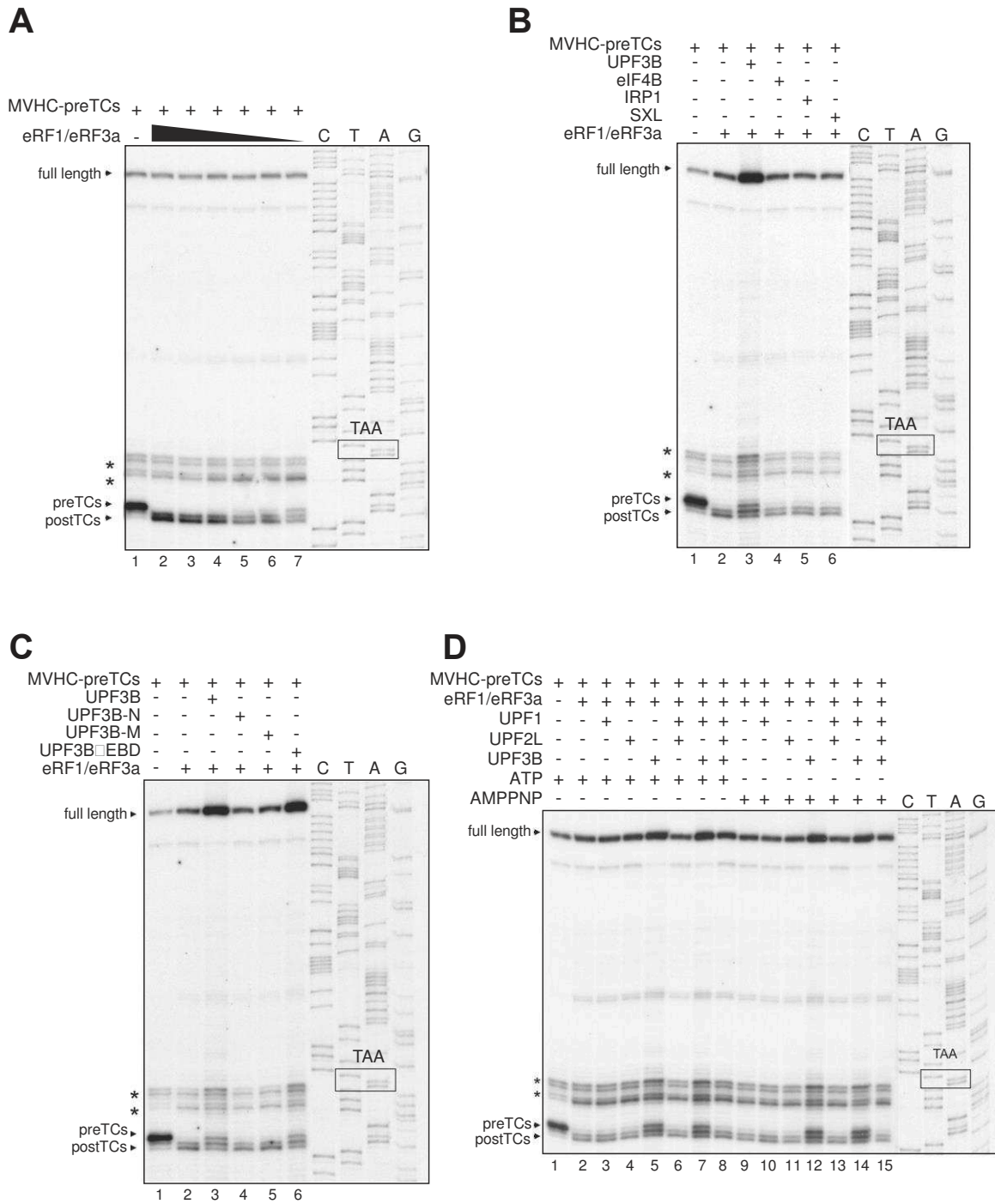


Figure EV2 Validation of the termination-delaying effect of UPF3B

A Toeprinting analysis of ribosomal complexes obtained by incubating MVHC-preTCs with decreasing amounts of eRFs. Representative example for the titration of eRF1 and eRF3a to identify concentrations slowing down the preTC-postTC transition. The amount used for the sample in lane 5 was chosen for further experiments with this batch of preTCs.

B Toeprinting analysis of ribosomal complexes obtained by incubating MVHC-preTCs with UPF3B, eIF4B, IRP1, SXL, or BSA at 1 mM free Mg^{2+} and 1mM ATP followed by termination with limiting amounts of eRF1 and eRF3a.

C Toeprinting analysis of ribosomal complexes obtained as in (B) by incubating MVHC-preTCs with UPF3B, UPF3B-N, UPF3B-M, UPF3B Δ EBD, or BSA.

D Toe-printing analysis of ribosomal complexes obtained as in Figure 1B in the presence of 1 mM ATP or AMPPNP, respectively.

A, B each represents 2 independent experiments. D represents 3 independent experiments.

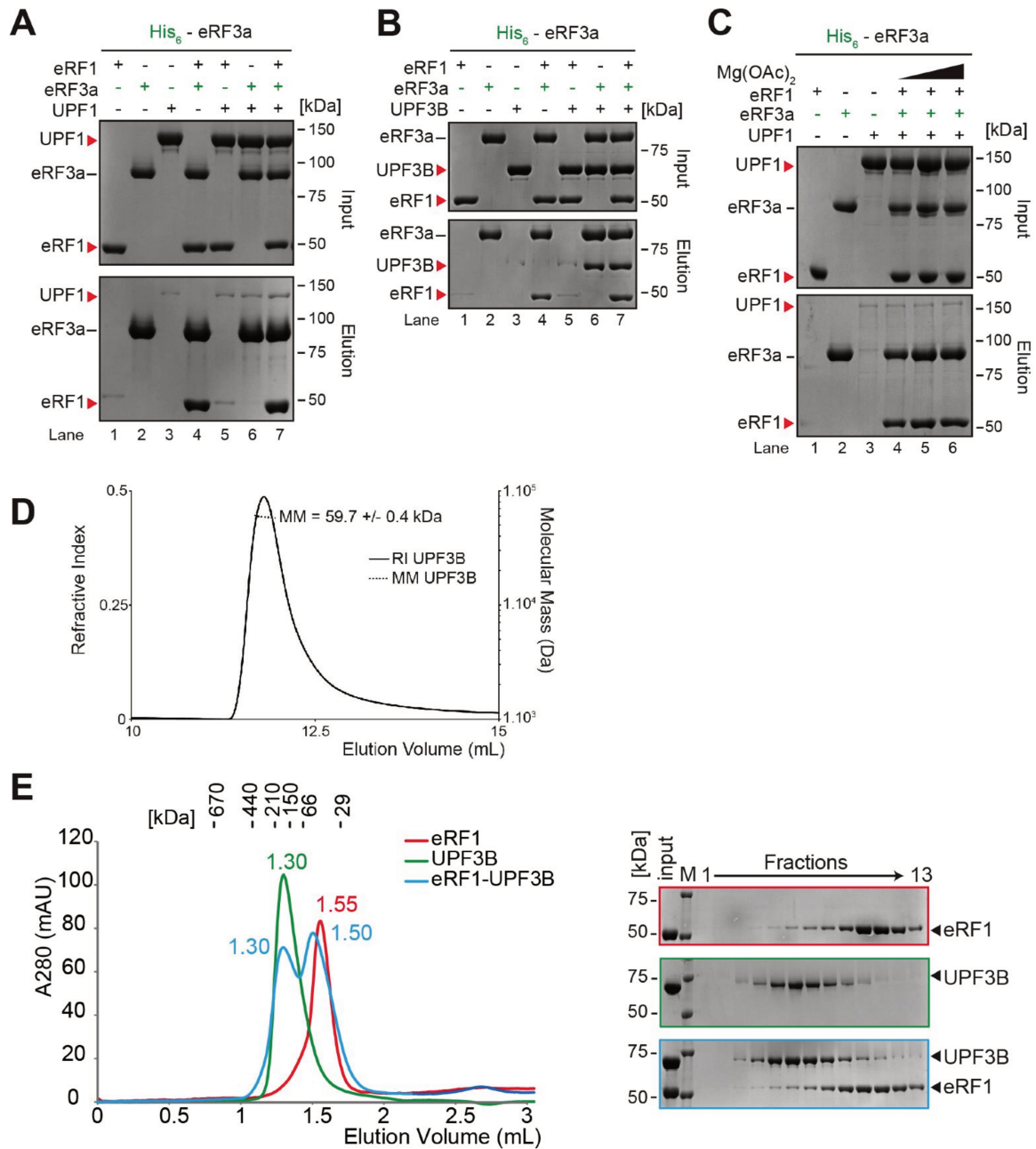


Figure EV3 Validation of UPF3B's complex formation with eRF1 and eRF3a

A In vitro pull-down of eRF1 and/or UPF1 with His-eRF3a. Protein mixtures before loading onto the beads (input) or after elution (eluate) were separated by SDS-PAGE.

B Pull-down experiment as in (A) with eRF1, UPF3B, and His-eRF3a.

C Pull-down experiment as in (B) with eRF1, UPF1, and His-eRF3a and at 0, 2.5, and 5 mM of Mg²⁺ (lanes 4-6), respectively.

D Molecular mass of UPF3B determined by size-exclusion chromatography using a Superdex 200 column combined with detection by multiangle laser light scattering and refractometry (SEC-MALLS-RI). The SEC elution profiles as monitored by refractometry (RI) are represented for UPF3B. The molecular mass (MM) of UPF3B calculated from light scattering and refractometry data is indicated.

E SEC elution profile of eRF1 (red), UPF3B (green), or both (blue). The elution volume (in mL) is indicated for each experiment. Calibration of the column was performed with globular proteins (shown above). Lower panel: SDS-PAGE analysis of eluate fractions. M: protein molecular weight standards (kDa).

A-C each represents 3 independent experiments. D, E each represents 2 independent experiments.

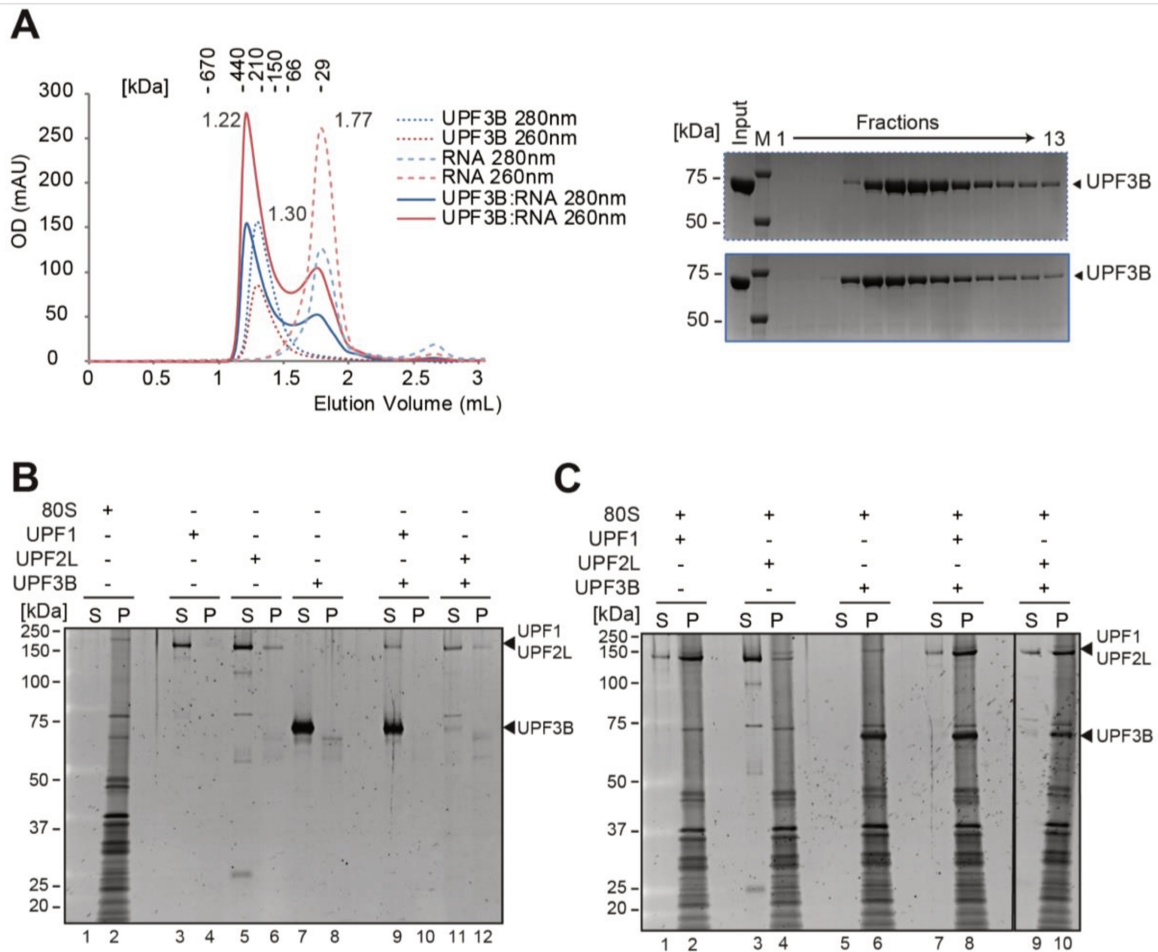


Figure EV4 UPF3B binds RNA and ribosomes

A Left: SEC elution profile of UPF3B (dotted lines), RNA (dashed lines) and the mix (solid lines). Optical density was recorded at 280 nm (blue) and at 260 nm (red). 40 μ M of UPF3B or RNA oligonucleotide (24mer) or both were loaded onto the Superdex200 column. The elution volumes are indicated next to the curves. Right: Eluate fractions of UPF3B alone (upper) and UPF3B-RNA mixes (lower) were analysed by SDS-PAGE. M: protein molecular weight standards (kDa).

B Sucrose cushion co-sedimentation analysis of UPF1, UPF2L, or UPF3B or in combinations as indicated. After ultracentrifugation, the supernatant (S) and pellet (P) fractions were analysed by SDS-PAGE.

C. Sucrose cushion co-sedimentation analysis of UPF1, UPF2L, or UPF3B as in (B) but in the presence of 80S ribosomes.

A represents 2 independent experiments. B, C each represents 4 independent experiments

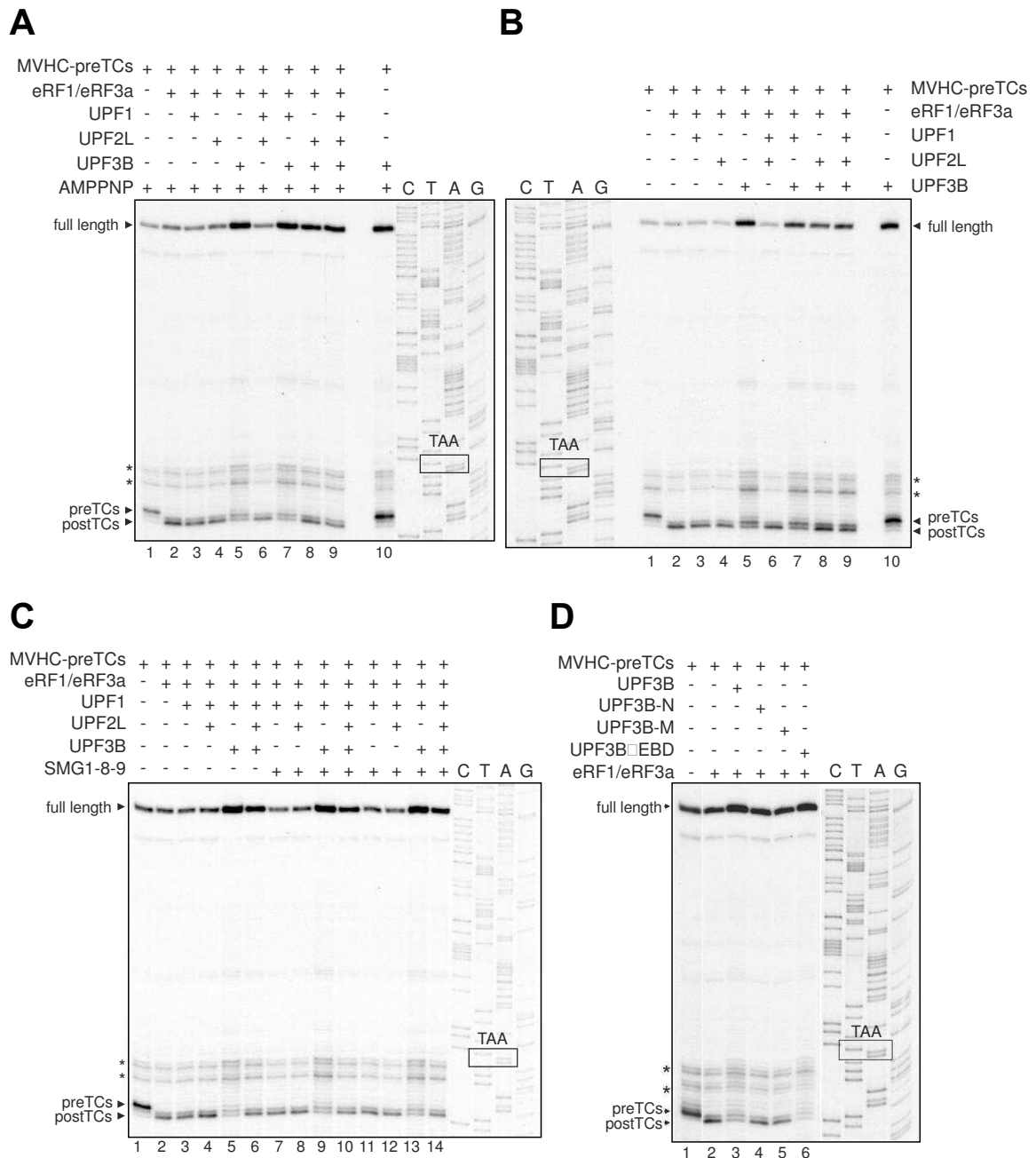


Figure EV5 UPF3B's postTC-dissolving activity is independent of ATP and SMG1-8-9 and requires both the RRM and the middle domain

A, B Toe-printing analysis of ribosomal complexes as in Figure 6A, but in the presence of 1 mM AMPPNP (A) or without adenosin nucleotide (B).

C Impact of UPF1-phosphorylation on efficient translation termination and on ribosome dissociation by UPF3B. Toe-printing analysis of ribosomal complexes obtained by incubating preTCs formed on MVHC-STOP mRNA (MVHC-preTCs) with UPF1, UPF2L, UPF3B, or BSA at 1 mM free Mg^{2+} , and 1 mM ATP. In lanes 7-10 UPF1 was incubated with SMG1-8-9 and ATP for 30 min at 37 °C either alone (lane 7) or in the presence of UPF2L, UPF3B, or both (lanes 8-

10) before preTCs were added to the mixture and again incubated for 10 min. In lanes 11-14 UPF1 was incubated with ATP and SMG1-8-9 for 30 min. Then, UPF2L and/or UPF3B were added for additional 15 min (lanes 12-14). Finally, MVHC-preTCs were added to the mixtures for 10 min followed by translation termination by eRF1 and eRF3a.

D Toeprinting analysis of ribosomal complexes obtained by incubating MVHC-preTCs with UPF3B, UPF3B-N, UPF3B-M, UPF3B Δ EBD, or BSA followed by termination with saturating amounts of eRF1 and eRF3a.

A represents 3 independent experiments. B, C each represents 2 independent experiments.

Supplementary Material and Methods

Plasmids

The pPROExHtb_eRF1 plasmid was generated by subcloning the PCR-amplified gene encoding from pQE30_eRF1 Frolova (Frolova et al., 2000) into pPROExHtb (Life Technologies) using restriction enzymes NcoI and NotI. The plasmid pET21d_UPF2L (121-1227) was generated by subcloning pPROExHtb_UPF2 (121-1227) into pET21d (EMD Biosciences) using restriction enzymes NcoI and NotI. pFastBacHtb_eRF3a was generated by subcloning the NcoI/HindIII fragment encoding full-size wildtype eRF3a from pET15b-eRF3a into pFastBacHtb (Life Technologies). Deletion constructs for pFast-BacHtb_UPF3B or pFastBacHtb_eRF3a were engineered by Self-SLIC, an insert-free SLIC reaction (Li and Elledge, 2007). Plasmids encoding human UPF1, UPF2L, UPF3A and UPF3B were generated by subcloning NcoI/NotI digested fragments from the respective pCI Neo / pcDNA vectors (Promega) into pFastBacHtb. Plasmids pCIneo-FLAG-eRF1, -eRF3a, and eRF3a variant plasmids as well as pCIneo-V5-UPF1, -UPF2, and -UPF3B plasmids for eukaryotic expression have been described (Ivanov, Gehring et al., 2008).

Protein production and purification

UPF1(115-914) and UPF1(295-914) were expressed from plasmids pET28-UPF1(115-914) and pET28a-UPF1(295-914) and purified as described (Chamieh et al., 2008). His-tagged human eRF3a, UPF1, UPF2L and UPF3B were expressed using the Multibac expression system (Fitzgerald et al., 2006). His-tagged eRF1 and UPF2L were expressed in the E. coli strain BL21-Gold(DE3) (Life Technologies). Cells were lysed in buffer A (25 mM HEPES-KOH, 10 mM imidazole, 300 mM KCl, 5 mM 2-mercaptoethanol, 5% v/v glycerol, pH 7.5) supplemented with protease inhibitor cocktail (Roche) and 0.1% NP40 for the insect cell expressed proteins. Lysed cells were centrifuged at 30,000 x g, 30 min. The supernatant was subjected to Ni-NTA affinity chromatography (QIAGEN). After removal of the His-tag with Tobacco Etch Virus (TEV) protease, proteins were further purified using a HiTrap QXL column (GE Healthcare); followed by cation exchange chromatography using a HiTrap SP/HP column (GE Healthcare) for UPF3B. UPF1, eRF1 and eRF3a were further purified by size-exclusion chromatography (SEC) using a Superdex 200 column (GE Healthcare) equilibrated with buffer B (25 mM HEPES-KOH, 300 mM KCl, 5 mM Dithiothreitol (DTT), 5% v/v glycerol, pH 7.5). The SMG1-8-9 complex was expressed in HEK-293T cells and purified via its streptavidin-binding tag and SEC as described (Deniaud et al., 2015). For in vitro termination, ATPase and in vitro phosphorylation assays all proteins used were diluted to 3 μ M in the protein storage buffer (25 mM Tris, pH 7.5, 150 mM NaCl, 1mM Mg(OAc)₂, 1 μ M ZnSO₄, 1mM DTT, 10% glycerol). Aliquots were stored at -80°C.

Pulldown assays to probe protein-protein interaction using purified proteins

All experiments were performed with 20 μ M of each protein in the final reaction volume of 20 μ L in buffer C (25 mM HEPES/KOH, 150 mM KCl, 10 mM imidazole, 0.05% Tween20, 5 mM DTT, 5% v/v glycerol, pH 7.5), if not indicated otherwise. The protein mixtures were incubated for 1 hour on ice, subsequently 20 μ L of Ni NTA agarose (QIAGEN) was added to the mix and incubated for 1 hour on ice. The reaction mixtures were washed 4 times with 200 μ L of buffer C, and proteins were eluted using buffer C supplemented with 200 mM imidazole. 8 μ L of SDS loading dye were mixed with either 2 μ L of input reactions or 20 μ L for the eluted complexes. 5 μ L of the input sample and 10 μ L of the elution sample were loaded onto a 10 or 12% SDS-PAGE gel.

Size Exclusion Chromatography

Size exclusion chromatography (SEC) was performed under physiological conditions similar to those used for the reconstitution of the UPF1-UPF2-UPF3-EJC complex (Melero et al., 2012) and for the purification of the SMG1-8-9 complex (Deniaud et al., 2015). Briefly, for SEC, 40 μ M of each protein was added in a final reaction volume of 60 μ L in buffer D (25 mM HEPES/KOH, 200 mM KCl, 3 mM Mg(OAc)₂, 0.05% Tween20, 5 mM DTT, 5% v/v glycerol, pH 7.5). The protein mixtures were incubated for 1 hour on ice before loading onto a Superdex 200 PC3.2/30 column (AEKTA micro system, GE Healthcare). 10 μ L of each elution fraction was loaded onto a 10% SDS-PAGE gel. For the UPF3B-RNA interaction experiment, 40 μ M of a 24-nucleotide long RNA oligonucleotide (5'-CCCAGGTGCTGCCGTCAGCTCAGGG-3') was mixed with 40 μ M UPF3B.

Size Exclusion Chromatography coupled to Multiple Angle Laser Light Scattering (SEC-MALLS)

SEC-MALLS of UPF3B was performed with a Superdex-200 increase column (GE Healthcare) equilibrated with 25 mM HEPES-KOH, 300 mM KCl, 5 mM DTT, 5% v/v glycerol, pH 7.5. The column was calibrated with globular standard proteins. The experiments were performed at 20°C with a flowrate of 0.5 mL.min⁻¹. A DAWN-HELEOS II detector (Wyatt Technology Corp.) with a laser emitting at 690 nm was used for detection. The protein concentration was determined on-line by differential refractive index measurements, using an Optilab T-rEX detector (Wyatt Technology Corp.) and a refractive index increment, dn/dc, of 0.185 mL.g⁻¹. The weight-averaged molar masses were calculated using the ASTRA software (Wyatt Technology Corp.).

Ribosome binding experiments

For co-sedimentation experiments, 5 pmol of rabbit 80S ribosomes were mixed with a ten-fold molar excess of UPF1, UPF2L, and UPF3B in 20 μ L of 25 mM HEPES-KOH pH 7.5, 100 mM KOAc, 2.5 mM Mg(OAc)₂, 2 mM DTT and incubated for 1 hour on ice. Subsequently, the reaction mixtures were applied on a sucrose cushion (same buffer containing 250 mM KOAc and 750 mM sucrose) and spun for 3 h at 55,000 x g at 4°C using a TLA-55 rotor (Beckman). Supernatant and pellet fractions were analysed by SDS-PAGE followed by SYPRO Ruby (Thermo Scientific) staining.

ATPase assays

ATPase assays were performed in a total volume of 20 μ L essentially as described (Chamieh et al., 2008). Briefly, 1.5 pmol UPF1 either alone or in presence of 3 pmol UPF2L and/or 3 pmol UPF3B were mixed with 4 μ L 5x MES buffer (250 mM MES pH 6.5, 250 mM KOAc, 25 mM Mg(OAc)₂, 10 mM DTT, 0.5 mg/mL BSA) or 5 x translation buffer (100 mM Tris pH 7.5, 500 mM KCl, 12.5 mM MgCl₂, 10 mM DTT, 1.25 mM spermidine), 2 μ L Poly(U) RNA (Sigma, 2 mg/mL in H₂O) and H₂O to a final volume of 16 μ L. When variable protein compositions were tested, the total volume of proteins added was adjusted to equal using protein storage buffer. The reaction was started by adding 3.9 μ L 10 mM ATP and 0.1 μ L γ ³²P-ATP (Hartmann Analytic, 3000Ci/mmol). Reactions proceeded for 1 h at 30 or 37°C. 1.5 μ L per sample were spotted on PEI cellulose TLC plates (Merck) that had been pre-run in water. Plates were developed in 0.4M LiCl, 0.8M acetic acid, dried and visualized by autoradiography.

In vitro phosphorylation

1.2 pmol UPF1 either alone or in presence of various combinations of 2.4 pmol of UPF2L, UPF3B, eRF1/eRF3a and 40 fmol of SMG1-8-9 were mixed with 4 μ L 5 x translation buffer and H₂O to a final volume of 16 μ L. When variable protein compositions were tested, the total volume of proteins added was adjusted to equal using protein storage buffer. The reaction was started by adding 2.5 μ L 10 mM ATP and 1.5 μ L γ ³²P-ATP and was allowed to proceed for 30 min at 37°C. Samples were separated by SDS-PAGE and visualized by autoradiography.

Cell culture and transfections

HeLa cells were grown in DMEM and transfected in 10 cm plates using JetPrime transfection reagent (Polyplus), 1 – 4.5 μ g of the test plasmids, and 0.4 μ g of a YFP-plasmid. Empty pGEM3z vector (Promega) was used to adjust total amounts of transfected DNA.

Co-immunoprecipitation assays from transfected cells

24 hours after transfection, cells were harvested in 400 μL /10 cm plate of buffer E (20 mM Tris pH 7.5, 150 mM KCl, 0.1% NP40) supplemented with 0.3 mM MgCl_2 and EDTA-free complete (Sigma-Aldrich) and lysed 30 min on ice. Magnetic M2 anti-FLAG beads (Sigma-Aldrich) were used to immunoprecipitate FLAG-tagged complexes from RNaseA-treated (30 $\mu\text{g}/\text{mL}$) cell lysates after 1 h incubation with the beads at 4°C. Beads were washed 8 times with buffer E supplemented with 0.6 mM MgCl_2 . Tubes were changed before the last wash. FLAG-complexes were eluted with 25 μL 0.1M glycine (pH 3.0) added to 6 μL 5 x loading buffer and neutralized with 1.5 μL 1M Tris pH 7.5. 6 μL of the samples were loaded for anti-FLAG detection and 20 μL for anti-V5 detection, separated by SDS-PAGE and analysed by immunoblotting using anti-FLAG and anti-V5- antibodies (both Sigma-Aldrich).

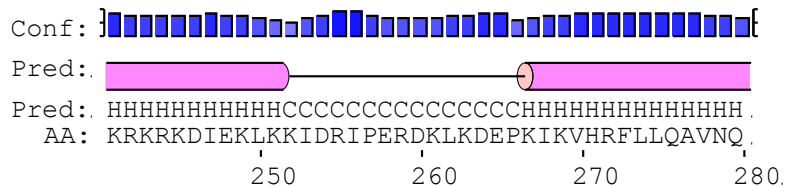
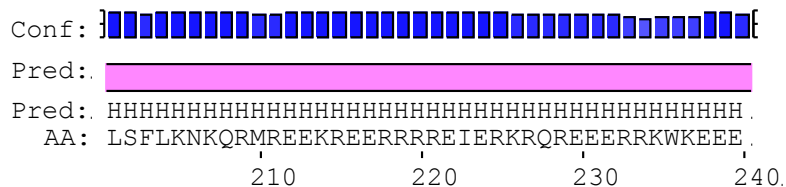
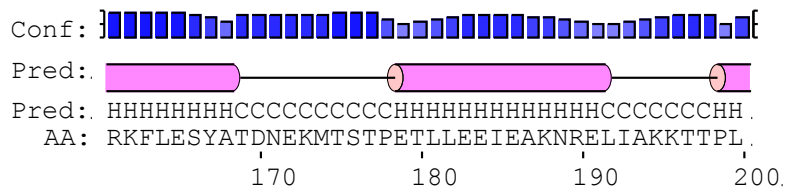
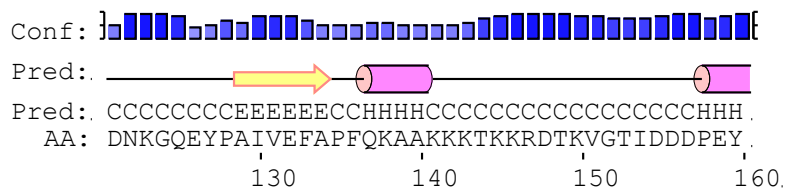
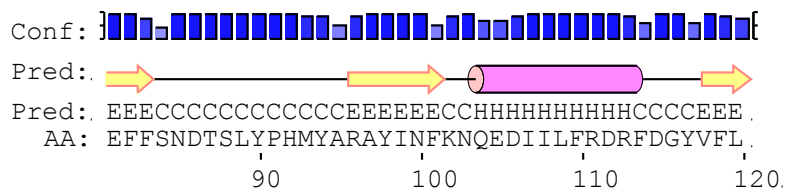
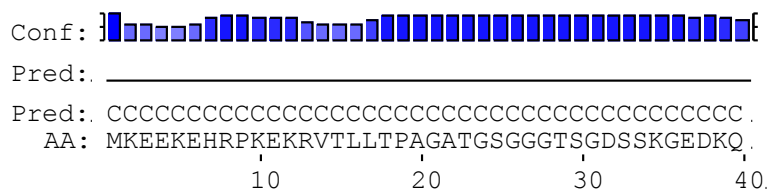
Pre-termination complex assembly and purification

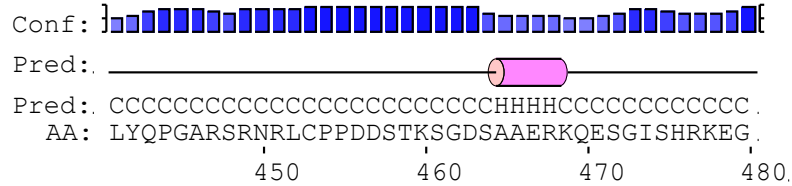
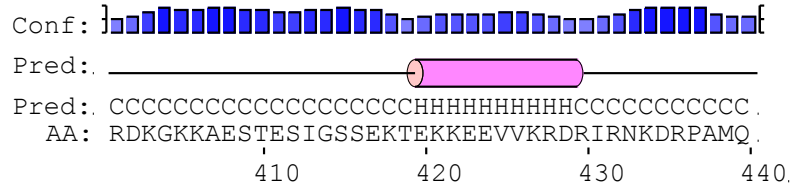
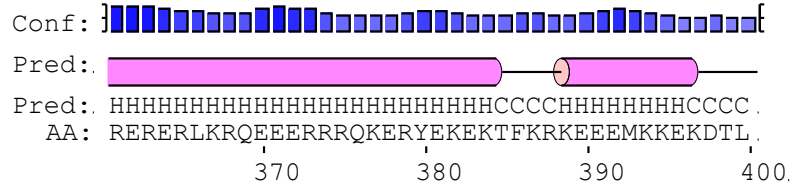
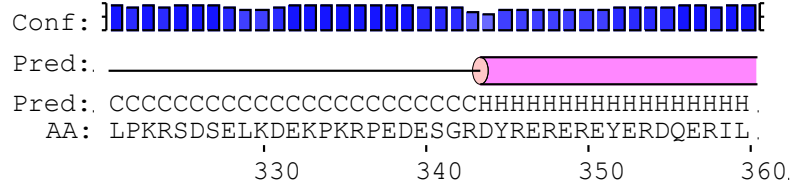
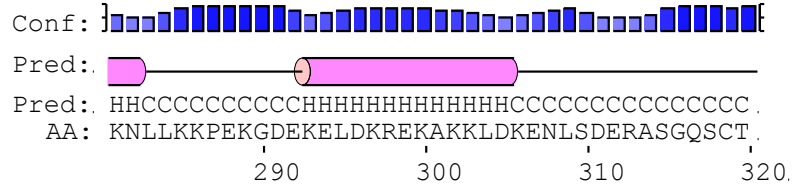
Pre-termination complexes (preTC) were assembled as described (Alkalaeva et al., 2006) with the following modifications: The translation reaction performed in translation buffer D (20 mM Tris-HCl, pH 7.5, 50 mM KOAc, 1.3 mM free MgCl_2 , 2 mM DTT, 0.25 mM spermidine) supplemented with 200 U RNase inhibitor (RiboLock, Fermentas), 1 mM ATP, 0.2 mM GTP, 35 pmol of MVHC-stop mRNA, 35 pmol initiator-tRNA_t (acylated with [³⁵S]-methionine for peptide release assays), 75 μg total tRNA (acylated with individual amino acids), 50 pmol purified human ribosomal subunits (40S and 60S), 100 pmol eIF2, 50 pmol eIF3, 80 pmol eIF4G Δ , eIF4A, eIF4B, eIF1, eIF1A, eIF5, eIF5B Δ each, 200 pmol eEF1H and 50 pmol eEF2 in the volume of 500 μL . The reaction mix was incubated for 40 min at 37°C. Subsequently, the reaction mix was loaded onto a 10–30% w/w linear sucrose density gradient (SDG) prepared in buffer D with 5 mM MgCl_2 and centrifuged for 115 min at 4°C at 50 000 rpm using a Beckman SW60 rotor. The fractions corresponding to preTC complexes


9 Appendix

(A) Secondary structure prediction of human UPF3B

(B) Multiple species alignment of UPF3

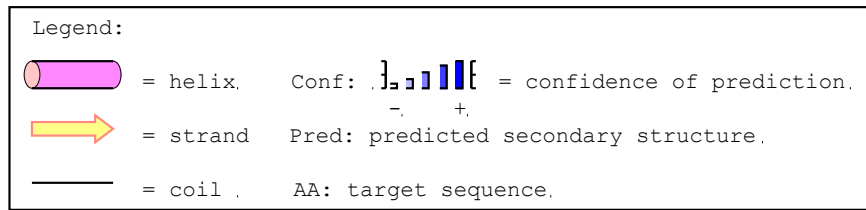




Conf: 

Pred: .

Pred: .CCC
 AA: .GEE.



sp|Q9BZI7-2|REN3B_HUMAN

1 10 20 30
sp|Q9BZI7-2|REN3B_HUMANMKEEK.E..HRP.....KEKR...VTLTTPAGATG..SGGGTS
sp|Q9H1J1|REN3A_HUMANMRSEKEG..AGGLRAAAVAARGPSGREKLSA...LEVQFHRDSQQQEAETPPT
tr|Q3ULJ3|UPF3_MOUSEMRSEEG..AGGLGAALAAARGPSWREKLS...SETHCRRESPRKESAAPPA
tr|Q7SXF0|UPF3B_DANREMKEDKEN..TRP.....REKK...VEIKC.....
sp|BOS733|REN3A_DANREMRSEKEQ..RTGS.....REGS...VEIQFRDC.....
tr|Q9W1H3|UPF3_DROMEMAETF.....E
sp|Q10267|UPF3_SCHPO
sp|P48412|UPF3_YEAST MSNVAGELKNSEGGKKGRGNRYHNKNRGKSKNETVDPKKNENKVNNAATNATHNNSKGRNN

sp|Q9BZI7-2|REN3B_HUMAN

alpha1
40 50 60 70
sp|Q9BZI7-2|REN3B_HUMAN GDS....SKGEDKQDRNKKKKELSKVVIRRLPPFLTKKQLQELHLPF.....
sp|Q9H1J1|REN3A_HUMAN SSS....GCGGAGKPREKRTALS KVVIRRLPPGLTKKQLLEQLRPL.....
tr|Q3ULJ3|UPF3_MOUSE PT....LSESGAGKPREKRTALS KVVIRRLPPGLTKKQLLEQLRPL.....
tr|Q7SXF0|UPF3_MOUSEDENDKQEKPCREKRTALS KVVIRRLPPFLTKKEDLEQLRPL.....
sp|BOS733|REN3A_DANREDNAAVNPKHKKKELSKVVIRRLPPSLSKDQLQELHLPF.....
tr|Q9W1H3|UPF3_DROME PKE....KSKASRRKDKKDTNQIVKIVMRHLPPMTMTAQLDQVGP.....
sp|Q10267|UPF3_SCHPOMAPDLSKRLPC KLVLFNLPFLPEQVFLQSIINSF.....
sp|P48412|UPF3_YEAST NKRRNREYYNKRKARLGLKSTENEGFKLVIRLPPNLTADFEFFAILRDNNDGDKQDIIQ

sp|Q9BZI7-2|REN3B_HUMAN

80 90 100 110 120
sp|Q9BZI7-2|REN3B_HUMAN ...PEHDYFEFFS..NDLSIYPHMYARAYINFKN..QEDIIIFRDRFDGYVFDLNKQGEY
sp|Q9H1J1|REN3A_HUMAN ...PAHDYFEFFA..ADLSIYPHLYSRAYNFRN..PDDIILFRDRFDGYIFLDSKGLLEY
tr|Q3ULJ3|UPF3_MOUSE ...PAHDYFEVVA..ADLSIYPHLYSRAYNFRN..PDDIILFRDRFDGYIFLDSKGLLEY
tr|Q7SXF0|UPF3_MOUSE ...PELDYFEFFS..NDLSIYPHLYSRAYNFRN..QDDIVLFRDRFDGYVFDLNKQGEY
sp|BOS733|REN3A_DANRE ...PSFDYFEFFP..ADQSIYPHLYSRAYNFRN..PDDIIFRDRFDGYVFDLNKQGEY
tr|Q9W1H3|UPF3_DROME ...PENDSYCYCK..ADWSLQGEATCRAIDMSSKDIGEVVQFRDRFDGYVFDHKKGEY
sp|Q10267|UPF3_SCHPO ...LPHVWHRFSSKSKATVGTSELLSFAYLKFQS..ATAVQEFFRVYQGHFTIDKKNNTY
sp|P48412|UPF3_YEAST GKLYSDFCFEGHYSKVFENKSTYSRCNLEFDN..LSDLERCANFIRKCKFDLNKNDIT

sp|Q9BZI7-2|REN3B_HUMAN

130 140 150 160 170 180
sp|Q9BZI7-2|REN3B_HUMAN PAIVEFAPFQKAAKKTKRDKVGTIDDDPEYRKFLESYATDNKMTSTPET..LLEEI
sp|Q9H1J1|REN3A_HUMAN PAVVEFAPFQKIAKKLKRDAAKTGSIEDDPEYKRFLETTCYVEEKTSA NPET..LLGEM
tr|Q3ULJ3|UPF3_MOUSE PAVVEFAPFQKIAKKLKRDAAKTGSIEDDPEYKRFLETTCYVEEKTSA NPET..LLGEI
tr|Q7SXF0|UPF3_MOUSE PAIVEFAPFQKVAKKSRRKDAKSTGIDDDADYKRFLEFYNGDEEKS SPNPET..LLEEI
sp|BOS733|REN3A_DANRE PAVVEFAPFQKVSRRKDAKAGTIEEDPEYRFFLENYSCDEEKS MANPET..LLGEI
tr|Q9W1H3|UPF3_DROME MAIVEYAPFQCFLLKRNDDSKVNTIESEPHYQEFKRLAEREASRMDGV..KIIDF
tr|Q10267|UPF3_SCHPO RAIVTIAPFYQKIPPSKVKADSLDLSGSLEQDPKQEFKVVQRESYSQ..TASND..VI...
sp|P48412|UPF3_YEAST IPDMKLSYVKKFTQTSKDAALVGTIEEDPEYKRFLENSMKQLNEDEYSFQDFSVLKSIL

sp|Q9BZI7-2|REN3B_HUMAN

190 200 210 220 230
sp|Q9BZI7-2|REN3B_HUMAN EAK.....NRELIARKTTPLLFLYKKN...KQRMREEKREERRRREIEKRRQRBEERRK
sp|Q9H1J1|REN3A_HUMAN EAK.....NRELIARRTTPLLFLYKKNRKLKQRIREEKREERRRRELEKRRLRBEERKR
tr|Q3ULJ3|UPF3_MOUSE EAK.....NRELIARRTTPLLFLYKKNRKLKQRLREEKREERRRRELEKRRLRBEERKR
tr|Q7SXF0|UPF3_MOUSE EAK.....NRELIARKTTPLLFLYKKN...KQRIREEKREERRRRELEKRRLRBEERKR
sp|BOS733|REN3A_DANRE EAK.....NRELIARKTTPLLFLYKKNRKLKQRIREEKREERRRRELEKRRLRBEERKR
tr|Q9W1H3|UPF3_DROME NFE.....RTEEKVKSSTPLLYLANKKK...RREARRRREKRRKREEQK...
sp|Q10267|UPF3_SCHPOEKLQTSSTPLLYLANEKKNNAVVEKGSK..PSKKS VKAKKLR LAEKPA
sp|P48412|UPF3_YEAST EKFEFSKSIENKILAE RTERVITELVGTGDKVKKNKN...K KKNKNAKKKFKEEEA SA

sp|Q9BZI7-2|REN3B_HUMAN

240 250 260 270 280
sp|Q9BZI7-2|REN3B_HUMAN WKEEE..KRRKRDIEKLLKIDRIPERDK...LKDEPKTKLLKKEPKG.DEKELDRRE.KA.
sp|Q9H1J1|REN3A_HUMAN RREEE..RCKKKEETDKQKKA.....EKEVRIKLLKKEPKG.EEPTTEKPKERGG.
tr|Q3ULJ3|UPF3_MOUSE RREED..RCKRKEAERH.KRA.....EKDVRIKLLKKEETG.EEVATEKPKERGG.
tr|Q7SXF0|UPF3_MOUSE WREED..RRKKEAEKLLKVEKASEKDKDQHKDEQPKIKLLRKEPEKA.DDGEAEKPKDKP.
sp|BOS733|REN3A_DANRE RREEE..RQKRKEAEKQKKS.....EKEIKIKLLKKECDR.DD VDSRLKDKG.
tr|Q9W1H3|UPF3_DROMELL.....RLAAQSD.....ASKLKEAEGGGG.GDTKPKAKKD.
sp|Q10267|UPF3_SCHPO SNNSK...AGKSSQESKKS KAPA.....ESAAAVIKEDKVVDRKKS KKTTP.
sp|P48412|UPF3_YEAST KIPKKRNRGKRRKRENRKSTISK.....TKNSNVVITIEEA..GKEV LKQRRK KML

sp|Q9BZI7-2|REN3B_HUMAN

290 300 310 320 330 340
sp|Q9BZI7-2|REN3B_HUMAN ..KLLDKENLSDERASGQSTLPKRSDSELKDEKPKRPEDESGRDYREREREY...R
sp|Q9H1J1|REN3A_HUMAN ..EEIDTGGGKQESCAGAVVKARPMEG.SLEEPQETSHSGSDKHEHRDVRSQE...
tr|Q3ULJ3|UPF3_MOUSE ..EAVGAGDEKQEDRLVA...SQPET...AGERLQDTSDEKPEPDKRSR...
tr|Q7SXF0|UPF3_MOUSE ..KKQDRERQKEDRPSGG..DLKKRQNGEHREKGGKPEDVGHKEVDRDGERE...R
sp|BOS733|REN3A_DANRE ..DSGETEKNRWE..KPGHTKSKD...SKDNRSQMENDKEQREHGRR...
tr|Q9W1H3|UPF3_DROME ..VKD.....PQSSGS.....QANDAKASRSKRRTERDQRREEHEQRKLVKR
sp|Q10267|UPF3_SCHPO ..VSNSTASQA.....SENASDKKTKEKKS...
sp|P48412|UPF3_YEAST IQEKLKINSNSQPQSSSAQ.T..QPS.....FQP...KLNLFVPRVKILHR

sp|Q9BZI7-2|REN3B_HUMAN 350 360

sp|Q9BZI7-2|REN3B_HUMAN D QERILRERERLRQEEERRRQEKERY

sp|Q9H1J1|REN3A_HUMAN QESEAQRVYHVDGRRHRRAHH

tr|Q3ULJ3|UPF3_MOUSE KDPEYSRCHPDTCKHSSSHS

tr|Q7SXF0|UPF3_DANRE DR DRERERRQKEKERIRRQDEERRRRREHQ

sp|B0S733|REN3A_DANRE QRDKDHRGRDEERKRQRHHY

tr|Q9WLH3|UPF3_DROME DKKKDDGQKQDKQDKQDKKQKPKSSGKQNKNSKSM DIVILKKANKPESNESLDVPSTSNAA

sp|Q10267|UPF3_SCHPO SGKQKIASKKKDQLTTDNNV

sp|P48412|UPF3_YEAST DDTKK

sp|Q9BZI7-2|REN3B_HUMAN 370 380 390 400

sp|Q9BZI7-2|REN3B_HUMAN EKEKTFKRKEEMKKKKDTLRRDKGKKAESTE . SIGS SEK

sp|Q9H1J1|REN3A_HUMAN EPERLSRSEDEQRWVGKGPQDRGKKGSDS . GAPGEAMERLGR

tr|Q3ULJ3|UPF3_MOUSE EFARFSRNEDEAKWVGKGFQDRGKKGQDG SVPMVAERSGK

tr|Q7SXF0|UPF3_DANRE DGENTYRKREEEGKKDKKERVWKKRKNEHTGE . SSGSARPEKSSR

sp|B0S733|REN3A_DANRE EFDKFMRR . KEETKWKGGYQDRAKKDQHHGYSYCPETGDKLKG

tr|Q9WLH3|UPF3_DROME EASKEKPATENTETPEAAVKVFTPAARGGKKEKRTGADKQPAGSAH ETAAE

sp|Q10267|UPF3_SCHPO

sp|P48412|UPF3_YEAST

sp|Q9BZI7-2|REN3B_HUMAN 410 420 430 440 450 460

sp|Q9BZI7-2|REN3B_HUMAN TEKKEEVVKRDRIIRNKKDRPAMQLYQP GARSNRLCPPDDSTKSGDSAAERKQESGISH

sp|Q9H1J1|REN3A_HUMAN AQRCDSPAPRKERLANKKDRPALQLYD PGARFRARECGNRRIC KAE

tr|Q3ULJ3|UPF3_MOUSE EHKEYDSLGP RKDRLGHKAQ

tr|Q7SXF0|UPF3_DANRE DSKKEESARKDRIIRNKKDRPAIQLYQP GSRNRTRGGGGGGTGGDGPAAEKRAEREAKK

sp|B0S733|REN3A_DANRE ED REDMGSRKERIRNKKDRPAMQLYQP GARNRKRMSGNKTFDFPPI SPEHAGEHCYKT

tr|Q9WLH3|UPF3_DROME AIKAAQFRASEERRIIRNKKDRPSTAIYQPKARIRASDEL PQAGGKDGSDGEASVVEEKTS

sp|Q10267|UPF3_SCHPO

sp|P48412|UPF3_YEAST

sp|Q9BZI7-2|REN3B_HUMAN 470

sp|Q9BZI7-2|REN3B_HUMAN RKEGGEE

sp|Q9H1J1|REN3A_HUMAN GSGTGPEKREEAE

tr|Q3ULJ3|UPF3_MOUSE

tr|Q7SXF0|UPF3_DANRE NQEKGAE

sp|B0S733|REN3A_DANRE VIGTGSEKSADE

tr|Q9WLH3|UPF3_DROME KRNRKRNRRNKPKPKVKCELETRRFSSKSSSSTSVK

sp|Q10267|UPF3_SCHPO

sp|P48412|UPF3_YEAST

10 Acknowledgments

This journey would not have been possible and completed with the support of numerous people. I am very thankful to every present and past members of EMBL, Grenoble who have helped me in making wonderful memories.

I would like to thank my supervisor Christiane Scahffitzel for giving me the opportunity to be a part of the project and for providing me with great scientific environment and for the guidance and the support and the discussions that have molded me to become scientifically strong.

I would like to thank my TAC members: Stephen Cusack, John Briggs and Carlo Petosa for their input, advice and motivation during the past four years. Especially Stephen for adopting me into his lab and being supportive, patient, and believing in me.

I would like to thank my jury members: Bertrand Seraphin, Robbie J Loewith, Uwe Schaltner and Stephen Cusack for taking their time to evaluate my thesis.

I am very grateful our collaborator Elena Alkaleva (Engelhardt Institute of Molecular Biology, Moscow) for her great support on the in vitro translation system and for the numerous the discussions on the various projects. I would also like to thank our collabartors on the UPF3B project: Gabriele Neu-Yilik, Beate Amthor, Matthias Hentze and Andreas Kulozik (MMU, Heidelberg).

I would like to thank various platforms and facilities at EMBL, Grenoble for a great support. Especially the IBS EM facility and Wim Hagen at EMBL, Heidelberg. Mani for freezing the grids, data collection and helping me to get started the microscope and data analysis.

I would like to thank everyone who supported me during this period. Etienne, for all the fun times in the lab, scientific discussions and as a great team member. Karine and Boris for the immense help in the various projects. Aurelien for helping me to get started with the SMG1C project. Petra, Wiebke, Taiana and Isai for the gal support and for always being there for me scientifically and emotionally. Matze for getting me started with crystallography. Alice, Emiko, Fred, Patricia, Irina, Catarina, Erika, Jesus, Guillaume, Francesco, Sonia, Kapil, Sarah, Mathieu, Jelger, Alex, Kyle, Esther, Paul, Maxime, and Greg who have helped me at various stages. Sowmya, Keerthi, Sri, Vipin, Satya and Gayathri as great friends and as part of the Indian mafia.

Last but not least my parents and my sister for being very supportive at every step.

Résumés

Le système de contrôle appelé dégradation des ARNm non-sens (NMD) permet de détecter puis de dégrader des ARNm contenant un codon de terminaison prématuré (PTC). Les facteurs principaux de la NMD : UPF1, UPF2 et UPF3 reconnaissent les PTCs en interagissant avec les facteurs de terminaison eRF1, eRF3 et la protéine poly (A) binding (PABP). La reconstitution d'un système de traduction *in vitro* a permis d'étudier la terminaison de la traduction en présence des facteurs PABP et UPF1, à l'aide de méthodes de biochimie et de cryo-microscopie électronique. L'étude du rôle du facteur de NMD UPF3B dans la terminaison de la traduction a mis en évidence une double action de cette protéine ; tout d'abord, un retardement de la reconnaissance du codon stop et également la promotion de la dissociation du ribosome. Ce travail a également permis de mettre en évidence une nouvelle interaction entre UPF3B et la kinase SMG1-8-9 et de montrer comment cette interaction affecte l'état de phosphorylation de UPF1. Les résultats de cette étude montrent une interaction complexe entre les différents facteurs de NMD et la kinase SMG1.

Nonsense-mediated mRNA decay (NMD) is an important eukaryotic quality control mechanism that recognizes and degrades mRNA containing a premature termination codon (PTC). Up-frameshift proteins constitute the conserved core NMD factors (UPF1, UPF2 and UPF3). They mediate the recognition of a NMD substrate, i.e. a ribosome stalled at a PTC. UPF proteins were shown to associate with eukaryotic release factors (eRF1 and eRF3) and were suggested to impede translation termination. We showed that, at a normal termination codon, poly (A) binding protein (PABP) stimulates translation termination by directly interacting with eRF3a. Using a reconstituted *in vitro* translation system, we studied translation termination in the presence of the factors PABP and UPF1 using biochemistry and single particle electron cryo-microscopy (Cryo-EM). Additionally, we analyzed the role of the other NMD factors UPF2 and UPF3B in translation termination *in vitro*. We discovered a novel role for UPF3B in translation termination. Moreover, we observed a novel interaction between UPF3B and the SMG1-8-9 kinase complex. The presence of UPF3B affects the kinase activity of SMG1 and thus the phosphorylation state of UPF1. Our results highlight a much more complex interplay of the NMD factors with the translation termination machinery and SMG1 kinase than anticipated.